# Merkel cell polyomavirus small T antigen's role in cell motility


## Gabrielė Stakaitytė

**BSc (Hons)**


Submitted in accordance with the requirements for the degree of
Doctor of Philosophy


University of Leeds

Faculty of Biological Sciences

School of Molecular and Cellular Biology


September 2016

The candidate confirms that the work submitted is her own and that appropriate credit has been given where reference has been made to the work of others. This copy has been supplied on the understanding that it is copyright material and that no quotation from the thesis may be published without proper acknowledgment.

This thesis is dedicated to my son Kernius. I hope that one day my journey in science will inspire him to undertake one himself.

# Acknowledgements

My thanks to Whitehouse laboratory members past and present, and especially to my supervisor Adrian Whitehouse. His help, support, and advice made this project possible. I would also like to thank Andrew Macdonald, Jamel Mankouri, and Jonathan Lippiat, as well as their group members, for their collaboration. These and many others at Leeds Virology have made my time spent here doing my PhD a fruitful and pleasant one. My project was further enriched by input from the Bioimaging and Flow Cytometry Facility, and I would like to thank Gareth Howell, Sally Boxall, and Brian Jackson (also a valued Whitehouse lab alumnus) for their help.

I would like to thank the BBSRC for funding my project and the White Rose DTP for all the additional training and support provided. Furthermore, I would like to thank the Educational Outreach department for the opportunity to act as an Educational Outreach Fellow. A special thanks goes to Rose Bavage and Jack Goode.

Finally, I would like to thank my whole family (mum, dad, brother, sister, and husband) for supporting me and believing in me these four years.

# Abstract

Merkel cell carcinoma (MCC) is an aggressive skin cancer of neuroendocrine origin with a high likelihood of recurrence and metastasis. In 2008, Merkel cell polyomavirus (MCPyV) was discovered monoclonally integrated within the host genome of at least 80% of MCC tumours. MCPyV transforms and maintains MCC tumours via the expression of the large and small tumour (LT and ST) antigens. Specifically, ST is thought to be the major transforming factor in the tumourigenesis of MCC. Since the discovery of MCPyV, a number of mechanisms have been suggested to account for replication and tumour formation, but to date, little is known about potential links between MCPyV T antigen expression and the highly metastatic nature of MCC.

In this thesis, the link between MCPyV and MCC metastasis is explored by focusing on the role of MCPyV ST in promoting cell motility. Cell motility and migration is a complex, multi-step, and multi-component process, intrinsic in cancer progression and metastasis. Previous work in the Whitehouse laboratory has implicated the microtubule network in MCPyV ST-induced cell motility. This thesis builds upon those findings to show that MCPyV ST-induced cell motility is dependent on multiple factors, including the activity of integrin receptors, Rho-family GTPases and the actin cytoskeleton, and intracellular chloride channels. This thesis also further explores the MCPyV ST-PP4C interaction in MCPyV ST-induced cell motility and proposes a mechanism by which this interaction activates integrin receptors to promote cell motility, thereby contributing to the metastatic nature of MCC. Furthermore, the relocalisation of intracellular chloride channels CLIC1 and CLIC4 to the cell surface is shown to be important in MCPyV ST-induced cell motility.

Overall, results presented herein describe a novel mechanism by which

a tumour virus induces cell motility, ultimately leading to cancer metastasis. Therefore, there may be implications for the potential future therapeutic targets for disseminated MCC.

# Abbreviations

| | |
|---|---|
| °C | degrees Celsius |
| % | percentage |
| 4E-BP1 | 4E-binding protein 1 |
| A | adenine |
| A/Ala | alanine |
| ADAM | a disintegrin and metalloproteinase |
| AIDS | acquired immunodeficiency syndrome |
| ALTO | alternative large T open reading frame |
| AMP | adenosine monophosphate |
| AP-1 | activator protein 1 |
| APyV | avian polyomavirus |
| Arp2/3 | actin related proteins 2 and 3 |
| ATM | Ataxia telangiectasia mutated |
| ATP | adenosine triphosphate |
| ATPase | adenosine triphosphatase |
| ATR | ATM and Rad3-related |
| BatPyV | bat polyomavirus |
| BET | bromodomain and extra terminal |
| BKPyV | BK polyomavirus |
| BPyV | bovine polyomavirus |
| Brd4 | bromodomain containing protein 4 |
| BSA | bovine serum albiumin |
| Bub1 | budding uninhibited by benzimidazoles 1 |
| C | cytosine |
| C/Cys | cysteine |
| CaCC | calcium-activated chloride channel |
| $CaCl_2$ | calcium chloride |
| CaPyV | canary polyomavirus |
| CBP | CREB binding protein |
| CCL20 | C–C motif chemokine ligand 20 |

| | |
|---|---|
| CD | cluster of differentiation |
| cDNA | complementary DNA |
| Cdc42 | cell division cycle 42 |
| CDK | cyclin-dependent kinase |
| C/EBPbeta | CCAAT enhancer binding protein beta |
| CFTR | cystic fibrosis transmembrane conductance regulator |
| CIP | calf intestinal (alkaline phosphatase) |
| CLIC | intracellular chloride channel |
| CLR7 | cullin-RING E3 ubiquitin ligase complex 7 |
| CK | cytokeratin |
| CMV | cytomegalovirus |
| c-myc | cellular myelocytomatosis oncogene |
| Cos7 | CV-1 (simian) in origin |
| CPyV | crow polyomavirus |
| CR1 | conserved region 1 |
| CREB | cyclic AMP response element binding |
| c-Src | cellular sarcoma |
| Cul7 | cullin 7 |
| CXCL9 | C–X–C motif chemokine ligand 9 |
| D/Asp | aspartate |
| DAPI | 4', 6-Diamidino-2-Phenylindole |
| DBD | DNA-binding domain |
| Dbl | dichaete beadex lethal |
| DDR | DNA damage response |
| $dH_2O$ | distilled water |
| DIDS | 4,4'-diisothiocyano-2,2'-stilbenedisulfonic acid |
| DMEM | Dulbecco modified eagle medium |
| DMSO | dimethyl sulphoxide |
| DNA | deoxyribonucleic acid |
| DNase | deoxyribonuclease |
| dNTP | deoxyribonucleoside triphosphate |
| ds | double-stranded |
| DTS | digital transcriptome subtraction |
| E1A | early region 1A |
| E2F | E2 factor |
| E/Glu | glutamate |

| | |
|---|---|
| EBNA2 | EBV nuclear antigen 2 |
| EBV | Epstein-Barr virus |
| *E. coli* | *Escherichia coli* |
| ECL | enhanced chemiluminescence |
| Ect2 | epithelial cell transforming 2 |
| ECM | extracellular matrix |
| EDTA | ethylenediaminetetraacetic acid disodium salt |
| EE | glutamate-glutamate |
| EGFP | enhanced green fluorescent protein |
| EGTA | (ethylene glycol-bis(β-aminoethyl ether)-N,N,N′,N′-tetraacetic acid |
| eIF4E | eukaryotic translation initiation factor 4E |
| ELISA | enzyme-linked immunosorbent assay |
| EMT | epithelial to mesenchymal trasition |
| EP300 | E1A binding protein 300 |
| ERK | extracellular signal-regulated kinases |
| Ets | E26 transformation-specific |
| F/Phe | phenylalanine |
| F-actin | filamentous actin |
| FAK | focal adhesion kinase |
| FAM111A | family with sequence similarity 111 member A |
| FBXW7 (Fbw7) | F-box and WD repeat domain containing 7 |
| FCS | foetal calf serum |
| FDA | Food and Drug Administration |
| Fgd1 | FYVE, RhoGEF and PH domain containing 1 |
| FGFR | fibroblast growth factor recpetor |
| FPyV | finch polyomavirus |
| g | gravity |
| G | guanine |
| G/Gly | glycine |
| GABA | γ-aminobutyric acid |
| G-actin | globular actin |
| GAG | glycosaminoglycan |
| GAP | GTPase-activating protein |
| GAPDH | glyceraldehyde 3-phosphate dehydrogenase |
| GDI | GDP-dissociation inhibitor |

| | |
|---|---|
| GDP | guanosine diphosphate |
| GEF | guanine exchange factor |
| GFP | green fluorescent protein |
| GHPyV | goose hemorrhagic polyomavirus |
| GM130 | Golgi marker 130 |
| GPCR | G-protein coupled receptor |
| GTP | guanidine triphosphate |
| GTPase | guanosine triphosphatase |
| Gu-HCl | guanidine hydrochloride |
| H/His | histidine |
| $H_2O$ | water |
| HA | haemagglutinin |
| HaPyV | hamster polyomavirus |
| HBV | hepatitis B virus |
| HBx | HBV protein X |
| HCl | hydrochloric acid |
| HCV | hepatitis C virus |
| HEK | human embryonic kidney |
| HEPES | 4-(2-hydroxyethyl)-1-piperazineethanesulfonic acid |
| HIF | hypoxia inducible factor |
| HOPS | homotrophic fusion and protein sorting |
| HPV | human papillomavirus |
| HPyV | human polyomavirus |
| H-ras | human rat sarcoma |
| HRP | horseradish peroxidase |
| Hsc70 | heat shock chaperone 70 |
| hTERT | human telomerase reverse transcriptase |
| HTLV-1 | human T-cell leukaemia virus 1 |
| I/Ile | isoleucine |
| IκB | inhibitor of kappa B |
| IF | immunofluorescence |
| IFN | interferon |
| IgG | immunoglobulin G |
| IKK | IκB kinase enzyme complex |
| IL | interleukin |
| IP | immunoprecipitation |

| | |
|---|---|
| IPTG | isopropyl-β-D-thio-galactoside |
| IRS1 | insulin receptor substrate 1 |
| IRSp53 | insulin receptor substrate protein 53 |
| JCPyV | JC polyomavirus |
| K/Lys | lysine |
| KCl | potassium chloride |
| kDa | kiloDalton |
| KIPyV | Karolinska Institute polyomavirus |
| KOAc | potassium acetate |
| KOH | potassium hydroxide |
| KPNA | karyopherin alpha |
| KSHV | Kaposi's sarcoma-associated herpesvirus |
| L/Leu | leucine |
| LB | Luria's broth |
| LIMK | LIM domain kinase |
| LMP1 | latent membrane protein 1 |
| LPyV | B-lymphotropic polyomavirus |
| LSD | LT stabilisation domain |
| LT | large T antigen |
| LXCXE | lysine–x–cysteine–x–glutamate |
| M | molar |
| M/Met | methionine |
| MAPK | mitogen activated protein kinase |
| MCC | Merkel cell carcinoma |
| MCPyV | Merkel cell polyomavirus |
| mDia2 | mammalian diaphanous 2 |
| mg | miligram |
| $MgCl_2$ | magnesium chloride |
| $MgSO_4$ | magnesium sulphate |
| miRNA | micro RNA |
| ml | mililitre |
| ML-141 | 4-[4,5-Dihydro-5-(4-methoxyphenyl)-3-phenyl-1H-pyrazol-1-yl]benzenesulfonamide |
| mm | milimetre |
| mM | milimolar |
| MMP | matrix metalloprotease |

| | |
|---|---|
| $MnCl_2$ | manganese chloride |
| MOPS | 3-(N-morpholino)propanesulfonic acid |
| MPTV | murine pneumotropic virus |
| MPyV | murine polyomavirus |
| MRN | MRE11/RAD50/NBS1 |
| mRNA | messenger RNA |
| MT | middle T antigen |
| MT1-MMP | matrix transmembrane metalloproteinase 1 |
| MTOC | microtubule organising centre |
| mTOR | mammalian target of rapamycin |
| mTORC | mTOR complex |
| MTS | 3-(4,5-dimethylthiazol-2-yl)-5-(3-carboxymethoxyphenyl)-2-(4-sulfophenyl)-2H-tetrazolium |
| MUR | Merkel cell polyomavirus unique region |
| MWPyV | Malawi polyomavirus |
| MXPyV | Mexico polyomavirus |
| N/Asn | asparagine |
| NaCl | sodium chloride |
| $Na_2CO_3$ | sodium carbonate |
| NaOH | sodium hydroxide |
| Nbs1 | nijmegen breakage syndrome 1 |
| NCCR | non-coding control region |
| NDEL1 | uclear distribution protein nudE-like 1 |
| NEMO | NF-κB essential modulator |
| NF-κB | nuclear factor κB |
| ng | nanogram |
| NJPyV | New Jersey polyomavirus |
| NLS | nuclear localisation signal |
| nm | nanometre |
| nM | nanomolar |
| NP-40 | tergitol-type NP-40 |
| NPF | nucleation-promoting factor |
| NPPB | 5-Nitro-2-(3-phenylpropylamino)benzoic acid |
| NSC23766 | N6-[2-[[4-(Diethylamino)-1-methylbutyl]amino]-6-methyl-4-pyrimidinyl]-2-methyl-4,6-quinolinediamine trihydrochloride |
| N-WASP | neural Wiscott-Aldrich protein |

| | |
|---|---|
| OBD | origin binding domain |
| OD | optical density |
| OraPyV | orangutan polyomavirus |
| ORF | open reading frame |
| *ori* | origin of replication |
| Q/Gln | glutamine |
| P/Pro | proline |
| p53 | protein 53 |
| p64 | protein 64 |
| p65 | protein 65 |
| p107 | protein 107 |
| p115RhoGEF | protein 115 RhoGEF |
| p130 | protein 130 |
| PAGE | polyacrylamide gel electrophoresis |
| PAMP | pathogen associated molecular pattern |
| PBS | phosphate buffered saline |
| PCNA | proliferating cell nuclear antigen |
| PCR | polymerase chain reaction |
| PD-1 | programmed cell death protein 1 |
| PEA3 | Phosphatidylinositol-4-phosphate 5-kinase 3 |
| PET | polyethylene tetraphthalate |
| PI-3K | phosphatidylinositol 3-kinase |
| PLC$\gamma$-1 | phospholipase C gamma 1 |
| PML | progressive multifocal leukoencephalopathy |
| pmol | picomole |
| PP1C | protein phosphatase 1 catalytic subunit |
| PP2A | protein phosphatase 2A |
| PP4 | protein phosphatase 4 |
| PP4C | protein phosphatase 4 catalytic subunit |
| pRb | retinoblastoma protein |
| PRR | pattern recognition receptor |
| psi | pounds per square inch |
| R/Arg | arginine |
| Rac | Ras-related C3 botulinum toxin substrate |
| RACE | rapid amplification of cDNA ends |
| RacPyV | racoon polyomavirus |

| | |
|---|---|
| RbCl | rubidium chloride |
| RCA | rolling circle amplification |
| RFC | replication factor C |
| RGDS | arginine–glycine–aspartate–serine |
| RGES | arginine–glycine–glutamate–serine |
| Rho | Ras homolog gene family |
| RIAA | Indanyloxyacetic acid 94, R(+)-Methylindazone |
| RNA | ribonucleic acid |
| RNase | ribonuclease |
| RNA pol II | RNA polymerase II |
| ROCK | Rho-kinase |
| RPA | replication protein A |
| RPMI | Roswell Park Memorial Institute medium |
| RSV | Rous sarcoma virus |
| RT | reverse transcriptase |
| RT-qPCR | RT quantitative PCR |
| RTK | receptor tyrosine kinase |
| S/Ser | serine |
| SA12 | simian agent 12 |
| SCF | SKP1–cullin1–F-box |
| SDS | sodium dodecyl sulphate |
| SFK | Src-family kinase |
| Shc | Src homology and collagen homology |
| SILAC | stable isotope labelling with amino acids in cell culture |
| siRNA | small interfering RNA |
| SqPyV | squirrel polyomavirus |
| ST | small T antigen |
| STLPyV | Saint Louis polyomavirus |
| SV40 | simian virus 40 |
| T | thymine |
| T/Thr | threonine |
| TANK | TRAF family member-associated NF-κB activator |
| TBE | tris-borate-EDTA buffer |
| TBS | tris buffered-saline |
| TEF1 | thyroid embryonic factor 1 |
| TEMED | N-N-N′-N′-tetramethylethylenediamine |

| | |
|---|---|
| TGF | transforming growth factor |
| Tim-3 | T cell immunoglobulin and mucin domain 3 |
| TK | tyrosine kinase |
| TLR | toll-like receptor |
| TNF | tumour necrosis factor |
| Tris | tris-(hydroxymethyl)-aminoethane |
| TSPyV | trichodysplasia spinulosa-associated polyomavirus |
| U | unit |
| UV | ultraviolet |
| V | volt |
| V/Val | valine |
| VEGF | vascular endothelial growth factor |
| vFLIP | viral FLICE inhibitory protein |
| VLP | virus-like particle |
| VP | viral protein |
| v-Src | viral sarcoma |
| VSOP | voltage-sensing domain only protein |
| v/v | volume over volume |
| W/Trp | tryptophan |
| WASP | Wiskott-Aldrich syndrome protein |
| WAVE | WASP-family verprolin-homologous protein |
| WHIM | warts, hypogammaglobulinaema, infections and myelokathexis |
| WNT | wingless-type MMTV integration site family member |
| WHO | World Health Organisation |
| WUPyV | Washington University polyomavirus |
| w/v | weight over volume |
| Y/Tyr | tyrosine |
| YM155 | 4,9-dihydro-1-(2-methoxyethyl)2-methyl-4,9-dioxo-3-(2-pyrazinylmethyl)-1H-naphth[2,3-d]imidazolium, bromide |
| ZCL278 | 2-(4-Bromo-2-chlorophenoxy)-N-[[[4-[[(4,6-dimethyl-2-pyrimidinyl)amino]sulfonyl]phenyl]amino] thioxomethyl]acetamide |
| Zn | zinc |
| ZO-1 | zonula occludens-1 |

| | |
|---|---|
| α | alpha |
| β | beta |
| γ | gamma |
| Δ | delta |
| κ | kappa |
| μg | microgram |
| μl | microlitre |
| μm | micrometre |
| μM | micromolar |

# Contents


**1 Introduction** **1**

1.1 Oncogenic viruses . . . 2

1.2 Polyomaviruses . . . 3

1.2.1 Classification of polyomaviruses . . . 4

1.2.2 Human polyomaviruses . . . 5

1.2.3 The polyomavirus genome . . . 7

1.2.4 The polyomavirus life cycle . . . 9

1.2.5 Polyomavirus early proteins . . . 10

1.2.5.1 The large T antigen . . . 11

1.2.5.2 The small T antigen . . . 14

1.2.5.3 The middle T antigen . . . 16

1.2.5.4 Other T antigen locus transcripts . . . 17

1.2.6 Polyomaviruses and cancer . . . 17

1.2.6.1 Polyomavirus oncogenicity . . . 18

1.2.6.2 The large T antigen in transformation . . . 18

1.2.6.3 The small T antigen in transformation . . . 20

1.2.6.4 The middle T antigen in transformation . . . 22

1.3 Merkel cell carcinoma . . . 22

1.3.1 Merkel cells . . . 22

1.3.2 Merkel cell carcinoma presentation . . . 24

1.3.3 Merkel cell carcinoma epidemiology . . . 25

1.3.4 Merkel cell carcinoma prognosis and treatment . . . 26

1.4 Merkel cell polyomavirus . . . 27

1.4.1 Merkel cell polyomavirus phylogeny . . . 27

1.4.2 Merkel cell polyomavirus genome organisation . . . 29

1.4.2.1 Merkel cell polyomavirus NCCR . . . 30

1.4.2.2 Merkel cell polyomavirus T antigen locus . . . 30

1.4.2.3 Merkel cell polyomavirus late proteins . . . . . 32
1.4.2.4 Merkel cell polyomavirus miRNA . . . . . 33
1.4.3 Merkel cell polyomavirus life cycle . . . . . 33
1.4.3.1 Merkel cell polyomavirus attachment and entry . . 34
1.4.3.2 Merkel cell polyomavirus replication . . . . . 35
1.4.3.3 Merkel cell polyomavirus and the immune response 37
1.4.3.4 Merkel cell polyomavirus assembly and egress . . 40
1.4.4 Merkel cell polyomavirus-induced tumourigenesis . . . . . 41
1.4.4.1 The role of LT in Merkel cell polyomavirus-induced tumourigenesis . . . . . 43
1.4.4.2 The role of ST in Merkel cell polyomavirus-induced tumourigenesis . . . . . 43
1.5 Merkel cell carcinoma treatment . . . . . 46
1.6 Cell motility . . . . . 47
1.6.1 The actin cytoskeleton . . . . . 48
1.6.1.1 Actin structures in cell motility . . . . . 50
1.6.1.2 Signalling cascades in actin regulation . . . . . 52
1.6.2 The microtubule network and intermediate filaments . . . . 52
1.6.3 Ion channels in cell motility . . . . . 53
1.6.3.1 Cell membrane potential . . . . . 53
1.6.3.2 Cell volume changes . . . . . 54
1.6.4 Tumour viruses and cell motility . . . . . 56
1.6.5 Cell migration . . . . . 59
1.7 Cancer metastasis . . . . . 61
1.7.1 Loss of cell adhesion . . . . . 61
1.7.2 Gain of cell motility . . . . . 63
1.7.3 Dissemination via the vasculature . . . . . 64
1.7.4 Colonisation and secondary tumour growth . . . . . 64
1.8 Thesis Aims . . . . . 65

**2 Materials and methods** **67**
2.1 Materials . . . . . 68
2.1.1 Chemicals . . . . . 68
2.1.2 Enzymes . . . . . 68
2.1.3 Antibodies and beads . . . . . 68
2.1.4 Mammalian cell culture reagents . . . . . 69

2.1.5 Cell lines . . . 69
2.1.6 Oligonucleotides . . . 70
2.1.7 Plasmid constructs . . . 71
2.1.8 siRNA constructs . . . 72
2.1.9 Inhibitors . . . 72
2.2 Methods . . . 73
2.2.1 Molecular cloning . . . 73
2.2.1.1 PCR amplification . . . 74
2.2.1.2 DNA gel electrophoresis . . . 74
2.2.1.3 DNA gel purification . . . 74
2.2.1.4 DNA ligation . . . 75
2.2.1.5 DNA restriction digestion . . . 75
2.2.1.6 Preparation of *E. coli* DH5α chemically competent cells . . . 75
2.2.1.7 Transformation of chemically competent cells . . . 76
2.2.1.8 Small scale (mini prep) DNA purification . . . 76
2.2.1.9 Large scale (maxi prep) DNA purification . . . 77
2.2.1.10 DNA sequencing . . . 78
2.2.2 Mammalian cell culture experiments . . . 78
2.2.2.1 Generating inducible cell lines . . . 79
2.2.2.2 Induction of inducible cell lines . . . 79
2.2.2.3 Plasmid DNA transfection . . . 79
2.2.2.4 siRNA transfection . . . 80
2.2.2.5 Addition of inhibitors . . . 80
2.2.3 Cell viability (MTS) assay . . . 80
2.2.4 Immunofluorescence . . . 81
2.2.4.1 Staining the actin cytoskeleton . . . 81
2.2.5 Protein expression and immunoblotting . . . 82
2.2.5.1 Preparation of mammalian cell lysates . . . 82
2.2.5.2 Determination of protein concentration . . . 82
2.2.5.3 Preparation of tumour and cell samples . . . 83
2.2.5.4 Tris-glycine SDS-polyacrylamide gel electrophoresis (PAGE) . . . 83
2.2.5.5 Western (immuno-) blotting . . . 84
2.2.6 Co-immunoprecipitation . . . 84
2.2.7 Cell motility experiments . . . 85

2.2.7.1 Life cell imaging . . . 85
2.2.7.2 Filopodia analysis . . . 85
2.2.7.3 Polarity assay . . . 85
2.2.7.4 Haptotaxis migration assay . . . 86
2.2.8 Cell surface protein analysis . . . 86
2.2.8.1 Flow cytometry . . . 86
2.2.9 Patch-clamping assay . . . 88
2.2.10 Gene expression analysis . . . 88
2.2.10.1 RNA extraction . . . 88
2.2.10.2 DNase I treatment . . . 89
2.2.10.3 Reverse transcription . . . 89
2.2.10.4 Ethanol precipitation . . . 89
2.2.10.5 RT-qPCR . . . 90
2.2.11 Statistical analysis . . . 90

**3 Merkel cell polyomavirus small T antigen enhances cell motility via Rho-GTPase-induced filopodia formation 91**
3.1 Introduction . . . 92
3.2 Quantitative proteomic analysis shows MCPyV ST expression affects actin-associated proteins . . . 93
3.3 MCPyV T antigen-positive MCC tumours express actin-associated proteins . . . 96
3.4 MCPyV ST expression induces the formation of actin-based protrusions . . . 97
3.5 MCPyV ST expression induces the formation of filopodia . . . 100
3.6 i293-GFP and i239-GFP-ST cell line generation using the 293 FlipIn™ system . . . 102
3.7 MCPyV ST induces cell motility in i293 and in MCC13 cells . . . 103
3.8 MCPyV ST-induced cell motility is directional . . . 104
3.9 MCPyV ST-induced cell motility is dependent on the action of Rho-family GTPases . . . 107
3.10 MCPyV ST-induced filopodia formation depends on the activity of the Rho-family GTPases . . . 111
3.11 Discussion . . . 114

**4 The interaction between MCPyV ST and PP4C is required for initiating**

**cell motility through the dephosphorylation of β1 integrin** **116**
4.1 Introduction . . . 117
4.2 Interaction of MCPyV ST with PP4C is required for cell motility . . 118
4.3 MCPyV ST interaction with the catalytic subunit of PP4 is required for filopodia formation . . . 122
4.4 The 102 residue of MCPyV ST is important in PP4C binding, MCPyV ST-induced cell motility, and filopodia formation . . . 125
4.5 Phosphomimetic mutants of Cdc42 and Rac1 show diminished filopodia formation upon MCPyV ST expression . . . 129
4.6 Expression of MCPyV ST does not affect the phosphorylation status of Cdc42 or Rac1 . . . 132
4.7 Integrin activity inhibition affects MCPyV ST-induced cell motility 132
4.8 Inhibition of integrin activity affects MCPyV ST-induced filopodia formation . . . 139
4.9 Expression of MCPyV ST affects the phosphorylation of β1 integrin at Thr788/789 . . . 141
4.10 Discussion . . . 143

**5 Merkel cell polyomavirus small T antigen-induced cell motility depends on the activity of intracellular chloride channels** **146**
5.1 Introduction . . . 147
5.2 MCPyV ST expression increases the activity of ion channels . . . 148
5.3 Broad-spectrum chloride channel inhibitors affect MCPyV ST-induced cell motility . . . 149
5.4 Disruption of MCPyV ST-induced cell motility by broad-spectrum chloride channels is not additive . . . 155
5.5 Disruption of MCPyV ST-induced cell motility by broad-spectrum chloride channels is reversible . . . 158
5.6 Broad-spectrum chloride channel inhibitors affect MCPyV ST-induced filopodia formation . . . 160
5.7 Quantitative proteomic analysis shows that MCPyV ST expression affects CLIC family protein levels . . . 162
5.8 MCPyV-positive MCC tumours express CLIC family proteins . . . 164
5.9 Depletion of CLIC1 and CLIC4 disrupts MCPyV ST-induced cell motility . . . 165

5.10 CLIC1 and CLIC4 show increased plasma membrane localisation upon MCPyV ST expression . . . . . 168
5.11 Discussion . . . . . 171

**6 Final discussion and future perspectives** **173**
6.1 Final discussion and future perspectives . . . . . 174

**References** **234**

# List of Figures


1.1 A phylogenetic tree of polyomaviruses based on whole genome sequences . . . 5
1.2 A generalised polyomavirus genome, including the non-coding control region, the early gene region and the late gene region . . . 8
1.3 The polyomavirus life cycle in a permissive cell line . . . 9
1.4 The structure of SV40 LT . . . 12
1.5 The structure of SV40 ST . . . 14
1.6 The structure of MPyV MT . . . 16
1.7 Effect of LT on cell proliferation . . . 20
1.8 Interaction of ST with PP2A . . . 21
1.9 Skin layers in the context of Merkel cells . . . 23
1.10 Merkel cell carcinoma presentation . . . 24
1.11 Merkel cell polyomavirus phylogeny . . . 28
1.12 The Merkel cell polyomavirus genome . . . 29
1.13 The Merkel cell polyomavirus T antigen locus and its gene products 31
1.14 MCPyV attachment and entry . . . 35
1.15 NF-κB signalling in the cellular immune response . . . 40
1.16 Merkel cell polyomavirus-induced tumourigenesis . . . 42
1.17 MCPyV ST promotes cell proliferation downstream of the Akt pathway . . . 45
1.18 The action of Arp2/3 and NPFs in the formation of actin fibres . . . 49
1.19 Cellular protrusions in cell motility . . . 51
1.20 Volume changes in cell migration . . . 55
1.21 Tumour viruses in the cell motility pathway . . . 58
1.22 Modes of cell migration . . . 60
1.23 Tumour spread from the primary site . . . 62

2.1 Isotype controls (rabbit and mouse) for flow cytometry experiments 87

3.1 Actin-associated proteins are upregulated upon MCPyV ST expression . . . 95
3.2 Actin-associated proteins are expressed in MCPyV-positive MCC tumours . . . 96
3.3 Cell imaging shows an increase in actin-based protrusions in ST-expressing cells . . . 98
3.4 Cell imaging quantification shows an increase in actin-based protrusions in ST-expressing cells . . . 99
3.5 Screening of filopodia-associated proteins indicates MCPyV ST expression induces filopodia formation . . . 101
3.6 Production of GFP-expressing and GFP-tagged MCPyV ST-expressing inducible cell lines . . . 102
3.7 Live cell imaging shows MCPyV ST expression enhances cell motility 104
3.8 Cell imaging shows MCPyV ST induces directional cell motility . . . 106
3.9 Cell viability assays for Rho-family GTPase inhibitors . . . 108
3.10 Live cell imaging shows a dependence of MCPyV ST-induced cell motility on Cdc42 and RhoA in i293 cells . . . 109
3.11 Live cell imaging shows a dependence of MCPyV ST-induced cell motility on Cdc42 and RhoA in MCC13 cells . . . 110
3.12 Cell imaging shows that Rho-family GTPase inhibitors reduce MCPyV ST-induced filopodia formation . . . 112
3.13 Cell imaging shows that Cdc42 and RhoA transdominant mutants reduce MCPyV ST-induced filopodia formation . . . 113

4.1 Live cell imaging shows that a MCPyV ST mutant that cannot bind PP2A Aβ or PP4C affects cell motility . . . 120
4.2 Live cell imaging shows that PP2A and PP4C transdominant mutants affect MCPyV ST-induced cell motility . . . 121
4.3 Cell imaging shows that a MCPyV ST mutant that cannot bind PP2A Aβ or PP4C disrupts filopodia formation . . . 123
4.4 Cell imaging shows the transdominant mutant of PP4C disrupts MCPyV ST-induced filopodia formation . . . 124
4.5 MCPyV ST 102 amino acid residue is critical for PP4C binding . . . 126
4.6 Live cell imaging shows that MCPyV ST mutants that cannot bind PP4C reduce MCPyV ST-induced cell motility . . . 127

4.7 Cell imaging shows that MCPyV ST mutants that cannot bind PP4C disrupt filopodia formation . . . 128
4.8 Cell imaging shows that the phosphomimetic Cdc42S71E mutant reduces MCPyV ST-induced filopodia formation . . . 130
4.9 Cell imaging shows that the phosphomimetic Rac1S71E mutant reduces MCPyV ST-induced filopodia formation . . . 131
4.10 MCPyV ST expression does not affect the phosphorylation status of Cdc42/Rac1 . . . 132
4.11 Cell viability assays for RGDS and RGES . . . 134
4.12 Integrin inhibitor RGDS reduces MCPyV ST-induced cell motility in i293 cells . . . 135
4.13 Integrin inhibitor RGDS reduces MCPyV ST-induced cell motility in MCC13 cells . . . 136
4.14 Control peptide RGES does not reduce MCPyV ST-induced cell motility in i293 cells . . . 137
4.15 Control peptide RGES does not reduce MCPyV ST-induced cell motility in MCC13 cells . . . 138
4.16 Integrin inhibitor RGDS reduces MCPyV ST-induced filopodia formation . . . 140
4.17 MCPyV ST expression reduces the phosphorylation levels of β1 integrin at Thr 788/789 residues . . . 142
4.18 A model for MCPyV ST-induced cell motility . . . 143

5.1 Patch clamping of HEK-293 cells shows an increase in current upon MCPyV ST expression . . . 149
5.2 Cell viability assays for broad-spectrum chloride channel inhibitors 151
5.3 Live cell imaging shows blocking chloride channels with broad-spectrum inhibitors reduces MCPyV ST-induced cell motility in i293 cells . . . 152
5.4 Live cell imaging shows blocking chloride channels with broad-spectrum inhibitors reduces MCPyV ST-induced cell motility in MCC13 cells . . . 153
5.5 Haptotaxis assay shows blocking chloride channels with broad-spectrum inhibitors reduces MCPyV ST-induced cell migration . . . 154

5.6 Live cell imaging shows the effect of broad-spectrum chloride channel inhibitors on MCPyV ST-induced cell motility in i293 cells is non-additive . . . 156
5.7 Live cell imaging shows the effect of broad-spectrum chloride channel inhibitors on MCPyV ST-induced cell motility in MCC13 cells is non-additive . . . 157
5.8 Live cell imaging shows the effect of broad-spectrum chloride channel inhibitors on MCPyV ST-induced cell motility is reversible . . . 159
5.9 Cell imaging shows that broad-spectrum chloride channe inhibitors reduce MCPyV ST-induced filopodia formation . . . 161
5.10 CLIC family proteins are upregulated upon MCPyV ST expression 163
5.11 CLIC family proteins are expressed in MCPyV-positive MCC tumours . . . 164
5.12 Live cell imaging shows CLIC1 and/or CLIC4 depletion reduces MCPyV ST-induced cell motility in i293 cells . . . 166
5.13 Live cell imaging shows knocking down CLIC1 and/or CLIC4 reduces MCPyV ST-induced cell motility in MCC13 cells . . . 167
5.14 Flow cytometry shows relocalisation of CLIC1 and CLIC4 to the cell surface . . . 170

# List of Tables


1.1 Human tumour viruses . . . . . 3
1.2 Human polyomaviruses . . . . . 7
1.3 Polyomavirus large T antigen binding partners . . . . . 13

2.1 Enzymes and their suppliers . . . . . 68
2.2 Primary antibodies, their origins, their working dilutions, and their suppliers . . . . . 70
2.3 Oligonucleotides used in cloning or RT-qPCR, including sequences for both forward and reverse oligo pairs . . . . . 71
2.4 Plasmid constructs and their sources . . . . . 72
2.5 Small molecule inhibitors, their working concentrations and suppliers. i293 cells include HEK-293 and derived cell lines . . . . . 73
2.6 Reagents and their volumes to prepare a range of tris-glycine polyacrylamide running gels . . . . . 83

3.1 Quantitative proteomic analysis shows an increase in actin-associated protein levels upon MCPyV ST expression . . . . . 94

5.1 Quantitative proteomic analysis shows an increase in CLIC family protein levels upon MCPyV ST expression . . . . . 162

# Chapter 1

# Introduction

## 1.1 Oncogenic viruses

Cancer is the cause of approximately 13% of deaths worldwide, more than AIDS, tuberculosis, and malaria combined [1]. It remains a growing public health concern, with prevention, management, and treatment costing individuals, charities, and governments billions. In 2010 alone, the associated cost of cancer care in the US was $124.57 billion, estimated to grow to $157.77 billion in 2020 [2]. In the UK, 2 million people live with cancer, a figure expected to rise by a million a decade. It is projected that by 2040, almost a quarter of people aged 65 will be cancer survivors [3].

There are many different causes of cancer, among them viruses and other infectious agents. 12.7 million new cancer cases occurred in 2008, and 16.1% (i.e. around 2 million new cancer cases) are attributed to infection. There is a clear geographic and economic divide in the distribution of infection-related cancers: 22.9% of cases in underdeveloped countries (32.7% of that in sub-Saharan Africa) vs 7.4% in developed countries (3.3% of that in Australia and New Zealand). The vast majority of these new cases, 1.9 million, were due to either Hepatitis B and C virus, human papillomavirus (HPV) or *Helicobacter pylori* infections, which resulted in mainly liver, cervix/uteri or gastric cancers. Around half the infection-related cancers in women were cervix/uteri, more than 80% in men were liver or gastric. In addition, around 30% of infection-attributable cases occur in people younger than 50 years [4].

Thus, there is a clear role for viruses in the global burden of cancer. The field of tumour virology began in the early 20th century, with experiments performed on chickens by Francis Rous in the USA and by Vilhelm Ellerman and Oluf Bang in Denmark. In 1908, they showed that avian erythroblastosis can be transmitted between chickens using a cell-free tumour extract. Three years later, in 1911, Rous showed that a sarcomatous chest tumour can also be transmitted between chickens using a cell-free tumour extract [5]. However, these findings were considered mere curiosities by the wider scientific community, and tumour virology did not garner much attention until the 1930s. In that decade, Rous returned to tumour virology, and worked on the cottontail rabbit papilomavirus [6], including investigations of the co-carcinogenic effects of coal tars on virus-induced tumours [7].

In the 1950s, two transforming mouse viruses were discovered: murine leukaemia

retrovirus (MLV) and murine polyomavirus (MPyV) [8]. This led to increased interest in tumour viruses, accelerated by the discovery of simian virus 40 (SV40) in the 1960s [9]. Research on SV40 has yielded many important discoveries in the field of molecular cell biology, e.g. identification of the p53 tumour suppressor [10], the first nuclear localisation signal [11], and tyrosine phosphorylation [12].

To date, 7 viruses have been conclusively linked to human cancers: Epstein-Barr virus (EBV), Hepatitis B virus (HBV), human T-lymphotropic virus 1 (HTLV-1), high risk human papillomaviruses (HPV16 and HPV18), Hepatitis C virus (HCV), Kaposi's sarcoma herpesvirus (KSHV) and Merkel cell polyomavirus (MCPyV). Table 1.1 provides information on year of discovery, associated cancers and genome type.

**Table 1.1: Human tumour viruses**

| Virus | Discovery | Major associated cancers | Genome | Refs |
|---|---|---|---|---|
| EBV | 1964 | Burkitt's lymphoma and nasopharyngeal carcinoma | Large dsDNA | [13] |
| HBV | 1965 | Hepatocellular carcinoma | ss and dsDNA | [14] |
| HTLV-1 | 1980 | Adult T cell lymphoma | Retrovirus RNA | [15] |
| HPV16, HPV18 | 1983-1984 | Cervical, penile, head and neck cancers | Small dsDNA | [16] [17] |
| HCV | 1989 | Hepatocellular carcinoma | (+)RNA | [18] |
| KSHV | 1994 | Kaposi's sarcoma, primary effusion lymphoma (PEL), multicentric Castleman's disease | Large dsDNA | [19] |
| MCPyV | 2008 | Merkel cell carcinoma | Small dsDNA | [20] |

ss: single-stranded, ds: double stranded, (+): positive strand

## 1.2 Polyomaviruses

The *Polyomaviridae* family of viruses is characterised by circular, double-stranded DNA genomes capable of infecting a variety of mammals and birds. The first polyomaviruses to be characterised, in the 1950s and 1960s respectively, were MPyV and SV40. The former was discovered when it was observed that filterable extracts from murine leukaemia could induce tumours in the parotid gland

of neonatal mice [8]. The latter was identified in African green monkey kidney cells, which were used in the production of the polio vaccine [9]. Historically, polyomaviruses were classified together with papillomaviruses into the papova virus family, but since the 7th International Committee on Taxonomy of Viruses (ICTV) report in 2001, it has been recognised that they are a distinct family of small double-stranded DNA viruses. Currently, polyomaviruses are known to infect birds, rodents, cattle, and primates, but an individual viral species has a very narrow host range and cell specificity.

### 1.2.1 Classification of polyomaviruses

Historically, polyomaviruses were classified into one genus. However, in 2010, the ICTV reclassified polyomaviruses into 3 separate genera: *Orthopolyomavirus* and *Wukipolyomavirus* for mammalian virus species and *Avipolyomavirus* for bird virus species. Figure 1.1 shows the phylogenetic relationship among polyomaviruses based on whole genomic nucleotide sequences.

There are some startling differences between the genera. For example, while mammalian polyomaviruses have a narrow host and cell specificity, avian polyomaviruses have a much broader host range [21]. Conversely, while a number of mammalian polyomaviruses display tumourigenicity under certain conditions (discussed in Section 1.2.6), avian polyomaviruses are agents of inflammation in non-immunosuppressed hosts [22].

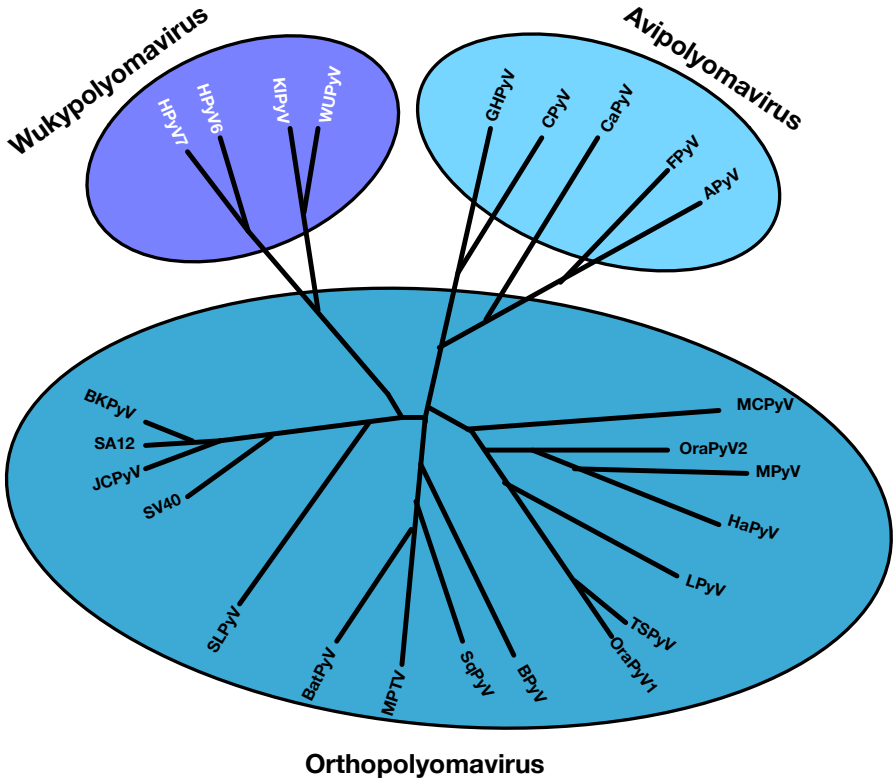


**Figure 1.1: A phylogenetic tree of polyomaviruses based on whole genome sequences.** Three large groups are distinguished: wukipolyomaviruses, avipolyomaviruses and orthopolyomaviruses.

### 1.2.2 Human polyomaviruses

Twelve human polyomaviruses have been discovered to date, ten of them since 2007. The first two human polyomaviruses were identified in 1971 from two different patient samples, and named after the initials of the patients: JC polyomavirus (JCPyV) and BK polyomavirus (BKPyV).

JCPyV was isolated from the brain tissue of a patient suffering from progressive multifocal leukoencephalopathy (PML), a disease characterised by the demyelination of the central nervous system [23]. It has since been conclusively determined that JCPyV is the causative agent of PML [24], and that the virus is a common childhood infection, with a seroprevalence of 70–90% of the adult population [25]. In an immunocompetent host, JCPyV establishes a latent, asymptomatic infection in the gastrointestinal tract and kidneys [26], but in an immunocompro-

mised host, it can reactivate and establish a lytic infection in oligodendrocytes, leading to PML [27].

BKPyV was identified from a urine sample of a kidney transplant recipient presenting with chronic pyelonephritis and advanced renal failure [28]. Like JCPyV, BKPyV is prevalent in approximately 80% of the adult population, with an asymptomatic, latent presence [29]. Upon immunosuppression, BKPyV can reactivate and enter a lytic replication cycle, and, in the context of kidney transplants, the virus can cause polyomavirus-associated nephropathy (PVAN), which is associated with 50% allograft failure [30].

Currently, there is somewhat of a renaissance in human polyomavirus discovery. Table 1.2 summarises all the human polyomaviruses known so far. Only Merkel cell polyomavirus (discussed in detail in Section 1.4) and Trichodysplasia Spinulosa-associated polyomavirus (TSPyV) have been implicated in disease. TSPyV causes a rare skin disease, Trichodysplasia Spinulosa, but only in conditions of immunosuppression [31]. The role of the remaining new human polyomaviruses in disease is under investigation, but so far it is unclear whether they are involved in any pathologies.

**Table 1.2: Human polyomaviruses**

| Virus | Discovery | Origin | Refs |
|---|---|---|---|
| JCPyV | 1971 | Brain tissue extract of PML patient | [23] |
| BKPyV | 1971 | Urine of renal translpant patient | [28] |
| KIPyV | 2007 | Respiratory tract (acute infection) | [32] |
| WUPyV | 2007 | Respiratory tract (acute infection) | [33] |
| MCPyV | 2008 | Merkel cell carcinoma (MCC) tumour | [20] |
| HPyV6 | 2010 | Healthy skin samples | [34] |
| HPyV7 | 2010 | Healthy skin samples | [34] |
| TSPyV | 2010 | Skin samples from TS patient | [31] |
| HPyV9 | 2011 | Healthy skin and serum samples | [35] |
| MWPyV (HPyV10, MXPyV) | 2012 | Healthy stool sample, WHIM patient sample, acute diarrhoea sample | [36] [37] [38] |
| HPyV12 | 2013 | Liver resection sample | [39] |
| STLPyV | 2013 | Healthy stool sample | [40] |
| NJPyV | 2014 | Muscle biopsy of pancreatic transplant patient | [41] |

J. C. and B. K.: patient initials, PML: progressive multifocal leukoencephalopathy, KI: Karolinska Institute, WU: Washington University, St. Luis, TS: trichodysplasia spinulosa, MW: Malawi, MX: Mexico, STL: St Louis, NJ: New Jersey

### 1.2.3 The polyomavirus genome

The polyomavirus genome is an approximately 5,000 base pair circle of double-stranded DNA, with a non-coding control region (NCCR) flanked by an early gene region on one side and a late gene region on the other. The NCCR contains the early and late promoters, their transcription start sites and the origin of replication.

The early and late gene regions are encoded on opposite strands of the template DNA. The early gene region encodes the large T antigen (LT) and the small T antigen (ST). In addition, alternatively spliced variants of LT (LT' in Figure 1.2) have been characterised for some polyomaviruses, such as MCPyV [42]. MCPyV has also been found to encode an alternative large T open reading frame (ALTO) transcript [43]. The newly-discovered STLPyV may express 229T, a third early transcript that shares the first 190 residues of small T antigen with an additional 39 residues from an alternative reading frame of LT [40]. However, none of the human polyomaviruses seem to encode a middle T antigen, which is present in

other mammalian polyomaviruses, such as MPyV [44].

The late gene region encodes the viral coat proteins VP1, VP2, and VP3. SV40 encodes an additional viroporin, VP4 [45]. The reading frames for VP2, VP3 and VP4 are identical, but translation starts at successive initiating AUG codons to generate the different proteins. SV40, JCPyV, and BKPyV late transcripts also encode the agnoprotein [46], a small protein of as-yet-unknown function. Figure 1.2 shows the generalised polyomavirus genome.

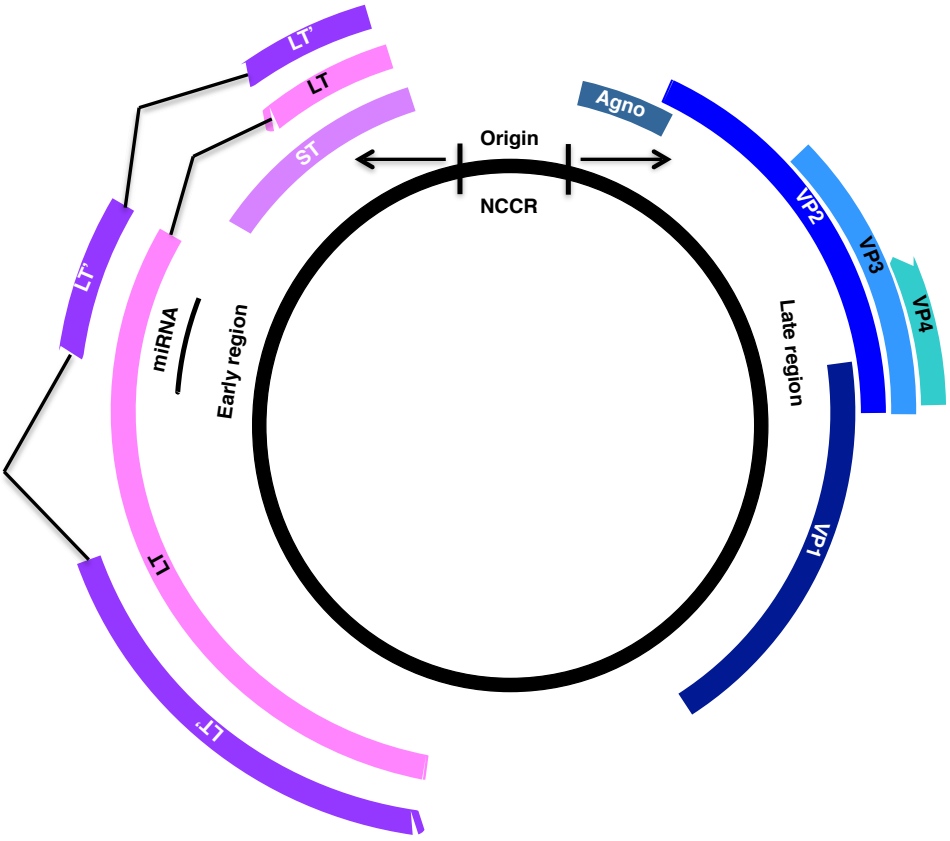


**Figure 1.2: A generalised polyomavirus genome, including the non-coding control region, the early gene region and the late gene region.** The early gene region commonly encodes LT, ST, and at least one alternative T antigen product (LT'). The late gene region encodes the structural VP proteins, and, in some polyomaviruses, the agnoprotein. Some polyomaviruses also express a microRNA. Agno: agnoprotein, LT: large T antigen, LT;: alternatively-spliced T antigen product, miRNA: polyomavirus-expressed micro RNA, NCCR: non-coding control region, ST: small T antigen, VP: viral protein/

### 1.2.4 The polyomavirus life cycle

The polyomavirus life cycle reflects the nature of DNA viruses, with entry both into the cell and into the nucleus. A generalised polyomavirus life cycle is summarised in Figure 1.3, using the SV40 lytic life cycle as the model.

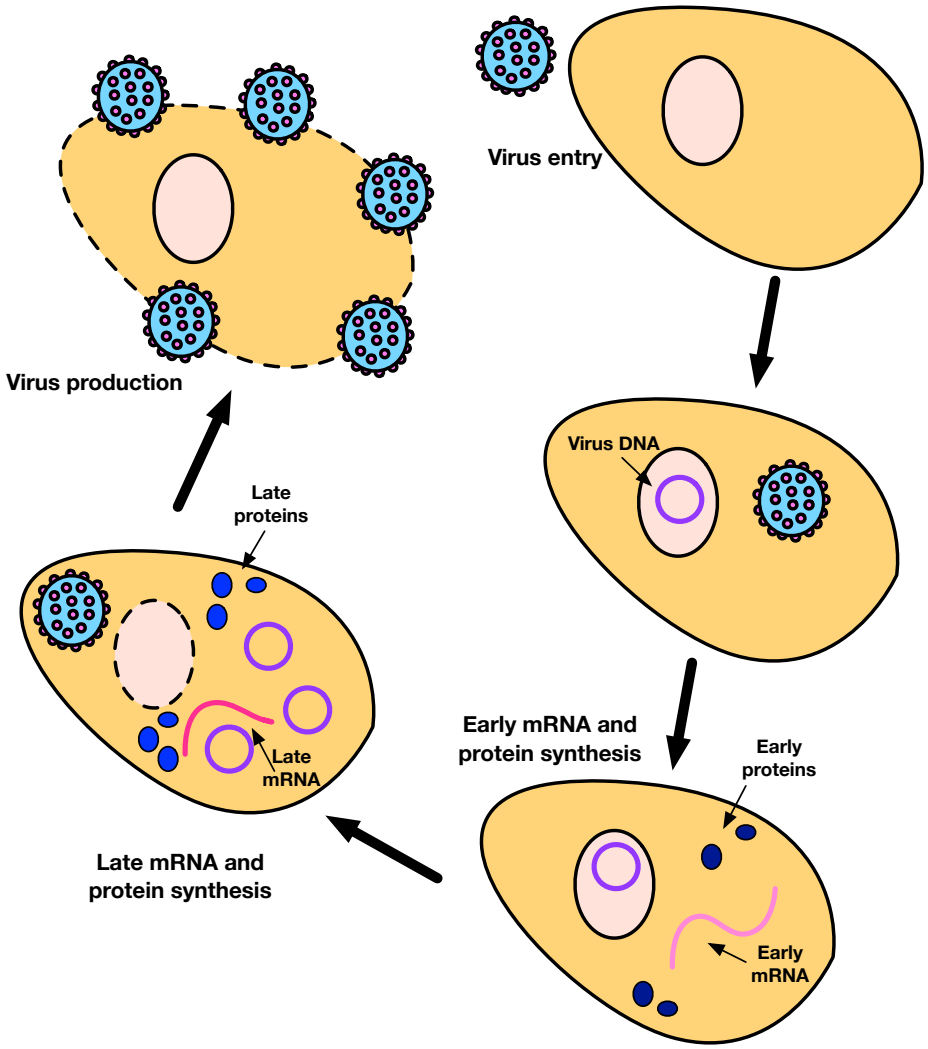


**Figure 1.3: The polyomavirus life cycle in a permissive cell line.** SV40 is taken as a model for the polyomavirus life cycle as its replication has been most widely studied.

In order to infect an animal cell, a virus first attaches to specific receptor molecules on the cell surface. SV40 entry is mediated by attachment to sialic acid moieties. The ganglioside GM1 is thought to be required in many cases for SV40 entry [47], but attachment to the major histocompatibility complex (MHC) has also been

observed [48]. MPyV and BKPyV bind to sialylated glycans, e.g. GT1B [49] [50], while JCPyV is tropic for $\alpha$-2-6-linked sialic acids [51].

Polyomaviruses enter the cell through endocytosis, but the mechanism of this vary for different viruses. SV40, for example, depends on caveolin-mediated endocytosis [52], while JCPyV utilises a clathrin-dependent mechanism [53]. After entry, the virus must be transported to the nucleus to continue its lifecycle. All three SV40 VPs have nuclear localisation signals (NLS) [54]. In addition, JCPyV VP1 also contains an NLS sequence, which allows binding to cellular importins and entry into the nucleus via the nuclear pore complex (NPC) [55].

Polyomavirus DNA is transcribed and replicated in the host cell nucleus. After entering the nucleus and uncoating, the early gene region is transcribed, with SV40 LT being able to transactivate the early promoter region as well as binding to the origin of replication to promote the replication of the viral genome [56]. Polyomavirus transcription, translation, and replication depend on host cell machinery, including proteins expressed only during S-phase, thus both LT and ST promote entry of the host cell into S-phase.

Once a sufficient concentration of LT is reached, it acts to inhibit the activity of the early promoter and instead activates the late promoter to drive the production of the structural proteins [56]. Translated structural proteins are re-imported into the nucleus, where virion assembly takes place. Virion assembly occurs by addition and organisation of the capsid proteins around the viral minichromosome, rather than by incorporation of DNA into pre-formed capsids [57] Each VP1 pentamer combines with a molecule of either VP2 [58] or VP3 [59] due to strong hydrophobic interactions. Interestingly, studies using capsid proteins with mutated NLS indicated that VP1 and VP2/3 are transported to the nucleus as a single unit [54]. This suggests that $VP1_5VP2/3$ is the building block for the SV40 capsid.

### 1.2.5 Polyomavirus early proteins

All polyomaviruses encode at least two proteins in the early region of their genome. LT and ST are ubiquitous among polyomaviruses, and are required for viral replication. They are produced from one transcript via differential splicing, and share a common amino-terminal region (first 80–82 residues) [60]. The known products of the T antigen locus are discussed in the following sections.

The functions of T antigens are commonly discussed in terms of SV40 and MPyV, as their early gene products are the most widely characterised. LT and ST promote the switch to S phase in quiescent host cells, and thus are required for viral DNA replication [61]. The S phase switch ensures the presence of the necessary host cell machinery to replicate viral DNA, since polyomaviruses do not encode any proteins for DNA synthesis [60]. This process is considered to result in polyomavirus-induced cellular transformation, as early gene expression in non-permissive cells results in aberrant cell cycle stimulation and interference with host cell signalling pathways [62].

#### 1.2.5.1 The large T antigen

LT is one of the products of the polyomavirus early transcript. It is a protein of approximately 700 amino acids, with an amino-terminal DnaJ domain, common to all T antigen transcripts, and a unique carboxy-terminal domain. The DnaJ domain contains the Hsc70 binding domain and the highly conserved Cr1 domain. The unique region contains multiple different protein binding domains (discussed below), a DNA-binding domain, a nuclear localisation signal (NLS), a zinc (Zn) finger domain and an ATPase domain. Figure 1.4 shows the structure of SV40 LT.

LT is involved in viral DNA replication, binding to the origin of replication within the NCCR and promoting DNA unwinding and transcription/replication complex formation via its DNA-binding and ATPase domains [63], [64]. In addition, SV40 [65] and JCPyV [66] LTs can promote the transcription of late region genes. In addition, LT promotes cell cycle dysregulation and host cell entry into S phase [60].

These functions depend on the ability of LT to bind to a wide variety of host cell proteins. SV40 LT can bind to a number of factors associated with DNA replication. For instance, the J domain and the ATPase domain of SV40 LT are necessary to directly bind to the catalytic subunit of DNA polymerase-$\alpha$ *in vitro* [67]. SV40 LT can also bind to replication protein A (RPA), a factor involved in replication assembly [68]. In addition, SV40 LT, like all polyomavirus LT studied, forms a hexameric complex to initiate DNA replication via its helicase function. Two of these LT complexes are required, binding in head-to-head configuration to the viral origin of repliation. In addition to LT, this helicase complex also contains

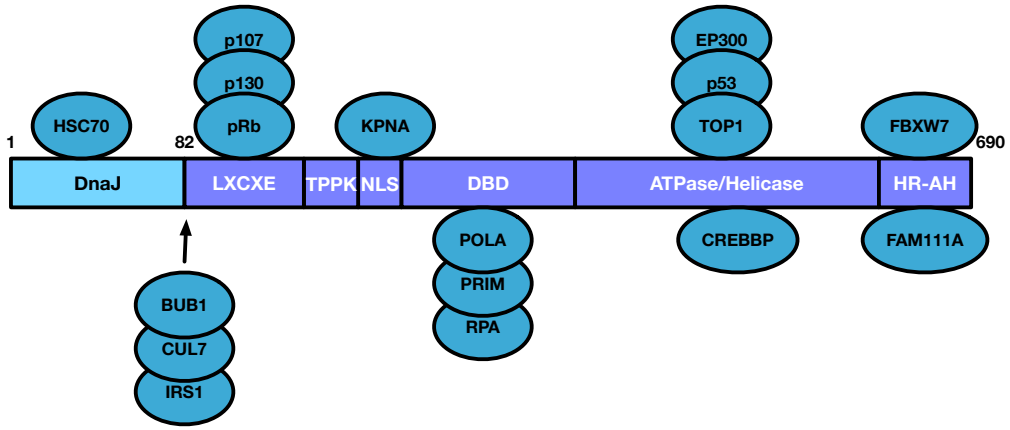


**Figure 1.4: The structure of SV40 LT.** SV40 LT contains an amino-terminal DnaJ domain that binds Hsc70, and multiple domains with many different binding partners, including a nuclear localisation signal, a DNA-binding domain, and an ATPase/helicase domain. BUB1: budding uninhibited by benzimidazoles 1 protein, CREBBP: CREB-binding protein, CUL7: cullin 7 protein, DBD: DNA-binding domain, EP300: E1A-binding protein 300, FAM111A: family with sequence similarity 111 member A, FBXW7: F-box and WD repeat domain containing 7, HSC70: heat shock chaperone 70, IRS1: insulin receptor substrate 1, KPNA: karyopherin alpha, NLS: nuclear localisation signal, POLA: DNA polymerase alpha, pRB: retinoblastoma protein, PRIM: DNA primase, RPA: replication protein A, TOP1: topoisoerase 1.

the host factors nucleolin and topoisomerase [69].

In addition to its function in viral DNA replication, LT also promotes host cell entry into S phase. A number of cellular proteins regulate the progression of the cell from $G_1$ to S-phase. One such protein is the retinoblastoma protein (pRb), a tumour suppressor which binds to and sequesters the E2F transcription factor. Phosphorylation of pRb releases the E2F transcription factor, allowing the switch to S-phase [70] [71]. SV40 LT binds to and sequesters pRb [72] and pRb family proteins (e.g. p107 and p130), allowing for the release of E2F [73]. BKPyV LT can also reduce the levels of pRb family proteins by promoting the proteolysis of p130 and other pRb family members in mouse fibroblast cells [74]. In addition, the Hsc70-binding domain of LT has *cis*-acting properties aiding in the dissociation of E2F from pRb in an ATPase-dependent manner [75]. As such, there appears to be ample redundancy in subverting the pRb signalling pathways by LT.

**Table 1.3: Polyomavirus large T antigen binding partners**

| Protein | Function | Effect of LT binding | Refs |
|---|---|---|---|
| Cullin7 (CUL7) | Core part of Cullin-RING E3 ubiquitin ligase complex 7 (CLR7) | Suppresses activity of CLR7, leading to impaired proteolysis of insulin receptor substrate 1 (IRS1) | [76] |
| Insulin receptor substrate 1 (IRS1) | Part of the insulin response pathway | Translocation of IRS1 into the nucleus, leading to inhibition of DDR | [77] [78] |
| β-catenin | Part of the Wnt signalling pathway | Increased stability of β-catenin and enhancement of target gene (e.g. c-myc) activation | [79] [80] |
| Thyroid embryonic factor-1 (TEF-1) | Transcription factor | Early-to-late switch in viral gene expression | [81] |
| p300/CREB-binding protein (CBP)* | Transcriptional adapter proteins | LT acetylation | [82] |
| Bub1 | Mitotic spindle checkpoint protein | Perturbation of the spindle checkpoint leading to genomic instability | [83] |
| Nbs1 | Part of the MRN complex in DDR | Disruption of DNA replication control | [84] |

* Indirect interaction through p53.

p53 is another significant tumour suppressor targeted by polyomavirus LT. It is a crucial regulator of cell cycle, apoptosis, and DNA damage repair (DDR) processes [85]. SV40, JCPyV and BKPyV LTs all bind p53 in an ATP-dependant manner [86] [87] [74]. LT sequestration of pRb leads to the transcription of E2F-responsive genes, which in turn lead to the activation of p53 and transcription of p53-responsive genes [88]. Activation of p53 normally leads to the arrest of cell growth and apoptosis. In order to prevent this cascade, LT binds p53, which stops p53 from accessing gene promoter regions and renders it transcriptionally inactive [89] [90]. SV40 LT expression is therefore sufficient to downregulate the expression of p53-responsive genes [91]. In permissive cell lines, this facilitates viral replication, but in non-permissive cell lines, it can lead to cellular transformation.

LT binding to pRb and p53 has been widely studied. However, LT binds to a number of other host cell factors. Table 1.3 lists a selection of other known LT binding partners, their functions, and the effect LT binding achieves.

Polyomavirus LT binding to host cell proteins has the primary purpose of promoting the switch to S-phase and facilitating viral replication. However, in non-permissive cell lines, this can lead to cellular transformation and tumourigenesis. The role of LT in cancer will be discussed in Sections 1.2.6.2 and 1.4.4.1

#### 1.2.5.2 The small T antigen

ST is 17kDa protein comprising 170 amino acids. The amino-terminal portion of ST contains the shared DnaJ domain, while the carboxy-terminal region is unique to ST in most polyomaviruses, although the MPyV MT amino-terminal region shares most of this sequence. This portion of ST contains the protein phosphatase 2A (PP2A) binding domain (CxxP/CxC). PP2A is the major cellular serine/threonine (Ser/Thr) phosphatase [92]. In many polyomaviruses, the interaction between ST and PP2A is considered to be the major function of the viral protein. Figure 1.5 shows the structure of SV40 ST.

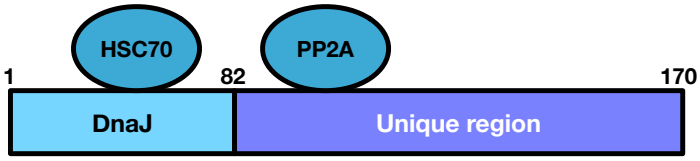


**Figure 1.5: The structure of SV40 ST.** SV40 ST shares the DnaJ domain with SV40 LT, and contains a unique region that binds PP2A. HSC70: heat shock chaperone 70, PP2A: protein phosphatase 2A.

PP2A is a heterotrimeric holoenzyme, made up of subunits A, B, and C. Subunit A is 65 kDa in size and acts as the scaffold. The carboxy-terminus of subunit A binds to subunit C (32 kDa), which functions as a catalytically-active phosphatase [93]. Subunit B binds to subunit A through its amino-terminal region [94], and the variety of these subunits allows for the regulation of substrate specificity [92]. Due to its ability to dephosphorylate a wide range of substrates, PP2A is an important regulator of multiple downstream signalling pathways, involved in apoptosis, cell cycle regulation, and proteolysis [95]. The ability of ST to bind PP2A gives

polyomaviruses access to these signalling pathways, thus subverting them for viral replication. Crystallisation studies of SV40 ST have determined that both the DnaJ and the unique domain are involved in binding with the PP2A A subunit, particularly to the A$\alpha$ isoform [96]. Furthermore, both SV40 and JCPyV ST bind directly to the A subunit and thus come into contact with the C subunit [97] [98]. The SV40 ST PP2A A subunit binding site overlaps with the B subunit binding site [99], indicating that ST competes with B subunits for A subunit binding.

These findings suggest that ST may function as a negative inhibitor or a positive activator of the PP2A holoenzyme, or potentially both, as some evidence suggests. In other words, replacing the B subunit with ST may inhibit dephosphorylation of specific substrates, such as Raf, MEK and ERK in the MAP kinase pathway [100], but it may also redirect PP2A to different cellular targets. For example, SV40 ST increases the dephosphorylation of histone protein H1 by PP2A [101]. In permissive cell lines, the interaction of ST with PP2A likely facilitates viral replication, while in non-permissive cell lines it may contribute to cellular transformation.

While polyomavirus LT is thought to be the main driver of viral replication, an auxiliary role in enhancing the function of LT has also been uncovered for ST. Supporting this, expression of SV40 ST mutants leads to reduced viral replication [102], while expression of ST increases early promoter and LT-mediated late promoter activity [103] [56]. Thus although ST is not essential for polyomavirus replication, it does have a role in increasing replication efficiency.

The interaction of ST with PP2A contributes to viral replication by helping disrupt the cell cycle and drive cells into S-phase [104]. One example of this is MPyV ST, which activates the MAP kinase cascade in a PP2A-dependent manner, resulting in increased binding by transcription factors such as AP-1 to stimulate the transition from $G_1$ to S-phase [100]. In addition, ST can decrease the levels of a cyclin-dependent kinase (CDK) inhibitor, p27/kip1 [105]. p27/kip1 prevents efficient complex formation between CDK4 and pRb, which normally leads to cell cycle arrest [106]. It is possible that ST binding to PP2A reduces the dephosphorylation of cyclin E/cdk2, which regulates p27/kip1, in turn leading to cell cycle progression. Finally, ST expression stimulates other factors involved in cell cycle progression, including cyclin D1, cyclin B, and thymidine kinase [107].

#### 1.2.5.3 The middle T antigen

Alternative splicing of rodent polyomavirus early transcript results in the production of MT, a 55kDa protein. The amino-terminal region of MT is identical to that of ST (apart from the last 4 carboxy-terminal amino acids), sharing the DnaJ and PP2A binding domains. The carboxy-terminal part of MT is unique and contains multiple phosphorylation sites. This part of MT is also hydrophobic, and able to span the lipid bilayer [108]. Figure 1.6 shows the structure of MPyV MT.

MPyV MT can bind the origin of replication and affects the expression of a number of host cell transcription factors, e.g. AP-1 transcrption factors [109], including c-Jun [110], and the Ets protein family of transcription factors such as PEA3 [111]), thus facilitating viral replication. MT is also important in virion assembly, as absence of MT expression leads to inefficient virion assembly due to aberrant phosphorylation of VP1 [112]. Despite this, transcripts of MT have not been identified in human polyomaviruses so far.

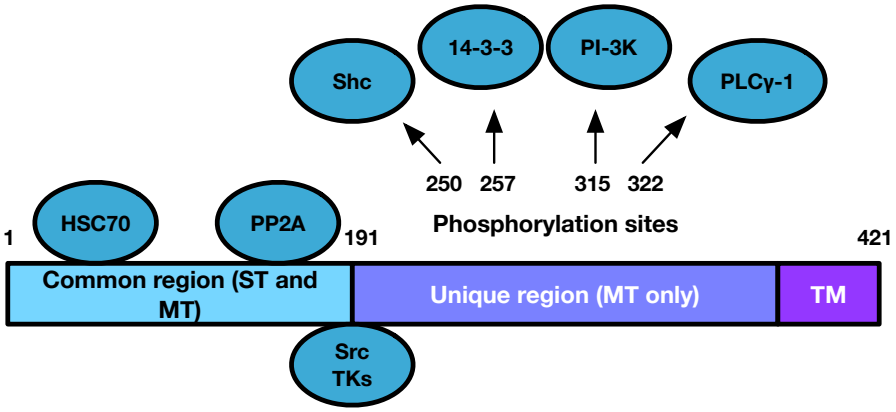


**Figure 1.6: The structure of MPyV MT.** MPyV MT contains an amino-terminal common region with ST that binds Hsc70 and PP2A. The unique region of MPyV MT contains multiple phosphorylation sites that lead to the activation of various cellular factors. A carboxy-terminal transmembrane (TM) domain is also present. HSC70: heat shock chaperone 70, PI-3K: phosphatidylinositol 3-kinase, PLC$\gamma$-1: phospholipase C gamma 1, PP2A: protein phosphatase 2A, Shc: Src, TKs: tyrosine kinases, TM: transmembrane domain

Like ST, MT can bind both isoforms of PP2A (A$\alpha$ and A$\beta$) [113], which activates c-Jun via this interaction [114]. In addition, MT can associate and sequester Src family tyrosine kinases (TKs) in a PP2A-dependent manner [115]. In addition, the

amino-terminal domain of MT is involved in this function [115] [116]. Binding of Src TKs to MT leads to the phosphorylation of MT at residues 250, 257, 315, and 322 [117]. Phosphorylation at any of the specific sites then leads to the activation of a number of important pathway initiators. For instance, phosphorylation of Tyr 315 leads to the activation of phosphatidylinositol 3'-Kinase (PI-3K), and is associated with MT-facilitated tumourigenesis [118].

#### 1.2.5.4 Other T antigen locus transcripts

LT, ST, and MT are the three most widely investigated of T antigen transcripts. In addition to these, many polyomaviruses encode other proteins in the early gene locus. For example, SV40 produces 17kT via alternative splicing from the amino-terminus of LT [119]. The functions of 17kT are not clear, although there is some evidence that it may contribute to promoting cell proliferation [120]. In addition, 17kT can rescue LT activity and immortalise human fibroblasts [121].

Another polyomavirus that encodes additional early proteins is JCPyV: T135, T136 and T165. T135 and T136 are composed of the amino-terminus of LT, while T165 comprises the amino-terminal LT region and the last 32 amino acids of LT carboxy-terminus [122]. These proteins are expressed during JCPyV lytic infection, and play an important role in viral replication [123]. In addition, there is evidence to suggest that these alternative T proteins may contribute to cellular transformation [124].

MCPyV also encodes additional early proteins which will be discussed in Sections 1.4.2.2.3 and 1.4.2.2.4.

### 1.2.6 Polyomaviruses and cancer

A number of polyomaviruses have been shown to be directly oncogenic, including the model viruses SV40 and MPyV. Both of these classic polyomaviruses can transform rodent cells and have been demonstrated to cause tumours in mice [125], [126]. Polyomaviruses tend to have a narrow host and cell specificity. Therefore only one or a few cell types will permit productive replication of a specific polyomavirus, and may contribute to the ability of several different polyomaviruses to transform non-permissive cells.

#### 1.2.6.1 Polyomavirus oncogenicity

Polyomaviruses have been observed integrated into host cell chromosomal DNA. This occurs when the viruses infect non-permissive cell lines, and has previously been demonstrated for SV40 [127], MPyV [128], JCPyV [129] and BKPyV [130], alongside MCPyV, whose integration is discussed in detail in Section 1.4.4. However, the role of most human polyomaviruses in cancer remains controversial.

JCPyV and BKPyV were proposed to have oncogenic properties soon after their initial isolation [131] [132]. However, their role in cancer remains controversial due to high seroprevalence in healthy individuals. There have been single case reports of BKPyV oncogenicity in urothelial and renal tubular malignancies [133] [134] in kidney transplant patients. Conversely, in other reports, BKPyV is not found convincingly in such tumors [135] [136]. However, there are also reports on the detection of BKPyV DNA in colorectal, pancreatic, brain, prostate, and a range of sarcoma tumours [137]. All in all, no causative link has been established. At the moment, WHO classifies BKPyV and JCPyV as "possibly carcinogenic to humans" (Group 2B) [138].

Currently there is no evidence to suggest that KIPyV and WUPyV are oncogenic, although KIPyV VP1 DNA was found in 9/20 lung cancer cases of unknown origin [139]. HPyV6, HPyV7, TSPyV, HPyV9, and HPyV10 have not been conclusively linked to any malignancies. In fact, the only human polyomavirus currently known to cause cancer is MCPyV.

A striking example of an oncogenic polyomavirus in a non-human mammalian species is the racoon polyomavirus (RacPyV). It has been associated with 100% of neuroglial tumours in wild-ranging racoons. Interestingly, it does not appear to integrate into the host genome and persists in tumours in an episomal form [140].

#### 1.2.6.2 The large T antigen in transformation

In oncogenic polyomaviruses, the T antigen transcripts play the major role in cellular transformation. It appears that the DnaJ domain is of vital importance for transformation as well as for viral replication, as SV40 LT and ST DnaJ deletions inhibit transformation [141]. The DnaJ domain, through its functions in promoting S-phase entry, likely promotes replication in permissive cells and transforma-

tion in non-permissive cells. In addition, the DnaJ domain contains the conserved Cr1 domain, which functions analogously to the adenovirus E1A protein. Both LT and E1A bind p300, the cellular transcriptional co-factor, facilitating cellular transformation [142].

SV40 LT alone can transform rat fibroblast cells [143], due to LT binding to the tumour suppressor proteins, p53 and pRb [62]. The cell cycle checkpoint protein p53 is activated by cell stress and blocks DNA replication under non-permissive conditions. p53 promotes the expression of genes that induce DNA repair, cell cycle arrest, and apoptosis [144]. Binding of SV40 LT to p53 inhibits its activity and induces inappropriate cell proliferation [10]. pRb controls entry into S-phase, and is bound to E2F outside of this part of the cell cycle. pRb phosphorylation disrupts this complex and permits E2F to activate the transcription of genes needed for cell cycle progression. LT binding to pRb inhibits its interaction with E2F and, again, induces cell proliferation [72]. Figure 1.7 illustrates the effect of LT on cell proliferation. However, mutations within LT that do not abrogate its ability to bind either pRb or p53 can inhibit transformation, thus other LT functions must contribute to tumourigenesis [145]. For example, BKPyV and SV40 LT have the ability to induce mutagenic effects in the host DNA by more than 100-fold, through LT binding to Mre11, a double-stranded break response component [62] [60].

As referred to in Table 1.3, LT can bind to a whole host of different cellular factors, and these interactions can also play a role in transformation. For example, the interaction of SV40 LT with cullin7 is important in tumourigenesis, as LT mutants that are defective in cullin7 binding are unable to transform primary mouse embryo fibroblasts [146]. IRS1 is another important binding partner, and dominant negative IRS1 expression inhibits anchorage-independent growth of JCPyV LT-transformed cells [78]. This suggests the possibility that LT utilises more than one mechanism for inducing anchorage-independent growth. Another contributing mechanism of LT-induced tumourigenesis is via the Wnt pathway, which has been associated with tumour formation and progression [147]. JCPyV LT can directly bind β-catenin, a component of this pathway, and this interaction is thought to enhance the stability of β-catenin and enhancing activation of target genes, such as c-myc [79]. Furthermore, thyroid embryonic factor-1 (TEF-1), a transcription factor, has been identified as a binding partner of SV40 LT. This interaction allows LT to inhibit TEF-1-mediated repression of the late viral pro-

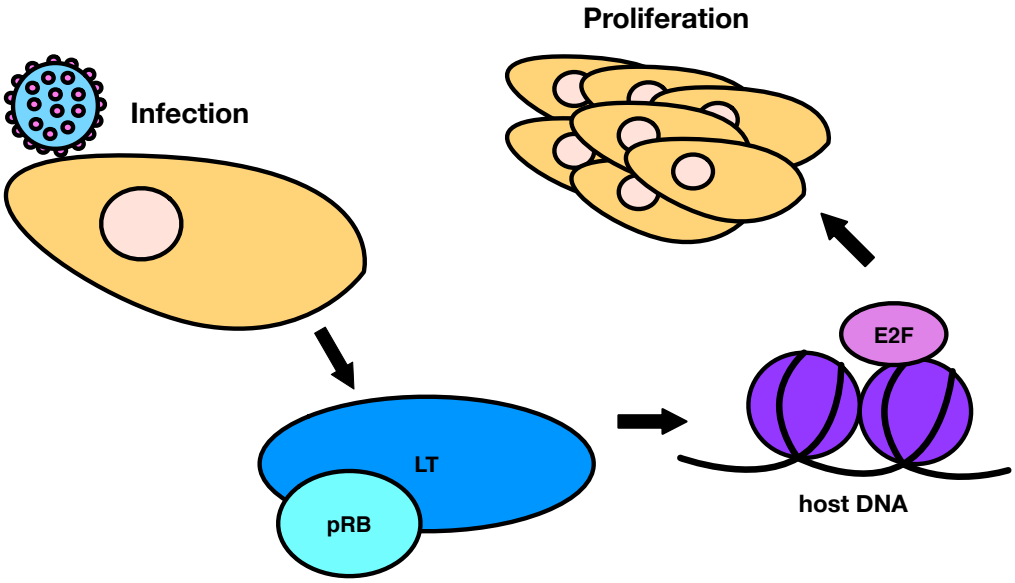


**Figure 1.7: Effect of LT on cell proliferation.** Upon MCPyV infection and T antigen expression, LT binds the regulatory protein pRb, thus inactivating it. This allows E2F to activate the transcription of cell cycle progression-associated genes, which switches the cell into S-phase and leads to cell proliferation. E2F: transcription factor E2F, LT: large T antigen, pRB: retinoblastoma protein.

moter, thereby stimulating DNA replication [81]. It may also play a role in transformation, as LT mutants unable to bind TEF-1 showed reduced numbers of foci in transformation assays [148].

#### 1.2.6.3 The small T antigen in transformation

In SV40 and other oncogenic polyomaviruses, ST plays an accessory role in transformation. The interaction of ST with PP2A stimulates cell entry into S-phase, which in non-permissive cells can contribute to cellular transformation. When LT expression is low, ST is required in SV40-driven transformation of rodent cells [149]. Interestingly, for SV40 to fully transform human cells, both LT and ST expression is required, in combination with oncogenic H-ras and hTERT [150]. In this setting, ST is essential for cell cycle progression, anchorage independent growth, and transformation [150].

The ST-PP2A interaction (Figure 1.8) inhibits the dephosphorylation, promoting stabilisation of c-myc [151], an important transcription factor [152]. This effect

alters cell proliferation, cell growth, and apoptosis signalling, all of which can contribute to transformation [153]. In addition, ST activates a number of other transcription factors, e.g. AP-1, CREB, and NF-κB, all of which have been implicated in tumourigenesis [154] [155] [156]. ST can also induce the PI-3K pathway activation, which has been implicated in tumourigenesis [157]. The result is the phosphorylation of targets like Akt, a Ser/Thr kinase important in cell persistence, metabolism, and angiogenesis [100].

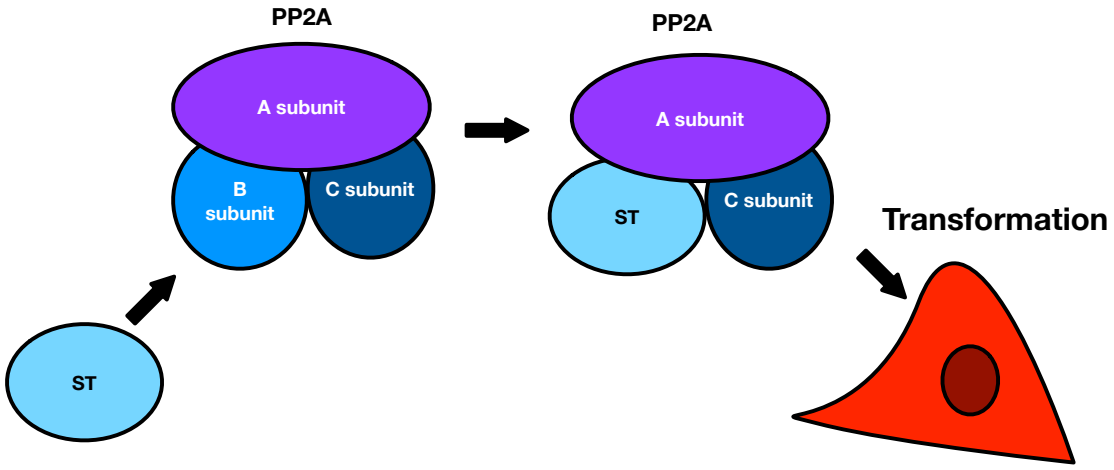


**Figure 1.8: Interaction of ST with PP2A.** Polyomavirus ST competes with the B subunit of PP2A for binding to the structural A subunit and the catalytic C subunit. In SV40, this interaction between ST and PP2A Aα leads to cell transformation. Although the interaction of MCPyV ST with PP2A Aα may not be necessary for transformation, interaction with PP2A Aβ or the related PP4C may play a role. A subunit: scaffold, B subunit: regulatory, C subunit: catalytic, PP2A: protein phosphatase 2A, ST: small T antigen.

Another fascinating aspect of the role ST plays in transformation is the upregulation of telomerase upon SV40 ST expression, which together with the ST-induced inhibition of Akt dephosphorylation [158] promotes an increase in telomerase phosphorylation and activity, leading to cell immortalisation. In addition, the ST-PP2A interaction may have an effect in the hyperphosphorylation of Bub1, a mitotic spindle checkpoint protein [159], which can induce tumourigenesis and aneuploidy [160].

#### 1.2.6.4 The middle T antigen in transformation

Unlike SV40 and many other polyomaviruses, MT is thought to be the major transforming factor in rodent polyomaviruses. MPyV MT expression alone has been shown to induce transformation in rat cells [161]. Structurally, the carboxy-terminal hydrophobic region is required for transformation, as deletion of the last six amino acids of this region fully ablates the ability of MT to induce transformation [162]. Furthermore, both the amino-terminal and carboxy-terminal regions are required for MT binding to various cellular protein kinases [116] [162], and through these interactions, as well as with PP2A, MT-induced transformation is enhanced.

## 1.3 Merkel cell carcinoma

Merkel cell carcinoma (MCC) was first described in 1972 by Cyril Toker [163], as a flesh-coloured or bluish-red glassy painless nodule with solid trabeculae in five different areas (forearm, lip, face, leg and buttock) of two older men and three older women. Toker named the cancer trabecular carcinoma of the skin to describe these tumours, due to the assumption that they represented an endocrine, sweat gland-derived carcinoma.

MCC is now described as a rare and highly malignant primary neuroendocrine carcinoma of the skin. Over 90% of cases arise in sun-exposed areas of the body, particularly around the head and neck. This suggests that sunlight, primarily as ultraviolet radiation, plays a role in the development of MCC. MCC can also develop on the trunk and genitals but at a frequency of under 10% [164]. MCC metastasises to other parts of the body by transiting through the lymphatic drainage [165], and metastases have been reported at distant sites including the pancreas and breast [166], the heart [167], and the palatine tonsil [168].

### 1.3.1 Merkel cells

Merkel cells are mechanoreceptors, first described by the German histopathologist Friedrich Sigmund Merkel at the end of the $19^{th}$ century [169]. The Merkel

cell-neurite complex is one of the four main classes of mammalian sensory receptors, for sensing light touch, shape, texture, and curvature [170]. Figure 1.9 shows that this receptor complex is made up of Merkel cells situated at the epidermal/dermal border and the afferent somatosensory fibres that stimulate them [169]. These complexes are located in touch sensitive regions of the skin, e.g. surfaces of the hands and feet, whisker follicles, and touch domes, i.e. specialised epithelial structures in hairy skin [171].

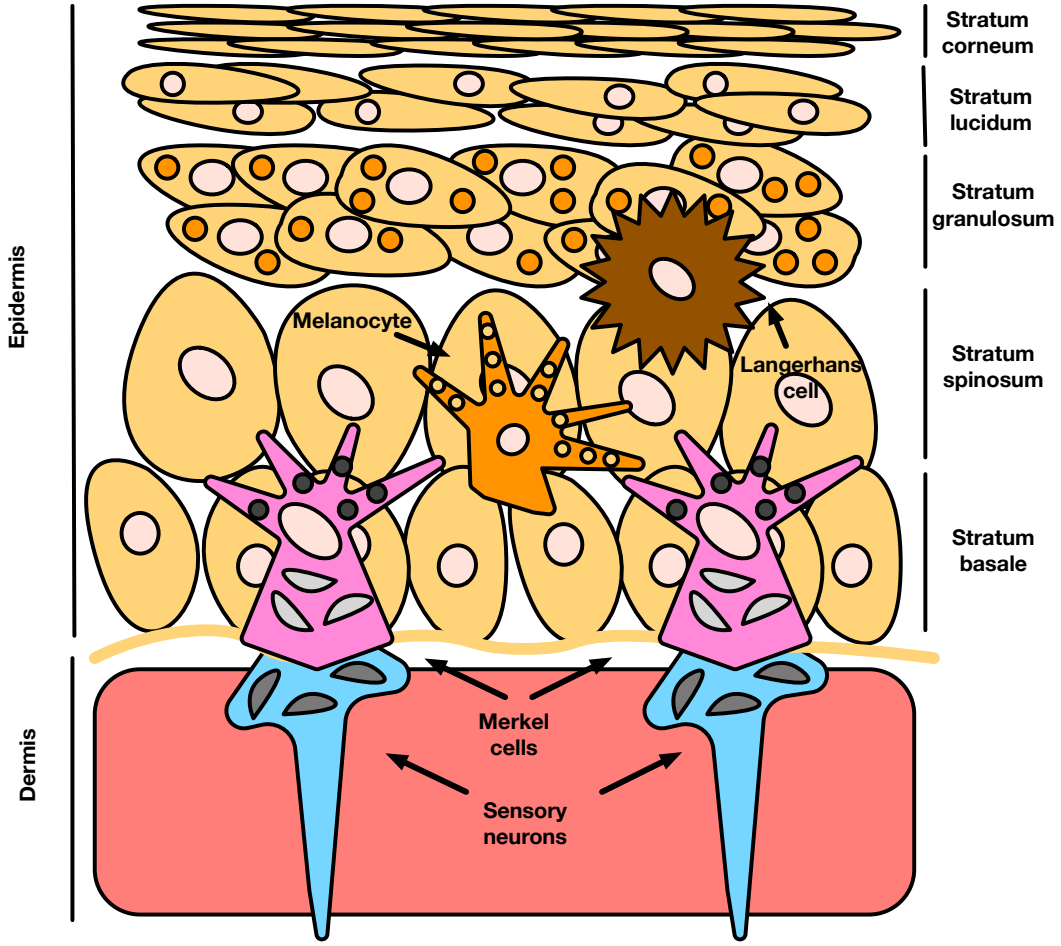


**Figure 1.9: Skin layers in the context of Merkel cells.** All skin layers are shown, as well as the Merkel cell-neurite complex at the epidermal/dermal border.

Merkel cells are oval and approximately 10–15 µm in diameter with spinous projections on the surface [171]. The exact mechanism of action of Merkel cells is as yet unclear, although there is evidence that neuropeptides accumulate near the

nerve fibre junctions and are required for synaptic transmission via voltage gated ion channels [172]. In addition, histochemical markers indicate that Merkel cells may also act in a paracrine manner [172].

The origin of Merkel cells was disputed for a long time. Conflicted evidence suggested descent from skin or from the neural crest. *Atoh1* is a transcription factor expressed by and necessary for the production of Merkel cells [173] [174]. Selective deletion of *Atoh1* from the neural crest in mice had no effect on the Merkel cell population, while deleting the gene from the skin lineage resulted in the loss of Merkel cells in all areas of the skin. This study provided conclusive evidence that mammalian Merkel cells are of epidermal origin [170].

### 1.3.2 Merkel cell carcinoma presentation

MCC primary tumours present as pink or purple nodules, less than 2mm in diameter, or as a mass more than 2mm in diameter (Figure 1.10A) [175]. These tumours are visibly similar to small-cell lung carcinoma and Ewings sarcoma tumours [176], and have historically been difficult to identify.

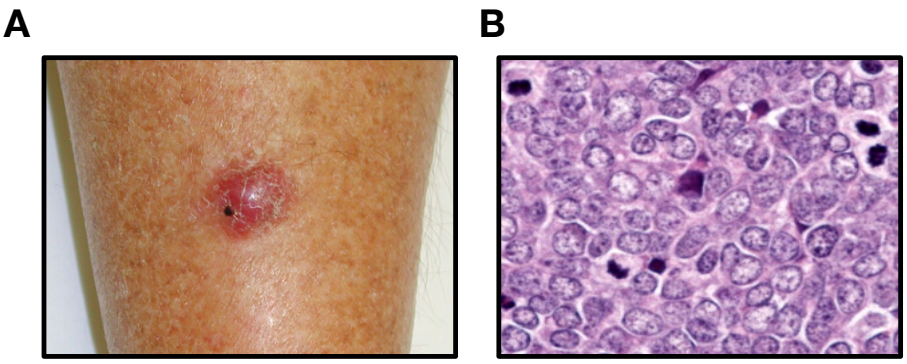


**Figure 1.10: Merkel cell carcinoma presentation.** (A) A primary MCC tumour nodule present on the leg of a patient (provided by Howard Peach, Leeds Teaching Hospital NHS Trust, UK). (B) MCC tumour cells characterised by dispersed granular chromatin, scanty cytoplasm and large nuclei [177].

Under the microscope, an MCC tumour appears as a lesion of nested or stranded small round cells, with an oval or round nucleus, dispersed granular chromatin and scanty cytoplasm, in a bed of vascular and infiltrating cells (Figure 1.10B) [178]. Recently, an effective detection system has been established, based on the

findings that MCC cells display a specific arrangement of cytokeratin 20 (CK20) filaments [179]. CK20 is now used as a specific and highly sensitive MCC biomarker which can clearly distinguish MCC from other tumours.

On the other hand, while most MCC tumours are CK20-positive and CK7-negative, a few CK20-negative and CK7-positive tumours have been characterised [180]. Therefore, several other biomarkers are used, such as chromatogranin, somatostatin, and neuron-specific enolase [179] [181]. Overall, clinical MCC diagnosis normally includes reactivity to CK20, a thyroid transcription factor, leukocyte common antigen, and one of the above neuro-endocrine markers [176].

### 1.3.3 Merkel cell carcinoma epidemiology

MCC is considered to be a rare cancer. The annual incidence of MCC is 0.6 per 100,000, but is increasing, with around 1,600 new cases per year in the US [182]. Overall, there has been a tripling of cases in the last 20 years [183], and this rise in MCC is a worldwide trend. In Australia, between 1986–2001, the age-adjusted incidence rose at an annual increase of 8% [184]. In the Netherlands, the incidence increased from 0.17 per 100,000 in 1993–1997 to 0.35 per 100,000 in 2003–2007 [185]. The median age at diagnosis is 76.2 years for women and 73.6 years for men. Only 4% of patients are diagnosed at 49 years or younger, and it is extremely rare in children [186]. MCC cases are 11-fold to 13-fold greater in patients with AIDS and 5-fold to 10-fold greater for people with a solid organ transplant [187]. 66% of MCCs present with local disease, 27% with nodal disease and 7% metastatic disease. Patients with local disease had a 64% relative survival at five years, as compared to 39% in regional nodal disease and 18% in metastatic disease [188]. The increase in MCC incidence is partially due to recent advances in diagnostic techniques, especially CK20 staining.

UV light appears to be an important factor in MCC. For example, there is a positive correlation between geographic UVB radiation indices and age-adjusted MCC incidence among Caucasians [184]. In general, pale skin is a risk factor for MCC, with 94.9% of patients being of European origin with tumours in the head and neck region, and patients of African origin making up only 1% of MCC cases [186]. Immunosuppression is another known risk factor for the development of MCC, specifically in immunosuppressed patients with T-cell dysfunc-

tion, i.e., solid organ transplant recipients, AIDS patients and chronic lymphocytic leukemia patients. Interestingly, there have been cases of MCC regressing following improvement in immune [189] function and sudden clearance of MCC after recognition by the immune system [190].

### 1.3.4 Merkel cell carcinoma prognosis and treatment

The clinical staging system for MCC is a four-tier arrangement. Stage I disease is classified as a localised tumour with a nodule of less than 2 mm, stage II disease as a localised tumour with a mass of more than 2 mm, stage III disease as a regional metastasis, and Stage IV disease as a distant metastasis [191]. This is the general system, and it can be modified to reflect individual differences in regional metastases and other factors [192].

MCC is highly aggressive, with 28% of patients dying within the first 2 years of diagnosis and over 55% of patients dying within 5 years due to the high rate of metastasis [193]. 45% of MCCs recur locally, 70% present with early involvement of local lymph nodes, and half of MCCs result in distant metastases. The mortality rate for patients with distant metastases is 80% [194]. This high mortality rate of MCC is due to the metastatic nature of the tumour [182]. Despite this, there are currently no specific therapeutic treatments available for MCC.

Currently MCC is treated with a wide surgical excision of the primary tumour, including a pathological verification of complete tumour removal, followed by ionising radiation therapy to decrease the incidence of local recurrence [195] [176]. If the tumour has metastasised to local lymph nodes, the treatment involves surgical removal of tumours, lymphadenectomy, and radiation therapy at the excision sites and lymph nodes [191]. Distant metastasis is treated with broad-spectrum chemotherapy, including cyclophosphamide, anthracyclines, and etoposide. The prognosis upon diagnosis of distant metastases has a median survival of 21.5 months [196].

## 1.4 Merkel cell polyomavirus

MCPyV is a double-stranded DNA virus of the *Polyomaviridae* family. It was discovered in 2008 by Patrick S. Moore and Yuan Chang at the University of Pennsylvania, who utilised digital transcriptome subtraction (DTS), a novel method of detecting viruses in cancerous tissue. DTS involves extracting mRNA from tumour cells, converting it to cDNA to prepare a library, and then pyrosequencing. The cDNA obtained is then compared to known human sequences, and matching stretches of DNA are subtracted, leaving the remainder as likely non-human. The remaining sequences are then compared against the pathogen sequence database. The analysis highlighted a sequence related to polyomaviruses, but distinct enough to be considered a novel virus [20].

3' rapid amplification of cDNA ends (3'-RACE) followed by viral genome walking were used to generate a complete circularised MCPyV genome. Generation of identical RACE products from both primary and metastatic tumours found in lymph nodes indicated clonal viral integration prior to tumour formation and metastasis [20]. This suggests that MCPyV is not a passenger virus, but a contributing factor to MCC development and progression.

Overall, MCPyV is thought to be clonally integrated into and thus to be the causative agent of MCC in 80–97% of cases, depending on the technique utilised [20] [197].

Although MCC is a rare disease, MCPyV is prevalent in the general population. Enzyme-linked immunosorbent assays (ELISA) that detect MCPyV structural proteins VP1 and VP2 highlight the fact that 50% of children under 15 and 80% of healthy adults are infected with MCPyV. Therefore, it is now thought that MCPyV is a common skin commensal [198].

### 1.4.1 Merkel cell polyomavirus phylogeny

A number of phylogenetic studies of human polyomaviruses have been conducted, using VP1, VP2 and LT sequences (Figure 1.11) [36]. Initially, it was thought that MCPyV is most closely related to the African Green Monkey Lymphotrophic polyomavirus [199], but more recent analysis suggest that it is more closely related to MPyV and Chimpanzee polyomavirus (ChPyV), as these viruses

share high sequence homology of their VP2 and LT genes [36]. In addition, the MCPyV VP1 gene is closely related to that of ChPyV and HPyV9 [36].

MCPyV is currently classified as belonging to the Orthopolyomavirus genus of the *Polyomaviridae* family [200]. Interestingly, MCPyV LT, VP1, and VP2 all share a high degree of sequence homology with TSPyV [36]. This may be reflected in the fact that both MCPyV and TSPyV are common skin commensals.

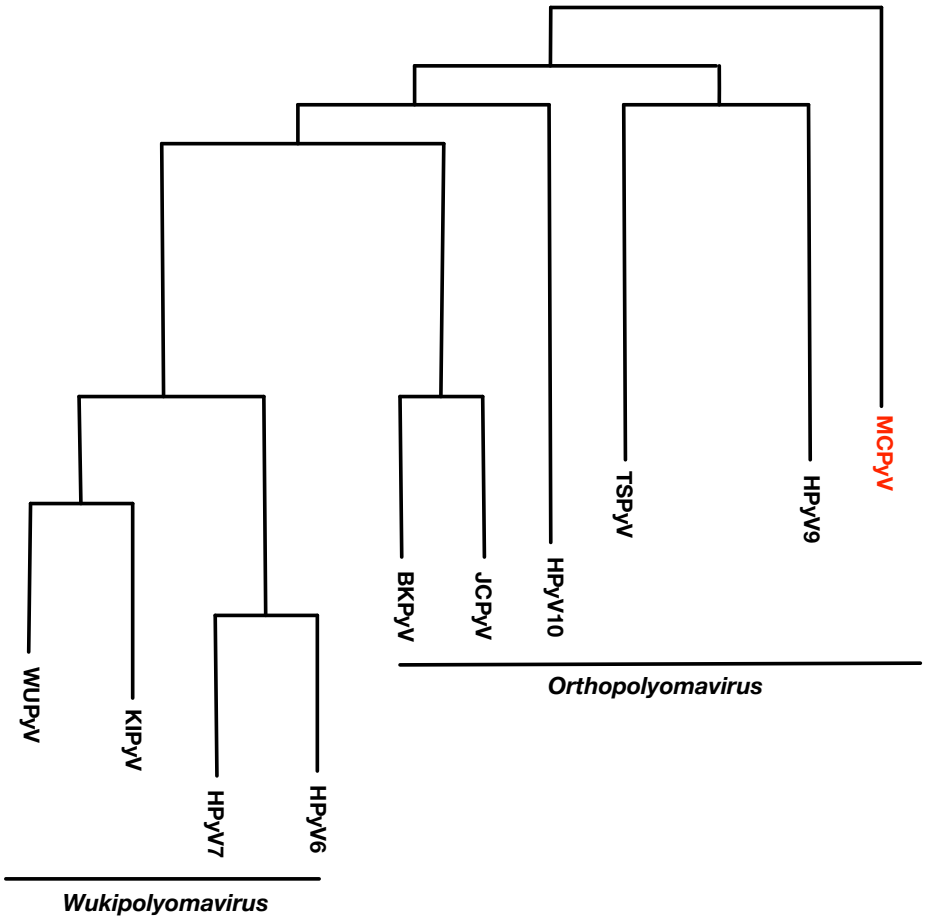


**Figure 1.11: Merkel cell polyomavirus phylogeny.** Whole genome nucleotide sequence analysis was performed using a maximum likelihood phylogenetic analysis. Phylogenetic analysis suggests that among human polyomaviruses MCPyV is most closely related to TSPyV, HPyV9, HPyV10 [201].

There also seems to be variability within the MCPyV genome. For example, Japanese and Asian strains of the virus form a distinct dominant clade, as do Caucasian strains [202]. It is yet unclear whether differences between clades affect MCPyV pathogenesis, but this is a novel and important field of research.

### 1.4.2 Merkel cell polyomavirus genome organisation

The MCPyV genome structure is closely related to that of other polyomaviruses. It comprises 5387 base pairs, with a non-coding control region (NCCR), that contains the bipartite origin of replication separating the early and late gene coding regions. This separation allows for temporal control of viral gene expression [20]. Figure 1.12 illustrates the MCPyV genome.

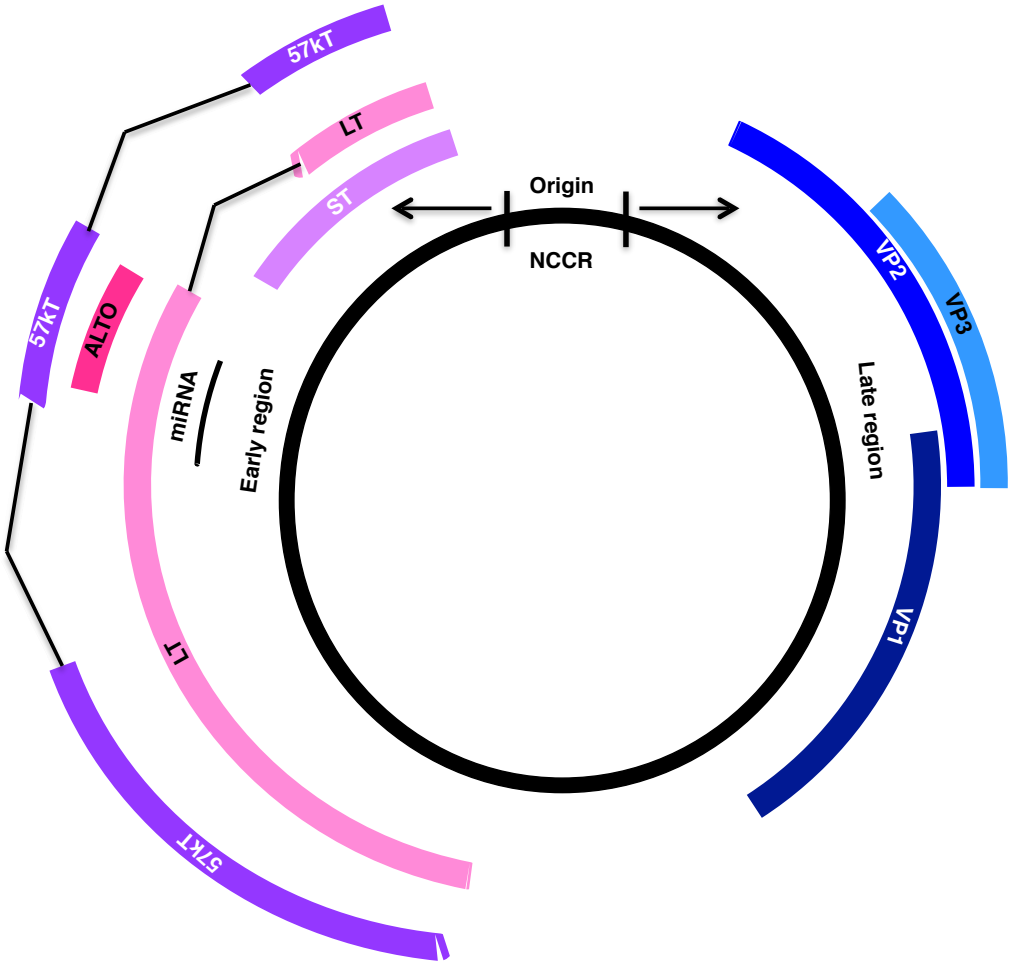


**Figure 1.12: The Merkel cell polyomavirus genome.** NCCR contains the bipartite origin of replication. The early gene region encodes LT, ST, 57kT, ALTO, and the miRNA. The late gene region encodes the capsid proteins (VP1-3). 57kT: 57 kiloDalton T antigen, ALTO: alternative large T open reading frame, LT: large T antigen, miRNA: microRNA, NCCR: non-coding control region, ST: small T antigen, VP: viral protein.

#### 1.4.2.1 Merkel cell polyomavirus NCCR

The MCPyV NCCR contains a 71 base pair long origin of replication (*ori*). Similar to other polyomaviruses, *ori* has an AT-rich region, an early enhancer domain and a binding site for LT to initiate viral replication. The LT binding site is made up of ten guanine-rich pentanucleotide sequences: eight corresponding to the general polyomavirus consensus of 5'-GAGGG-3', one with a 5'-GGGGC-3' sequence and one with a 5'-GAGCC-3' sequence. The proximity and number of sequences are distinct from other polyomaviruses [203].

#### 1.4.2.2 Merkel cell polyomavirus T antigen locus

The MCPyV T antigen locus comprises approximately 3,000 base pairs in length, and is transcribed as a single transcript. Post-transcriptional splicing produces LT, ST, and the 57 kiloDalton (57kT) T antigens [20]. MCPyV LT, ST and 57kT all share the same amino-terminal region including the DnaJ domain. However, alternative splicing produces a distinct carboxy-terminus, which determines the variability in the functions of the spliced products. Figure 1.13 illustrates the different T antigen locus-encoded proteins.

##### 1.4.2.2.1 Merkel cell polyomavirus LT

MCPyV LT consists of 816 amino acids and is spliced together from two exons. It has numerous functions in MCPyV infection, including the initiation of viral replication and manipulation of the host cell cycle, which will be discussed in more depth below. MCPyV LT contains several conserved domains found across polyomaviruses: the pRb binding domain, a NLS, and the OBD region. The carboxy-terminal half of LT has viral DNA binding and helicase features [204]. The presence of a NLS allows MCPyV LT to localise to the nucleus when expressed in mammalian cells [205]. In general, MCPyV LT binds to similar cellular factors elaborated on in Section 1.2.5.1 and Table 1.3. It has equivalent DNA-binding and helicase functionality as SV40 LT [206]. However, despite the similarities in binding partners, MCPyV LT shares only 34% sequence identity with SV40 LT [204]. It also contains the MCPyV unique region (MUR), a 200 amino acid sequence found between the first exon and the OBD [207]. This unique region binds the host factor Vam6p and causes it to relocalise to the nucleus [207].

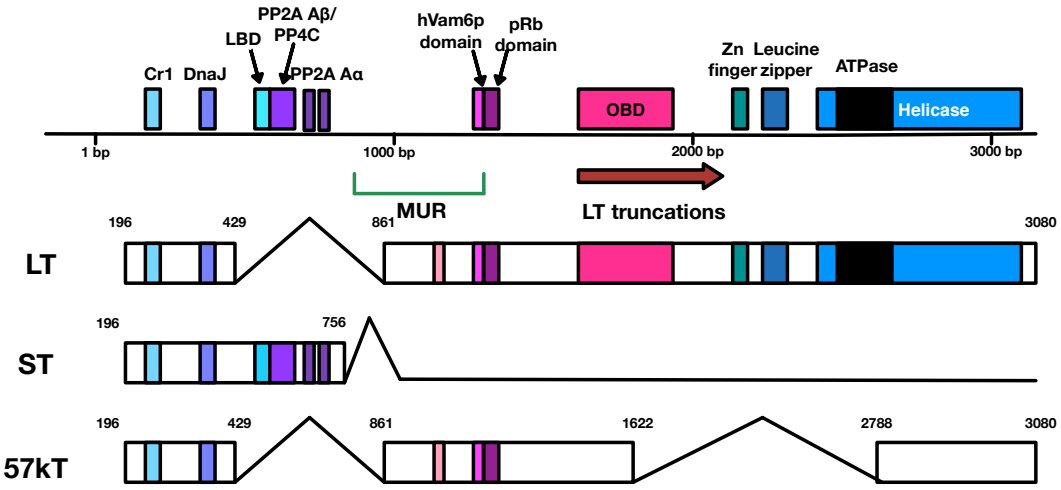


**Figure 1.13: The Merkel cell polyomavirus T antigen locus and its gene products.** The schematic shows the relative locations of each gene that encode specific protein binding domains and splicing patterns associated with differential splicing of the primary early transcript. The three T antigens are LT, ST and 57kT. All three encode CR1 (LXXLL) and DnaJ (HPDKGG) domains. ST also contains two PP2A A$\alpha$ binding sites (R7 and L142), a PP2A A$\beta$/PP4C binding site (amino acids 97–111) and an large T antigen-stabilisation domain (LSD, amino acids 91–95). LT shares the pRb binding domain with 57kT and has unique origin binding (OBD), zinc finger, leucine zipper, ATPase and helicase domains. The MCPyV-unique region (MUR) of LT contains the hVam6p binding site.

In addition, the MUR encodes a miRNA [208].

#### 1.4.2.2.2 Merkel cell polyomavirus ST

MCPyV ST consists of 186 amino acids, with a unique carboxy-terminal region produced by transcriptional read-through of the exon splice site used by LT and 57kT. ST localises to the nucleus and the cytoplasm [60]. It contains the common polyomavirus PP2A binding site [20]. However, recently, an alternative PP2A and/or protein phosphatase 4C (PP4C) binding site near the carboxy-terminus has also been discovered, which may have a role in protecting MCPyV from the cellular immune response [209] and in cell motility [210]. MCPyV ST also contains a LT-binding domain (LBD), which stabilises LT and aids in the replication of the MCPyV genome [211]. In addition, recent evidence suggests that MCPyV ST may also be an iron-sulphur cluster protein, which may also enhance LT-mediated viral replication [212].

#### 1.4.2.2.3 Merkel cell polyomavirus 57kT

MCPyV 57kT is 432 amino acids in length. It is the product of alternative splicing linking three exons, and shares the DnaJ domain and CR1 epitope with LT and ST, as well as the MUR region and the pRb-binding domain. 57kT is homologous with SV40 17kT [44], which is known to promote cell proliferation [120].

#### 1.4.2.2.4 Merkel cell polyomavirus ALTO

As well as the three T antigen products, the MCPyV early gene locus also encodes a fourth protein, the alternative T antigen open reading frame (ALTO). ALTO is encoded by overprinting within the T antigen locus, and is transcribed from the MUR region of LT. Phylogenetic analysis shows that ALTO may be evolutionarily related to MPyV MT. It has a hydrophobic carboxy-terminus, analogous to MT, and this region is required for its subcellular localisation [43]. No known function of ALTO has been described to date.

### 1.4.2.3 Merkel cell polyomavirus late proteins

The MCPyV late gene region contains three open reading frames which encode the capsid/structural proteins, VP1, VP2, and VP3. Three structural proteins are typical for all polyomaviruses. VP1 is the major capsid protein, VP2 is the minor capsid protein, and they have been shown to self-assemble into virus like particles (VLPs) *in vitro* [213] [214]. It is unclear whether VP3 is expressed at all, as its sequence is not conserved and it does not form part of the capsid [215].

The MCPyV capsid is non-enveloped and icosahedral, made up of 72 pentamers of VP1. The overall capsid size is around 40–55 nm, similar to other polyomaviruses, with a VP1 to VP2 ratio of 5:2 [215]. The structure of VP1 monomers has been crystallographically shown to be two antiparallel β sheets that form a β-sandwich structure with a jelly-roll topology. The overall shape of VP1 is a symmetrical, ring-shaped homopentamer arranged around a central axis with variable loops that create unique interaction surfaces on the outside of the pentamer. It also has a NLS at its amino-terminus, showing a diffuse nuclear staining pattern [216].

MCPyV VP2 appears to be superfluous to entry in most cell lines studied, and it does not affect viral DNA packaging, viral protein trafficking, or cell receptor

binding. It is possible that myristoylation of VP2 may help disrupt cellular membranes [216]. VP2 lacks a NLS, but co-expression with VP1 redistributes VP2 into the nucleus [215].

#### 1.4.2.4 Merkel cell polyomavirus miRNA

SV40, BKPyV and JCPyV all encode microRNAs (miRNAs) which regulate early gene transcription [217] [218]. In SV40, these miRNAs are complementary to and target early gene transcripts for degradation at late stages of infection [217]. MCPyV encodes a 22-nucleotide-long miRNA, MCPyV-miR-M1-5p, antisense to the LT gene sequence [208]. It regulates the expression of the early genes and reduces levels of early gene transcripts in a negative feedback loop to facilitate the switch from early to late gene expression [208]. It may also have a role in transformation, as its expression is preserved in at least half of MCPyV-positive MCC tumours [219].

### 1.4.3 Merkel cell polyomavirus life cycle

The cellular tropism for MCPyV infection has not yet been firmly established, as MCPyV was discovered within a tumour rather than within the milieu of its natural host. The origin of MCC as well as the fact that MCPyV virions are shed from the skin of healthy adults indicate an epidermal source of host cells [34]. However, recent data suggests human dermal fibroblasts as natural host cells for MCPyV, which can also support productive MCPyV infection [220]. In addition, MCPyV pseudovirions can infect human skin-derived primary keratinocytes (HEKa) and transformed melanocytes, but not primary transformed keratinocytes (HeCat) or primary melanocytes, or, indeed, sixty human tumour cell lines investigated [221]. Regardless, a MCPyV genome capable of productive viral infection has been established [215] [222]. In one instance, a full-length wild-type MCPyV genome was isolated from surface skin swabs of healthy adult volunteers, and the DNA was amplified using random hexamer-primed rolling circle amplification (RCA) [215]. In the other case, a synthetic MCPyV genomic clone was generated from sequence data of MCPyV genomes [222]. Both of these approaches have produced plasmids, such as pR17b, containing the full recircularised MCPyV genome.

Currently, efficient replication of the MCPyV viral genome, both early and late gene expression and viral particle formation, can be achieved by transfection of the pR17b plasmid in HEK-293 cells that overexpress the MCPyV LT and ST *in trans*, known as HEK-293-4T cells [223]. This viral replication system is key to understanding the MCPyV life cycle and viral-host interactions that contribute to MCC pathology. As mentioned above, human dermal fibroblasts have been suggested as the natural host for MCPyV, allowing a new cell culture model to be developed. MCPyV infection of dermal fibroblasts is facilitated by epithelial and fibroblast growth factors as well as the β-catenin signalling pathway [220]. This cell culture model will most likely be invaluable in future studies of the viral life cycle and MCC tumourigenesis.

#### 1.4.3.1 Merkel cell polyomavirus attachment and entry

Most polyomaviruses, such as MPyV, SV40, and BKPyV use sialic acid-containing glycolipids, or gangliosides, for initial attachment to host cells [224] [225]. However, MCPyV appears to involve glycosaminoglycans, in particular heparan sulphate and chondroitin sulphate, for initial attachment [223]. In addition to this initial binding, binding to gangliosides, specifically Gt1b, which carries three different sialic acids, is required for post-attachment entry [223]. MCPyV can still attach to cells deficient in gangliosides, although this leads to impaired MCPyV gene transduction [223]. X-ray crystallography has determined that the MCPyV VP1 has a shallow binding site for cellular glycans containing sialic acid with a Neu5Ac moiety, specifically a linear Neu5Ac-α2,3-Gal motif. Interestingly, mutating these binding sites has no effect on initial virus attachment [216]. The current MCPyV entry model is a two-step attachment-and-entry process involving two separate types of host cell plasma membrane molecules, as shown in Figure 1.14.

The fact that MCPyV uses glycosaminoglycans for cellular attachment is similar to papillomavirus entry [226]. Papillomaviruses are exclusively tropic for keratinocytes, a type of epithelial cell. This similarity may be a possible example of convergent evolution, and further suggests the skin as host to MCPyV.

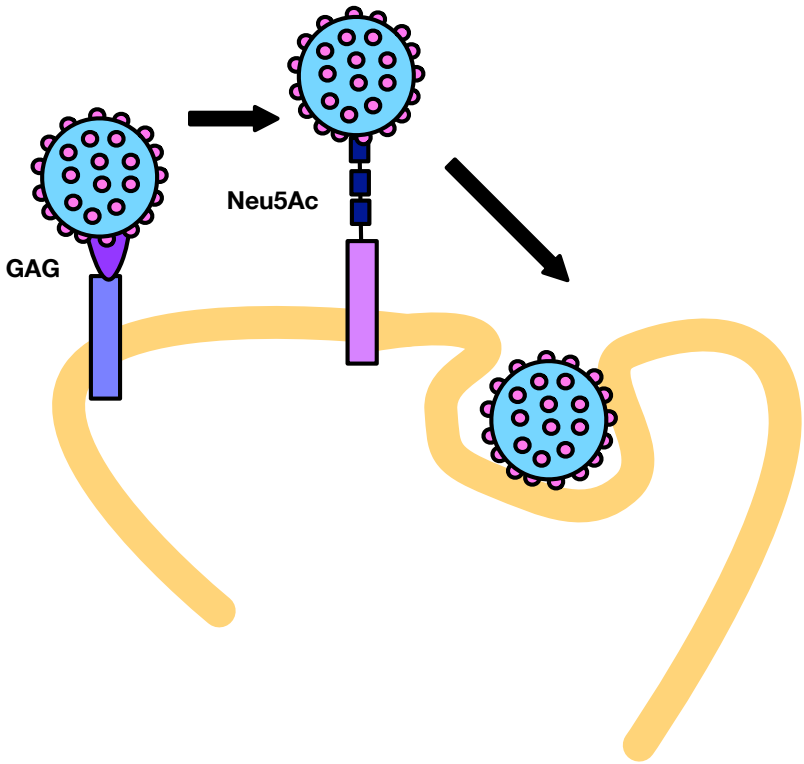


**Figure 1.14: MCPyV attachment and entry.** MCPyV entry is a two-step attachment-and-entry process. MCPyV binds GAG, specifically heparan sulphate as the initial mode of attachment. MCPyV then binds a ganglioside with a Neu5Ac motif to facilitate viral entry. GAG: glycosaminoglycan, Neu5Ac: N-acetylneuraminic acid-α2,3-galactose.

#### 1.4.3.2 Merkel cell polyomavirus replication

MCPyV is able to complete its replication cycle and form virions without inducing tumourigenesis in permissive cells. As other small DNA viruses, MCPyV relies upon many different host cell factors to replicate its genome. The expression of viral T antigens is essential for this function, and they are transcribed immediately upon virus entry into the nucleus of the host cell. LT and 57kT are transcribed first, with ST shortly afterwards [227]. The T antigens force the host cell to enter S-phase. This alters the cellular environment, making it more hospitable to viral replication.

In later stages of viral replication, it is suggested that further early gene transcription is inhibited by the MCPyV miRNA, likely by causing the degradation of early gene transcripts [208]. This then shifts the focus to the transcription of

the late region and also to the replication of the viral genome itself.

#### 1.4.3.2.1 The role of LT in Merkel cell polyomavirus replication

Polyomaviruses require expression of the LT antigen to initiate genome replication. LT oligomerises to form hexameric molecules, two of which bind to the *ori* in a head to head orientation [228]. The LT helicase domain then unwinds DNA and replication proceeds in a bidirectional manner, with the two hexamers moving in opposite directions. The LT OBD interacts with the *ori* by recognising the GAGGC-like motifs. A crystal structure of the *ori* shows that to initiate replication, three of these pentanucleotide sequences are required [229]. The number and proximity of LT binding sites on the origin likely allows for intermolecular OBD-OBD interactions between molecules of LT [203].

MCPyV LT is thought to function in a similar fashion to other polyomavirus LTs. However, there are several unique MCPyV LT-host interactions that affect viral replication. For example, MCPyV LT binds to the cytoplasmic vacuolar sorting protein, hVam6p, via its MUR domain [207]. hVam6p is a member of the homotrophic fusion and protein sorting (HOPS) complex, and it is redistributed from the cytoplasm to the nucleus upon MCPyV LT expression, resulting in a disruption of lysosome clustering. Overexpression of hVam6p leads to a reduction in MCPyV virus formation by more than 90%, suggesting an inhibitory role [227]. Furthermore, abrogating the hVam6p binding domain increases infectious virion production by 4-fold to 6-fold [207] [227]. The inhibitory role of hVam6p may function to diminish viral replication and establishing a persistent infection. Another factor important for MCPyV LT-mediated viral replication is the chromatin-associated bromodomain containing protein 4 (Brd4). Brd4 is a member of the BET protein family and plays a role in recruitment of cellular replication factors required for viral replication. The interaction of MCPyV LT with Brd4 helps recruit replication factor C (RFC) to MCPyV replication complexes [230]. RFC facilitates loading of the PCNA clamp and tethering of the processive DNA polymerase δ, and this action allows for the elongation of MCPyV DNA [227]. The importance of the MCPyV LT-Brd4 interaction is highlighted by findings that the expression of dominant negative Brd4 inhibits MCPyV replication [230]. In addition, DNA damage response (DDR) factors are also involved in MCPyV replication [231], with both DDR pathways, ATM and ATR, being involved. MCPyV LT expression relocalises DDR factors to the nucleus, into the replication foci where

they co-localise with LT [231]. Interestingly, both DDR [232] and Brd4 [233] activation and recruitment have been observed in HPV replication. These findings stress the importance of the DDR pathways in viral replication across multiple viral families.

#### 1.4.3.2.2 The role of ST in Merkel cell polyomavirus replication

While MCPyV LT is the primary factor in the replication of MCPyV DNA, it does not facilitate replication efficiently on its own. MCPyV ST is required to enhance replication, and its depletion leads to inhibition of replication [203]. This is in contrast to SV40 ST, as its co-expression has little effect on SV40 LT-mediated viral replication [234]. Interestingly, the mechanism by which MCPyV ST enhances viral replication does not depend on its ability to bind PP2A or Hsc70, and the equivalent SV40 ST domains cannot enhance MCPyV LT-mediated viral replication [234]. This suggests an alternative mechanism for MCPyV ST enhancement of viral replication.

One possible mechanism by which MCPyV ST could function in replication enhancement is by promoting the hyperphosphorylation of the translation regulator eIF4E binding protein (4E-BP1) [234]. This leads to increased production of cellular proteins, including host factors necessary for viral replication. In addition, MCPyV ST targets the cellular SCF ubiquitin E3 ligase complex, of which Fbw7 is the recognition component [235]. This complex targets MCPyV LT for proteasomal degradation, but binding of MCPyV ST to $SCF^{Fbw7}$ via its LSD region inhibits MCPyV LT degradation [211]. This prevents the turnover of MCPyV LT, whose half-life without MCPyV ST expression is 3-4 h, going up to 24 h when the two proteins are co-expressed [211].

Overall however, neither MCPyV ST nor MCPyV 57kT are sufficient for replication in the absence of MCPyV LT. Co-expressing MCPyV 57kT with MCPyV LT shows no increase in replication efficiency [203].

### 1.4.3.3 Merkel cell polyomavirus and the immune response

In order to establish an infection, viruses need to evade the cellular immune response. Host cells use innate immunity as a barrier against invaders, and pathogens of all types have evolved mechanism to evade or subvert it. MCPyV

T antigens appear to play an intriguing role in overcoming the innate immune response to allow the establishment of viral infection.

MCPyV ST downregulates the innate immune response by interfering with the NF-κB family of transcription factors [209]. NF-κB is an important regulator of a number genes involved in both the inflammatory and antiviral response. It is activated in response to various innate immunity signalling, for instance from pattern recognition receptors (PRRs). PRRs detect pathogen associated molecular patterns (PAMPs), e.g. proteins or nucleic acids. PAMP recognition results in the production of antimicrobial peptides, cytokines, and chemokines capable of fighting against and clearing microbial infections [236].

This recognition also activates a coordinated signalling cascade, leading to the activation of the IKK complex [236] [237]. The IKK complex consists of two catalytic components, IKKα and IKKβ, and a regulator subunit, NF-κB essential modulator (NEMO). NEMO is a molecular scaffold which can recruit upstream signalling complexes [237]. IKK activation causes the phosphorylation and degradation of IκB, which in turn induces the release of NF-κB from the complex. Free NF-κB translocates to the nucleus, where it stimulates the transcription of proinflammatory cytokine and type 1 interferon genes [236]. Figure 1.15 depicts the NF-κB signalling pathway.

Many viruses produce proteins that can interfere with NF-κB signalling [238], such as HCV core protein [239] and HPV E7 [240], both of which prevent IκB degradation. Furthermore, murine cytomegalovirus (mCMV) [241] and molluscum contagiosum poxvirus [242] directly target NEMO, disrupting IKK activation. Conversely, SV40 ST upregulates NF-κB activation in a PP2A-dependent manner, while some inflammatory targets like interleukin-8 (IL-8) are downregulated upon SV40 ST expression [107]. MCPyV ST is able to inhibit IKKα/IKKβ phosphorylation via an interaction with NEMO, thus preventing NF-κB release and translocation into the nucleus. This interaction appears to be dependent on protein phosphatases PP2A Aβ and/or PP4C [209]. Moreover, a number of NF-κB target genes are downregulated upon MCPyV ST expression, e.g. CCL20, IL-8, TANK, and CXCL-9 [209].

Viruses also act upstream of NF-κB to inhibit receptors involved in innate immunity, such as Toll-like receptors (TLRs), a subset of PRRs. EBV [243], HPV [244], and HBV [245] all downregulate TLR9 expression. TLR9 detects viral or

bacterial double-stranded DNA containing multiple non-methylated CpG motifs [236]. Upon recognition of pathogen DNA, TLR9 activates NF-κB in immune cells, which upregulates the production of inflammatory molecules [246]. MCPyV LT also inhibits TLR9 expression [247] by reducing the mRNA levels of the C/EBPβ transactivator, a positive regulator of the TLR9 promoter. This leads to greatly reduced binding of C/EBPβ to its response element on the TLR9 promoter, therefore MCPyV LT targeting of C/EBPβ may be important in establishing viral persistence [247].

It appears that MCPyV has a complex and multifaceted defence against innate immunity, targeting different parts of the various pathways and utilising both major T antigen products. This allows the virus to persist, and may even contribute to tumourigenesis.

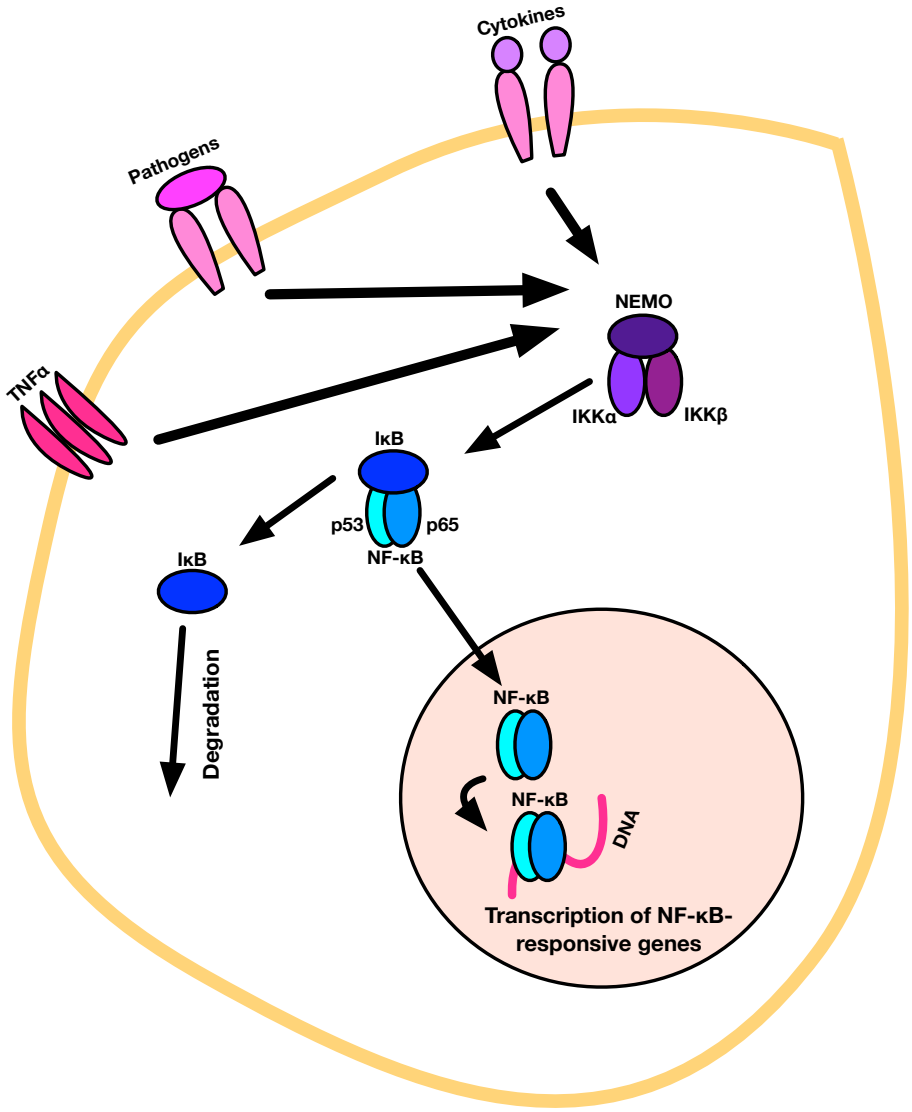


**Figure 1.15: NF-κB signalling in the cellular immune response.** PAMP recognition by PRRs or cytokine or TNFα stimulation of other receptors leads to the activation of the IKK complex. Activation leads to the proteasomal degradation of IκB and the release of NF-κB, which can then translocate into the nucleus and activate the transcription of genes that have functions in the innate immunity. IKK: IκB kinase complex, IκB: inhibitor of κB, NEMO: NF-κB essential modulator, NF-κB: nuclear factor κB, TNFα: tumour necrosis factor α.

#### 1.4.3.4 Merkel cell polyomavirus assembly and egress

Little is known about MCPyV virion assembly and egress, although more research may be forthcoming with the discovery of a potentially permissive cell

line [220]. MCPyV virions tend to cluster in the nucleus and its periphery before egress [222]. Unlike other polyomaviruses, including SV40, JCPyV, and BKPyV, MCPyV does not encode an agnoprotein, which is known to be important in virus particle assembly and maturation [248]. Nor does MCPyV encode an equivalent of the SV40 VP4, which triggers lytic virion release [249]. Therefore, an alternative mechanism must be utilised by MCPyV. It is possible that redistribution of the lysosomal factor, hVam6p, to the nucleus by MCPyV LT contributes to egress via lysosomal processing during virus replication [207].

Polyomavirus virion release is thought to occur primarily through cell lysis, although shedding of accumulated viral particles in SV40-infected cells has also been observed [250]. It is possible that if the natural host of MCPyV is a type of skin cell, lysis might not be required for release, as the natural process of keratinocyte desquamation may serve this purpose. The newly-developed dermal fibroblast cell culture model may help to fully address these specific questions about the MCPyV life cycle.

### 1.4.4 Merkel cell polyomavirus-induced tumourigenesis

MCPyV is a common skin commensal, usually acquired at some point during childhood. In contrast, MCC is rare, thus the development of the cancer following viral infection must require multiple contributing factors, such as age, immune suppression, and UV light. MCPyV is a direct carcinogen, since it expresses oncoproteins (the T antigens) that directly contribute to the transformation of the host cell. Supporting evidence for this comes from MCPyV-positive MCC cell lines which demonstrate growth arrest and cell death when both MCPyV LT and ST protein expression is depleted [251].

The major feature of MCPyV-positive MCC tumours is the presence of mutations in MCPyV LT that truncate it at the carboxy-terminus [42] [252]. These mutations lead to the loss of functional domains associated with viral replication, and are randomly distributed in different tumours, although with the consistent preservation of the pRb binding site. Therefore MCPyV LT proteins in different tumours vary in size, depending on where their specific truncating mutations lie [253].

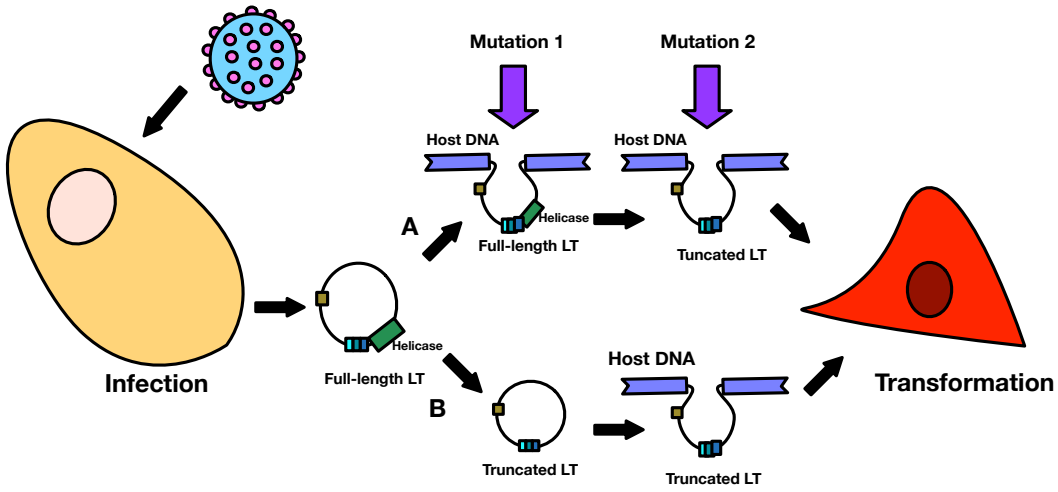


**Figure 1.16: Merkel cell polyomavirus-induced tumourigenesis.** MCPyV infection occurs in childhood in most cases. Loss of immunosurveillance leads to proliferation of the virus prior to tumourigenesis. At least two mutations are needed before MCPyV can transform cells. In model A, the first mutation is the integration of the full-length viral genome into host DNA, while the second mutation is the truncation of LT. In model B, truncation of LT occurs prior to integration. These changes in the virus lead to cellular transformation and tumour proliferation.

MCPyV-induced tumourigenesis has several key stages illustrated in Figure 1.16. Initially, the MCPyV genome integrates into the host chromosome in a monoclonal pattern [20] [254]. Upon integration, the viral genome retains the full length MCPyV LT, which can initiate host DNA replication, and this unlicensed replication results in fork collision and DNA breakage, thus leading to cell death [42]. Therefore, once MCPyV integrates, there is a strong selective pressure to eliminate MCPyV LT-mediated DNA replication and this is achieved via the truncation of MCPyV LT and the resulting loss of replication capabilities [253]. This requirement for two separate events may at least in part explain why MCPyV is so rare. Alternatively, it may be that MCPyV LT is truncated prior to integration [255]. To support this possibility, it has been shown that expression of truncated MCPyV LT upon exposure of UV radiation leads to defective DNA repair, leading to increased genomic instability which may promote MCPyV integration [256].

#### 1.4.4.1 The role of LT in Merkel cell polyomavirus-induced tumourigenesis

As mentioned in Section 1.4.4, MCPyV LT truncation is a defining feature of MCC tumours. However, current evidence suggests that neither full-length nor truncated MCPyV LT can initiate transformation [234]. Despite this, MCPyV LT is expressed in 75% of MCPyV-positive MCC tumours samples, and its DNA is present at around 5.2 copies per tumour cell [257]. This likely means that there is a role for MCPyV LT in MCPyV-induced tumourigenesis.

One reason why MCPyV LT cannot transform cells, unlike its SV40 counterpart, may be because all truncated MCPyV LT forms lose the p53 binding site [258]. However, truncated MCPyV LT is more effective at inducing cellular proliferation than full-length MCPyV LT, as the carboxy-terminal region, lost during truncation, exhibits growth inhibitory effects [258]. It is also possible that loss of the carboxy-terminal region prevents activation of host DDR and thus apoptosis, as p53 is not activated. This possibility is highlighted by the findings MCPyV infection results in the activation of the DDR pathway in a MCPyV LT-dependent manner [206]. In addition, MCPyV LT maintains its pRb binding domain after truncation, and this interaction is known to interfere with pRb binding to E2F and thus promotes cell proliferation [259].

MCPyV LT also increases the levels of the cellular oncoprotein, survivin [259]. Survivin is a member of the inhibitor-of-apoptosis family of proteins, and it is elevated in a number of cancers [260]. Survivin mRNA is increased 7-fold in MCPyV-positive MCC tumours, and MCPyV LT expression alone can upregulate survivin, whereas knocking down the T antigens decreases both the mRNA and protein levels of survivin, leading to cell death [259]. Survivin may be a viable drug target for MCPyV-positive MCC treatment, and a small molecule inhibitor, YM155 is able to initiate selective MCC cell death [259].

#### 1.4.4.2 The role of ST in Merkel cell polyomavirus-induced tumourigenesis

Unlike other oncogenic polyomaviruses, MCPyV ST seems to be the primary tumourigenic factor in MCC development. 92% of MCPyV-positive MCC tumours are positive for MCPyV ST, while only 75% are positive for MCPyV LT. Moreover, knock down of MCPyV ST induces cell growth arrest, and expression of MCPyV ST but not LT is sufficient to induce rodent fibroblast transformation, loss of con-

tact inhibition, and anchorage- and serum-independent growth [234]. All these features are typical of a viral oncogene, although it is uncharacteristic for a polyomavirus ST to be the main factor in tumourigenesis.

SV40 ST is an accessory to SV40-induced transformation, and primary contributes by targeting PP2A, specifically the A$\alpha$ subunit, to alter the substrate specificity of the holoenzyme (as discussed in Section 1.2.5.2). This interaction is critical for SV40 ST-facilitated transformation and cell proliferation. However, disrupting the equivalent MCPyV ST-PP2A A$\alpha$ interaction does not reduce the ability of MCPyV ST to induce rodent cell transformation and anchorage-independent colony formation [234]. Thus an alternative mechanism is utilised by MCPyV ST.

One possibility is that SV40 and MCPyV ST proteins affect the PI-3K-Akt-mTOR signalling pathway at different stages. This signalling pathway is an important regulator of translation in tumourigenesis [261] [262] [263]. SV40 ST activates the pathway by preventing the PP2A A$\alpha$-mediated dephosphorylation of Akt [100], however MCPyV ST has little effect at that stage of the Akt-mTOR pathway, instead acting downstream [234], at the level of the translation factor 4E-binding protein 1 (4E-BP1).

Cap-dependent translation depends on the binding of the eukaryotic translation initiation factor 4E (eIF4E) to mRNA molecules. eIF4E is part of the eIF4F complex that initiates ribosome recruitment [264]. This pathway is regulated by 4E-BP1, by binding eIF4E to prevent eIF4F complex formation [265]. 4E-BP1 is regulated by phosphorylation, whereupon it releases eIF4E, allowing assembly of eIF4F and cap-dependent translation [266]. 4E-BP1 is phosphorylated by mTOR, and MCPyV ST reduces the turnover of hyperphosphorylated 4E-BP1, which increases eIF4F activity and thus encourages cap-dependent translation. This effect of MCPyV ST on 4E-BP1 is independent of PP2A A$\alpha$ and Hsc70 binding [234]. Figure 1.17 illustrates the different stages of the PI-3K-Akt-mTOR pathway where SV40 and MCPyV ST proteins function.

Furthermore, the MCPyV ST LSD domain may be required for transformation, since a mutation within this region abrogates MCPyV ST ability to transform rodent cells, but does not affect the ability of MCPyV ST to bind PP2A A$\alpha$ [211].

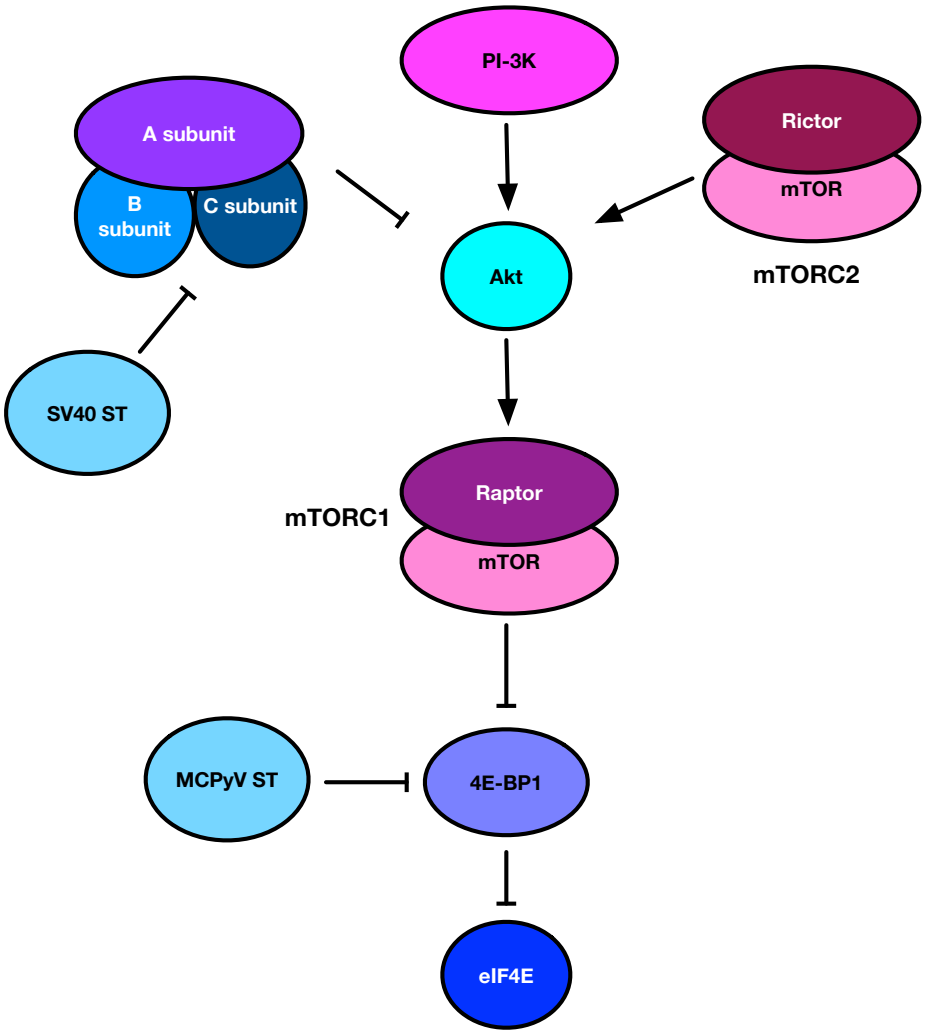


**Figure 1.17: MCPyV ST promotes cell proliferation downstream of the Akt pathway.** MCPyV ST targets the translational regulator 4E-BP1, and reduces hyperphosphorylated 4E-BP1 turnover, promoting eIF4E activity and cap-dependent translation. On the other hand, SV40 ST promotes Akt activity by preventing PP2A-mediated Akt dephosphorylation. 4E-BP1: 4E binding protein 1, eIF4E: eukaryotic translation initiation factor 4E, MCPyV: Merkel cell polyomavirus, mTOR: mammalian target of rapamycin, mTORC: mammalian target of rapamycin complex, PI-3K: phosphatidylinositol 3-kinase, ST: small T antigen, SV40: simian virus 40.

There is still some controversy as to the tumourigenic nature of MCPyV ST, because its levels in MCC cell lines and tissues appears to be low [267]. Regardless, it is more commonly detected in MCC tissues than MCPyV LT, and MCPyV ST depletion inhibits MCPyV-positive MCC cell growth [234]. It may also be the case that MCPyV ST is essential for initial transformation while MCPyV LT is

more important in subsequent persistence and proliferation of tumour cells.

## 1.5 Merkel cell carcinoma treatment

Conventional MCC treatment depends on the stage of cancer progression. If the tumour is localised, the standard therapy is surgical excision with 2-3 cm margins. If the cancer has metastasised into the regional lymph nodes, these are excised together with the primary tumour, and adjuvant radiotherapy to the tumour and regional lymph node sites is given. This mode of treatment has been associated with reduced risk of regional relapse [268]. MCC is a radiosensitive tumour, thus if surgery cannot be performed, radiation on its own can also be effective [269] For metastasised MCC, various regimens of broad-spectrum chemotherapy are used, such as anthracyclines, cyclophosphamide, etoposide, and platinum derivatives, alone or in combination, with a notoriously poor prognosis [196]. Therapies available for MCC at the moment are generic, but this is likely to change as the causative agent for the majority of cases has been discovered, and thus new drug targets are being researched. As MCPyV T antigen expression is necessary for the survival of MCPyV-positive MCC cells, both MCPyV LT and ST could be potential therapeutic targets.

Preliminary inhibitors of MCPyV-positive MCC have been identified *in vitro*. For instance, IFN reduces MCPyV LT expression and causes cell death in MPyV-positive MCCs [270], although IFN treatment did not induce a clinical response in two patients with late-stage MCPyV-positive MCC [271]. A more promising target is YM155, an inhibitor of surivin expression, which is cytotoxic in nanomolar quantities and shows a cytostatic, though not cytotoxic, effect in MCC mouse xenograft tumours in mice [259] [272]. At the moment, pazopanib, a small-molecule TK inhibitor, is undergoing a phase II clinical trial [273]. In addition, controlling MCPyV infection in immunosuppressed and elderly patients might be a preventative measure for MCC, and the FDA-approved drug trametinib has been suggested as a therapy [220]. Novel drugs, particularly those targeting the various interactions of MCPyV T antigens with host cellular proteins, will likely remain a focus of intense research.

MCC is an immunologically responsive cancer, as it contains viral antigens within the tumour cells. Improved immunosurveillance has been behind occasional

spontaneous regression of disseminated MCC tumours [274]. Thus in parallel to small molecule inhibitors, immuno-based treatments for MCPyV-positive MCC are also being researched. Specific T lymphocytes recognising various MCPyV epitopes have been identified, both within tumour cells and in the blood of both MCC patients and healthy test subjects [275]. 58 CD8+ T lymphocytes against 35 MCPyV T antigen epitopes have been identified, present only in MCC patients. Despite this response, MCC tumours persist and grown, thus it appears MCCs can inhibit T lymphocyte cytotoxicity or otherwise evade the immune response [276].

Alternatively, a DNA vaccine could be a viable therapy for MCC. Murine tumour models have demonstrated that it is possible to target both MCPyV LT and ST to induce CD4+ and CD8+ T lymphocyte responses [277] [278]. Furthermore, MCPyV-specific CD8+ T lymphocytes produce targetable exhaustion markers PD-1 and Tim-3 that are associated with reversible T-lymphocyte dysfunction [279]. Therefore, the investigation of potential antagonists of PD-1 and Tim-3 pathways may yield additional MCC treatment measures.

Due to the highly metastatic nature of Merkel cell carcinoma, designing drugs to inhibit this property would limit the mortality rate of late-stage disease. Uncovering the mechanism of what drives MCC metastasis is therefore of paramount importance, particularly determining the role of the T antigens. Interactions of, for example, ST with cellular factors at one or more stages of the motility pathways employed by cells are highly targetable, and inhibitors of such interactions would be of great interest in further research.

## 1.6 Cell motility

Cell motility is a vital part of the proper functioning of a number of different cell types. For example, movement of cells from one location to another is vital for embryonic development, migration of cells into a wound is important for healing, while cells of the immune system "patrol" tissues searching for pathogens and can migrate quickly under the influence of chemoattractants. On the other hand, cell motility in cancer is part of the metastatic cascade (discussed in Section 1.7), and is a sign of disease progression.

Prokaryotic cells and sperm cells use appendages such as cilia and flagella to propel themselves, while eukaryotic cell motility is much more complex, and often involves several different mechanisms. These mechanisms mainly involve changes in cell shape driven by rearrangements of the cytoskeleton. The eukaryotic cytoskeleton consists of three different types of filament: actin filaments, microtubules, and intermediate filaments.

### 1.6.1 The actin cytoskeleton

Actin is ubiquitous and universally conserved in eukaryotic cells, and is involved in muscle contraction, cell motility, cell division, cell signalling, cellular junctions, vesicle and organelle movement, and cell shape maintenance. Monomeric actin (G-actin) is globular and around 42 kDa. G-actin subunits polymerise into filaments (F-actin). Filament formation requires a sufficient concentration of G-actin for nucleation sites to form. Actin filaments are polar, with the plus end growing faster than the minus end. G-actin binds adenosine triphosphate (ATP), which is hydrolysed after the formation of filaments, and this may prime filaments for disassembly.

Actin, together with myosin, was first discovered in muscle in the 1940s, and in other cells in the 1960s. Currently, there are over 100 known accessory proteins and actin regulators [280]. A number of regulators are important in actin nucleation, contributing to the growth of actin filaments. The largest such regulator group are the formins, Rho-family GTPase-regulated proteins with a highly conserved FH2 domain [281]. Rho-family GTPases release formins from their autoinhibitory state, which allows them to promote the incorporation of G-actin monomers at the plus end of growing filaments [282]. Formins produce straight actin filaments.

However, the best-studied of the major actin regulators is the seven subunit actin-related protein complex (Arp2/3). Arp2/3 binds to the minus end of an actin filament and caps it, all the while initiating the assembly of a new filament at a Y angle. Thus Arp2/3 promotes actin branching, which is very important for cell motility. Arp2/3 relies on the co-operative functions of an array of nucleation-promoting factors (NPFs), as it has little nucleation capability on its own [283].

Class I NPFs have a WCA domain, composed of the WH2 region that binds actin

monomers, an ampiphatic linker, and an acidic peptide that binds Arp2/3. Class I NPFs include the Wiskott-Aldrich syndrome protein (WASP), neural WASP (N-WASP), and the WASP family verprolin homology proteins (WAVE1-3). N-WASP is the best-studied NPF, and it requires activation by a number of different proteins, including cortactin, in order to interact with Arp2/3 [284]. NPFs have roles in diverse aspects of cytoskeletal change. For example, N-WASP has roles in the formation of filopodia, membrane ruffles, and phagocytic structures, as well as in endocytosis [285]. The WAVE proteins function mainly in cell motility, although, for example, WAVE2 has also been implicated in forming cell-cell contacts [285].

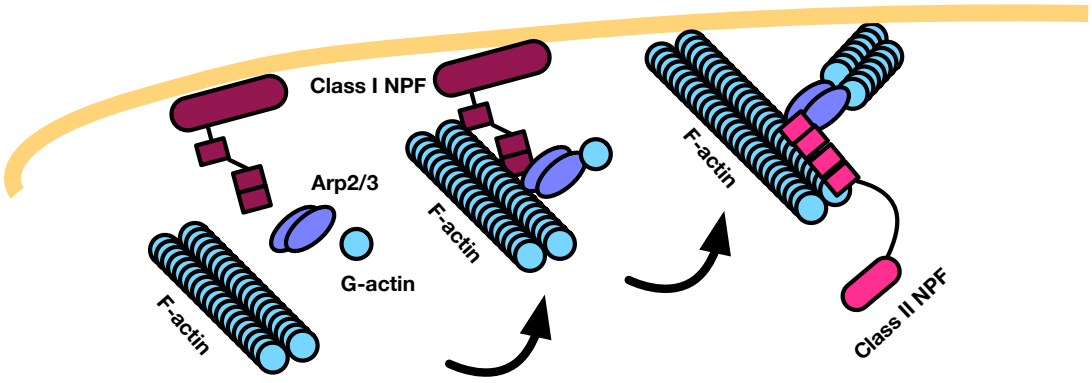


**Figure 1.18: The action of Arp2/3 and NPFs in the formation of actin fibres.** The Arp2/3 complex is recruited by Class I NPFs close to cellular membranes. The NPFs serve the purpose of bringing the Arp2/3 complex together with the first G-actin subunit in the new filament and generate a branch. Arp2/3 branch-points can be stabilised by F-actin-binding Class II NPFs, e.g. cortactin. Arp2/3: actin-related protein complex 2/3, F-actin: filamentous actin, G-actin: globular actin, NPF: nucleation-promoting factor.

Class II NPFs do not contain a WCA domain, and the best-studied of these is cortactin. It is important in a variety of actin-driven cellular processes, including cell migration and invasion, axon guidance and neuron morphogenesis, as well as tumour metastasis [286]. Cortactin binds and stabilises active Arp2/3 using an acidic amino-terminal peptide, while binding F-actin with its specific cortactin repeats domain. Cortactin stabilises actin filament Y-branches by preventing Arp2/3 from spontaneously dissociating [287]. Alone, cortactin is a weak NPF, but it interacts with N-WASP by releasing it from its autoinhibited state to help enhance Arp2/3 activation [287]. Figure 1.18 illustrates the function of Arp2/3 and its NPFs.

Actin turnover involves treadmilling, i.e. loss of G-actin monomers from the plus end of the filament, severing, i.e. cutting a filament into two without loss of polymer mass, and catastrophic disassembly. The latter two are facilitated by cofilin and a number of accessory factors, such as coronin [288]. In any case, actin turnover involves ATP hydrolysis, and returns G-actin monomers to the cytosolic pool, where they can be used to make new filaments.

#### 1.6.1.1 Actin structures in cell motility

The actin cytoskeleton is key in the formation of cellular protrusions: lamellipodia, filopodia, invadopodia, and non-apoptotic blebs, as illustrated in Figure 1.19 [285]. Filopodia are the simplest protrusive actin-based structures, thin cylinders that can extend tens of μms from out of the cortex of the cytoskeleton. They contain a tight bundle of actin filaments bundled together by accessory proteins such as fimbrin [289] and fascin [290]. Filopodia are considered to be early markers of cell motility, as they are utilised by cells to explore the surrounding area [291]. Lamellipodia are thin sheet-like projections dominating the leading edge of motile cells They are shaped by branched webs of actin filaments, with Arp2/3 complexes at the intersections between branches, with WAVE the primary NPF [292]. Lamellipodia are thought to be the major motile structures, actually responsible for moving cells forward. Invadopodia are specialised actin-rich protrusions able to break down the extracellular matrix (ECM). Arp2/3 and N-WASP are the main factors in invadopodia formation [293]. All these structures are also important in the mesenchymal form of migration (discussed in Section 1.6.5).

Actin is also involved in amoeboid migration, playing a role in the formation of membrane blebs. Blebbing occurs when the cortical actin meshwork becomes disrupted, leading to a large protrusion lacking F-actin. As the bleb grows, an actin cross-linker, ezrin, is recruited to its cortex, leading the the re-polymerisation of actin and the retraction of the bleb [294].

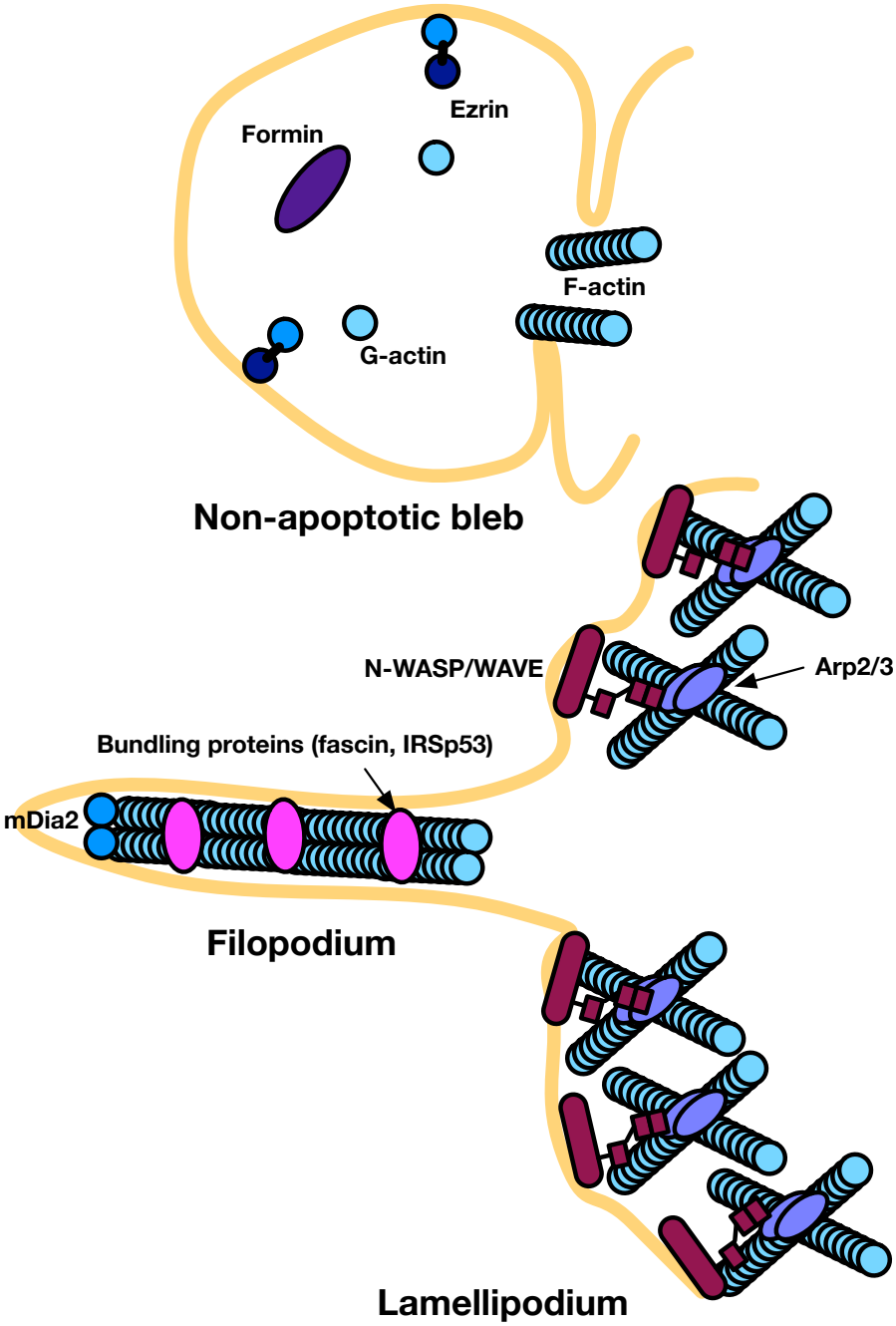


**Figure 1.19: Cellular protrusions in cell motility.** Lamellipodia and filopodia are actin-rich protrusions at the leading edge of mesenchymally-migrating cells. Non-apoptotic blebs are actin-poor protrusions involved in amoeboid migration. Arp2/3: actin-related protein complex 2/3, IRSp53: insulin receptor substrate protein 53, mDia2: mammalian diaphanous 2, N-WASP: neural Wiskott-Aldrich syndrome protein, WAVE: WASP family verprolin homology protein.

#### 1.6.1.2 Signalling cascades in actin regulation

Actin reorganisation, including the formation of motile structures and cell polarisation, depends on signalling cascades. Actin filament formation is directly dependent on the activity of Rho-family GTPases. These signal mediators activate NPFs such as N-WASP and WAVE1-3, recruiting the Arp2/3 complex. There are 22 known Rho-family GTPases in mammals, and three have been studied extensively: Rac, RhoA and Cdc42. Rac can induce the formation of lamellipodia, and is thought to be the main Rho-family GTPase involved in their extension, as it activates the major actin nucleator involved in lamellipodia, WAVE2 [295]. RhoA has been found to be active at the tailing edge of the motile cell, and is involved in the retraction of membrane protrusions [296] and formation of stress fibres [297]. Finally, Cdc42 is the major Rho-family GTPase involved in filopodia and invadopodia formation, activating N-WASP and the formin mDia2 [298].

Receptors that are ultimately responsible for changes in the actin cytoskeleton include G-protein coupled receptors (GPCRs), receptor tyrosine kinases (RTKs), and integrins [299]. Integrins, for instance, are involved in the formation of focal adhesions, which connect the actin cytoskeleton to the ECM. Integrin activation in turn leads to the activation of focal adhesion kinase (FAK) and Src kinase, which then affects factors that activate the Rho-family GTPases [299]. A simplified version of this pathway is illustrated in Figure 4.18.

### 1.6.2 The microtubule network and intermediate filaments

The microtubule network is important for cell maintenance and also functions in intracellular vesicle transport [300], organelle positioning [301], and mitotic spindle formation for segregation of chromosomes during mitosis [302]. In addition, the microtubule network facilitates the control of cell shape and polarised cell motility [303].

Microtubule growth is coordinated at the microtubule organising centre (MTOC), a structure that also plays a major role in cell division [304]. Microtubules are hollow tubes composed of $\alpha\beta$-tubulin heterodimers that form a dense cytoplasmic network. Their structure, just like F-actin, is polarised, with $\beta$-tubulin exposed at the plus and $\alpha$-tubulin exposed at the minus end. They can be formed either by *de novo* nucleation or by disruption of pre-existing structures [305]. There are

many accessory proteins that maintain the balance between microtubule growth and shrinkage, and are grouped into microtubule-stabilising and microtubule-destabilising proteins [306].

Intermediate filaments are a diverse group of structures that contribute to the overall cell shape, anchor organelles, and are structural components of the nuclear lamina, as well as being part of the cell-cell and cell-ECM junctions [307]. They are tissue-specific, and composed of different building blocks, e.g. vimentins (mesenchymal cells), keratin (epithelial cells), neurofilaments (neural cells), lamin (nuclear envelope), or desmin (muscle cells) [307]. Unlike the actin cytoskeleton or the microtubule network, intermediate filaments do not generally participate in cell motility.

### 1.6.3 Ion channels in cell motility

In addition to the cytoskeleton and all associated proteins, ion channels are also involved in cell motility. The role of ion channels in motility is related to their housekeeping functions, i.e. maintaining the cell membrane potential, and regulating cell volume, calcium concentration, and pH. Ion channels is a broad term covering channels that are permeable to potassium, sodium, chloride, calcium, and other ions.

Broadly speaking, regulating cell membrane potential and cell volume are the major contributions that ion channels make to cell motility, although some individual transporters have been found to be involved in cell motility in a manner that is not dependent on their conductive properties, e.g. as adhesion receptors [308].

#### 1.6.3.1 Cell membrane potential

Cell membrane potential plays a role in maintaining the cell volume and pH. In addition, it sets the electrical driving force for calcium influx and controls the gating of voltage-dependent calcium channels. The importance of this function for cell migration is illustrated in neutrophils, where proton channels (VSOP/Hv1) prevent the depolarisation of the cell membrane potential during respiratory burst

and thereby sustain calcium influx required for cell migration, while depletion or inhibition of these channels leads to defects in cell motility [309].

In addition, depolarisation of the cell membrane potential modulates the cytoskeleton [310] [311]. For instance, the actin network can sense cell membrane potential and this determines the actin polymerisation/depolymerisation ratio, affecting cell stiffness [312]. Changes in membrane potential strongly influence the electrical field of the cell, and changes in the electrical field can control the conformation and thus the activity of voltage-gated ion channels. Another example of the importance of the electric field is that it promotes the interaction of potassium Kv11.1 channels with β1 integrins. Kv11.1 activation causes the hyperpolarisation of the cell membrane, which in turn leads to the recruitment of downstream signalling molecules, like the focal adhesion kinase (FAK) and Rac1 [313]. Furthermore, recent research has shown that electric fields extend beyond the cell membrane into the cytosol [314], thus potential effects of changes to cell membrane potential brought on by ion channels towards cell motility could be much more extensive.

#### 1.6.3.2 Cell volume changes

The migratory cycle of a cell can be depicted as the gain of volume at the front of the cell and the loss of volume at the rear of the cell, as shown in Figure 1.20

Cell volume rises during the protrusion of lamellipodia and decreases during the retraction of the rear end. Local changes of up to 35% have been observed in cells [315] [316]. Studies on neutrophil migration have shown that their volume increases on chemotactic stimulation [317]. Volume changes remain restricted to one cell pole due to the elastic structure of the actin network and cytoplasm within lamellipodia, which prevents equalisation of local volume changes [318] [319] [320]. The cell body is softer and more deformable than lamellipodia [321], and lamellipodia are attached more firmly to the substratum as the cell moves [315]. Thus lamellipodia retain more fluid compared to the cell body when ion channels are activated, so local volume changes mechanically support protrusion and retraction of front and rear ends of the cell [322] [323] [316].

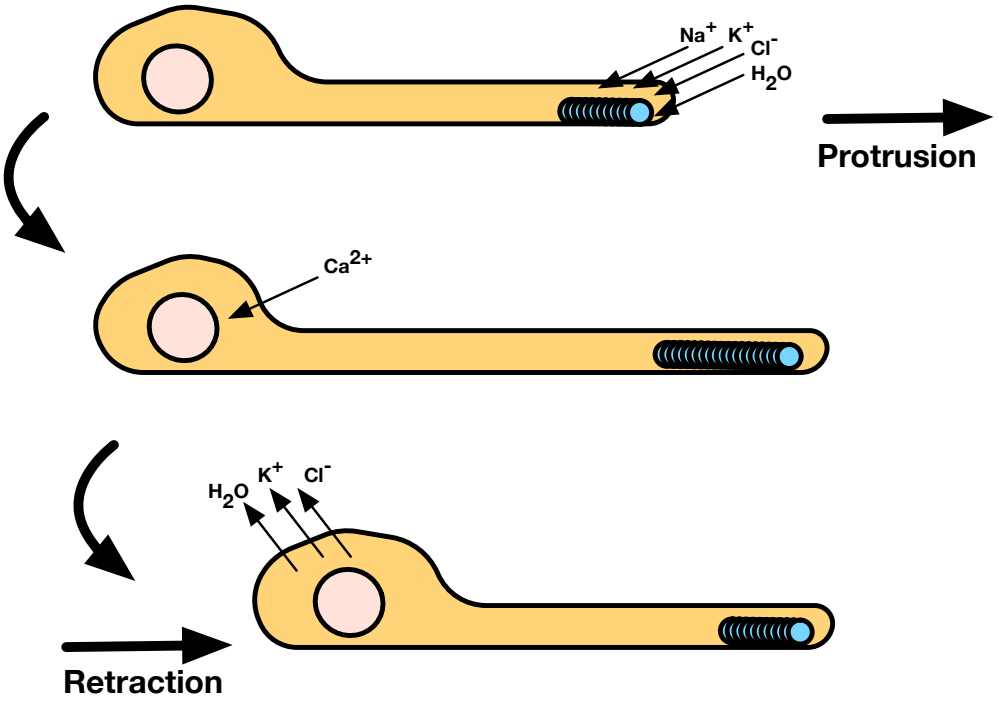


**Figure 1.20: Volume changes in cell migration.** Cell motility can be modelled as a cycle of isosmotic volume increase at the cell front and isosmotic volume decrease at the rear end. This process is facilitated by ion channels.

Amoeboid blebbing is another example of volume change in migrating cells. While blebs form mainly due to changes in intracellular volume distribution, there seems to be role for channels, as aquaporins have been found in the plasma membrane of blebs [324]. Furthermore, increasing the extracellular osmolarity inhibits bleb formation [325].

Cell volume regulation depends on ion channel activity. Cells return to their stable volume by either activating potassium or chloride channels and releasing potassium chloride and water (volume decrease) or by activating sodium, potassium, and chloride co-transport, sodium/hydrogen exchange, and non-selective cation channels to uptake potassium chloride and water (volume increase) [326]. Thus many ion channels are involved in cell volume regulation, and as such can be thought of as participating in cell motility, including KCa3.1 [327], Kv1.3 [328], to name but a few.

The actin cytoskeleton undergoes rapid polymerisation and depolymerisation following osmotic shrinkage or swelling, respectively [329] [330] [331]. Actin-

associated protein localisation is affected by volume changes as well, as in the case for cortactin [332] and ezrin [333]. The Rho-family GTPases are highly sensitive to cell volume changes [332] [334] [335]. These findings support the hypothesis that there is interdependence between ion channel activity, cell volume, and the cytoskeleton during cell motility.

### 1.6.4 Tumour viruses and cell motility

The actin cytoskeleton is co-opted by a number of different viruses for entry, replication, assembly, and egress. Thus, viruses need to interact with multiple factors involved in actin dynamics. Furthermore, some tumour viruses use their own oncoproteins to interfere with pathways that regulate cell motility. Figure 1.21 illustrates some of the viral proteins (oncogenic and not) that interfere with these signalling cascades.

Cellular morphology changes were observed early on in tumour virus research. The first oncoprotein to be associated with cytoskeletal changes was the RSV-encoded viral Src protein (v-Src). v-Src induces morphological changes in cells by reorganising actin stress fibres [336], and it also co-localises with actin-associated proteins in motile structures [337]. Furthermore, v-Src phosphorylates the actin-associated proteins vinculin [338] and cofilin [339], suggesting it is involved in invadopodia formation [340].

Another viral protein that affects the actin cytoskeleton is SV40 ST, which has been implicated in the loss of actin filaments [341]. The well-described SV40 ST-PP2A interaction leads to the rearrangement of filamentous actin network, causing Rac-induced lamellipodia formation, Cdc42-induced filopodia formation, and the loss of RhoA-dependent stress fibres [342]. This occurs due to SV40 ST expression increasing the levels of Rac1 and Cdc42, while reducing RhoA levels [342].

These actin cytoskeleton changes have also been seen in other tumour viruses. For example, EBV-transformed B cells show a 200-fold increase in fascin, a type of actin bundling protein [343], while EBV nuclear antigen 2 (EBNA2) interferes with Rho-family GTPase signalling by inducing PI-3K [344]. HBV protein X interacts with Rac1 to redistribute it to the tips of membrane protrusions [345], while HPV E7 enhances the accumulation of p27, a positive regulator of motility and

invasiveness, in the cytoplasm, leading to cell migration [346]. Finally, KSHV vFLIP protein promotes remodelling of the actin cytoskeleton via activation of the NF-κB pathway [347].

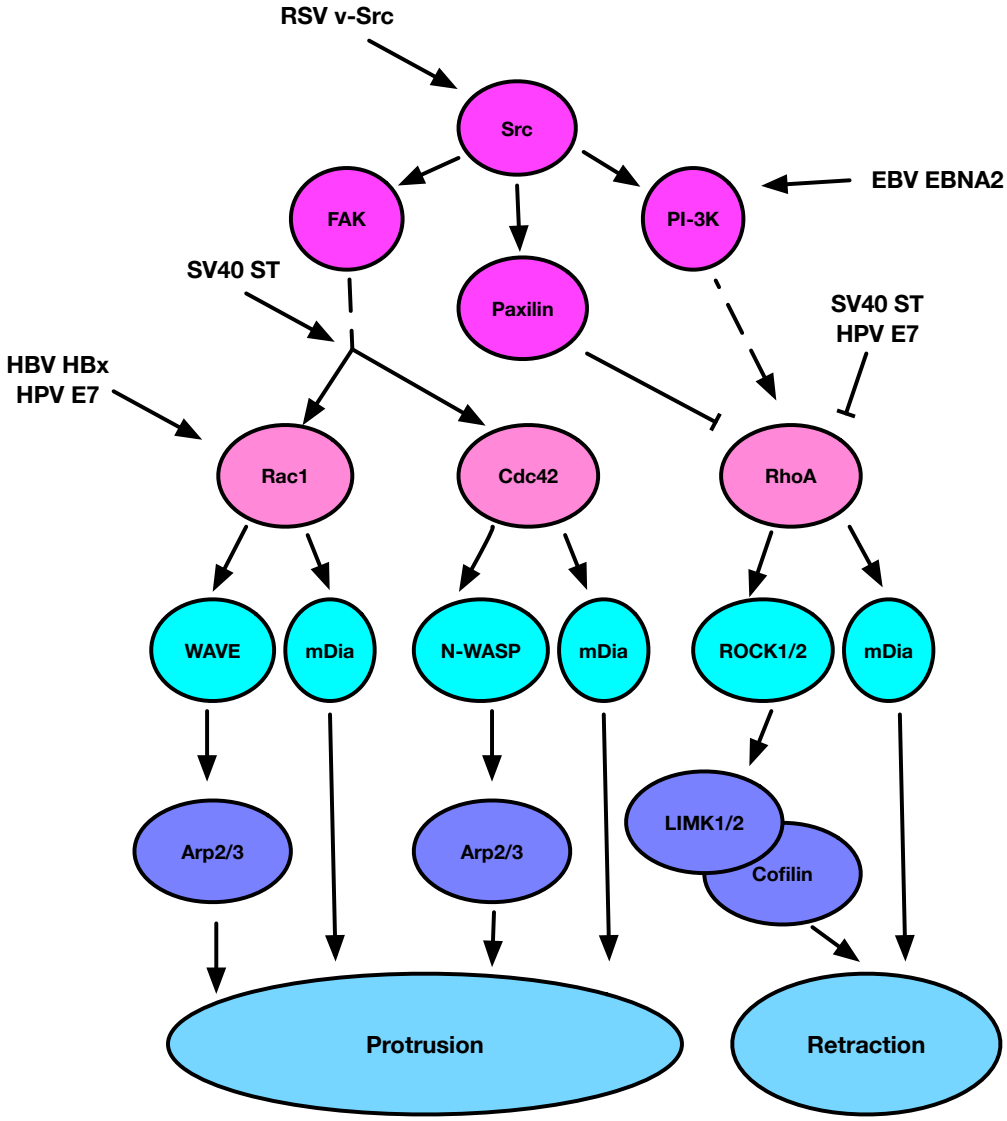


**Figure 1.21: Tumour viruses in the cell motility pathway.** SV40 ST upregulates Rac1 and Cdc42 while downregulating RhoA activity. HPV E7 upregulates Rac1 while downregulated RhoA activity. HBV HBx upregulates Rac1. EBV EBNA2 induces PI-3K and RSV v-Src induces Src activity. Direct phosphorylation/stimulation: black arrows. Inhibition: black lines, indirect interaction: dotted lines. Arp2/3: actin-related protein complex 2/3, Cdc42: cell division cycle protein 42, EBNA: EBV nuclear antigen, EBV: Epstein-Barr virus, FAK: focal adhesion kinase, HBV: hepatitis B virus, HBx: hepatitis B virus x protein, HPV: human papillomavirus, LIMK1/2: LIM domain kinase 1/2, mDia: mammalian diaphanous, N-WASP: neural Wiskott-Aldrich syndrome protein, PI-3K: phosphatidylinositol 3 kinase, Rac1: ras-related C3 botulinum toxin substrate 1, RhoA: ras homolog gene family, member A, ROCK1/2: rho-associated protein kinase 1/2, RhoA: RSV: Rous sarcoma virus, ST: small T antigen, SV40: simian virus 40, v-Src: viral Src, WAVE: WASP family verprolin homology protein [348].

Therefore, tumour viruses subvert the actin cytoskeleton both to affect cell motility, but also in other contexts. The major focus of this thesis is the effect of MCPyV ST on cell motility, thus the role of this oncoprotein in actin dynamics is important to consider, and it will be explored in the results sections.

### 1.6.5 Cell migration

Cell motility in eukaryotes can take several different forms. which are classified into three types: amoeboid, mesenchymal, and collective migration. Amoeboid migration is usually defined by the presence of plasma membrane blebs, weak or absent adhesion to the substratum and little or no ECM proteolysis [349]. On the other extreme, mesenchymal cell migration is a multi-step cycling type of cell motility mode characterised by cell polarisation to form a leading edge that extends actin-rich protrusions, e.g. lamellipodia and filopodia (Section 1.6.1.1). Such migration involves adhesive interactions with the substratum and proteolytic ECM remodelling. The final stage in mesenchymal migration is the retraction of the contractile cell rear to achieve cellular movement [350]. There is substantial interchangeability between these forms of cell migration, and it is not always clear cut which mode of migration a cell is undertaking [349]. Amoeboid and mesenchymal cell migration characterise single cell motility. Collective cell migration occurs when cells move as a sheet without breaking the cell-cell junctions between them [351]. Here, cells at the leading edge of movement generate proteases to degrade the ECM, creating a path [352]. Unlike mesenchymal migration, collective migration requires active adhesion complexes [350]. Less is known about this mode of cell migration, due to difficulties of *in vitro* modelling. The different types of motility are illustrated in Figure 1.22.

Cell migration can be separated into discrete components, including cell polarisation, protrusion formation, adhesion to the substratum, and retraction of the rear. Cell polarisation is defined as the presence of a stable front and rear, and often arises from the presence of directional cues, e.g. chemoattractants, substrate concentration differences, electric fields, or others, as well as combinations of different cues. In mesenchymal cell migration, the leading edge is characterised by actin-rich protrusions and adhesion to the substrate, while the rear edge is characterised by stable bundle and disassembly of adhesion [353]. The main Rho-family GTPase contributing to cell polarity is Cdc42 [354]. Protrusion formation,

discussed in Section 1.6.1.1, occurs at the leading edge, and is also regulated by Rho-family GTPases.

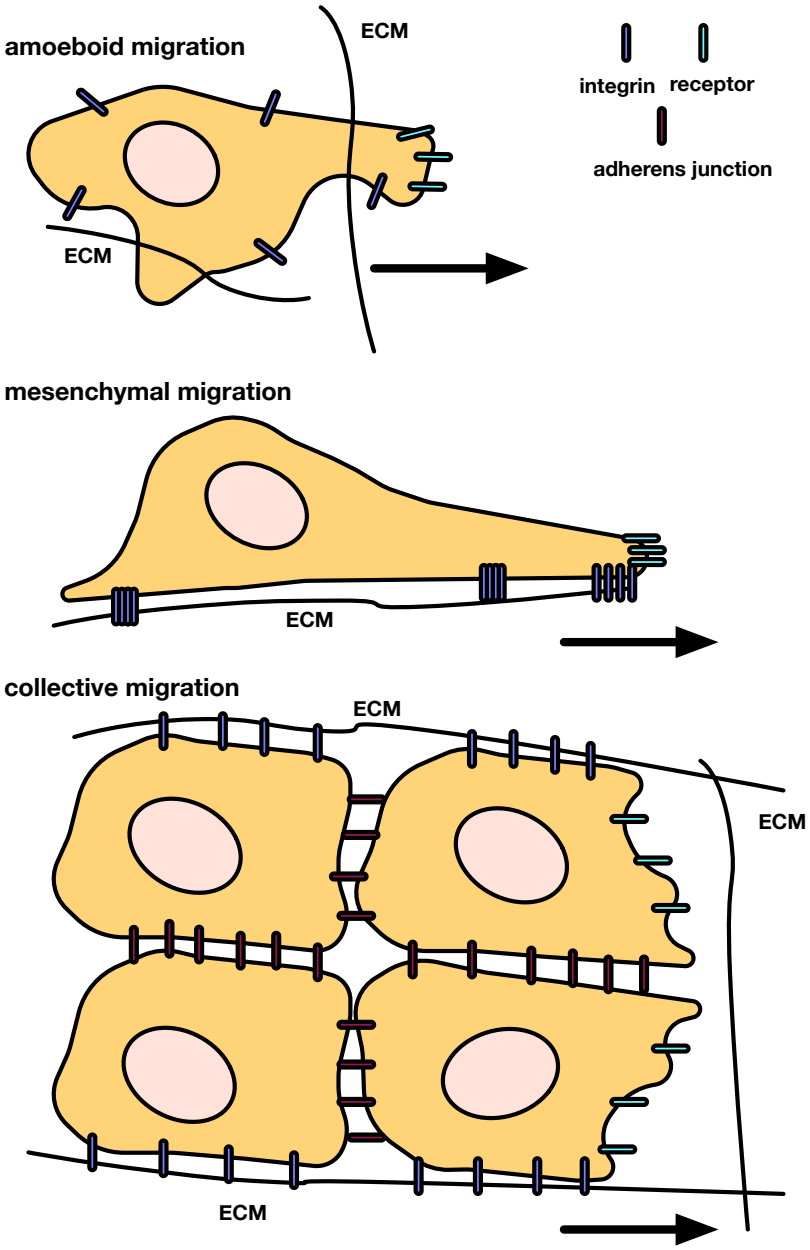


**Figure 1.22: Modes of cell migration.** Amoeboid motility is characterised by amorphous cell shape, random integrin distribution, and rapid changes in direction. Cells are able to squeeze through the ECM without degrading it. Mesenchymal motility is characterised by elongated morphology, and localised integrin contacts with the ECM. Cells need to degrade the ECM via the action of MMPs to migrate. Collective motility is characterised by groups or sheets of migratory cells, with many still retaining cell-cell contacts. Cells use MMPs to degrade the ECM. ECM: extracellular matrix.

Adhesion to the substratum is another important aspect of cell migration, and occurs mainly via the activity of integrin receptors. Ligand binding to integrins triggers signalling pathways regulating the formation of protrusions. This links the substratum to the actin cytoskeleton, which provides traction for migration [355]. Adhesion sites can be small, i.e. focal complexes, or large, i.e. focal adhesions. Adhesion sites close to the leading edge actively promote actin polymerisation and are quick to assemble/disassemble, while those further away from the leading edge are more stable, larger, and anchor bundles of actin filaments [356]. Adhesion sites are composed of many different proteins, including signalling complexes. Paxilin and FAK are two important kinases in adhesions [357], involved in regulating Rho-family GTPases. Other adhesion components, like talin, vinculin, and $\alpha$-actinin link the actin cytoskeleton to the substratum through integrins [358] [359] [360].

Finally, retraction of the rear requires the coordinated contraction of the actin cytoskeleton and the disassembly of adhesions at the trailing edge. This occurs in several different ways: contraction of actin to rip the adhesions, microtubule-induced disassembly, integrin endocytosis, and the proteolytic cleavage of proteins that link integrins to the actin cytoskeleton [361].

## 1.7 Cancer metastasis

Cancer metastasis is the primary cause of the vast majority of cancer-related deaths [362]. Metastasis is a complex process, with several discrete steps required for the formation of secondary tumour sites: loss of cell adhesion, gain of cell motility, dissemination via the vasculature, and colonisation of distant sites. Cell motility is thus a key stage of cancer metastasis, and the metastatic nature of MCC can be potentially linked to the effects of MCPyV ST on enhancing cell motility, first presented in the literature [210], and further explored in this thesis.

### 1.7.1 Loss of cell adhesion

Epithelial tissue is the primary origin of solid tumours, as it is composed of cell sheets separated from the basement membrane by stroma. These cell sheets are

organised into highly complex structures that require cell-cell and cell-ECM adhesion. During the early stages of metastasis, cells from the solid tumour needs to detach, thus cell adhesion complexes have to be deconstructed. Unsurprisingly, carcinoma cells lose adhesive properties [363]. Invasive tumours of epithelial origin show the loss of E-cadherin [364]. E-cadherin is a member of the tissue-specific cadherin family of transmembrane glycoproteins required to maintain tissue integrity [365]. Cadherins localise to cell junctions called zonula adherens and are responsible for calcium-dependent cell adhesion and signalling [366].

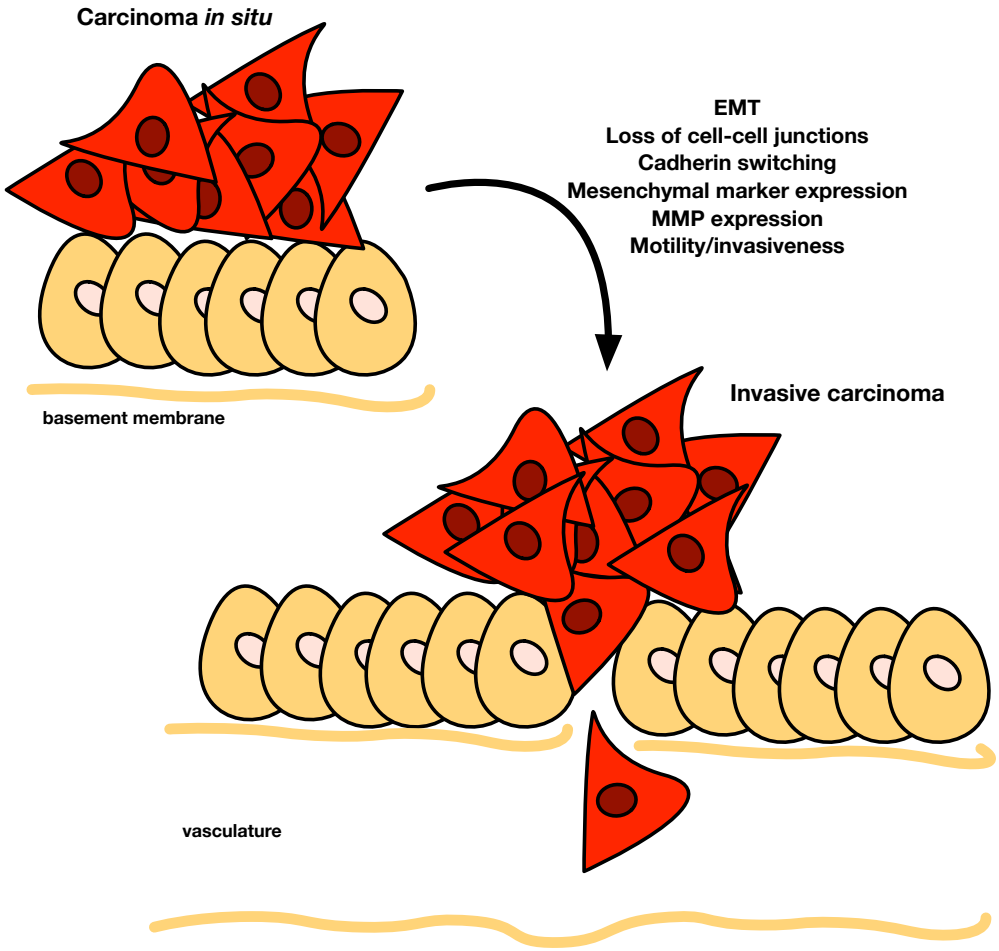


**Figure 1.23: Tumour spread from the primary site.** The process of a primary tumour spreading into the vasculature involves EMT, as cells gain motility and express specific markers, integrins, and MMPs. These factors are required for invasion of local tissue and passage through the basement membrane into the vasculature. EMT: epithelial-mesenchymal transition, MMP: matrix metalloproteinase.

A characteristic of many cancers, correlating with increased invasiveness, is a

process known as "cadherin switching", i.e. loss of E-cadherin and increased expression of N-cadherin [364]. This process is part of a wider process, epithelial-to-mesenchymal transition (EMT). EMT is characterised by a loss of cell polarity and epithelial proteins such as E-cadherin, occludins, claudins, catenins, and cytokeratin, all of which are responsible for maintaining cell-cell junctions, and a gain of a mesenchymal, migratory and invasive phenotype [367], as illustrated in Figure 1.23.

Multiple signalling pathways control EMT [367], and many of these are deregulated in metastatic tumours, through transcriptional repression, proteolytic degradation, or receptor domain cleavage [364]. In addition, increasing N-cadherin expression promotes tumour invasion via the activation of fibroblast growth factor receptor (FGFR), which stimulates cell survival, migration, and invasion [368].

Tumour viruses express a number of oncoproteins, which promote the loss of cell adhesions. For instance, HPV E6 expression promotes degradation of epithelial cell tight junctions through an interaction with E6AP, an ubiquitin ligase, which allows for proteosomal degradation of cell adhesion molecules, in an EMT-like manner [369] [370]. Furthermore, HBV HBx downregulates E-cadherin expression resulting in the loss of intracellular adhesion molecules [371]. In addition, SV40 ST promotes, in a PP2A-dependent manner, the redistribution and downregulation of E-cadherin, ZO-1, claudin-1, and occludin, all proteins involved in cell junctions [342]. MCC tumours also show a pronounced redistribution of E-cadherin from the cell membrane to the nucleus [372], suggesting mesenchymal qualities that promote the deadly invasive phenotype of the cancer.

### 1.7.2 Gain of cell motility

In order for tumour dissemination to be possible, cells must become motile. Cell motility and different types of migration have been extensively discussed in Section 1.6. Up to 40% of cancers undergo EMT and migrate in a mesenchymal manner [373], while cancers that do not undergo EMT tend to migrate in an amoeboid manner [374]. Collective motility has been demonstrated in breast, colon, and ovarian cancers [374].

### 1.7.3 Dissemination via the vasculature

The basement membrane is a barrier for invasive tumours of epithelial origin, which must be passed through to access the vasculature. It is important for epithelial structure and integrity, and consists of a dense network of proteoglycans and glycoproteins, including laminin and collagen. The basement membrane can be broken down by extracellular matrix proteases, which are normally under strict regulatory control by their localisation, inhibitors, and autoinhibition [375]. Therefore, malignant cells that use the mesenchymal mode of migration need to activate these proteases to degrade the ECM, which can further lead to the production of bioactive peptides able to mediate migration, angiogenesis, and tumour survival [374]. One subset of matrix proteases are are calcium-activated, zinc-containing matrix metalloproteinases (MMPs) [376].

DNA tumour viruses can promote matrix degradation and tumour invasion. For instance, HPV E7 and HBV HBx induce the expression of matrix transmembrane metalloproteinase 1 (MT1-MMP), which is crucial for the degradation of the ECM and activation of matrix metalloproteinase 2 and 9 (MMP2 and MMP9) [377], [345]. MT1-MMP expression promotes tumour growth and angiogenesis by upregulating expression of the vascular endothelial growth factor (VEGF), and this correlates with invasiveness [378]. Interestingly, induction of MMP gene expression by the WNT/β-catenin signalling pathway and other growth factors stimulates MCPyV infection. These findings could further the hypothesis that MCC risk factors such as UV radiation and ageing, known to stimulate WNT signalling and MMP expression, may promote viral infection, thus driving MCC [220].

### 1.7.4 Colonisation and secondary tumour growth

In order for tumour cells to access remote tissues and organs, they must access the vasculature. Angiogenesis is the process of growing new blood vessels, and is an important step in cancer malignancy. Angiogenesis prevents hypoxia and necrosis of the growing tumour, as well as providing nutrients and removing waste products [374]. VEGF is a key factor in angiogenesis, and some virus oncoproteins, e.g. EBV LMP1, can induce hypoxia-inducible factor 1 alpha (HIF-1$\alpha$) expression, which in turn promotes the expression of VEGF [379].

Entry into the vasculature is known as intravasation, and is initiated by tumour

cells orienting towards the vasculature and migrating towards it [374]. The vast majority of tumour cells are either trapped in the capillary bed or rapidly die in the circulatory system. Only a minority of tumour cells that enter the circulation can exit the vasculature and establish metastases [374]. Exit from the vasculature is extravasation and is largely dependent on the principles involved in intravasation. Establishment of tumour cells in new sites and eventual secondary tumour growth is not necessarily a random process. For example, breast, lung, and prostate cancers preferentially metastasise to bone tissue [380]. This suggests that the organ must be compatible with the metastasising cells, known as the seed and soil hypothesis.

## 1.8 Thesis Aims

The major aim of this thesis was to build upon earlier work in the Whitehouse laboratory investigating the role that MCPyV ST plays in cell motility and cancer metastasis.

MCPyV ST has been previously reported to affect the microtubule network, thereby promoting cell motility [210]. Chapter 3 describes the effect of MCPyV ST on the actin cytoskeleton, including morphological changes in several cell lines and the upregulation of a number of actin-associated proteins in cell culture and MCPyV-positive MCC tumour samples. The morphological changes upon MCPyV ST expression were shown to be filopodia formation, a marker for cell motility. In order to further explore MCPyV ST-induced cell motility, i293-GFP and i293-GFP-ST cell lines were developed, and increased motility upon MCPyV ST expression was confirmed. The Rho-family GTPases, particularly Cdc42 and RhoA, were implicated in MCPyV ST-induced cell motility and filopodia formation, using inhibitors and transdominant mutants.

Chapter 4 expands on the results of Chapter 3, as well as building on previous work implicating protein phosphatases in MCPyV ST-induced cell motility. Polyomavirus ST antigens contain binding sites required for interactions with cellular phosphatases, such as PP2A A$\alpha$ and PP2A A$\beta$ [234], and recent findings also show that MCPyV ST can bind to PP4C [209]. MCPyV ST PP4C non-binding mutants showed reduced cell motility and filopodia formation compared to wild-type MCPyV ST. The effect of phosphorylation on Rho-family GTPases was in-

vestigated, although results showed that MCPyV ST expression does not directly affect the phosphorylation status of Cdc42 or Rac1. Furthermore, the role of integrins was shown to be important in MCPyV ST-induced cell motility and filopodia formation, using inhibitory peptides. Finally, it was shown that integrin β1 shows reduced phosphorylation at the Thr788/789 upon MCPyV ST expression, but not upon the expression of MCPyV ST PP4C non-binding mutants. This led to a model by which the MCPyV ST-PP4C interaction leads to the dephosphorylation of integrin β1, which activates the downstream cell motility pathway.

Chapter 5 implicates chloride channels in MCPyV ST-induced cell motility. Patch clamping showed an increase in ion channel activity upon MCPyV ST expression, and inhibitor studies showed that chloride channels are involved in MCPyV ST-induced cell motility and filopodia formation. In addition, MCPyV ST expression upregulated the protein levels of two intracellular chloride channels, CLIC1 and CLIC4, both in cell culture and MCPyV-positive MCC tumour samples. Knockdown of CLIC1 and CLIC4 reduced MCPyV ST-induced cell motility. Furthermore, both were found to have increased redistribution to the cell surface upon MCPyV ST expression.

These findings stress the importance of the MCPyV ST-PP4C interaction as a potential therapeutic target to treat metastasised MCC. Results also show the first detailed molecular mechanism of MCPyV ST-induced cell motility and filopodia formation, incorporating the activity of integrin receptors and Rho-family GTPases. Furthermore, a novel avenue of chloride channel research in the context of MCC is presented, providing additional potential drug targets for disseminated MCC.

# Chapter 2

# Materials and methods

# 2.1 Materials

## 2.1.1 Chemicals

All analytical grade chemicals and solvents were provided by Sigma-Aldrich®, Melford Laboratories Ltd., and Life Technologies™, unless stated otherwise. Solutions were sterilised using 0.22 μm filters (Millex), or by autoclaving (121°C, 30 min, 15 psi). All water used throughout, unless mentioned otherwise, was deionised water sterilised through an ELGA PURELAB ultra machine (ELGA).

## 2.1.2 Enzymes

All restriction enzymes and supporting reagents were supplied by New England Biolabs® Inc, as well as Alkaline Phosphatase, Calf Intestinal (CIP) and the T4 DNA ligase. Other enzymes and their suppliers are listed in Table 2.1.

**Table 2.1: Enzymes and their suppliers**

| **Enzyme** | **Supplier** |
|---|---|
| Platinum® *Pfx* DNA polymerase | Life Technologies™ |
| Superscript® II reverse transcriptase | Life Technologies™ |
| Proteinase K | Life Technologies™ |
| RNase Out | Life Technologies™ |
| DNA-free™ DNase I treatment kit | Ambion™ |
| 2x SensiMix™ SYBR No-ROX Kit | Bioline Reagents Ltd |

## 2.1.3 Antibodies and beads

Primary antibodies were purchased from a number of suppliers and used at a variety of concentrations, details of which are listed in Table 2.2.

Horseradish peroxidase (HRP) conjugated anti-mouse and anti-rabbit secondary antibodies (Dako™) were used for immunoblotting at concentration of 1:5,000. Alexa-fluor conjugated anti-mouse and anti-rabbit Immunoglobulin G (IgG) antibodies (Life Technologies™) were used at a concentration of 1:500 for immunofluorescence microscopy and at a concentration of 1:200 for flow cytometry. To visualise actin, Alexa-fluor-tagged phalloidin (Life Technologies™), an actin inter-

calating agent, was used at a concentration of 1:10,000. The 2T2 antibody (kindly provided by Dr Christopher Buck, National Cancer Institute, Bethesda, MD), which recognises the DnaJ-domain leader peptides present in both MCPyV ST and MCPyV LT was used at a dilution of 1:5 for immunoblot analysis. Anti-Flag beads in agarose were purchased from Abcam™ and GFP-trap® beads were purchased from Clontech™.

### 2.1.4 Mammalian cell culture reagents

All mammalian tissue culture media and culture supplements were supplied by either Life Technologies™, Lonza™ or Sigma-Aldrich™. Selection antibiotics were provided by either InVivoGen™ or Life Technologies™. Transfection reagents used were Lipofectamine™ 2000 (Life Technologies™) for HEK-293-derived cell lines and *Trans*IT-X2® Dynamic Delivery System (Mirus LLC) for MCC13 cells and siRNA transfections.

### 2.1.5 Cell lines

The HEK 293 Flp-In™ cell line (HEK-239) was purchased from Life Technologies™. The i293-ST-flag (by Laura Knight), i293-GFP and i293-GFP-ST cell lines were derived from the HEK-293 cell line (see Chapter 3). The MCC13 cell line was purchased from Health Protection Agency Culture Collection.

**Table 2.2: Primary antibodies, their origins, their working dilutions, and their suppliers**

| Antibody (catalogue number) | Origin | Working dilution | Supplier |
|---|---|---|---|
| Anti-Flag (F7425) | Rabbit | 1:1,000 (WB), 1:250 (IF) | Sigma-Aldrich® |
| Anti-HA (H9658) | Mouse | 1:1,000 (WB), 1:250 (IF) | Sigma-Aldrich® |
| Anti-Myc (M4439) | Mouse | 1:1,000 (WB), 1:250 (IF) | Sigma-Aldrich® |
| Anti-EE (ab24627) | Mouse | 1:1,000 (WB), 1:250 (IF) | Abcam |
| Anti-GAPDH (ab8245) | Mouse | 1:5,000 (WB) | Abcam |
| Anti-GFP (632569) | Mouse | 1:5,000 (WB) | Living Colours |
| Anti-Arp3 (GTX115345S) | Rabbit | 1:1,000 (WB) | GeneTex |
| Anti-Cortactin (GTX11065) | Rabbit | 1:1,000 (WB) | GeneTex |
| Anti-Cofilin-1 (GTX11062) | Rabbit | 1:1,000 (WB) | GeneTex |
| Anti-GM130 (ab52649) | Rabbit | 1:200 (IF) | Abcam |
| Anti-Rac1/Cdc42 (phospho Ser71) (2461S) | Rabbit | 1:1,000 (WB) | CST |
| Anti-Integrin beta 1 (phospho T788 + T789) (ab5189) | Rabbit | 1:1,000 (WB) | Abcam |
| Anti-CLIC1 (sc-374202)/(ab77214) | Mouse | 1:1,000 (WB), 1:50 (FC) | Santa Cruz Biotech/Abcam |
| Anti-CLIC4 (sc-130723)/(ab183043) | Rabbit | 1:1,000 (WB), 1:50 (FC) | Santa Cruz Biotech/Abcam |
| Rabbit IgG1 isotype (abab172730) | Rabbit | 1:50 (FC) | Abcam |
| Mouse IgG1 isotype (ab91353) | Mouse | 1:50 (FC) | Abcam |

### 2.1.6 Oligonucleotides

Oligonucleotide primers for polymerase chain reaction (PCR) and real-time quantitative PCR (RT-qPCR) were supplied by Sigma-Aldrich®. The list of primers is shown in Table 2.3. Oligo(dT)$_{12–8}$ was supplied by Promega.

**Table 2.3: Oligonucleotides used in cloning or RT-qPCR, including sequences for both forward and reverse oligo pairs**

| Oligonucleotide | Technique | Sequence |
|---|---|---|
| GFP Forward | Cloning | GGG (EcoRV)GAT ATC ATG GTG AGC AAG GGC GAG GAG |
| GFP Reverse | Cloning | CCC (ApaI)GGG CCC CTA GAA AAG GTG CAG ATG CAG |
| GFP-ST Forward | Cloning | GGG (KpnI)GGT ACC ATG GTG AGC AAG GGC GAG GAG |
| GFP-ST Reverse | Cloning | CCC (NotI)GCG GCC GCT TAT CTA GAT CCG GTG GAT CC |
| Arp3 Forward | RT-qPCR | TTC ATC ACC CTC CTT TGA GC |
| Arp3 Reverse | RT-qPCR | GTG TGG TGG ACT GTG GCA |
| Cortactin Forward | RT-qPCR | TAA TCC AAT GAG GAA TTT CCA |
| Cortactin Reverse | RT-qPCR | TAG AGC CTG GTG CCT GGG |
| Cofilin-1 Forward | RT-qPCR | TGA CAC CAT CAG AGA CAG CC |
| Cofilin-1 Reverse | RT-qPCR | TCC TAC TAA ACG GAA GGG GC |
| CLIC1 Forward | RT-qPCR | GAC ACC TTC CAT CTT CAG CAC T |
| CLIC1 Reverse | RT-qPCR | CAA GAA TTC AAA CCC AGC ACT C |
| CLIC4 Forward | RT-qPCR | CAT CCG TTT TGA CTT CAC TGT TG |
| CLIC4 Reverse | RT-qPCR | AGG AGT TGT ATT TAG TGT GAC GA |
| GAPDH Forward | RT-qPCR | TGT CAG TGG TGG ACC TGA C |
| GAPDH Reverse | RT-qPCR | GTG GTC GTT GAG GGC AAT G |

### 2.1.7 Plasmid constructs

Table 2.4 lists plasmid constructs, either purchased or supplied by other laboratories.

**Table 2.4: Plasmid constructs and their sources**

| Construct | Source |
|---|---|
| pcDNA5-FRT-TO | Life Technologies™ |
| pEGFP-C1 | Clontech |
| pEGFP-ST | David Griffiths, University of Leeds, UK |
| pcDNA5-ST-Flag | David Griffiths, University of Leeds, UK |
| pEGFP-ST:R7A | Hussein Abdul-Sada, University of Leeds, UK |
| pEGFP-ST:Δ95–111 | Hussein Abdul-Sada, University of Leeds, UK |
| pEGFP-ST102A | Hussein Abdul-Sada, University of Leeds, UK |
| pEGFP-ST103A | Hussein Abdul-Sada, University of Leeds, UK |
| RL-PP4C-HA | Tse-Hua Tan, National Health Research Institute, Taiwan |
| pcDNA3.1-HA-PP2A Cα | Peter Cron, University of Basel, Switzerland |
| pEGFP-mDia2 | Shuh Narumiya, University of Kyoto, Japan |
| pRK5myc-IRSp53 | Laura Machesky, Beatson Institute for Cancer Research, UK |
| pcDNA3-EGFP-Cdc42-T17N | Gary Bokoch (Addgene plasmid 12976) |
| pcDNA3-EGFP-Rac1-T17N | Klaus Hahn (Addgene plasmid 13721) |
| pcDNA3-EGFP-RhoA-T19N | Gary Bokoch (Addgene plasmid 12967) |
| pcDNA3.1-Cdc42-HA | Ralf Gerhard, MH-Hannover, Germany |
| pcDNA3.1-Rac1-HA | Ralf Gerhard, MH-Hannover, Germany |
| pcDNA3.1-Cdc42S71E-HA | Ralf Gerhard, MH-Hannover, Germany |
| pcDNA3.1-Rac1S71E-HA | Ralf Gerhard, MH-Hannover, Germany |

### 2.1.8 siRNA constructs

siRNA constructs to knock down CLIC1 and CLIC4, as well as the negative control scramble siRNA were purchased from Life Technologies™.

### 2.1.9 Inhibitors

Table 2.5 lists small-molecule and peptide inhibitors from a number of different suppliers.

**Table 2.5: Small molecule inhibitors, their working concentrations and suppliers. i293 cells include HEK-293 and derived cell lines**

| Inhibitor (CAS number) | Working concentration | Supplier |
|---|---|---|
| ML-141 (CAS 71203-35-5) | 15 μM (i293), 30 μM (MCC13) | Tocris Bioscience |
| NSC23766 (CAS 733767-34-5) | 50 μM (i293), 100 μM (MCC13) | Santa Cruz Biotechnology |
| ZCL278 (CAS 587841-73-4) | 50 μM (i293), 100 μM (MCC13) | Tocris Bioscience |
| Rhosin (CAS 1173671-63-0) | 30 μM (i293), 60 μM (MCC13) | Merk Millipore |
| R(+)-IAA-94 (RIAA) (CAS 54197-31-8) | 50 μM (i293), 100 μM (MCC13) | Sigma-Aldrich® |
| NPPB (CAS 107254-86-4) | 25 μM (i293), 50 μM (MCC13) | Tocris Bioscience |
| DIDS (CAS 207233-90-7) | 50 μM (i293), 100 μM (MCC13) | Sigma-Aldrich® |
| RGDS (CAS 91037-65-9) | Various non-toxic | Sigma-Aldrich® |
| RGES (CAS 93674-97-6) | Various non-toxic | AnaSpec |

## 2.2 Methods

### 2.2.1 Molecular cloning

DNA was amplified using PCR and separated by agarose gel electrophoresis, then gel purified and ligated into a linearised double stranded DNA vector. This was done via the Zero Blunt® (Life Technologies$^{TM}$) cloning vector kit. Table 2.4 and Table 2.5 list recombinant vectors and the corresponding primers used for PCR amplification of the inserted fragments. After amplification in chemically competent bacteria and purification of plasmid DNA, presence of inserts was verified by restriction digest analysis. All constructs were sequenced to validate the identity of the inserted fragments. All cloning was carried out using *Escherichia coli* (*E.coli*) strain DH5α (Genotype: $F^-$, Ψ80d*lacZ*ΔM15, Δ(*lacZYA-argF*)U169, *deoR, recA1, endA1, hsdR17*($rk^-$, $mk^+$), *phoA, supE44*, $\lambda^-$, *thi-1, gyrA19,*

*relA1*).

#### 2.2.1.1 PCR amplification

All PCRs were prepared in 0.2 ml Greiner™ PCR tubes in a total volume of 50 µl. PCR mixes were made up according to the manufacturer's protocol (Life Technologies™). For cloning protocols, Platinum® *Pfx* DNA polyomerase was used. Each 50 µl reaction volume contained 0.2mM each of forward and reverse primer, 1× polymerase amplification buffer, 1.5 mM $MgSO_4$, 1–10 ng templated DNA and 1 µl DNA polymerase, with miliQ water making up the full volume. The PCR machine used was the TI-312 model from Therme™. The PCR cycle involved initial denaturation (94°C, 3 min), 35 cycles of denaturation (95°C, 30 s), annealing (55–62°C, 30 s) and extension (68°C, 1 min), followed by a final extension stage (68°C, 10 min). Reactions were done with the heated lid setting on to prevent sample evaporation. PCR products were analysed by agarose gel electrophoresis.

#### 2.2.1.2 DNA gel electrophoresis

Double stranded DNA fragments were separated by agarose gel electrophoresis, using 0.8–1.2% agarose gels. Agarose was dissolved in 1× TBE buffer [90 mM Tris-base, 2 mM EDTA, 80 mM boric acid] with 0.5 µg/ml ethidium bromide. A 6× solution of gel loading buffer [0.25% (w/v) Orange G dye, 30% (v/v) glycerol] was added to DNA samples at 1× final concentration. 1 kb DNA ladder (Life Technologies™) was loaded alongside samples. Electrophoresis was performed at 120 V in 1× TBE buffer using a Sub-Cell® or mini-Sub® Cell horizontal electrophoresis tanks (Bio-Rad Laboratories, Inc.). DNA bands were visualised under ultra-violet light using a transilluminator and images taken using the GeneGenius bio-imaging system (Syngene™).

#### 2.2.1.3 DNA gel purification

Following agarose gel electrophoresis, DNA fragments were excised using a sterile scalpel and purified using the QIAquick gel extraction kit (Qiagen), according to the manufacturer's instructions. The mass of the DNA gel slice was recorded

and then incubated for 10 min at 50°C with 3× gel volumes of buffer QG to melt the agarose, after which 1 gel volume of isopropanol was added to the sample. This solution was then applied to a QIAquick column and centrifuged for 1 min at 13,000 × g at room temperature. DNA bound to the membrane was washed using 750 µl PE buffer and centrifuged at 13,000 × g for 1 min at room temperature. DNA was eluted into a sterile microcentrifuge tube using 30 µl miliQ water, incubated for 1 min and centrifuged at 13,000 × g for 1 min at room temperature. Pure DNA was stored at -20°C.

#### 2.2.1.4 DNA ligation

A typical ligation reaction was set up in a total volume of 10 µl, using 5× T4 DNA ligase buffer, 1 U of T4 DNA ligase (both Life Technologies™), 10–100 ng linearised vector and varied molecular proportions of insert DNA. Reactions were performed at room temperature for 1 h. Ligation efficiency was determined via control reactions lacking either DNA insert or DNA ligase.

#### 2.2.1.5 DNA restriction digestion

DNA restriction digestions were carried out according to the manufacturer's protocol (New England Biolabs, Inc). All reactions were prepared in a volume of 20 µl in 10× CutSmart® buffer, with 1 U of restriction digest enzyme used per 1 µg of DNA. Double digests, using two restriction digest enzymes to minimise DNA loss as a result of purification of DNA, were done when possible. All digestion reactions were performed at 37°C for 2 h. If the DNA was to be subsequently used for ligation, CIP alkaline phosphatase (New England Biolabs, Inc) was added for 1 h at 37°C (1 U per 1 pmol of DNA). Resulting digests were terminated by heat inactivation at 65°C for 20 min. Resulting fragments were analysed by agarose gel electrophoresis (Section 2.2.1.2) and gel purified (Section 2.2.1.3).

#### 2.2.1.6 Preparation of *E. coli* DH5$\alpha$ chemically competent cells

Chemically competent *E. coli* were prepared using a rubidium chloride-based method and liquid cultures were grown in autoclaved Luria broth (LB) [1% (w/v) tryptone, 0.5% (w/v) NaCl, 0.5% (w/v) yeast extract, pH 7.5] and incubated at

37°C with shaking (200 rpm). DH5α cells were streak plated on LB agar plates [1% NaCl, 1% Tryptone, 0.5% Yeast Extract and 1.5% Agar] followed by overnight incubation at 37°C. One colony was used to inoculate 2 ml of LB media and incubated for 5–7 h at 37°C with shaking. 0.5ml of the culture was used to inoculate 50 ml of LB media and the cells were grown at 37°C with shaking until an OD600 of 0.3–0.6 was reached. The cells were subsequently pelleted by centrifugation at 5,000 × g for 5 min at 4°C. The pellet was resuspended in 40 ml ice-cold filter-sterilised TFB1 buffer [30 mM KOAc, 10 mM $CaCl_2$, 50 mM $MnCl_2$, 100 mM RbCl, 15% (v/v) glycerol, adjusted to pH 5.8 with acetic acid] and incubated for 5 min at 4°C. The cells were centrifuged at 5,000 × g for 5 min at 4°C, followed by gentle resuspension of cells in 2 ml ice-cold filter-sterilised TFB2 buffer [10 mM MOPS, 75 mM $CaCl_2$, 10 mM RbCl, 15% (v/v) glycerol, adjusted to pH 6.4 with KOH]. This was followed by incubation at 4°C for 15–60 min and subsequently cells were aliquoted and flash-frozen on dry ice. Competent cells were stored at -80°C.

#### 2.2.1.7 Transformation of chemically competent cells

100 ng of a pre-chilled DNA expression construct was mixed with a 50 µl aliquot of DH5α chemically competent cells, and incubated for 5–30 min at 4°C. Mixtures were then heat shocked for precisely 1 min at 42°C then placed for 2 min at 4°C. 250 µl of LB media were added to the samples and they were incubated with shaking at 37°C for 1 h. Samples were then spread plated onto LB agar containing the appropriate selective antibiotic (either ampicillin or kanamycin) at a concentration of 50 µg/ml. These plates were then incubated overnight at 37°C.

#### 2.2.1.8 Small scale (mini prep) DNA purification

QIAprep Spin miniprep kits (QIAGEN) were used for small scale DNA purification according the the manufacturer's protocol. Single transformed *E. coli* colonies were used to inoculate 5 ml of LB media each with appropriate antibiotic (50 µg/ml), followed by overnight incubation at 37°C with shaking. Cultures was pelleted by centrifugation at 5,000 × g for 5 min at room temperature, then resuspended in 250µl of Buffer P1[50 mM Tris-HCl (pH 8.0), 10 mM EDTA, 100 µg/ml RNaseA] in microcentrifuge tubes. 250 µl of Buffer P2 [200 mM NaOH, 1% (w/v) SDS] were added for cell lysis and the tubes was inverted 4–6 times.

350 µl of Buffer N3 [4.2 M Gu-HCl, 0.9 M KOAc (pH 4.8)] were added to neutralise the samples and the tubes were inverted again 4–6 times. The samples were centrifuged for 10 min at top speed in a table-top microcentrifuge. Supernatants were then transferred to QIAprep spin columns and centrifuged for 1 min at top speed to bind DNA. The columns were washed with 0.75 ml buffer PE [10 mM Tris-HCl (pH 7.5), 80% ethanol], centrifuged for 1 min at top speed, then the supernatants were emptied and the columns were re-centrifuged for 1 min to collect residual buffer. DNA was eluted into clean 1.5 ml microcentrifuge tubes with miliQ water (30 µl), incubated at room temperature for 1 min, then centrifuged for 1 min. Purity and concentration of DNA was measured using a NanoDrop-1000 spectrophotometer (NanoDrop Technologies) at 260/280 nm.

#### 2.2.1.9 Large scale (maxi prep) DNA purification

QIAGEN plasmid maxi kits were used for large scale DNA purification according to the manufacturer's protocol. Single transformed *E. coli* colonies were used to inoculate 5 ml of LB media each with appropriate antibiotic (50 µg/ml), followed by incubation at 37°C for 8 h with shaking. Day cultures were added to 200 ml LB media and incubated at 37°C overnight with shaking. The culture was then centrifuged at 5,000 × g for 20 min at 4°C. The cell pellet was then resuspended in 10 ml Buffer P1 [10 mM EDTA, 50 mM Tris-HCl (pH 8.0), 100 µg/ml RNaseA] and 10 ml Buffer P2 [1% SDS, 200 mM NaOH], then inverted 10 times and incubated at room temperature for 5 min. 10 ml of pre-chilled Buffer P3 [3 M KOAc, pH 5.5] was added, the mixture was inverted 10 times, and incubated at 4°C. Mixtures were centrifuged at 5,000 × g for 30 min at 4°C. The solution was added to a pre-equilibrated QIAGEN-tip 500 column and allowed to drain by gravity to bind DNA. The column was equilibrated with Buffer QBT [50 mM MOPS (pH 7.0), 750 mM NaCl, 0.15% (v/v) Triton X-100]. The column resin was subsequently washed twice with 30 ml Buffer QC [50 mM MOPS (pH 7.0), 1 M NaCl, 15% (v/v) isopropanol], followed by DNA elution by addition of 15 ml Buffer QF [15% (v/v) isopropanol, 1.25 M NaCl, 50 mM Tris-HCl]. To precipitate DNA, 10.5 ml isopropanol was added to the eluted solution and pelleted by centrifugation at 5,000 × g for 30 min at 4°C. The pellet was washed with 5 ml 75% ethanol and re-centrifuged for at 5,000 × g for 10 min at 4°C. The DNA pellet was subsequently air-dried and resuspended in 100–200 µl miliQ water. Purity and concentration

of DNA was measured using a NanoDrop-1000 spectrophotometer (NanoDrop Technologies) at 260/280 nm.

#### 2.2.1.10 DNA sequencing

DNA sequencing was done by GATC, London. Plasmid DNA was sent at a concentration of 30 ng/µl in a total volume of 50 µl. Sequencing data was analysed using BioEdit sequence alignment editor and ClustalW (EBI, UK) against corresponding reference sequences obtained from the NCBI database.

### 2.2.2 Mammalian cell culture experiments

HEK-293 Flp-In$^{TM}$, i293-ST-Flag, i293-GFP, i293-GFP-ST, and Cos7 cell lines were maintained in Dulbecco modified eagle medium (DMEM) (Life Technologies$^{TM}$), supplemented with 5 U/ml penicillin and streptomycin and 10% (v/v) foetal calf serum (FCS), (referred to as 10% DMEM). HEK-293 Flp-In$^{TM}$ cells were maintained in 10% DMEM supplemented with 100 µg/ml zeocin (Life Technologies$^{TM}$). i293-ST-Flag, i293-GFP and i293-GFP-ST cells lines were maintained in 10% DMEM supplemented with 100 µg/ml Hygromycin B (Life Technologies$^{TM}$). All above-mentioned cell lines were passaged every 3-4 days, removing the confluent cells layer using kinetic force from the surface of a 75 $cm^3$ tissue culture vessel (Sigma-Aldrich®) and split in a 1:10 to 1:20 ratio into new flasks made up to a total volume of 20 ml using 10% DMEM and supplemented with the corresponding selective antibiotic.

MCC13 cells were maintained in Roswell Park Memorial Institute (RPMI) media, supplemented with 5 U/ml penicillin and streptomycin and either 15% FCS or 10% FCS, respectively (15% RPMI or 10% RPMI). Cells were passaged every 3-4 days, removing the confluent cell layer by trypsinisation or using non-trypsin EDTA cell resuspension buffer (Life Technologies$^{TM}$), and the cells were subsequently split 1:20 into new flask containing 15% RPMI.

All cell lines were incubated in an InCu saFe Copper-Enriched Stainless Steel $CO_2$ incubator (Panasonic), with 5% $CO_2$ concentration, unless otherwise stated.

For long term storage, cells were aliquoted into 1.8 ml Cryotubes$^{TM}$ (NUNC$^{TM}$) at $1 \times 10^6$ cells/ml. Cells were resuspended in freezing media [90% (v/v) FCS,

10% (v/v) DMSO]. Cryotubes were then stored at -80°C for 24 h in an isopropanol containing freeze flask and transferred to liquid nitrogen for long term storage.

#### 2.2.2.1 Generating inducible cell lines

In order to generate cell lines capable of inducible expression of EGFP or GFP-tagged MCPyV ST (EGFP-ST), HEK-293 Flp-In™ cells were co-transfected with EGFP-C1 or EGFP-ST-C1 respectively and pPGK/Flip/ObpA (kindly supplied by M.Walsh, University of Sheffield, UK) at a 1:3 ratio, using 0.5 μg of EGFP or EGFP-ST and 1.5 μg pPGK/Flip/ObpA. The cell line was selected and maintained using Hygromycin B resistance at concentration of 100 μg/ml. Cells were monoclonally selected to ensure the resulting cell line was derived from a single cell colony.

#### 2.2.2.2 Induction of inducible cell lines

3 x $10^5$ cells (i293-ST-flag, i293-GFP or i293-GFP-ST) were seeded per 6-well plate in 2 ml 10% DMEM. 24 h later, 4 μl doxyclycline hyclate (Life Technologies™) was added to 2ml 10% DMEM and mixed, resulting in a final concentration of 2 μg/ml per well. Cells were grown under induction for 24, 48, or 72 h.

#### 2.2.2.3 Plasmid DNA transfection

A standard transfection protocol was followed for all assays unless stated otherwise. Approximately 5 x $10^5$ cells were seeded into a 6-well (35 mM diameter) plate 24 hours before transfection, to allow cells to grow to 70–80% confluence at transfection. All plasmid DNA transfections of HEK-293 and derived cell lines used Lipofectamine™ 2000, according to the manufacturer's protocol. For each reaction (1 well of a 6-well plate), 3 μl Lipofectamine™ 2000 was diluted in 100 μl Opti-MEM® (Life Technologies™) and mixed with 1 μg total plasmid DNA diluted in 100 μl Opti-MEM®. This mixture was incubated for 20 min at room temperature. Cell media was replaced with 1 ml of Opti-MEM®. After incubation, the transfection mixture was added to cells drop-wise. Cells were incubated at 37°C overnight. Subsequently Opti-MEM® was replaced with 10% DMEM and transfected DNA was allowed to express for 24, 48, or 72 h. All plasmid

DNA transfections of MCC13 cells used *Trans*IT-X2® Dynamic Delivery System (Mirus LLC), according to the manufacturer's protocol. For each reaction (1 well of a 6-well plate), 7.5 µl of the transfection reagent was mixed with 2.5 µg of plasmid DNA in 250 µl Opti-MEM®, incubated for 30 min and added drop-wise to cells in 1 ml/well Opti-MEM®. Cells were incubated at 37°C overnight. Subsequently Opti-MEM® was replaced with 15% RPMI and transfected DNA was allowed to express for 24, 48, or 72 h.

#### 2.2.2.4 siRNA transfection

A standard siRNA transfection protocol was followed for all assays unless stated otherwise. Approximately $3 \times 10^5$ cells were seeded into a 6-well plate 24 h before transfection. For each reaction, 10 nM of siRNA and 7.5 µl of *Trans*IT-X2® Dynamic Delivery System (Mirus LLC) were mixed in 250 µl of Opti-MEM®, incubated for 30 min and added drop-wise to cells in 1 ml/well Opti-MEM®. Cells were incubated at 37°C overnight. Subsequently Opti-MEM® was replaced with appropriate media and RNAi was allowed to proceed for at least 72 h.

#### 2.2.2.5 Addition of inhibitors

Approximately $5 \times 10^5$ cells were seeded into 6-well plates, and transfected and/or induced if appropriate. 24 h before harvesting, appropriate concentrations of inhibitors dissolved in DMSO were added (up to a final concentration of 1 µl/ml DMSO). 1 µl/ml of DMSO was also added to control cells. Otherwise, when cells were seeded into 96-well plates or otherwise, the number of cells and the amounts of inhibitors were adjusted accordingly.

### 2.2.3 Cell viability (MTS) assay

Approximately 5,000 cells per well were seeded into 96-well plates in quintuplicate for each treatment condition. Negative controls of cell-free medium, untreated cells and 1 µl/ml DMSO-treated cells were included. Cells were grown overnight and appropriately treated the following day. 24 h later, 20µl of CellTitre 96® AQueous One Solution Cell Proliferation Assay reagent (Promega) was added to each well. Cells were then incubated for approximately 1 h at 37°C, and

absorbance was read at 490 nm using the Infinite® F50 absorbance microplate reader (Tecan).

### 2.2.4 Immunofluorescence

Glass coverslips were sterilised in 100% ethanol and, placed in individual wells of a 6-well plate, and air-dried before were treatment with 0.01% poly-L-lysine solution (Life Technologies$^{TM}$) for 5 min at room temperature. Coverslips were washed 3× with 1 ml PBS and 3× with the appropriate culture medium. Approximately 2–3 × $10^5$ cells were seeded onto coverslips in their respective media and incubated for overnight at 37°C. Cells were either transfected, induced or both. Following the appropriate incubation time and manipulation, media was removed and the cell monolayer washed 3× in 2 ml PBS, followed by fixation in 2 ml PBS containing 4% (v/v) paraformaldehyde for 15 min at room temperature. The cell monolayer was washed 3× with 2 ml PBS and permeabilised (if appropriate) with 2 ml PBS containing 1% (v/v) Triton X-100 for 15 min. Cells were washed a further 3× in 2 ml PBS and blocked for 1 h at 37°C in 2 ml blocking solution [PBS, 1% (w/v) bovine serum albumin (BSA)]. After blocking, coverslips were transferred to a humidity chamber and incubated for 1 h at 37°C or overnight at 4°C with an appropriate primary antibody (see Table 2.2) diluted in blocking solution. Following incubation, cells were washed gently 5× with PBS and incubated with the appropriate AlexaFluor conjugated secondary antibody for 1 h at 37°C. Subsequently, cells were washed gently 5× with PBS and mounted on microscope slides using VECTORSHIELD® with DAPI mounting media (Vector Laboratories) to stain the nucleus. Cells were then visualised using the LSM700 META laser scanning inverted confocal microscope and ZEN 2011 image analysis software (Zeiss).

#### 2.2.4.1 Staining the actin cytoskeleton

The immunofluorescence microscopy protocol was followed. An actin stain, rhodamine phalloidin (Life Technologies$^{TM}$) was used at a 1:10,000 dilution in 1% BSA at room temperature for 20 min. This stain was either used after washing cells following permeabilisation with 1% (v/v) Triton X-100, if antibody staining was not required or following secondary antibody exposure. Cells were then

gently washed 5× with PBS and mounted using VECTORSHIELD® with DAPI.

### 2.2.5 Protein expression and immunoblotting

#### 2.2.5.1 Preparation of mammalian cell lysates

Cells were removed from the tissue culture plates by pipetting with 1 ml PBS. MCC13 cells were removed from the surface of the culture plate by scraping in 1 ml PBS. The cells suspension was then centrifuged at 3,500 × g at room temperature, washed 3× in 1 ml PBS, and re-centrifuged. The cell pellet was then resuspended and lysed in 100 µl pre-chilled RIPA lysis buffer [150 nM Tris-HCl, 50 mM Tris base ultrapure, 1% NP40, pH 7.6, supplemented with 1× protease inhibitor EDTA (Roche)]. Fresh 1× Phosphatase Inhibitor Cocktail 3 (Sigma-Aldrich®) was added if cells were to be probed for phosphorylated proteins. The samples were immediately mixed and incubated on ice for 30 min, with mixing every 5 min. The lysates were then centrifuged in a centrifuge at 13,200 × g for 10 min at 4°C. The supernatant was transferred to a clean microcentrifuge tube and stored at -20°C until further use.

#### 2.2.5.2 Determination of protein concentration

All protein concentrations were determined using the DC Protein Assay Kit (Bio-Rad Laboratories, Inc.), according to the manufacturer's protocol. 5 dilutions of a protein standard (BSA) were prepared in a 96-well plate, with concentrations ranging from 0.2 mg/ml to 1.5 mg/ml. This was used to prepare a standard curve for each plate measurement. The standard was prepared in the same buffer as the test protein samples to ensure accuracy of the standard curve. 5 µl of each standard and test sample were pipetted into the 96-well plate in triplicate. 20 µl of Reagent S was mixed thoroughly with 1 ml Reagent A, and 25 µl of the mixed solution were then added to each individual well, followed by 200 µl Solution B. The plate was then agitated for 20 min and the absorbance read at 620 nm using the Infinite® F50 absorbance microplate reader (Tecan). Protein concentrations of the test samples were determined by plotting a standard curve using the standard dilution series.

#### 2.2.5.3 Preparation of tumour and cell samples

Frozen MCC tumour samples (originally obtained from Professor Julia Newton-Bishop at St James University Hospital, Leeds) were physically homogenised using a mortar and pestle, then lysed for 1 hr using 10 ml pre-chilled RIPA lysis buffer, sonicated twice for 5 min (20 s on/10 s off), then lysed for further 30 min with mixing every 5 mins. The lysates were then centrifuged in a centrifuge at 13,200 $\times$ g for 10 min at 4°C. The supernatant was transferred to a clean micro-centrifuge tube and stored at -20°C until further use. A fresh skin sample from a consenting healthy donor (obtained by Professor Eric Blair at University of Leeds) was treated identically to the frozen tumour samples and used as the control in further experiments.

#### 2.2.5.4 Tris-glycine SDS-polyacrylamide gel electrophoresis (PAGE)

Tris-glycine polyacrylamide running gels (Table 2.6) were overlaid with stacking gels [per 1 ml: 170 µl acrylamide/bis acrylamide solution 37.5:1 (Severn Biotech Ltd), 130 µl 0.25M Tris-HCL (pH 6.8), 10 µl 10% (w/v) SDS, 670 µl miliQ water, 10 µl 10% ammonium persulfate, 2 µl TEMED].

**Table 2.6: Reagents and their volumes to prepare a range of tris-glycine polyacrylamide running gels**

| **Reagent** | **6%** | **8%** | **10%** | **12%** |
|---|---|---|---|---|
| milliQ water | 2.6 ml | 2.3 ml | 1.9 ml | 1.6 ml |
| Acrylamide/bisacrylamide (37.5:1) | 1 ml | 1.3 ml | 1.7 ml | 2.0 ml |
| 1 M Tris-HCl (pH 8.8) | 1.3 ml | 1.3ml | 1.3 ml | 1.3 ml |
| 10% (w/v) SDS | 50 µl | 50 µl | 50 µl | 50 µl |
| 10% (w/v) ammonium persuflate | 50 µl | 50 µl | 50 µl | 50 µl |
| TEMED | 4 µl | 3 µl | 2 µl | 2 µl |

2$\times$ protein solubilising buffer [50 mM Tris-HCl (pH 6.8), 2% (w/v) SDS, 20% (v/v) glycerol, 50 µg/ml Bromophenol Blue and 10 mM DTT] was added to protein lysates and the samples were denatured by heating at 95°C for 3–5 min. Heated samples were loaded onto appropriate polyacrylamide gels. Samples were loaded next to pre-stained protein ladder (Bio-Rad Laboratories, Inc.), as

an indicator of molecular weight (kDa). Prior to sample loading, gels were immersed in Tris-glycine running buffer [0.25 M Tris-base, 192 mM glycine, 0.1% (w/v) SDS]. Gels were run at 180 V for $\tilde{4}5$ min or until the solubilising buffer reached the bottom to the gel. All SDS-PAGE was carried out using a Bio-Rad$^{TM}$ Mini-PROTEAN 3 cell (Bio-Rad Laboratories, Inc.), set up according to the manufacturer's instructions. Proteins were then analysed by western blot.

#### 2.2.5.5 Western (immuno-) blotting

Proteins from SDS-PAGE gels were transferred onto Thermo Scientific$^{TM}$ Pierce$^{TM}$ Nitrocellulose membranes (Thermo Fisher Scientific Inc.), using the Bio-Rad Mini Trans-Blot Electrophoretic Transfer Cell (Bio-Rad Laboratories, Inc.), according to the manufacturer's protocol. 4 pieces of Whatman 3 mm filter paper, 1 SDS-PAGE gels and one nitrocellulose membrane were soaked in transfer buffer [25 mM Tris-base, 190 mM glycine, 20% (v/v) methanol] and placed in a cassette in sequential order. Proteins were transferred from the gel to the membrane at 100 V for 1–2 h, depending upon protein size, followed by incubation of the membrane in 5% TBS-Tween blocking buffer [500 mM NaCl, 20 mM Tris, 0.1% (v/v) Tween-20, 5% non-fat dried milk (Marvel)] at room temperature for 1 h. Subsequently, the membrane was incubated in the corresponding primary antibody (See Table 2.3 for concentrations) diluted in 1% TBS-Tween blocking buffer [500 mM NaCl, 20 mM Tris, 0.1% (v/v) Tween-20, 1% non-fat dried milk (Marvel)] overnight at 4°C. The membranes were then washed 3× for 5 min in 1× TBS-tween buffer [20 mM Tris, 0.1% Tween-20, 500 mM NaCl], and incubated for 1 h at room temperature in the appropriate secondary antibody. The membranes were then washed 3× for 5 min in 1× TBS-tween solution. Protein bands were then visualised by enhanced chemiluminescence using EZ-ECL enhancer solutions A and B kit (Geneflow$^{TM}$) (1:1 ratio) and exposed to ECL$^{TM}$ hyperfilm (Amersham$^{TM}$). Films were developed using a Konica SRX-101A developer. All incubations and washes were done with agitation.

### 2.2.6 Co-immunoprecipitation

MCC13 cells were seeded at $5 \times 10^5$ and transfected for 12 h. 24 h later cells were harvested and lysed in 1 ml lysis buffer supplemented with protease inhibitor

cocktail. Cell lysates were then incubated with GFP-TRAP A beads (Chromotek) for 2 h at room temperature. Beads were then washed 3× in ice-cold PBS, resuspended in 2× protein solubilising buffer and analysed by immunoblotting with appropriate antibodies.

### 2.2.7 Cell motility experiments

#### 2.2.7.1 Life cell imaging

i293-GFP, i293-GFP-ST or MCC13 cells were seed at a density of $1 \times 10^5$ cells per well in 6-well plates, grown overnight, and either induced with doxycycline hyclate at 2 μg/ml or transfected with 1 or 2.5 μg of plasmid DNA per well using the appropriate transfection reagent. Cells were incubated for 24 h at 37°C, and, if applicable, inhibitors were added at appropriate concentrations for another 24 h. Cells were then imaged using the IncuCyte$^{TM}$ Live-Cell Imaging System (Essen BioScience), as per the manufacturer's protocol. Imaging was performed every 30 min over the course of 24 or 48 h and cell motility was then analysed using Image J software.

#### 2.2.7.2 Filopodia analysis

Cells were prepared as described for immunofluorescence, and, if appropriate, induced, transfected and/or treated with inhibitors. Cells were visualised visualised using the LSM700 META laser scanning inverted confocal microscope (n = 75 for each condition), and filopodia were counted and their length measured using ImageJ software.

#### 2.2.7.3 Polarity assay

i293-GFP and i293-GFP-ST were seeded at a density of $5 \times 10^5$ on coverslips. After 24 hours cells were either induced with 2 μg/ml doxycycline hyclate or transfected. 6 h pre-fixation, cells were scratched using a p200 tip across the coverslip, washed 3× with media and left to move back into the wound gap. Cells were then fixed and stained for Golgi structures. Cells were visualised visualised using the LSM700 META laser scanning inverted confocal microscope (n = 75 for

each condition) and scored for polarity if the Golgi apparatus was seen in front of the nucleus towards the wound gap, using ZEN 2011 image analysis software (Zeiss).

#### 2.2.7.4 Haptotaxis migration assay

HEK-293 Flp-In®, i293-GFP and i293-GFP-ST cells were seeded at $3 \times 10^5$ per 6-well plate, and induced with doxycycline hyclate if appropriate for 24 h. Cells were then treated with 1 µl/ml DMSO or appropriate concentrations of chloride-channel inhibitors (Table 2.5) for 24 h. $1 \times 10^6$ cell suspensions in triplicate were prepared in serum-free DMEM containing the appropriate inhibitors. CytoSelect™ 24-well Haptotaxis Assay, Collagen I plates (Cell Biolabs, Inc) were prepared according to the manufacturer's instructions. 500 µl 10% DMEM was added to the bottom of the wells and 300 µl of cell suspension was added to the insert. Cells were allowed to migrate towards the FCS chemoattractant for 24 h. Then media was aspirated, inserts washed, transferred to clean wells and stained for 10 min at room temperature in 400 µl of the Cell Stain Solution provided. Inserts were then transferred to clean wells with 200 µl Cell Extraction Solution and agitated for 10 min. 100 µl of each sample was transferred to a 96-well plate and read at 560 nm using the Infinite® F50 absorbance microplate reader (Tecan).

### 2.2.8 Cell surface protein analysis

#### 2.2.8.1 Flow cytometry

HEK-293 Flp-In® cells were seeded at $3 \times 10^5$ density in 6-well plates, then mock transfected or transfected with 1 µg EGFP or EGFP-ST per well using the standard Lipofectamine®2000 protocol for 6 h. 24 h post-transfection cells were harvested, washed with ice-cold PBS and resuspended at 1–2 $\times$ $10^6$ cells/ml in staining buffer [PBS, 10% FCS, 1% (w/v) sodium azide]. Cells were then fixed with 2% paraformaldehyde for 10 min at 37°C, centrifuged at 1,000 $\times$ g and washed 3$\times$ with staining buffer. Cells were then incubated with appropriate dilutions of primary antibody or staining buffer only for 1 h at room temperature in the dark, washed 3$\times$ with staining buffer and incubated with Alexa-Fluor-tagged secondary antibody or staining buffer only for 1 h at room temperature in the

dark. Cells were then washed 3× with staining buffer and finally resuspended in 500 µl of staining buffer. Flow cytometry was performed immediately after staining. Flow cytometry experiments were performed in triplicate, and each experiment included unstained and secondary-only stained controls. Isotype controls were also performed for all antibodies used and the gates were set according to Figure 2.1.

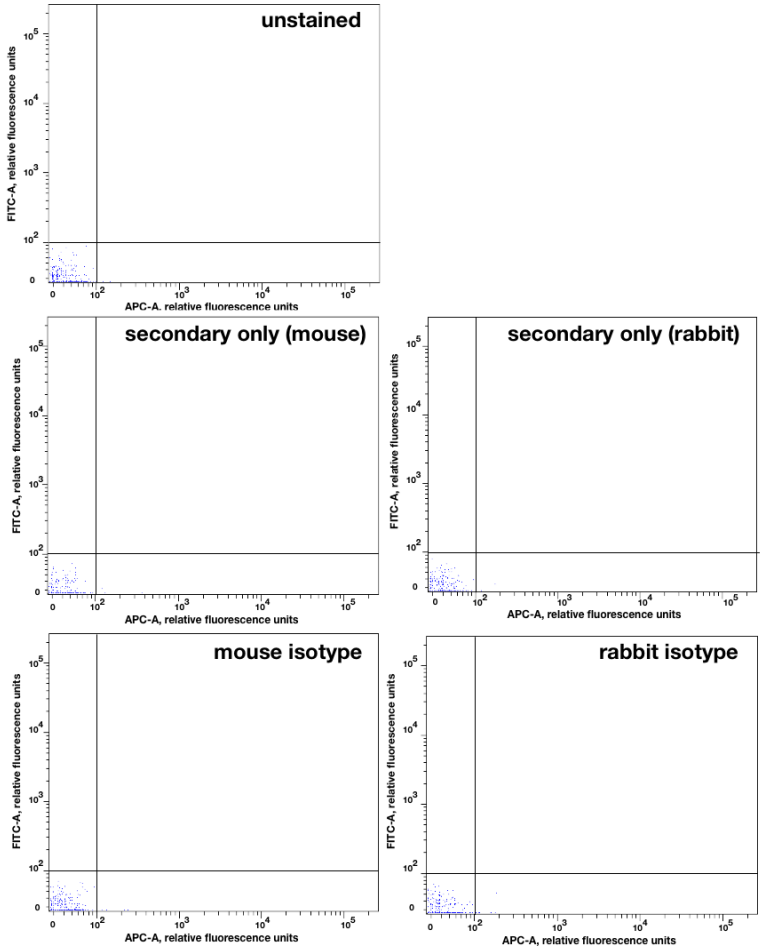


**Figure 2.1: Isotype controls (rabbit and mouse) for flow cytometry experiments.** HEK-293 cells were grown in 6-well plates for 24 h. Cells were fixed with 2% paraformaldehyde, then stained with rabbit and mouse isotype control antibodies before performing flow cytometry. FITC-A corresponds to EGFP fluorescence and APC-A corresponds to secondary antibody staining.

### 2.2.9 Patch-clamping assay

HEK-293 cells were seeded at 3 $\times$ $10^5$ in 6-well plates, then transfected with 1 µg EGFP or EGFP-ST using Trans-IT-LT1 reagent (Mirus) and studied by electrophysiology 2–5 days later. Patch pipettes were pulled from thin-walled filamented borosilicate glass capillaries (Harvard Apparatus) and had resistances between 2–4 MΩ in the experimental solutions. The intracellular pipette solution contained 135 mM KCl, 20 mM NaCl, 1 mM $CaCI_2$, 1 mM $MgCI_2$, 11 mM EGTA, 10mM HEPES, pH 7.3, the extracellular bath solution contained 140 mM NaCI, 5 mM KOH, 2 mM $CaCI_2$, 1 mM $MgCI_2$, 10 mM HEPES, 30 mM D-mannitol, pH 7.4. Membrane currents were recorded from single fluorescing cells using the whole-cell configuration of the patch clamp technique using a HEKA EPC-10 amplifier under the control of PatchMaster software (HEKA Electronik), filtered at 3 kHz and digitised at 10 kHz. Cells were held at -80 mV and pulses were applied to potentials between -100 and +100 mV. Current-voltage relationships were constructed for each cell by plotting the steady-state current at the end of the pulse against the pipette potential.

### 2.2.10 Gene expression analysis

#### 2.2.10.1 RNA extraction

i293-ST-Flag cells were seeded at a density of 4 $\times$ $10^5$ in triplicate per condition (uninduced and induced) and induced for 48 h with 2 µg/ml doxycycline hyclate. Cells were then directly lysed by addition of 1ml TRIzol reagent (Life Technologies$^{TM}$) per well, mixed by pipetting in an RNase-free microcentrifuge tube, and incubated at room temperature for 5 min. Subsequently, 200 µl chloroform was added per sample, and samples were vortexed for 15 s and incubated at room temperature for 3 min. Samples were then centrifuged at 12,000 $\times$ g for 15 min at 4°C. The top aqueous/colourless phase ($\tilde{5}$00 µl) was transferred to a fresh RNase-free microcentrifuge tube. RNA was then precipitated by adding 500 µl isopropanol and incubating samples at room temperature for 10 min before centrifugation at 12,000 $\times$ g for 10 min at 4°C. The supernatants were carefully aspirated and the pellets washed in 1 ml 75% ethanol and briefly vortexed, followed by centrifugation at 7,500 $\times$ g for 5 min at 4°C. The supernatants were once again aspirated and the pellets air-dried for 5 min. The pellets were resuspended

in 49 µl DEPC-treated water and 1µl RNaseOUT™ (Life Technologies™) and incubated at 57°C for 10 min. The RNA was stored at -80°C or treated immediately with DNase I treated and reverse transcribed.

#### 2.2.10.2 DNase I treatment

A DNase I kit (Ambion™) was used to remove contaminating DNA from extracted RNA samples as per the manufacturer's protocol. 0.1 volume of DNase reaction buffer and 0.5 µl Amplification Grade DNase I were added to each sample, gently mixed and incubated for 30 min. After incubation, 0.1 volume of Stop solution was added, samples were mixed thoroughly and heated at 70°C for 10 min. Samples were then briefly chilled on ice. The RNA concentration was measured using a NanoDrop-1000 spectrophotometer (NanoDrop Technologies) at 280 nm wavelength. Samples diluted in RNase-free water to a final concentration of 50 ng/µl.

#### 2.2.10.3 Reverse transcription

Superscript™ II Reverse Transcriptase (Life Technologies™) was used to synthesise cDNA from the total extracted cellular RNA, according to the manufacturer's protocol. The initial sample mixture contained 1 µg DNase I treated RNA , 1 µl 10 mM dNTP mix, 1 µl Oligo(dT)12-18 primer and made up to a total volume of 12 µl. Samples were then mixed and incubated at 65°C for 5 minutes and then quick-chilled on ice. Following this, 4 µl 5X First-Strand buffer, 2 µl 0.1 M DTT, 1 µl RNaseOUT™ and 1 µl Superscript™ II Reverse Transcriptase were added per sample. Samples were mixed and incubated at 42°C for 50 minutes, followed by enzyme inactivation at 70°C for 15 minutes. This was then followed by ethanol precipitation to remove dNTPs.

#### 2.2.10.4 Ethanol precipitation

2 µl 3 M sodium acetate (pH 5.6) and 60 µl ice cold 100% ethanol were added to each cDNA sample (Section 2.2.10.3) and mixed, followed by incubation at 4°C for 10 minutes. Samples were then centrifuged at 12,000 × g for 10 minutes at 4°C. The pellets were washed in 1 ml ice cold 100% ethanol and centrifuged

again at 12,000 × g for 10 minutes at 4°C. The supernatants were removed and the pellets briefly air-dried. The cDNA pellets were resuspened in 20 µl nuclease-free water (Sigma$^{TM}$). The cDNA concentration was measured using a NanoDrop-1000 spectrophotometer (NanoDrop Technologies) at 260 mM and diluted to 2 ng/µl in nuclease-free water.

#### 2.2.10.5 RT-qPCR

RT-qPCR samples were set up in Corbett tubes and a pre-chilled Corbett tube rack (Corbett Life Sciences). Each primer pair were added in duplicate to RNA samples extracted at different times (biological replicates). The PCR master mix contained the following for each reaction: 10 µl SensiMixPlus SYBR$^{TM}$ No-ROX (Quantace$^{TM}$), 1 µl primer mix (10 µM of both forward and reverse primers), 5 µl nuclease-free water and 4 µl cDNA (10 ng final amount). The PCRs were performed using a Rotor-Gene$^{TM}$ Q 5plex MRM Platform (Qiagen$^{TM}$) using a 3 Step with Melt program. A typical PCR cycle parameter consisted of 95°C for 10 min and then 35 cycles of: 95°C for 15 s, 60°C for 30 s, and 72°C for 20 s. Quantitative analysis was then performed using the comparative CT method as previously described [381].

### 2.2.11 Statistical analysis

All experiments where statistical significance is given have biological replicates of n = 3 or more. Between-condition significance was measured using the Student's two-tailed t-test for independent samples. Data is presented as bar charts with standard deviation error bars.

# Chapter 3

# Merkel cell polyomavirus small T antigen enhances cell motility via Rho-GTPase-induced filopodia formation

## 3.1 Introduction

MCPyV has been established as the causative agent of the vast majority of MCCs. It is clonally integrated in genomes of both primary and secondary MCC tumours [20], and MCPyV LT derived from MCC tumours carries a tumour-specific mutation which renders the virus replication-incompetent [42]. MCC is a highly aggressive neuroendocrine cancer, with a propensity to spread via the lymphatic system [382]. It has a poor 5 year prognosis [193], likely due to its metastatic character.

The spread of cancer cells from the primary solid tumour to remote sites, leading to the growth of secondary tumours, is a key problem facing cancer treatment. This process, known as metastasis, results in more than 90% of cancer associated-deaths [383]. The clinical importance of cancer metastasis cannot be overstated, and while many aspects have yet to be elucidated, cell motility is considered one of the major underlying processes.

Cell motility is complex, involving multiple signalling cascades and a large variety of cellular factors. An important component of cell motility is the actin cytoskeleton, with a number of actin-associated proteins implicated in tumour progression in a variety of different cancers [384] [385] [386]. In addition, the actin cytoskeleton provides the backbone of motile cellular structures, such as lamellipodia, filopodia, or invadopodia. Filopodia, for instance, are structures used to explore the immediate surroundings of a cell. They are considered to be early markers of cell motility [387]. Therefore appearance of filopodia around the cellular periphery can indicate a motile phenotype.

Cell motility requires the remodelling of the actin cytoskeleton. This function is controlled by the Rho-family GTPases, a large group of signal mediators that are vitally important in the motility pathway. The Rho-family GTPases affect both the microtubule network and the actin cytoskeleton [388]. The three most widely studied Rho-family GTPases are Cdc42, Rac1 and RhoA. Simply put, Cdc42 is involved in filopodia formation [389], Rac1 in lamellipodia formation [390], and RhoA in stress fibre formation [297]. While this classification is broadly valid, recent research has shown that the functions of Rho-family GTPases are more complex, involving cross-talk in the cell motility cascade. For instance, filopodia formation is not exclusively due to Cdc42 signalling [391]. Importantly, Rho-

family GTPases are not only vital for the normal functioning of many different cell types, but also play a role in cancer [392] [393] [394]. For example, overexpression of RhoA has been observed in a number malignancies, including breast, colon, lung, and gastric cancers [395] [396] [397].

This chapter begins with the initial observation of changes to the actin cytoskeleton, actin-associated protein expression and cell motility upon MCPyV ST expression. It then focuses on the involvement of the Rho-family GTPases in MCPyV ST-induced cell motility and filopodia formation.

## 3.2 Quantitative proteomic analysis shows MCPyV ST expression affects actin-associated proteins

Regulation of the actin cytoskeleton and associated proteins is an integral part of cell motility. A SILAC-based quantitative proteomic approach was undertaken to determine potential alterations in the host cell proteome upon inducible MCPyV ST expression in a HEK-293-derived i293-ST cell line (previously described in [210]). The microtubule network and the actin cytoskeleton were both observed to be upregulated upon MCPyV ST expression. For example MCPyV ST expression results in the upregulation of the microtubule-associated protein, stathmin, which affects microtubule dissociation [398] [210]. Moreover, the same approach highlighted that a number of proteins associated with the regulation of the actin cytoskeleton were also upregulated upon MCPyV ST expression. These proteins are shown in Table 3.1.

In order to confirm increased levels in actin-associated proteins, i293-ST cells remained uninduced or were induced with doxycycline hyclate for 48 h. In addition, MCC13 and Cos7 cells were transfected with EGFP or EGFP-ST. Cell lysates were analysed by immunoblotting, and upregulation of actin-associated proteins Arp3, cortactin, and cofilin-1 was confirmed upon expression of MCPyV ST, both in 293 and in MCC13 cells, while cortactin and cofilin-1 upregulation was further confirmed in the non-human Cos7 cell line (Figure 3.1A). Arp3 increased 4-fold in i293-ST and MCC13 cells, cortactin increased 4-fold in i293-ST cells, 3-fold in MCC13 cells, and 5-fold in Cos7 cells, while cofilin-1 increased 2-fold in i293-ST and Cos7 cells, and 4-fold in MCC13 cells (Figure 3.1B).

**Table 3.1: Quantitative proteomic analysis shows an increase in actin-associated protein levels upon MCPyV ST expression**

| Protein | Fold change over uninduced | Peptide hits | Function |
|---|---|---|---|
| Cofilin-1 | 5.1 | 16 | Promotes rapid actin filament turnover [399] |
| Cortactin | 3.7 | 17 | Contributes to the organisation of the actin cytoskeleton and cell structure [287] |
| Actin-related protein 2/3 complex subunits | 3.9 | 13 | Regulates actin polymerisation and mediates the formation of branched actin networks [400] |

This increase in protein levels appears to be at the translation stage, as transcription levels, measured by RT-qPCR, are unchanged in i293-ST cells upon MCPyV ST expression (Figure 3.1C). This could be due to previous findings that MCPyV ST deregulates translation rather than transcription [234]. These results indicate that the actin cytoskeleton is also altered upon MCPyV ST expression, which may have implications in MCPyV ST-induced cell motility.

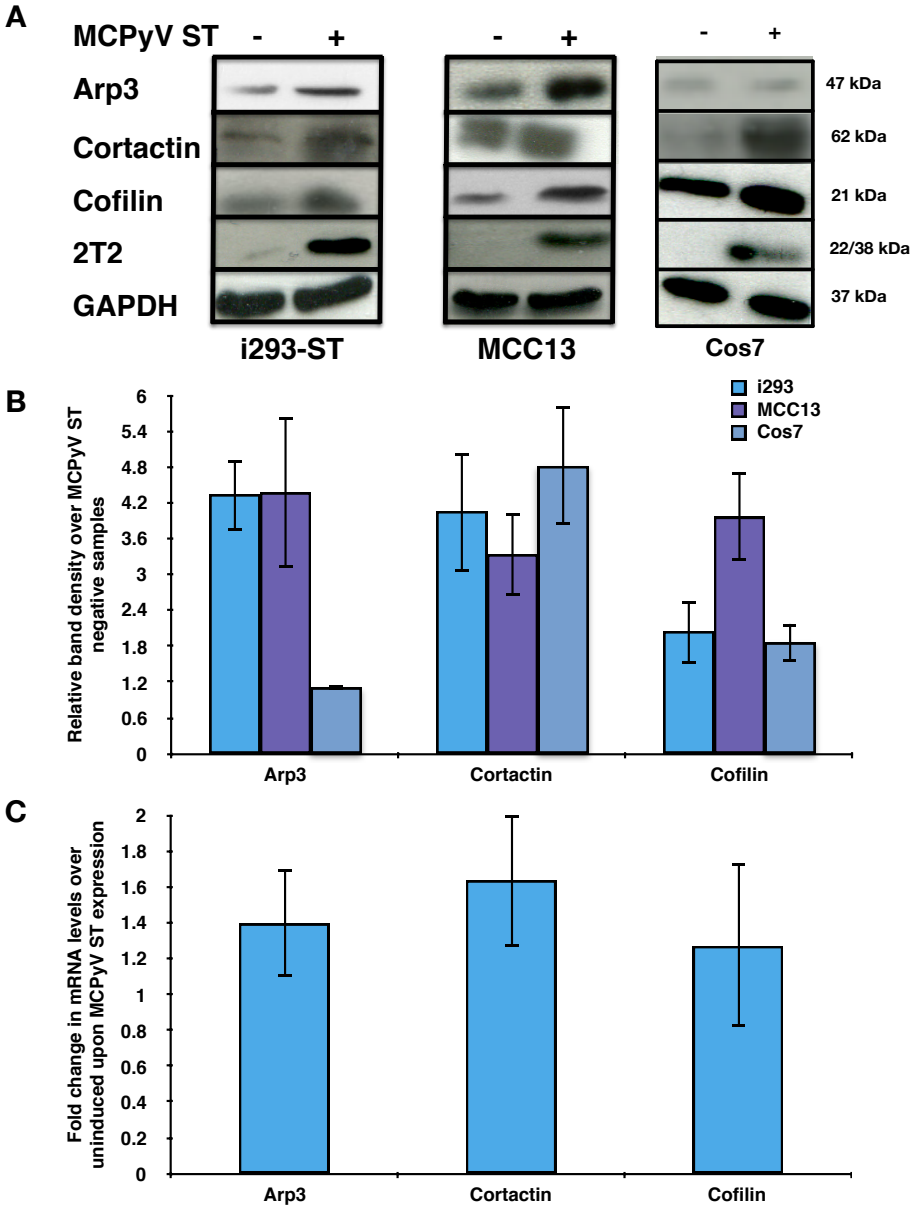


**Figure 3.1: Actin-associated proteins are upregulated upon MCPyV ST expression.** (A) i293-ST cells remained uninduced or were incubated for 48 h in the presence of doxycycline hyclate. After induction, cell lysates were probed for Arp3, cortactin and cofilin-1 using specific antibodies. MCC13 and Cos7 cells were transfected with 1 µg EGFP or EGFP-ST for 12 h. Lysates were probed for Arp3, cortactin, and cofilin-1. GAPDH was used as a measure of equal loading, the 2T2 hybridoma was used to probe for MCPyV ST expression. (B) Exposed film with immunoblotting results was scanned and uploaded onto ImageJ software, which was used to compare band density (n = 3). (C) i293-ST cells remained uninduced or were incubated for 48 h in the presence of doxycycline hyclate. After induction, cellular RNA was extracted using phenol/chloroform, reverse transcribed and RT-qPCR was performed. Transcript levels were analysed using the comparative CT method (n = 3).

## 3.3 MCPyV T antigen-positive MCC tumours express actin-associated proteins

MCPyV ST has been implicated in tumourigenesis [234], and MCPyV is found clonally integrated in MCPyV-positive MCC tumours [20]. In order to investigate whether actin-associated proteins are expressed and/or upregulated in MCPyV-positive MCC tumours, two unrelated MCC tumour samples were used (MCC1 and MCC2). Healthy skin was used as a negative control. All samples were homogenised, lysed, and sonicated, and then probed for Arp3, cortactin and cofilin-1. Arp3 and cortactin appear to be expressed to detectable levels in MCC1 and, to a lesser extent, MCC2, but not in the healthy skin sample, while cofilin-1 is upregulated in MCC1 compared to healthy skin, but not in MCC2 (Figure 3.2). This may be due to varying expression of MCPyV tumour antigens in samples or due to other unique tumour features. Overall, these results confirm the cell line results and further indicate that the actin cytoskeleton is affected upon MCPyV ST expression and may play a role in MCC tumourigenesis.

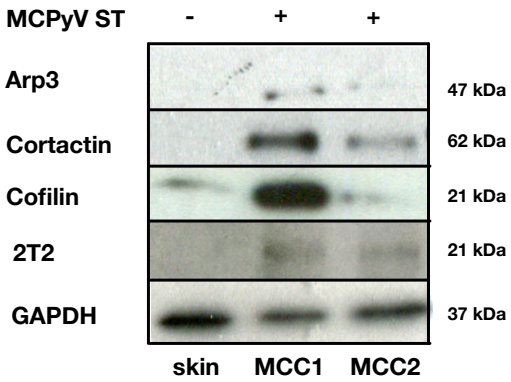


**Figure 3.2: Actin-associated proteins are expressed in MCPyV-positive MCC tumours.** Healthy skin, MCC1, and MCC2 were crushed using a mortar and pestle on dry ice, lysed with RIPA buffer for 30 min on ice and then further homogenised by sonication (5 min, 10 s on/10 s off). Tissue lysates were then probed for Arp3, cortactin and cofilin-1. GAPDH was used as a measure of equal loading, the 2T2 hybridoma was used to probe for MCPyV ST expression.

## 3.4 MCPyV ST expression induces the formation of actin-based protrusions

Altered actin-associated protein levels upon MCPyV ST expression indicated the possibility of actin cytoskeleton-related phenotypic changes. To examine any changes in MCPyV ST-expressing cells, HEK-293 cells were transfected with EGFP or EGFP-ST. Cells were then fixed and stained with rhodamine phalloidin, an actin-binding compound, to investigate any possible changes in the actin cytoskeleton. MCPyV ST-expressing HEK-293 cells showed a clear abundance of actin-based protrusions, compared to the much smoother cell periphery of EGFP-expressing HEK-293 cells (Figure 3.3A and Figure 3.4A). Similar results were also observed in MCPyV ST-expressing MCC13 and Cos7 cells, showing an increased number of longer protrusions, although the difference was less pronounced in MCC13 cells (Figure 3.3B and Figure 3.4B). In Cos7 cells, expression of MCPyV ST induced filopodia to a level comparable with HEK-293s (Figure 3.3C and Figure 3.4C). This different in results between cell lines may be due to the transformed nature of MCC13 cells.

To further quantify the increase in actin-based protrusions upon MCPyV ST expression, the protrusions were counted and their lengths measured using ImageJ software. Analysis showed a large increase in both the numbers and length of these actin-based protrusions in MCPyV ST-expressing HEK-293 and Cos7 cells, and an increase in longer actin-based protrusions in MCPyV ST-expressing MCC13 cells (Figure 3.4).

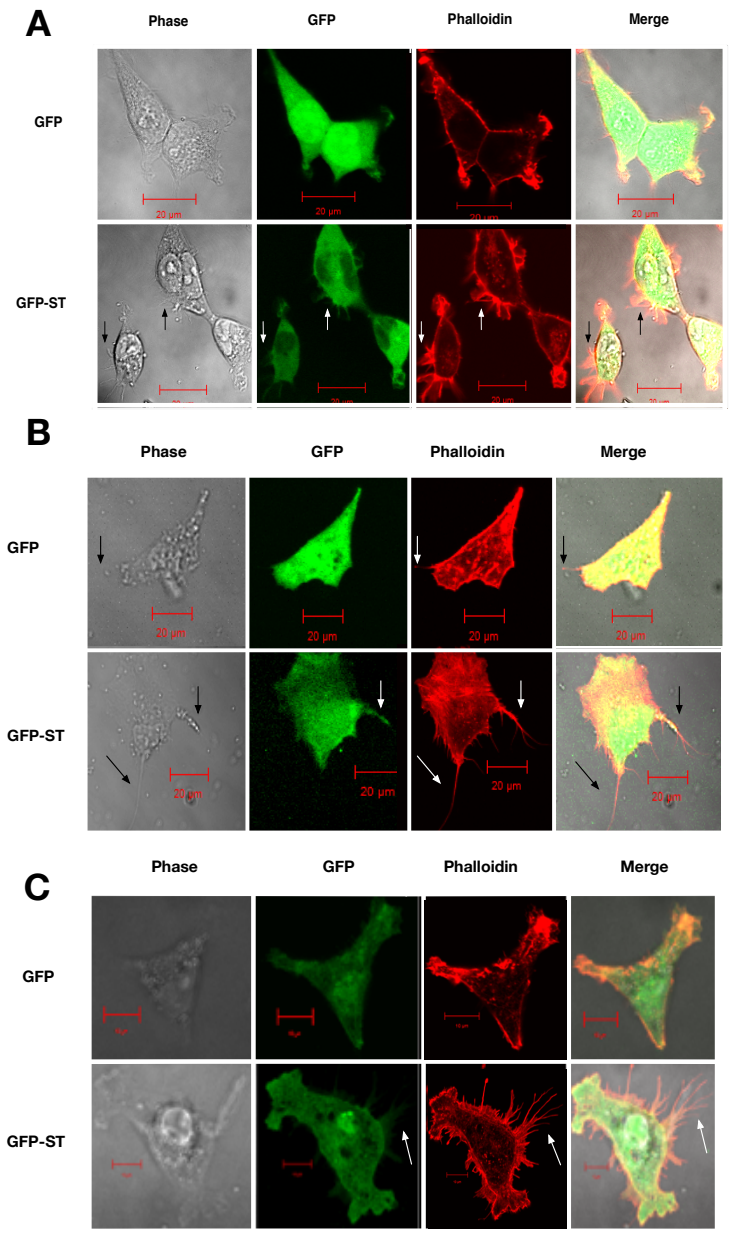


**Figure 3.3: Cell imaging shows an increase in actin-based protrusions in ST-expressing cells.** (A) HEK-293, (B) MCC13 or (C) Cos7 cells were transfected with 1 µg of either EGFP or EGFP-ST for 6 h or 12 h. Cells were fixed after 24 h and stained with rhodamine-phalloidin. Slides were then analysed using a Zeiss LSM 700 confocal laser scanning microscope.

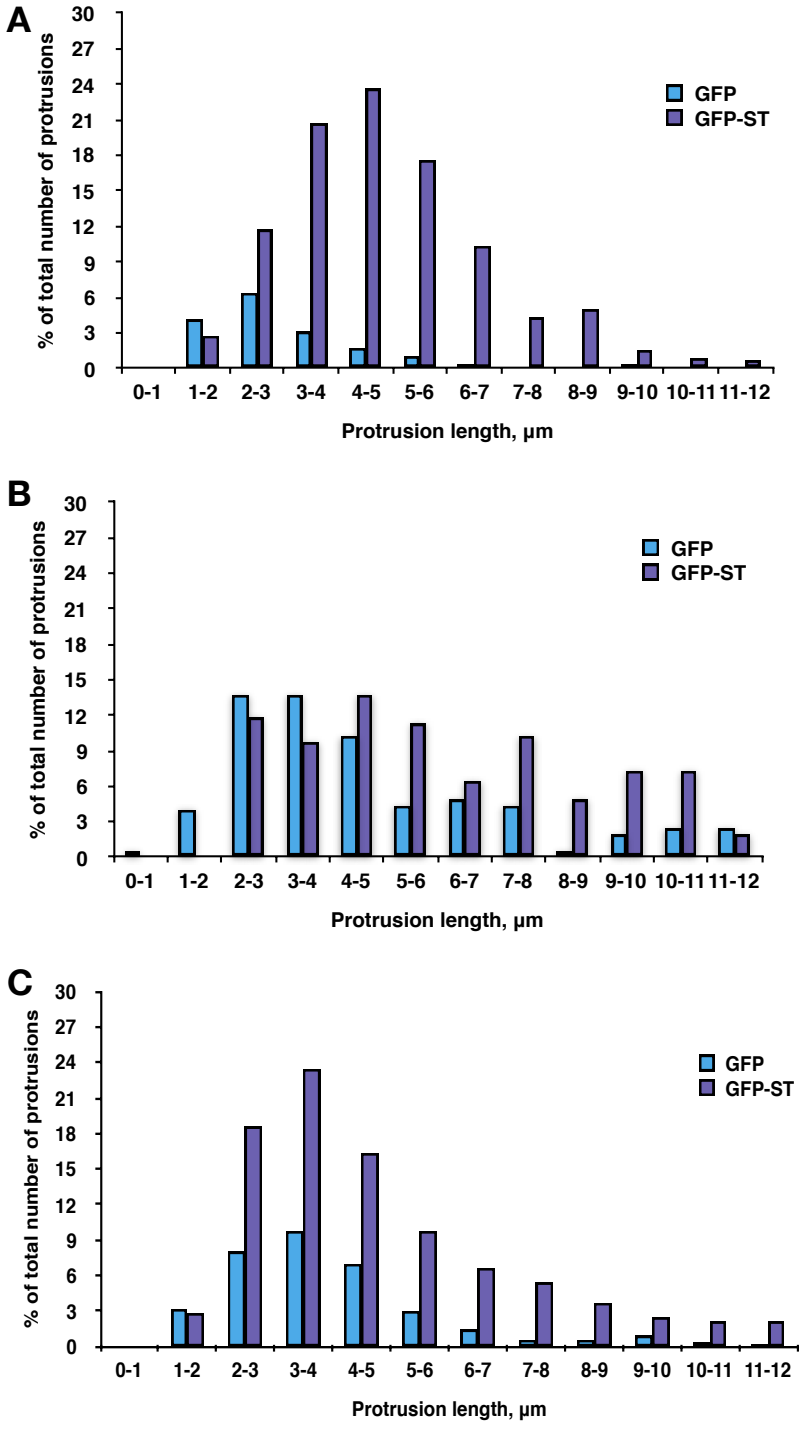


**Figure 3.4: Cell imaging quantification shows an increase in actin-based protrusions in ST-expressing cells.** Actin-based protrusions were counted for 75 cells per condition using ImageJ software, in (A) HEK-293, (B) MCC13 or (C) Cos7 cell lines. Quantifications are representative examples of 3 biological replicates.

## 3.5 MCPyV ST expression induces the formation of filopodia

The thin, filamentous nature of the actin-based protrusions formed upon MCPyV ST expression suggests a filopodia-like character. However, to conclusively characterise these protrusions, two filopodia-associated proteins were visualised using immunofluorescence in the absence and presence of MCPyV ST expression: mDia2 [401] and IRSp53 [298]. To visualise mDia2 localisation, HEK-293 cells were either transfected with EGFP-tagged mDia2 alone or co-transfected with Flag-tagged MCPyV ST (ST-flag) [209]. To visualise IRSp53 localisation, EGFP or EGFP-ST were co-transfected with myc-tagged IRSp53. Cells were then fixed and stained with rhodamine phalloidin to visualise actin-based structures. In control cells, mDia2 was seen to be diffuse in the cytoplasm, while in cells expressing MCPyV ST, mDia2 relocalised to the cell periphery and into the actin-based protrusions (Figure 3.4A). Likewise, IRSp53 was observed to be diffuse in the cytoplasm in control cells but relocalised to the cellular periphery and into the actin-based protrusions upon the expression of MCPyV ST (Figure 3.4B). Due to the known association of both mDia2 and IRSp53 with filopodia, this was the first marker-based indication that MCPyV ST expression induced filopodia formation specifically. To further confirm this conclusion, the localisation of an additional filopodia marker, myosin X [402], was visualised. HEK-293 cells were transfected with EGFP or EGFP-ST and stained for myosin X. Punctate foci of myosin X staining can be observed at the tips of MCPyV ST-induced actin-based protrusions (Figure 3.4C). Together, these results confirm that the protrusions induced by MCPyV ST expression are filopodia.

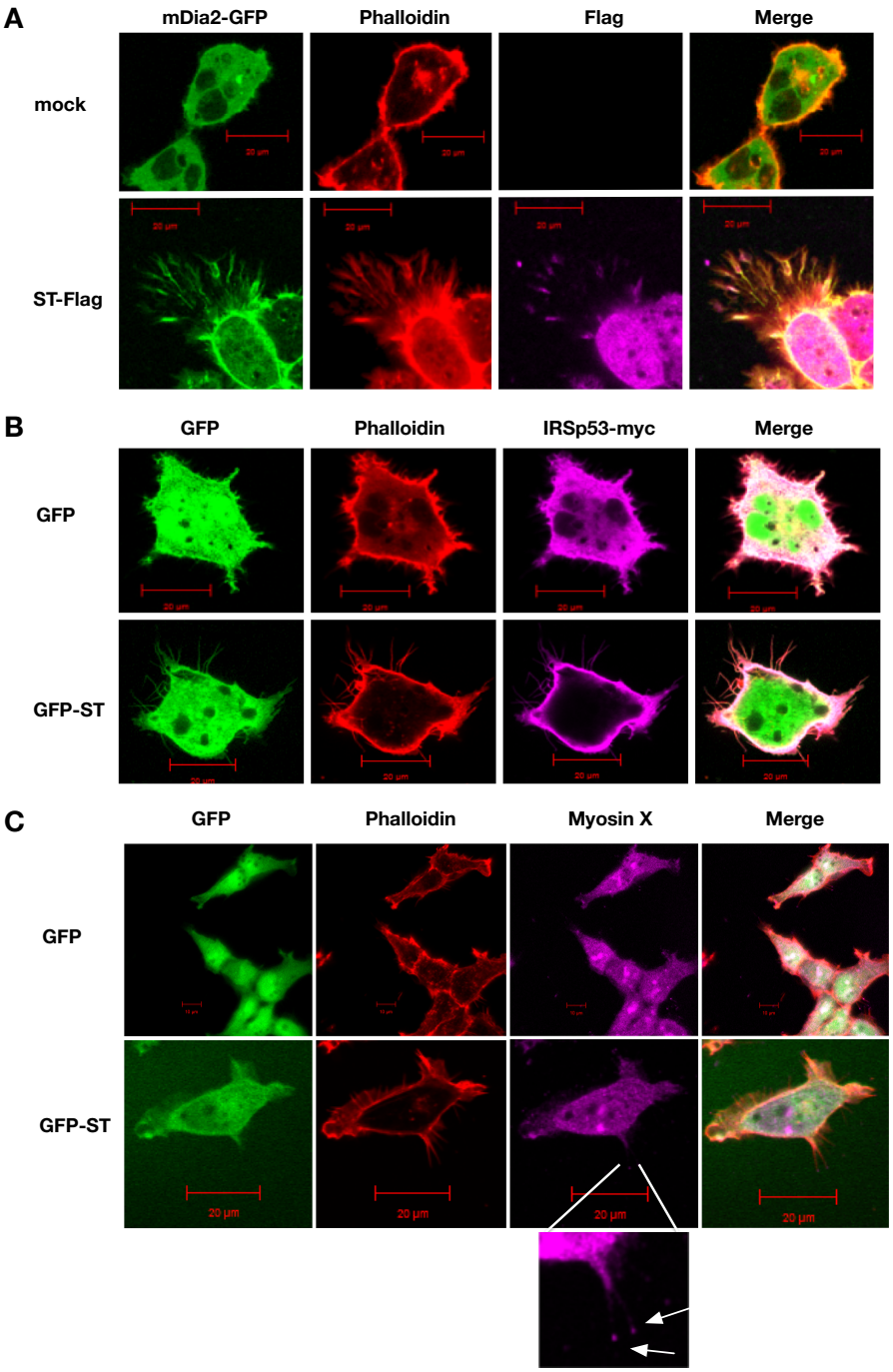


**Figure 3.5: Screening of filopodia-associated proteins indicates MCPyV ST expression induces filopodia formation.** (A) HEK-293 cells were either transfected with 1 µ g of EGFP-mDia2 or co-transfected with 1 µ g of EGFP-mDia2 and ST-Flag for 6 h. 12 h later cells were fixed and stained with rhodamine-phalloidin and specific antibodies. (B) HEK-293 cells were either co-transfected with 1 µg of EGFP and IRSp53-myc or co-transfected with 1 µg of EGFP-ST and IRSp53-myc for 6 h. 12 h later cells were fixed and stained with rhodamine-phalloidin and specific antibodies. (C) HEK-293 cells were either transfected with 1 µg of EGFP or EGFP- ST for 6 h. 12 h later cells were fixed and stained with rhodamine-phalloidin and specific antibodies. All slides were then analysed using a Zeiss LSM 700 confocal laser scanning microscope.

## 3.6 i293-GFP and i239-GFP-ST cell line generation using the 293 FlipIn™ system

In order to reliably and consistently express MCPyV ST with a fluorescent tag, two cell lines were produced: one that expressed GFP-tagged MCPyV ST (i293-GFP-ST) and a control cell line that expressed GFP (i293-GFP) under doxycycline hyclate induction. The GFP tag allows for motility to be observed in individual living cells as well as potentially observing the effects of MCPyV ST *in vivo*. The GFP gene from the pEGFP-C1 plasmid and the GFP-ST fused gene from a pEGFP-C1 backbone were subcloned first into pCR®-Blunt vectors and then into pcDNA5/FRT/TO vectors. Expression of both vectors was confirmed in HEK-239 cells (Figure 3.5A).

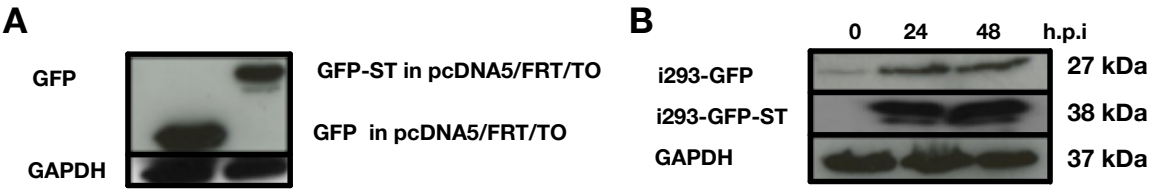


**Figure 3.6: Production of GFP-expressing and GFP-tagged MCPyV ST-expressing inducible cell lines.** (A) HEK-293 cells were transfected with 1 μg of EGFP-pcDNA5/FRT/TO or 1 μg of EGFP-ST-pcDNA5/FRT/TO. Immunoblotting shows expression of GFP or GFP-ST from pcDNA5/FRT/TO. (B) i293-GFP and i293-GFP-ST cells remained uninduced or were induced for 24 or 48 h using doxycycline hyclate. Immunoblotting shows expression of both GFP and GFP-ST from cells after induction. GAPDH was used as a loading control. h.p.i. - hours post induction.

The Flp-In® HEK-293 cell line was co-transfected with the Flp® plasmid and pcDNA5/FRT/TO with the GFP or GFP-ST insert at a 9:1 ratio. After an overnight transfection cells were grown in serum-supplemented DMEM with 100 μg/ml Hygromycin B to select cells with the integrated Flp-In® system. Single colonies were picked and grown under antibiotic selection. Clonal cell populations were tested for induced expression of either GFP or GFP-ST by adding doxycycline hyclate. Clones with highest expression and non-leaky promoters were selected and maintained. Both the i293-GFP and i293-GFP-ST cell lines express the desired proteins upon induction with doxycyline hylcate (Figure 3.5B). For the sake

of brevity, these cell lines will be referred to as i293s when discussed together.

## 3.7 MCPyV ST induces cell motility in i293 and in MCC13 cells

Filopodia are early markers of cell motility. Thus a marked increase in filopodia formation may correlate to increased in cell motility. In order to investigate this possibility, live cell imaging was performed for 24 h using i293-GFP and i293-GFP-ST cells, which were induced using doxycycline hyclate 24 h prior to imaging or MCC13 cells transfected with EGFP and EGFP-ST (Figure 3.6A). Distances travelled by individual cells were tracked using ImageJ (see the individual coloured traces), and analysis shows a significant ($p < 0.001$) increase in distance travelled by MCPyV ST-expressing cells over control cells (Figure 3.6B). Firstly, this suggests that the i293-GFP and i293-GFP-ST cell lines are functional and behave as expected depending on MCPyV ST expression. Secondly, it confirms the published findings [210] that MCPyV ST induced cell motility and this is measurable in single cells in different cell lines.

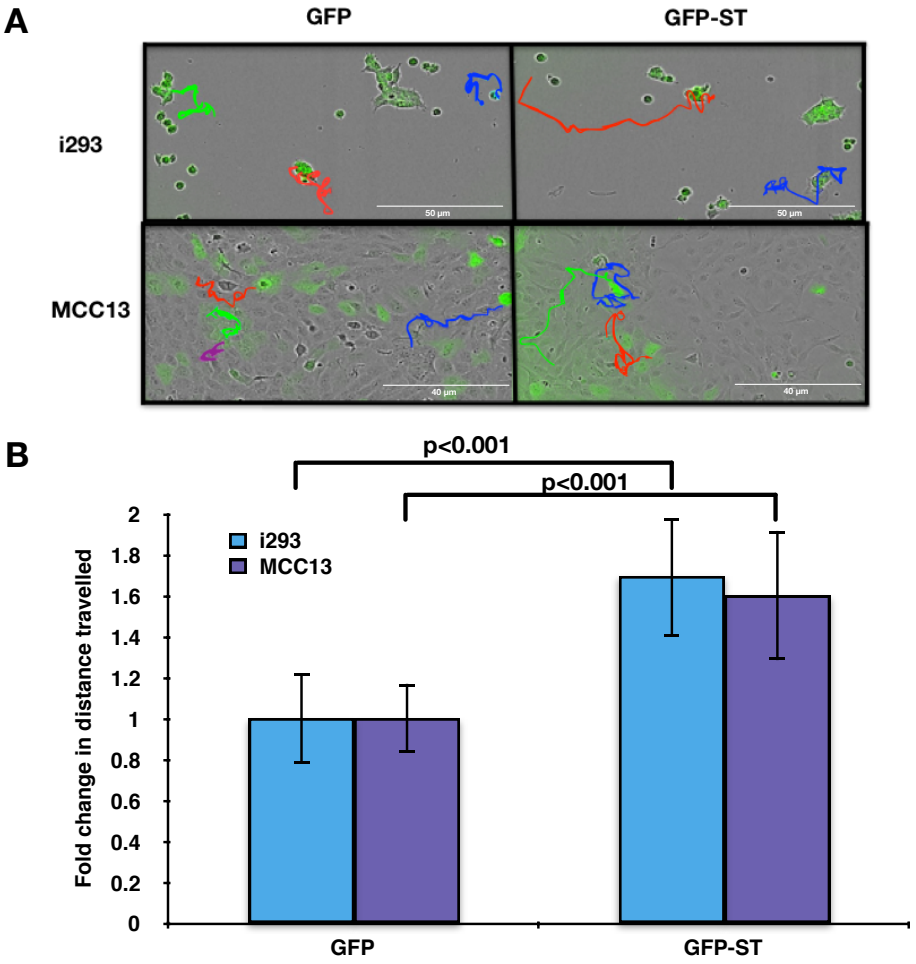


**Figure 3.7: Live cell imaging shows MCPyV ST expression enhances cell motility.** (A) i293-GFP and i293-GFP-ST cells were induced using doxycycline hyclate. After 24 h, cell motility was measured using the IncuCyte kinetic live cell imaging system. MCC13 cells were transfected with 1 µg EGFP or EGFP ST for 6 h. After 12 h cell motility was measured using the IncuCyte kinetic live cell imaging system. Images were taken every 30 min for a 24 h period. (B) The movement of cells was then tracked using Image J software (n = 30). Average cell movement was calculated and significance was tested using a two-tailed Student's t test.

## 3.8 MCPyV ST-induced cell motility is directional

Directional cell motility is an important feature of cell migration in cancer [403], as migratory cells tend to move away from the primary tumour site towards lymphatic or blood vessels. In order to determine whether MCPyV ST expression promotes directionality, i293-GFP and i293-GFP-expressing cells were induced

with doxycycline hyclate for 48 h on coverslips, then scratches were made across the coverslips and cells were left to grow into the scratches for 6 h. Cells were then fixed and stained for Golgi vesicles. Golgi vesicle presence in front of the nuclei of cells facing the gap is an indication of cell polarity, and thus an indirect indication of directionality [404] (Figure 3.7A). Quantification of the image indicated that MCPyV ST expression significantly ($p < 0.001$) increased the percentage of polarised cells (Figure 3.7B). This suggests that MCPyV ST expression induces directional cell motility.

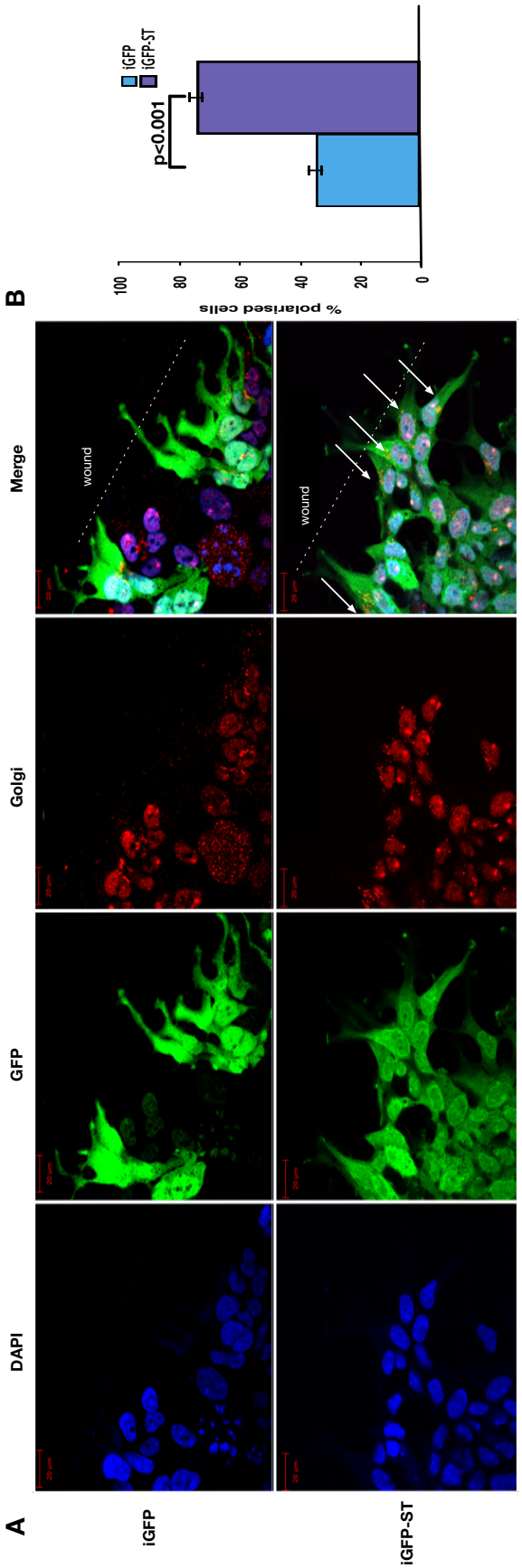


**Figure 3.8: Cell imaging shows MCPyV ST induces directional cell motility.** (A) i293-GFP and i293-GFP-ST cells, seeded on coverslips, were induced using doxycycline hyclate for 48 h. Scratches were made across the surface of the coverslips (3 per coverslip) and cells were then left to move into the gap for 6 h. Cells were then fixed, stained for the Golgi network and imaged using the LSM 700 microscope. (B) Individual cells (n = 50) facing the scratch gap were analysed and scored for Golgi particles in front of the nucleus (facing the gap). Significance was tested using a two-tailed Student's t-test.

## 3.9 MCPyV ST-induced cell motility is dependent on the action of Rho-family GTPases

The Rho-family GTPases are a superfamily of signalling molecules, a number of which have been implicated in increased cell motility and metastasis in various cancers [405] [406] [407]. They are also well characterised regulators of actin dynamics [388]. In order to determine whether Rho-family GTPases are involved in MCPyV ST-induced cell motility, a selection of inhibitors known to target Rho-family GTPases were utilised at non-cytotoxic concentrations as measured by MTS assay (Figure 3.8): ML141 and ZCL278 (Cdc42 inhibitors) [408] [409], NSC23766 (a Rac1 inhibitor) [410], and Rhosin (a RhoA inhibitor) [411]. i293-GFP and i293-GFP-ST cells were induced using doxycycline hyclate, while MCC13 cells were transfected with EGFP or EGFP-ST, and treated with each respective inhibitor for 24 h. Cells were then imaged using the IncuCyte kinetic imaging system, every 30 min for 24 h (Fiigure 3.9A and Figure 3.10A).

Distance travelled by individual cells were tracked using ImageJ software. No significant differences were observed among the average distances travelled by control cells not expressing MCPyV ST, in both untreated and treated cells with the Rho-family GTPase inhibitors (Figure 3.9B and Figure 3.10B). Conversely, MCPyV ST-expressing cells treated with both Cdc42 inhibitors and the RhoA inhibitor showed reduced cell motility ($p < 0.001$), while no significant reduction was observed when cells were treated with the Rac1 inhibitor (Figure 3.9B and Figure 3.10B). This suggests that Cdc42 and RhoA GTPases may be the main Rho-family GTPases involved in facilitating MCPyV ST-induced cell motility.

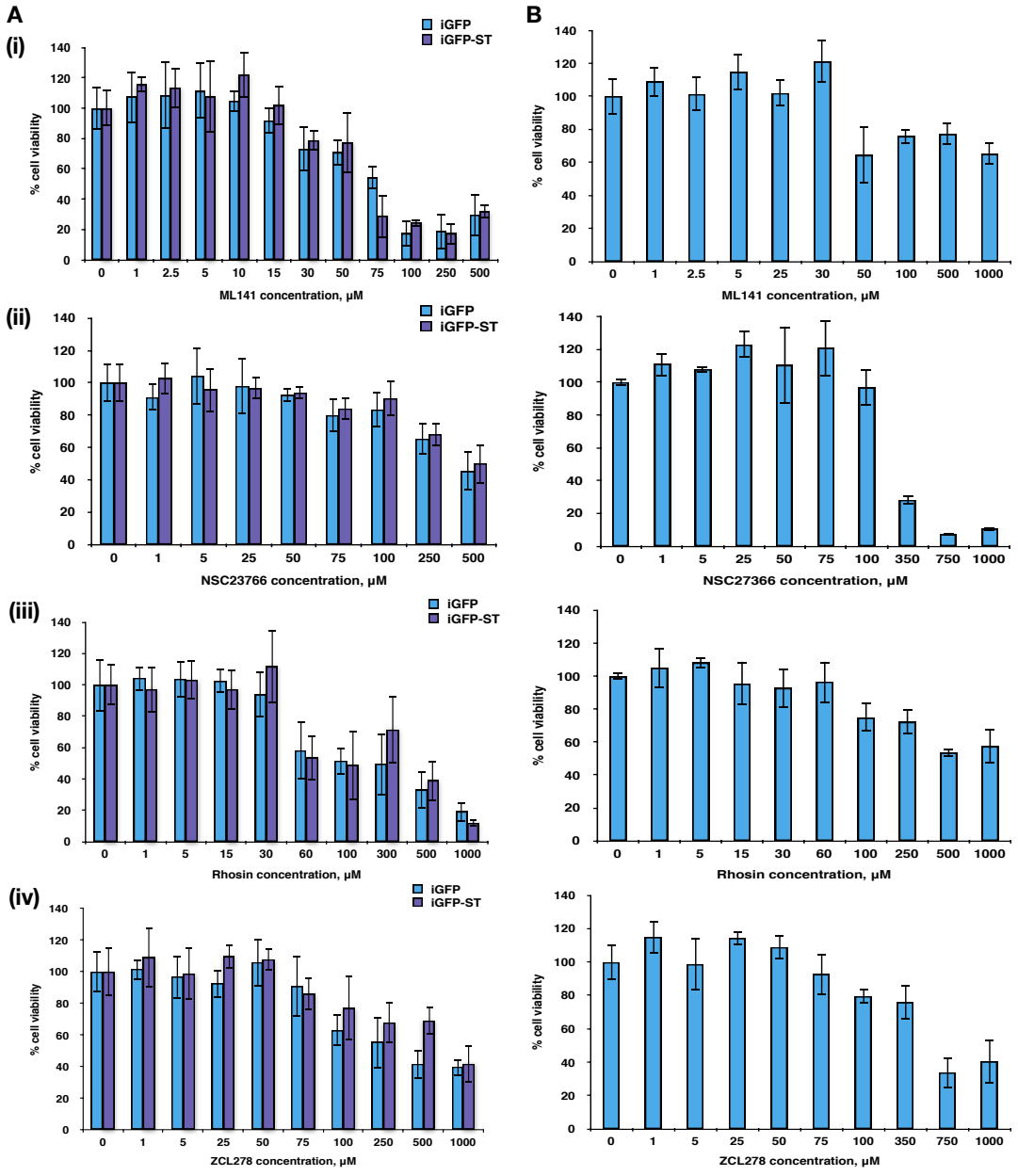


**Figure 3.9: Cell viability assays for Rho-family GTPase inhibitors.** (A) i293-GFP and i293-GFP-ST cells were induced for 24 h, then treated with inhibitors ((i) ML141, (ii) NSC27366, (iii) Rhosin, (iv) ZCL278) at different concentrations for 24 h. (B) MCC13 cells were grown for 24 h, then treated with inhibitors ((i) ML141, (ii) NSC27366, (iii) Rhosin, (iv) ZCL278) at different concentrations for 24 h. Cell viability was measured using the MTS assay. Highest concentration of each inhibitor at >80% viability was used for further experiments.

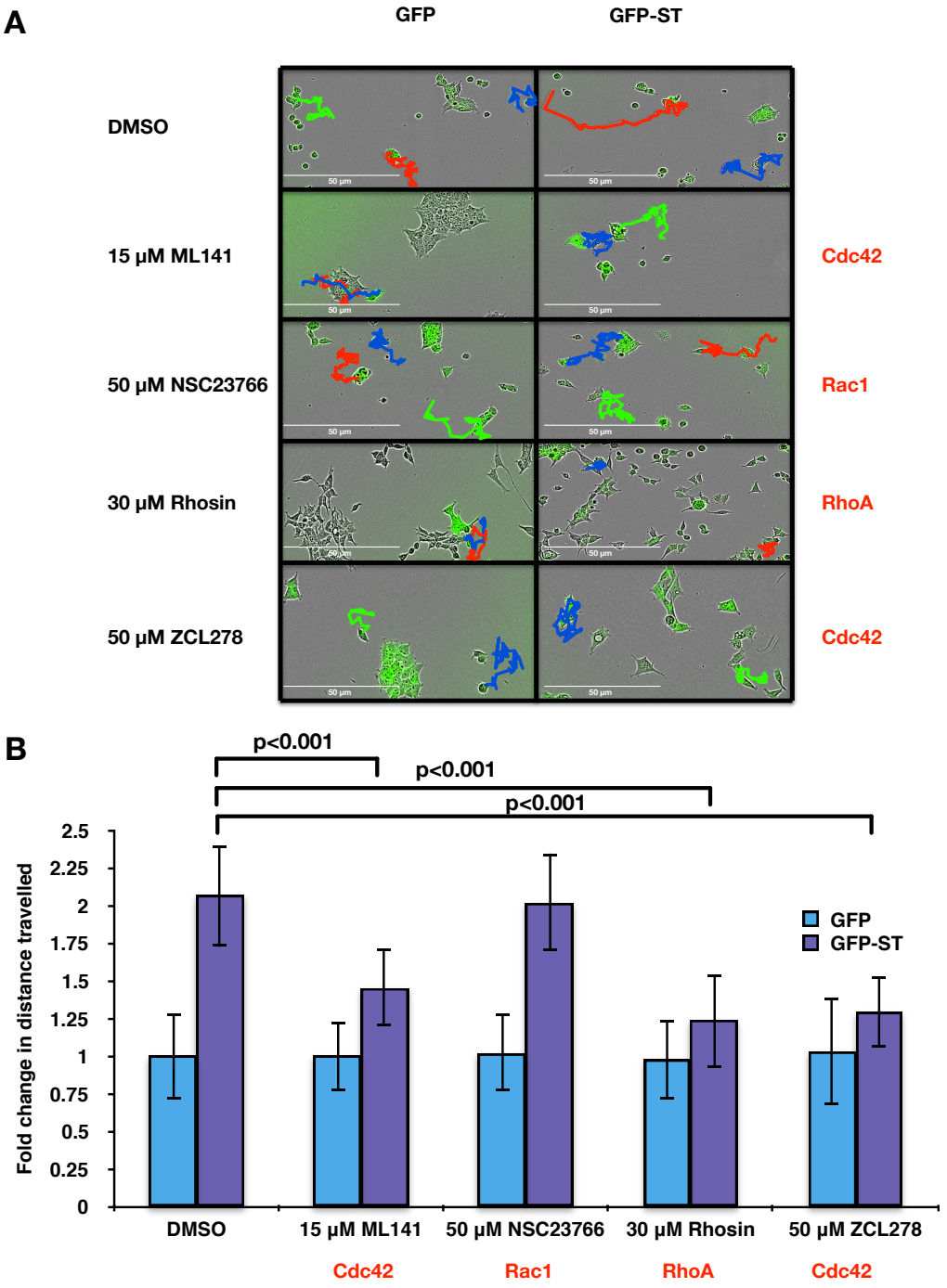


**Figure 3.10: Live cell imaging shows a dependence of MCPyV ST-induced cell motility on Cdc42 and RhoA in i293 cells.** (A) i293-GFP and i293-GFP-ST cells were induced using doxycycline hyclate and treated with 1 µg/µl DMSO, 15 µM of ML141, 50 µM of NSC23766 or ZCL278, or 30 µM of Rhosin. After 24 h, cell motility was measured using the IncuCyte kinetic imaging system. Images were taken for 30 min for a 24 h period. (B) The movement of cells was then tracked using ImageJ software (n = 25). Average cell movement was calculated and significance was tested using a two-tailed Student's t-test.

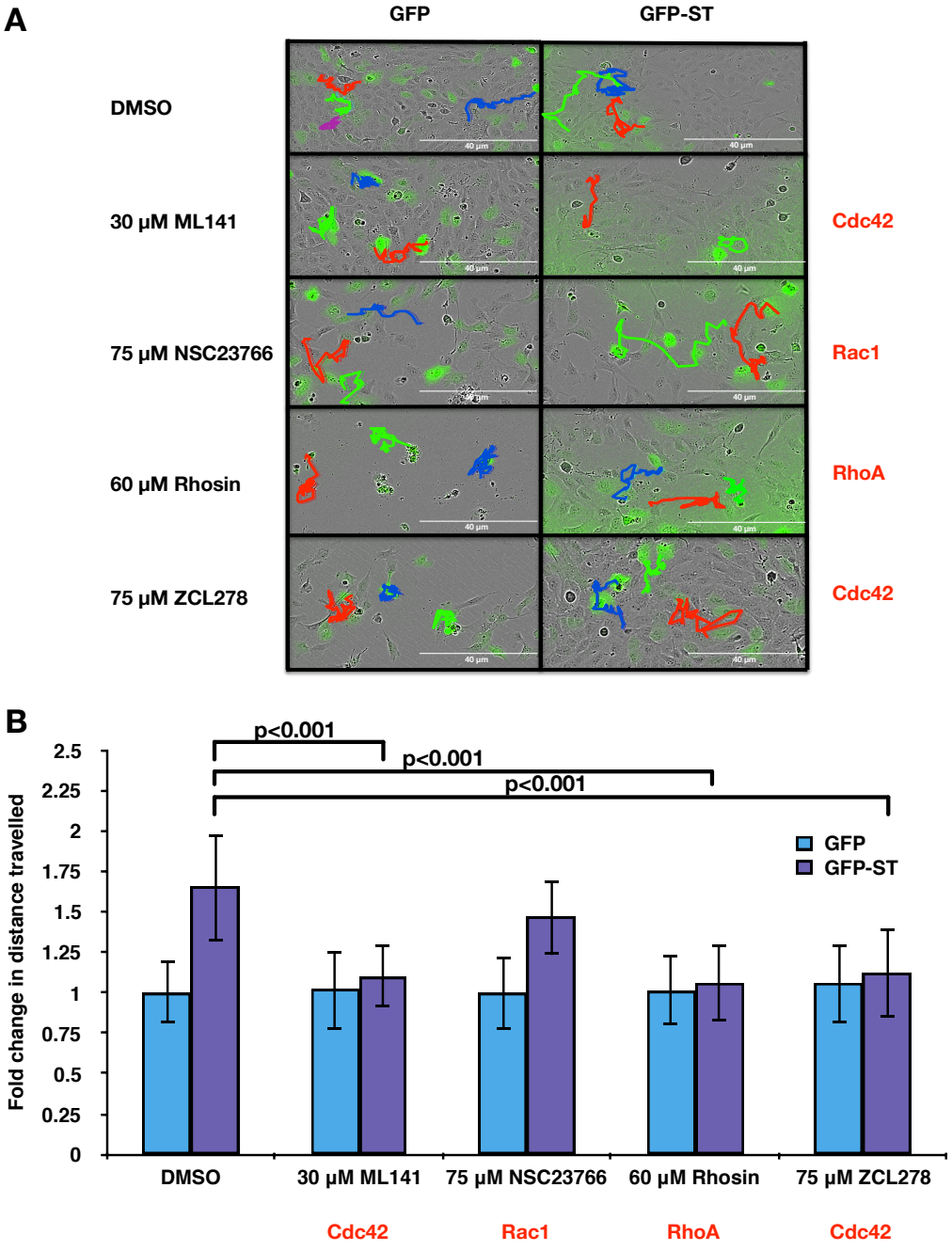


**Figure 3.11: Live cell imaging shows a dependence of MCPyV ST-induced cell motility on Cdc42 and RhoA in MCC13 cells.** (A) MCC13 cells were transfected for 12 h with 1µg of EGFP and EGFP-ST, and treated for 24 h with 1 µg/µl DMSO, 30 µM of ML141, 75 µM of NSC23766 or ZCL278, or 60 µM of Rhosin. Cell motility was measured using an IncuCyte kinetic live cell imaging system. Images were taken for 30 min for a 24 h period. (B) The movement of cells was then tracked using ImageJ software (n = 25). Average cell movement was calculated and significance was tested using a two-tailed Student's t-test.

## 3.10 MCPyV ST-induced filopodia formation depends on the activity of the Rho-family GTPases

Due to the previous results of an observed effect of Rho-family GTPases on MCPyV ST-induced cell motility, it was hypothesised that MCPyV ST-induced filopodia formation may also be affected by Rho-family GTPase inhibitors. Specifically, it was speculated that Cdc42 and/or RhoA inhibition might reduce MCPyV ST-induced filopodia formation. In order to explore this possibility, HEK-293 cells were transfected with EGFP or EGFP-ST cells, and treated with the specific Rho-family GTPase inhibitors (ML141, NSC27366, Rhosin and ZCL278) for 24 h. Cells were then fixed and stained with rhodamine phalloidin to observe actin-based structures (Figure 3.11A). Quantitative analysis of filopodia showed a decrease in filopodia formation when MCPyV ST-expressing cells were treated with any of the Rho-GTPase inhibitors (Figure 3.11B), suggesting that these signal mediators are involved in MCPyV ST-induced filopodia formation. It may be that all 3 major Rho-family GTPases are involved in MCPyV ST-induced filopodia formation but not cell motility. However, to further explore the possibility of any differences on MCPyV ST-induced filopodia formation by Rho-family GTPases, HEK-293 cells were co-transfected with ST-Flag and Rho-family GTPase transdominant (TD) mutants: pcDNA-5-GFP-Cdc42-T17N, pcDNA5-GFP-Rac1-T17N, or pcDNA5-GFP-RhoA-T19N (Figure 3.12A). These TD mutants are catalytically inactive and inhibit endogenous Cdc42, Rac1 and RhoA activity respectively. Cells were then fixed and stained with rhodamine phalloidin to visualise actin-based structures.

Quantitative analysis of filopodia showed a small decrease in filopodia upon co-expression of MCPyV ST with the Rac1 TD mutant. However, a marked decrease was observed when cells are co-transfected with either the Cdc42 TD mutant or the RhoA TD mutant, which confirms the observation of the live cell imaging data (Figure 3.12B). These findings suggest a definitive role for Cdc42 and RhoA in MCPyV ST-induced filopodia formation, and further indicate that these Rho-family GTPases are involved in MCPyV ST-induced cell motility.

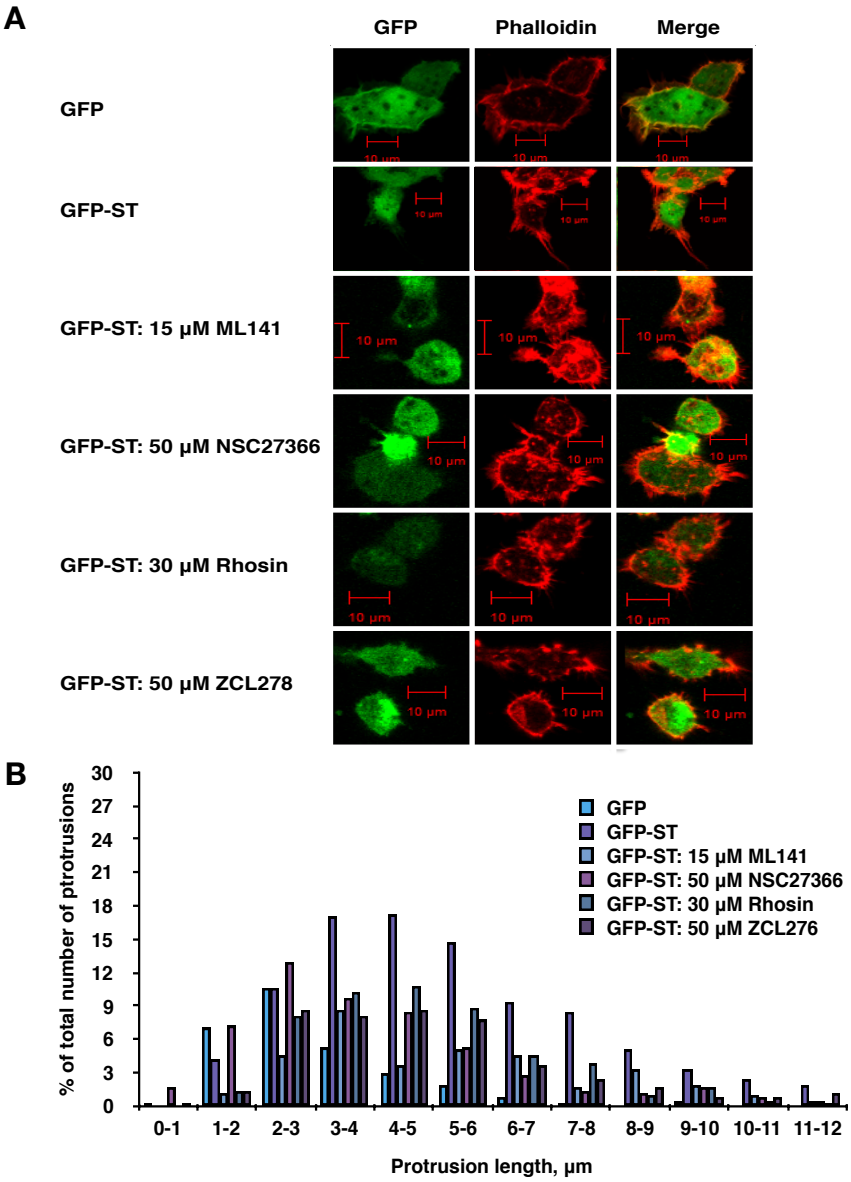


**Figure 3.12: Cell imaging shows that Rho-family GTPase inhibitors reduce MCPyV ST-induced filopodia formation.** (A) HEK-293 cells were transfected with 1 µg EGFP or EGFP-ST for 6 h and treated with 1 µg/µl DMSO, 15 µM of ML141, 50 µM of NSC23766 or ZCL278, or 30 µM of Rhosin. After 24 h cells were fixed and stained with rhodamine-phalloidin. All slides were then analysed using a Zeiss LSM 700 confocal laser scanning microscope. (B) Actin-based protrusions were counted for 75 cells per condition using ImageJ software. Quantifications are representative examples of 3 biological replicates.

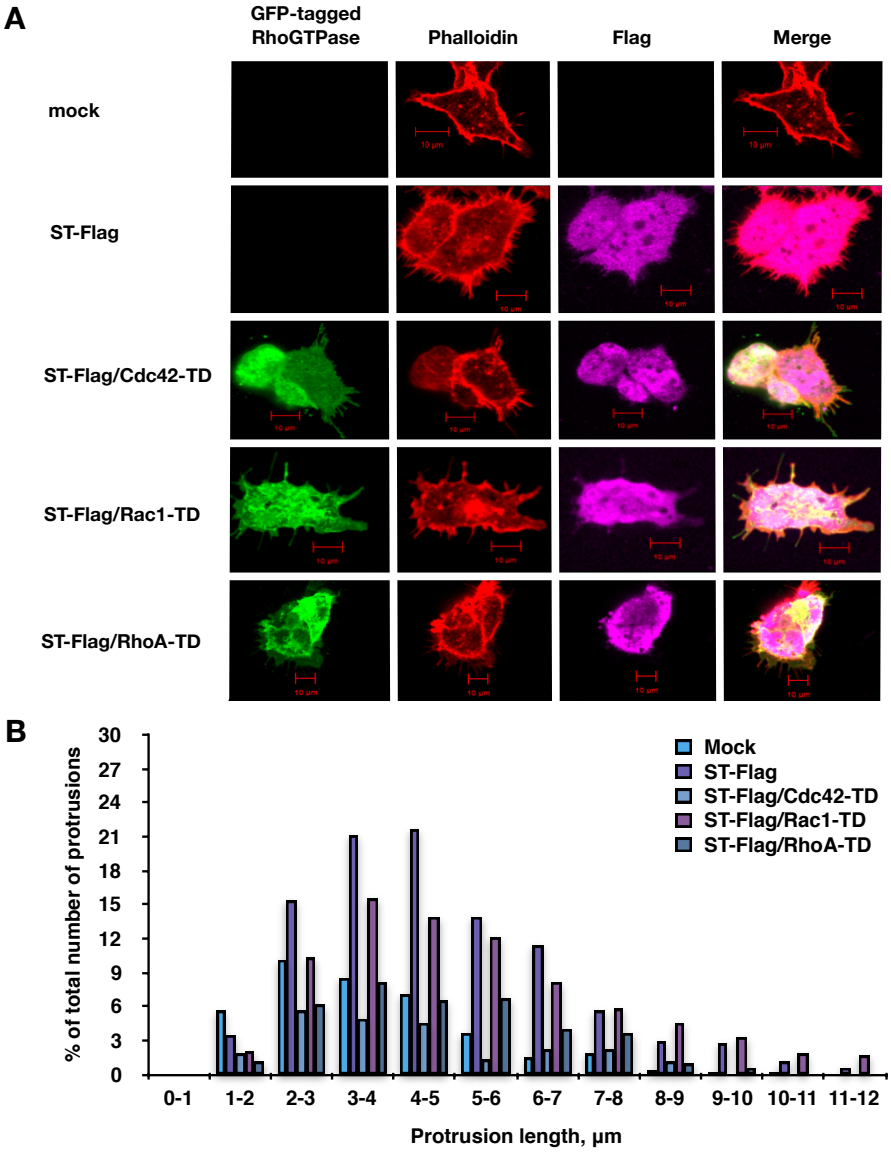


**Figure 3.13: Cell imaging shows that Cdc42 and RhoA transdominant mutants reduce MCPyV ST-induced filopodia formation.** (A) HEK-293 cells were mock transfected, transfected with 1 µg ST-Flag or co-transfected with 1 µg ST-Flag and pcDNA5-GFP-Cdc42-T17N, pcDNA5-GFP-Rac1-T17N, or pcDNA5-GFP-RhoA-T19N for 6 h. 12 h later cells were fixed and stained with rhodamine-phalloidin. All slides were then analysed using a Zeiss LSM 700 confocal laser scanning microscope. (B) Actin-based protrusions were counted for 75 cells per condition using ImageJ software. Quantifications are representative examples of 3 biological replicates.

## 3.11 Discussion

MCPyV ST has been shown to promote the destabilisation of microtubules via enhancing the expression of stathmin [210]. Data presented in this chapter show that in addition to the microtubule network, the actin cytoskeleton undergoes changes upon MCPyV ST expression. This is visible both in changes in protein expression and in the increase in filopodia numbers. These changes were observed to greater or lesser degrees in different cell lines: HEK-293, MCC13 and Cos7 cells. In addition, expression or upregulation of actin-associated proteins was observed in MCC tumours when compared to a MCC-negative healthy skin sample.

Observations involving increased filopodia and changes in actin-associated protein levels upon MCPyV ST expression led to an investigation of changes in cell motility. Data presented in this chapter show an increase in cell motility when MCPyV ST is expressed, in i293 and MCC13 cells. In addition, data in i293 cells suggests that MCPyV ST-induced cell motility is directional, which is significant in a metastatic context [403].

Rho-family GTPases have been widely studied and shown to be important in the cell motility pathway. Therefore, their effect upon MCPyV ST-induced cell motility was investigated, and findings presented herein suggest that Cdc42 and RhoA appear to be involved in MCPyV ST-induced cell motility and filopodia formation, with Rac1 potentially playing a smaller role. This involvement of Rho-family GTPases is not without precedent, as other oncogenic viruses have been reported to affect the Rho-family GTPases. The best-known example is SV40 ST, whose activity leads to the rearrangement of filamentous actin networks, including Rac-induced lamellipodia formation, Cdc42-induced filopodia formation and loss of RhoA-dependent stress fibres. Levels of Rac1 and Cdc42 are increased in cells expressing SV40 ST, while levels of RhoA are decreased [342]. Thus it is possible that a similar process is occurring in cells expressing MCPyV ST, except through interaction with PP4C instead of PP2A (this argument will be expanded upon in Chapter 4).

Rho-family GTPases are primarily regulated via GTP cycling, with a whole range of factors stimulating or depressing GTPase activity. Rho-family GTPase activators are known as guanine exchange factors (GEFs), promoting the exchange of

inactive GDP molecules for active GTP molecules. GEFs in turn are regulated by a whole range of cellular receptors [412]. In addition, Rho-family GTPases are negatively regulated by GTPase activity promoters (GAPs) and guanine dissociation inhibitors (GDIs), which are also regulated by cellular receptors and other upstream mediators [413]. Investigation of which of these numerous factors are important in MCPyV ST-induced cell motility is beyond the scope of this thesis, but well worth researching in the future. Chapter 4 expands upon the investigation of MCPyV ST-induced cell motility, including the role of phosphatases and receptors, to develop a potential model.

# Chapter 4

# The interaction between MCPyV ST and PP4C is required for initiating cell motility through the dephosphorylation of β1 integrin

## 4.1 Introduction

The cell motility pathway is a complex and dynamic series of interactions between a multitude of cellular factors. Within the pathway, protein phosphorylation and dephosphorylation have been shown to be important methods of signal transduction [414] [415].

MCPyV ST has been shown to interact with cellular protein phosphatases PP2A [416] and PP4 [209] [416]. PP2A is the major serine/threonine phosphatase in mammalian cells, and is well-characterised, ubiquitous and evolutionarily conserved [92]. It has three different subunits: the scaffold subunit A, the regulatory subunit B, and the catalytic subunit C. MCPyV ST is know to bind to two different A subunits of PP2A: A$\alpha$ and A$\beta$ [209]. This binding of polyomavirus ST outcompetes B subunit binding, resulting in altered substrate specificity [417]. However, surprisingly, disrupting the PP2A binding site within MCPyV ST does not affect the tumourigenic potential of the oncoprotein [234].

PP4 is a less well-characterised cellular phosphatase, but its catalytic subunit (PP4C) has been shown to interact with MCPyV ST [209]. This interaction has been implicated in regulating the NF-$\kappa$B pathway [209] and in microtubule dissociation [210].

In Chapter 3, the Rho-family GTPases were implicated in MCPyV ST-induced cell motility and filopodia formation. As discussed, Rho-family GTPases are central to the cell motility pathway; however, the pathway starts upstream of Rho-family GTPases, via cellular receptors, such as the trans-membrane integrin receptors. In humans, integrins exist as $\alpha\beta$ heterodimers, with 24 types of $\alpha$ subunits and 9 types of $\beta$ subunits. Some types are found in specific tissues (e.g. $\alpha 3\beta 2$ in platelets [418]) while others are widely expressed (e.g. $\alpha 5\alpha 1$) [419]. Integrins consist of large extracellular domains that bind the extracellular matrix (ECM) and short cytoplasmic tails that link to the actin cytoskeleton [420]. The main function of these receptors is to transmit signals from the ECM to the cell interior, and some of these signals affect cell motility [421] and cancer progression [422].

Integrins are regulated both externally and internally, by "inside-out" signals from kinases and phosphatases and "outside-in" signals by extracellular ligands, which are important for signalling cascades that regulate the cell motility pathway [423]. Several kinases have been shown to bind to $\beta$ subunits, including

Src-family kinases (SFKs) [424]. In addition, the catalytic subunit of protein phosphatase 1 (PP1C) has been shown to interact with αIIbβ3 [425]. These interactions are thought to initiate "outside-in" signalling from the ECM. Furthermore, a number of studies have shown the significance of phosphorylation in the activity of integrins, including β1 [426] [427]. For instance, PP2A can dephosphorylate β1 integrin at Thr788/789 [428].

The interaction of MCPyV with cellular protein phosphatases, and the role of MCPyV ST in inducing cell motility suggest that integrins may play a role in MCC metastasis. This chapter begins by implicating PP4C in MCPyV ST-induced cell motility and shows that integrins play a role in MCPyV ST-induced cell motility (with β1 integrin as the model). Results therefore suggest a mechanism for the action of the MCPyV ST-PP4C interaction in regulating the initiation of the cell motility pathway via the dephosphorylation of β1 integrin.

## 4.2 Interaction of MCPyV ST with PP4C is required for cell motility

It is well established that MCPyV ST interacts with protein phosphatases, specifically PP2A and PP4C [209]. In order to explore whether these interactions enhance cell motility, two mutants of MCPyV ST were utilised: EGFP-ST:R7A, which fails to interact with the Aα isoform of PP2A, and EGFP-ST:Δ95–111, which does not interact with the Aβ isoform of PP2A or PP4C.

HEK-239 and MCC13 cells were transfected with either EGFP, EGFP-ST, EGFP-ST:R7A, or EGFP-ST:Δ95–111, and live cell imaging performed for 24h (Figure 4.1A). Distances travelled by individual cells were then tracked using ImageJ. HEK-293 and MCC13 cells expressing EGFP-ST:Δ95–111 showed a significant ($p < 0.001$) decrease in distance travelled when compared to wild type MCPyV ST expressing cells. In contrast, HEK-293 cells expressing the EGFP-ST:R7A mutant did not show a significant decrease in motility, while MCC13 cells expressing the same construct resulted in a less motile phenotype (Figure 4.1B). Therefore, while these results do suggest a more significant role for PP2A Aβ and/or PP4C than PP2A Aα, further investigations were necessary to disambiguate the results.

In order to further examine results presented in Figure 4.1, i293-GFP-ST cells were

transfected with transdominant mutants of PP2A (PP2A-TD) or PP4C (PP4C-TD) for 6 h. Then i293-GFP and untransfected and transfected i293-GFP-ST cells were induced using doxycycline hyclate for 24 h. Cells were then imaged for 24 h (Figure 4.2A) and the distance travelled by individual cells was tracked using ImageJ. Cells co-expressing MCPyV ST with PP2A-TD showed a decrease in motility ($p < 0.001$). However, interestingly, cells co-expressing MCPyV ST with PP4C-TD showed a greater decrease in motility ($p < 0.001$) (Figure 4.2B), even though the level of expression of PP4C-TD is much lower than that of PP2A-TD. These results further suggested a more significant for PP4C; however, further work was necessary to resolve the issue of which phosphatase is central to MCPyV ST-induced cell motility.

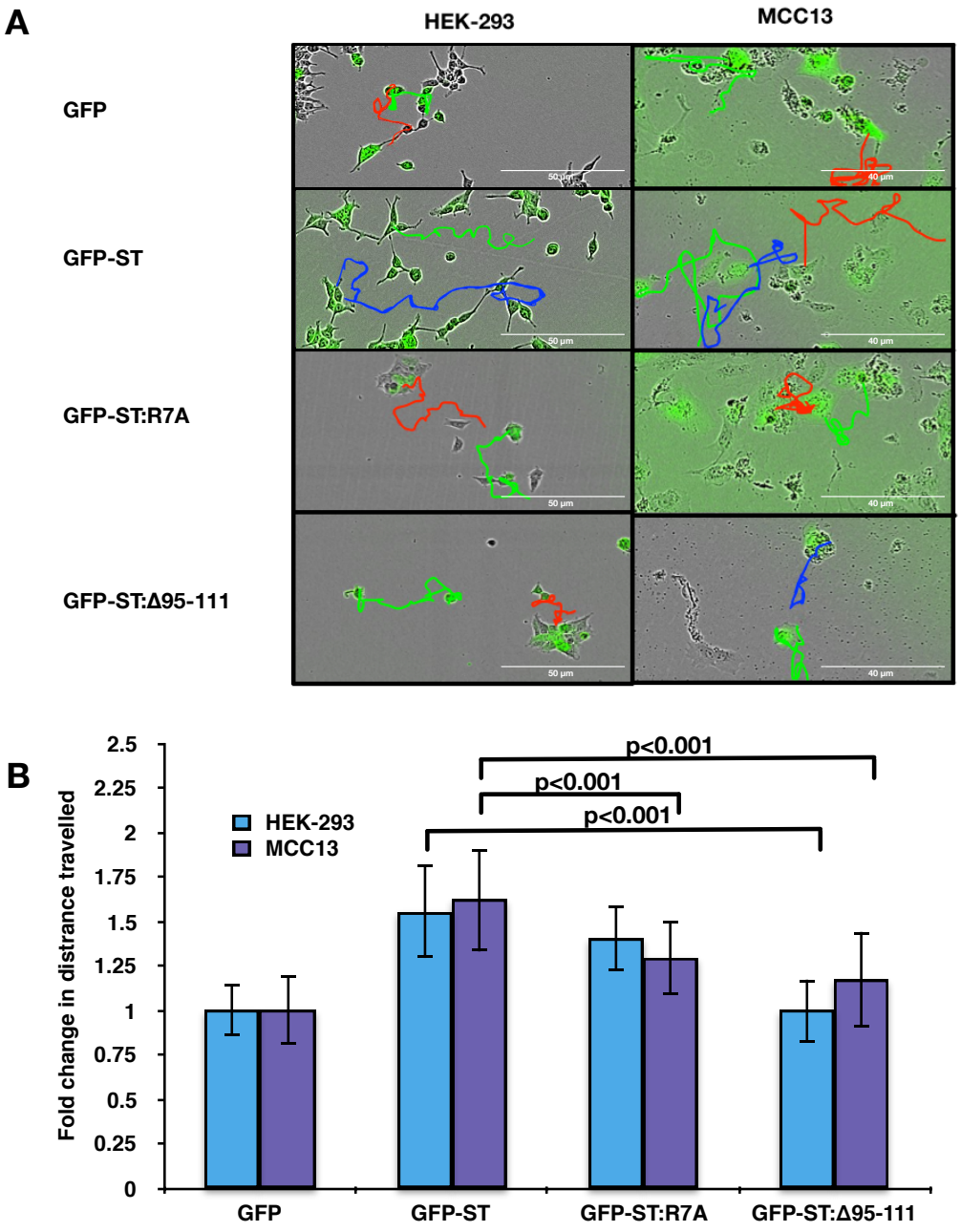


**Figure 4.1: Live cell imaging shows that a MCPyV ST mutant that cannot bind PP2A Aβ or PP4C affects cell motility.** (A) HEK-293 cells were transfected with 1 µg EGFP, EGFP-ST, EGFP-ST:R7A, and EGFP-ST:Δ95–111 for 6 h, while MCC13 cells were transfected with 1 µg EGFP, EGFP-ST, EGFP-ST:R7A and EGFP-ST:Δ95–111 for 12 h. After 12 h cell motility was measured using the IncuCyte kinetic live cell imaging system. Images were taken for 30 min for a 24 h period. (B) The movement of cells was then tracked using Image J software (n = 25). Average cell movement was calculated and significance was tested using a two-tailed Student's t test.

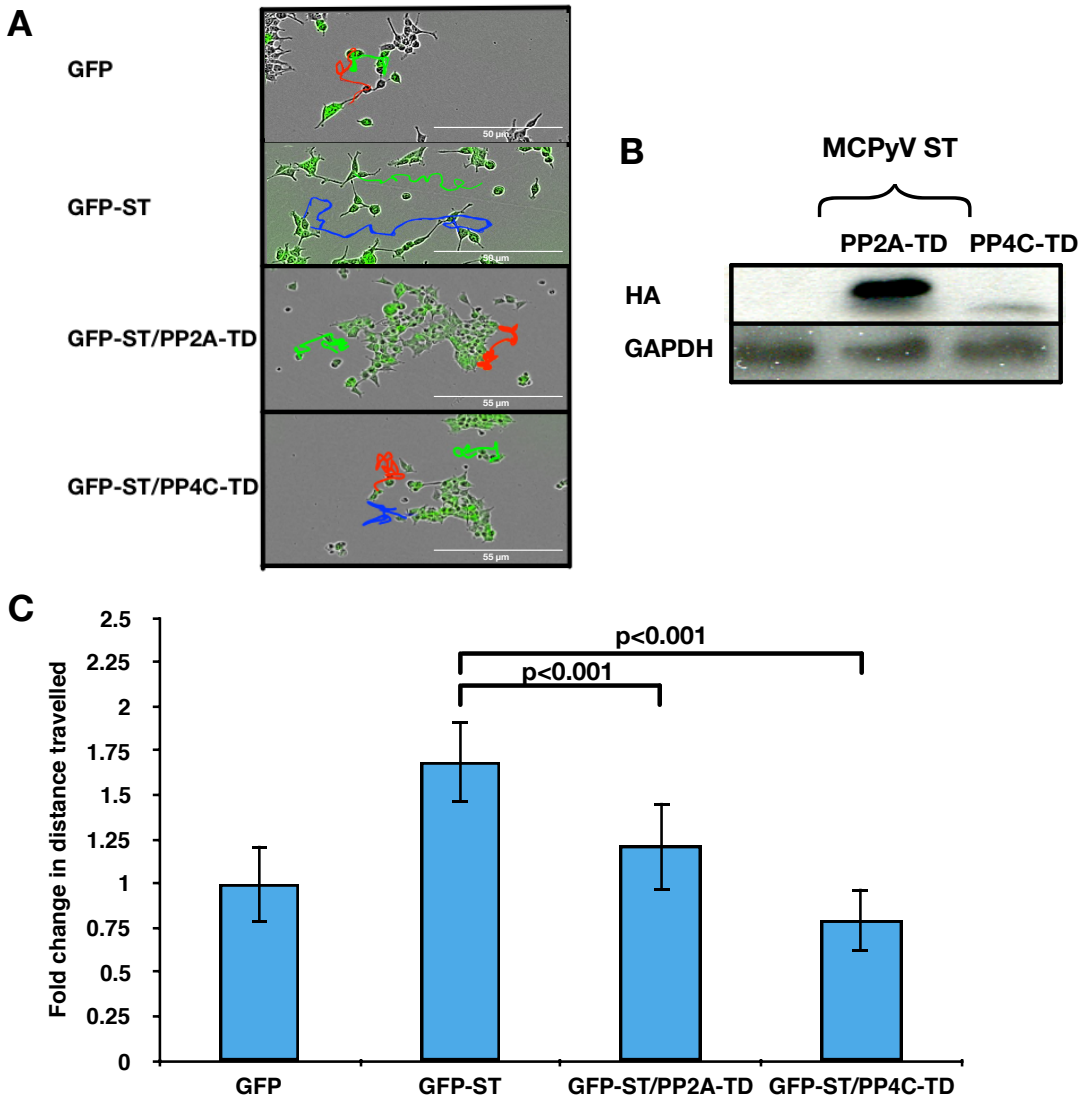


**Figure 4.2: Live cell imaging shows that PP2A and PP4C transdominant mutants affect MCPyV ST-induced cell motility.** (A) i293-GFP-ST cells were transfected with 1 µg PP2A-TD or PP4C-TD for 6 h. i293-GFP and transfected and untransfected i293-GFP-ST cells were induced with doxycycline hyclate for 24 h. Cell motility was measured using the IncuCyte kinetic live cell imaging system. Images were taken for 30 min for a 24 h period. (B) Expression of PP2A-TD and PP4C-TD in MCPyV ST-expressing cells was probed using the HA antibody. GAPDH was used as loading control. (C) The movement of cells was then tracked using Image J software (n = 25). Average cell movement was calculated and significance was tested using a two-tailed Student's t test.

## 4.3 MCPyV ST interaction with the catalytic subunit of PP4 is required for filopodia formation

Results from Chapter 3 showed that MCPyV ST expression induces filopodia formation. Therefore it was important to determine whether the interaction of MCPyV ST with PP2A A$\alpha$ or with PP2A A$\beta$ and/or PP4C is involved in the formation of MCPyV ST-induced filopodia formation. For this purpose, HEK-293 cells were transfected with either EGFP, EGFP-ST, EGFP-ST:R7A or EGFP-ST:$\Delta$95–111. Cells were then fixed and stained with rhodamine phalloidin to identify actin-based structures (Figure 4.3A). Results show that the expression of EGFP-ST:$\Delta$95–111 causes a reduction in filopodia formation compared to the expression of EGFP-ST or EGFP-ST:R7A. Quantitative analysis confirmed that the MCPyV ST 95-111 deletion mutant reduces the formation of filopodia, while the MCPyV ST R7A mutant has little effect (Figure 4.3B). However, this analysis was again not sufficient to determine which MCPyV ST-phosphatase interaction was important in cell motility and filopodia formation.

In order to specifically investigate whether PP4C activity affects MCPyV ST-induced filopodia formation, HEK-293 cells were transfected with EGFP or EGFP-ST in the absence and presence of PP4C-TD for 6h, fixed and stained for actin structures (Figure 4.4A). It must be noted that the transdominant mutant of PP2A could not be used in this analysis due to its expression resulting in aberrant cell phenotype as highlighted by confocal imaging (data not shown). Results show that cells co-expressing EGFP-ST and PP4C-TD show a marked decrease in filopodia formation when compared to cells expressing wild-type MCPyV ST. Quantification of filopodia confirmed these observations (Figure 4.4B). Together, these results point towards PP4C as the main cellular phosphatase involved in MCPyV ST-induced cell motility and filopodia formation.

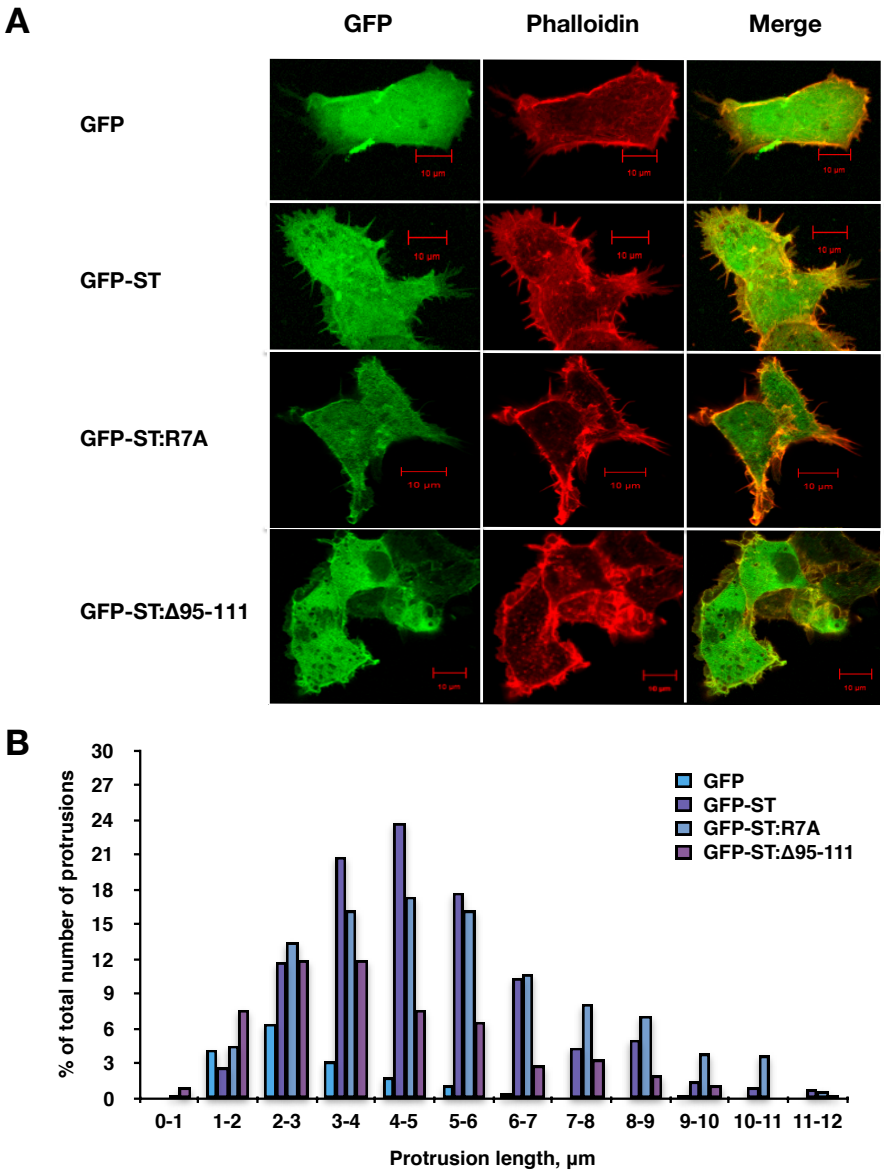


**Figure 4.3: Cell imaging shows that a MCPyV ST mutant that cannot bind PP2A Aβ or PP4C disrupts filopodia formation.** (A) HEK-293 cells were transfected with 1 μg EGFP, EGFP-ST, EGFP-ST:R7A, and EGFP-ST:Δ95–111 for 6 h. 24 h later cells were fixed and stained with rhodamine phalloidin. All slides were then analysed using a Zeiss LSM 700 confocal laser scanning microscope. (B) Actin-based protrusions were counted for 75 cells per condition using ImageJ software. Quantifications are representative examples of 3 biological replicates.

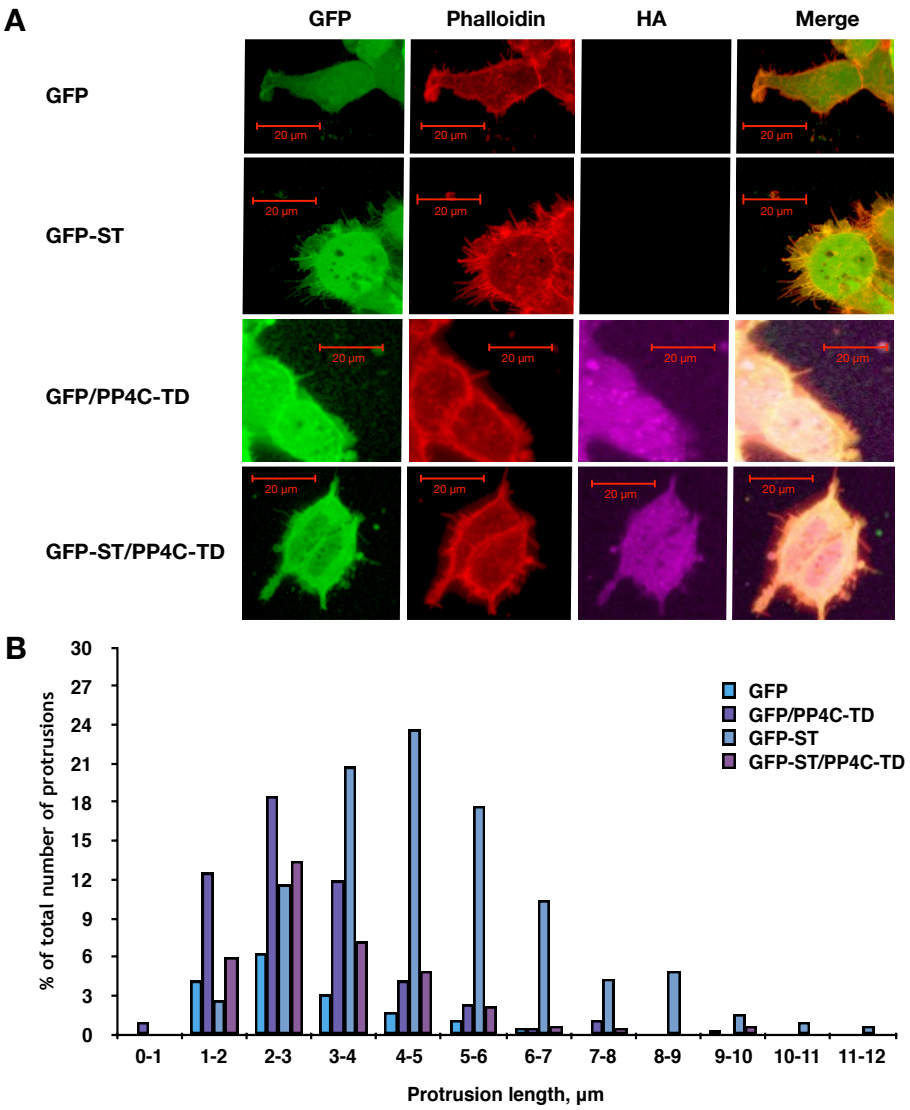


**Figure 4.4: Cell imaging shows the transdominant mutant of PP4C disrupts MCPyV ST-induced filopodia formation.** (A) HEK-293 cells were transfected with 1 µg EGFP, EGFP-ST or co-transfected with 1 µg EGFP and PP4C-TD or 1 µg EGFP-ST and PP4C-TD for 6 h. 24 h later cells were fixed and stained with rhodamine phalloidin. All slides were then analysed using a Zeiss LSM 700 confocal laser scanning microscope. (B) Actin-based protrusions were counted for 75 cells per condition using ImageJ software. Quantifications are representative examples of 3 biological replicates.

## 4.4 The 102 residue of MCPyV ST is important in PP4C binding, MCPyV ST-induced cell motility, and filopodia formation

Previous results suggested a possibly more significant role for PP4C compared to PP2A isoforms in MCPyV ST-induced cell motility. However, it could not be confirmed with the constructs available. Therefore, to conclusively determine which cellular phosphatase is responsible for MCPyV ST-induced cell motility and filopodia formation, additional alanine-scanning MCPyV ST mutants were produced using site-directed mutagenesis in the 95–111 region. This work was done by Husein Abdul-Sada. Immunoprecipitation experiments were then performed to identify a mutant that could distinguish between PP2A Aβ and PP4C. Results from pulldown experiments using PP4C-Flag showed that mutating a single residue (102) specifically abrogates PP4C binding (Figure 4.5A), while mutating the neighbouring residue (103) not only abrogates PP4C binding (Figure 4.5A) but also substantially reduces the interaction with PP2A Aβ (Figure 4.5B). These distinguishing MCPyV ST mutants could therefore be used to determine the specific interaction between MCPyV ST and cellular phosphatases that is necessary for enhancing cell motility and filopodia formation.

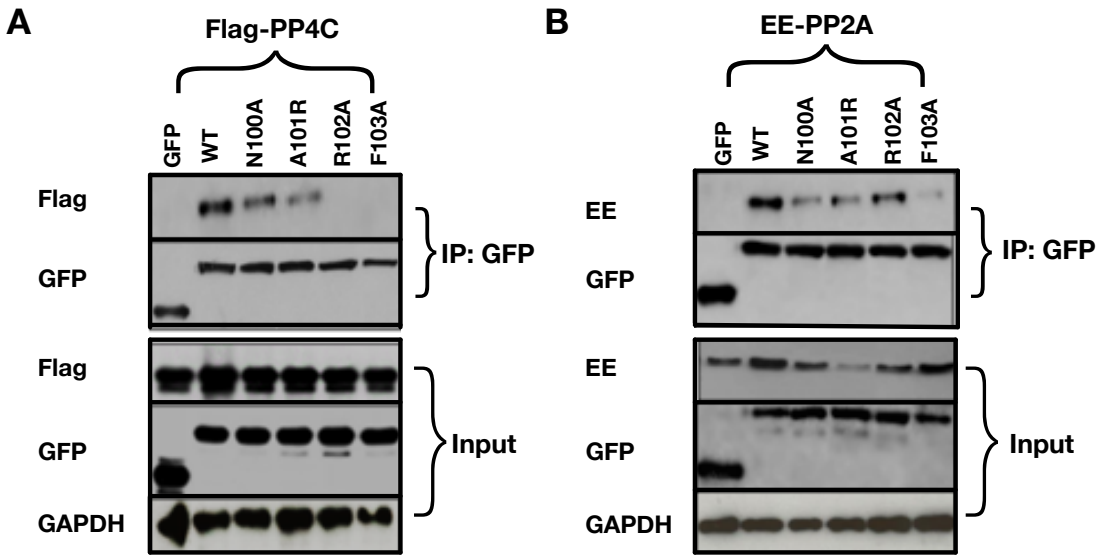


**Figure 4.5: MCPyV ST 102 amino acid residue is critical for PP4C binding.** (A) MCC13 cells were co-transfected with FLAG-PP4C and various EGFP-ST mutants for GFP-TRAP immunoprecipitation. Precipitates were probed for FLAG and GFP. Lysates were probed for FLAG and GFP to confirm successful expression and for GAPDH to verify equal protein loading. (B) MCC13 cells were co-transfected with EE-PP2A Aβ and various EGFP-ST mutants for GFP-TRAP immunoprecipitation. Precipitates were probed for FLAG and GFP. Lysates were probed for FLAG and GFP to confirm successful expression and for GAPDH to verify equal protein loading. This work was performed by Hussein Abdul-Sada.

To determine which specific cellular phosphatase is involved in MCPyV ST-induced cell motility and filopodia formation, HEK-293 or MCC13 cells were transfected with either EGFP, EGFP-ST, EGFP-ST102A, or EGFP-ST103A for 6 h. Cells were then imaged using the IncuCyte live cell imaging system, taking an image every 30 min for 24 h (Figure 4.6A), and cell motility was analysed using ImageJ software by tracing the tracks of individual cells, allowing quantification of the distance travelled. Results showed that HEK-293 and MCC13 cells expressing either EGFP-ST102A or EGFP-ST103A showed reduced cell motility in comparison to cells expressing EGFP-ST ($p < 0.001$) (Figure 4.6B). This suggests that the specific interaction of MCPyV ST with PP4C is required for MCPyV ST-induced cell motility.

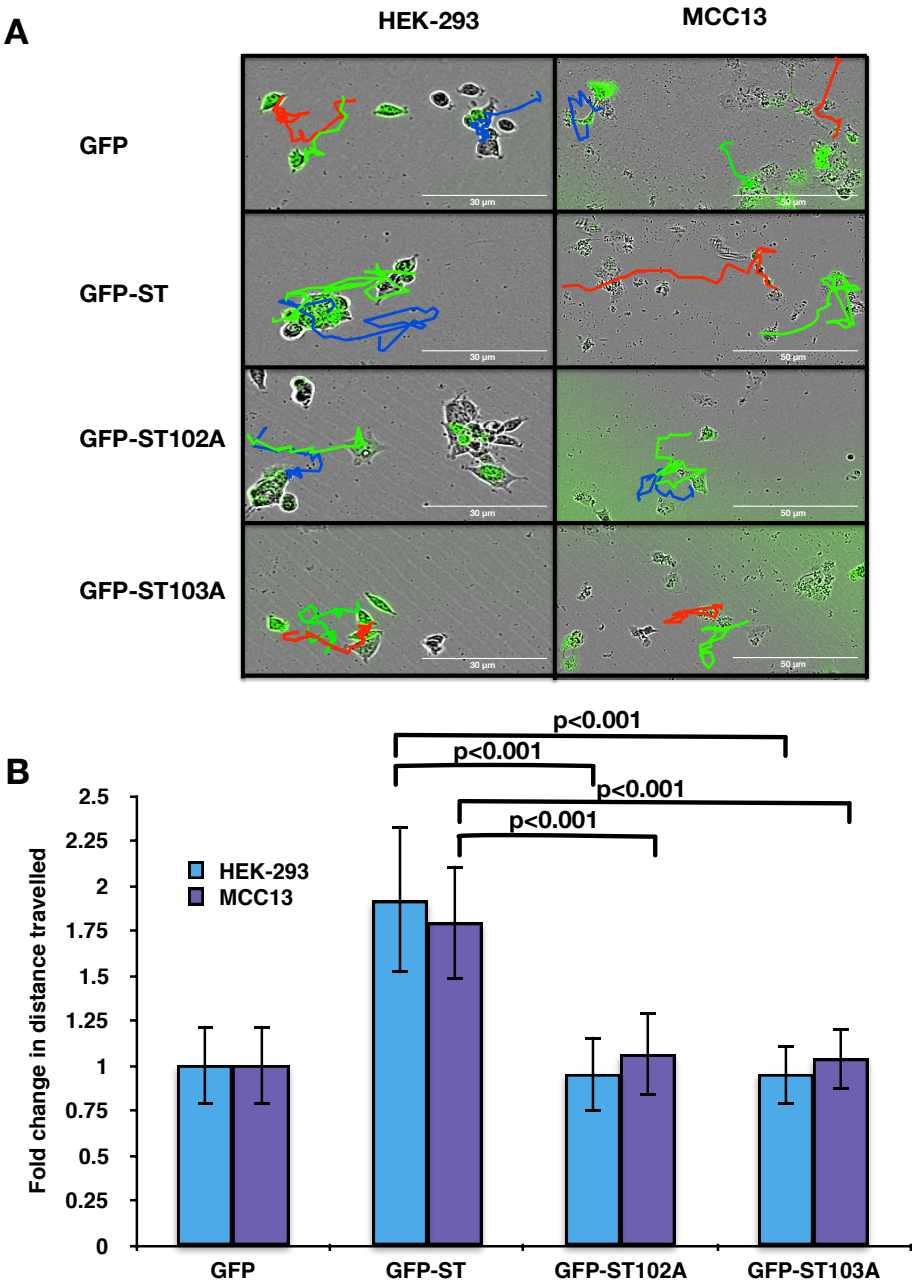


**Figure 4.6: Live cell imaging shows that MCPyV ST mutants that cannot bind PP4C reduce MCPyV ST-induced cell motility.** (A) HEK-293 or MCC13 cells were transfected with 1 μg EGFP, EGFP-ST, EGFP-ST102A or EGFP-ST103A for 6 h or 12 h. Cells were imaged using the IncuCyte live cell imaging system every 30 min for 24 h. The movement of cells was then tracked using ImageJ software. (B) Average cell movement was calculated (n = 25) and significance was tested using a two-tailed Student's t-test.

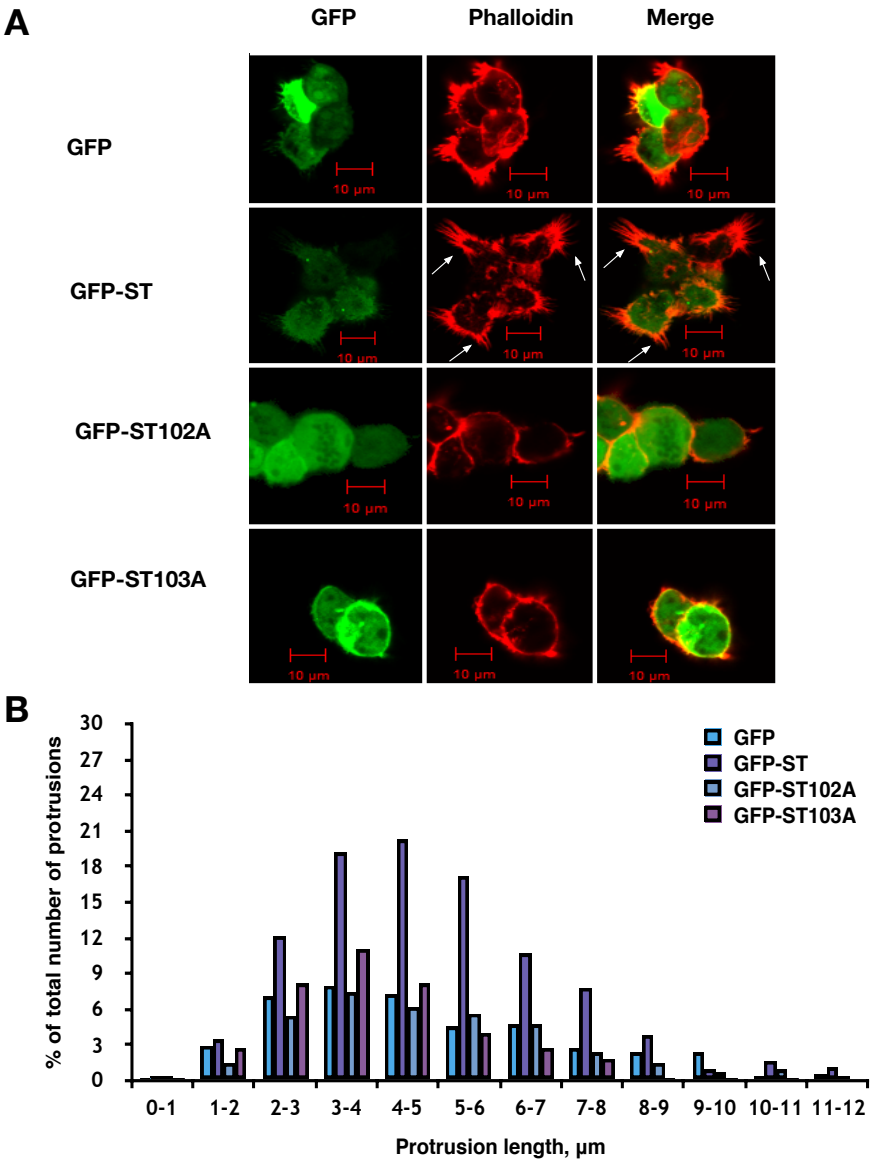


**Figure 4.7: Cell imaging shows that MCPyV ST mutants that cannot bind PP4C disrupt filopodia formation.** (A) HEK-293 cells were transfected with 1 µg EGFP, EGFP-ST, EGFP-ST102A or EGFP-ST103A for 6 h. 24 h later cells were fixed and stained with rhodamine phalloidin. All slides were then analysed using a Zeiss LSM 700 confocal laser scanning microscope. (B) Actin-based protrusions were counted for 75 cells per condition using ImageJ software. Quantifications are representative examples of 3 biological replicates.

To confirm the association between MCPyV ST, PP4C, and filopodia formation, HEK-293 cells were transfected with EGFP, EGFP-ST, EGFP-ST102A or EGFP-ST103A for 6 h, then fixed and stained with rhodamine phalloidin to observe

actin-based structures (Figure 4.7A). Together with quantitative analysis of filopodia formation (Figure 4.7B), results showed that cells expressing EGFP-ST102A and EGFP-ST103A showed a marked decrease in filopodia formation compared to cells expressing EGFP-ST. These results support the data gathered from live cell imaging experiments and further confirm the importance of the specific interaction of MCPyV ST with PP4C to induce cell motility and filopodia formation.

## 4.5 Phosphomimetic mutants of Cdc42 and Rac1 show diminished filopodia formation upon MCPyV ST expression

Having determined the role of PP4C in MCPyV ST-induced cell motility and filopodia formation, the next stage was to determine where the MCPyV ST-PP4C interaction might be important in the cell motility pathway. Initially, research was focused on the Rho-family GTPases, as there is evidence that they can be regulated by phosphorylation [429]. Specifically, phosphomimetic mutants of Cdc42 and Rac1 at the Ser71 residue have shown altered activity, with the Rac1 mutant having reduced ability to induce the formation of membrane ruffles and showing reduced GTP binding [430]. Therefore, it was hypothesised that overexpression of phosphomimetic mutants of Cdc42 and/or Rac1 may result in a decrease in filopodia formation upon MCPyV ST expression compared to cells expressing MCPyV ST alone.

To test this hypothesis, HEK-293 cells were transfected with EGFP or EGFP-ST in the presence of one of the following: Cdc42-HA, Cdc42S71E-HA (phosphomimetic), Rac1-HA, or Rac1S71E-HA (phosphomimetic). Cells were then fixed and stained with rhodamine phalloidin to observe actin structures and HA antibody to visualise the Rho-family GTPase constructs (Figures 4.8A and 4.9A). Quantitative analysis of filopodia showed a decrease in filopodia formation when cells co-expressed MCPyV ST and either of the phosphomimetic Rho-family GTPase mutants (Figures 4.8B and 4.9B). These results suggested that the MCPyV ST-PP4C interaction may be acting at the level of the Rho-family GTPases in the cell motility cascade.

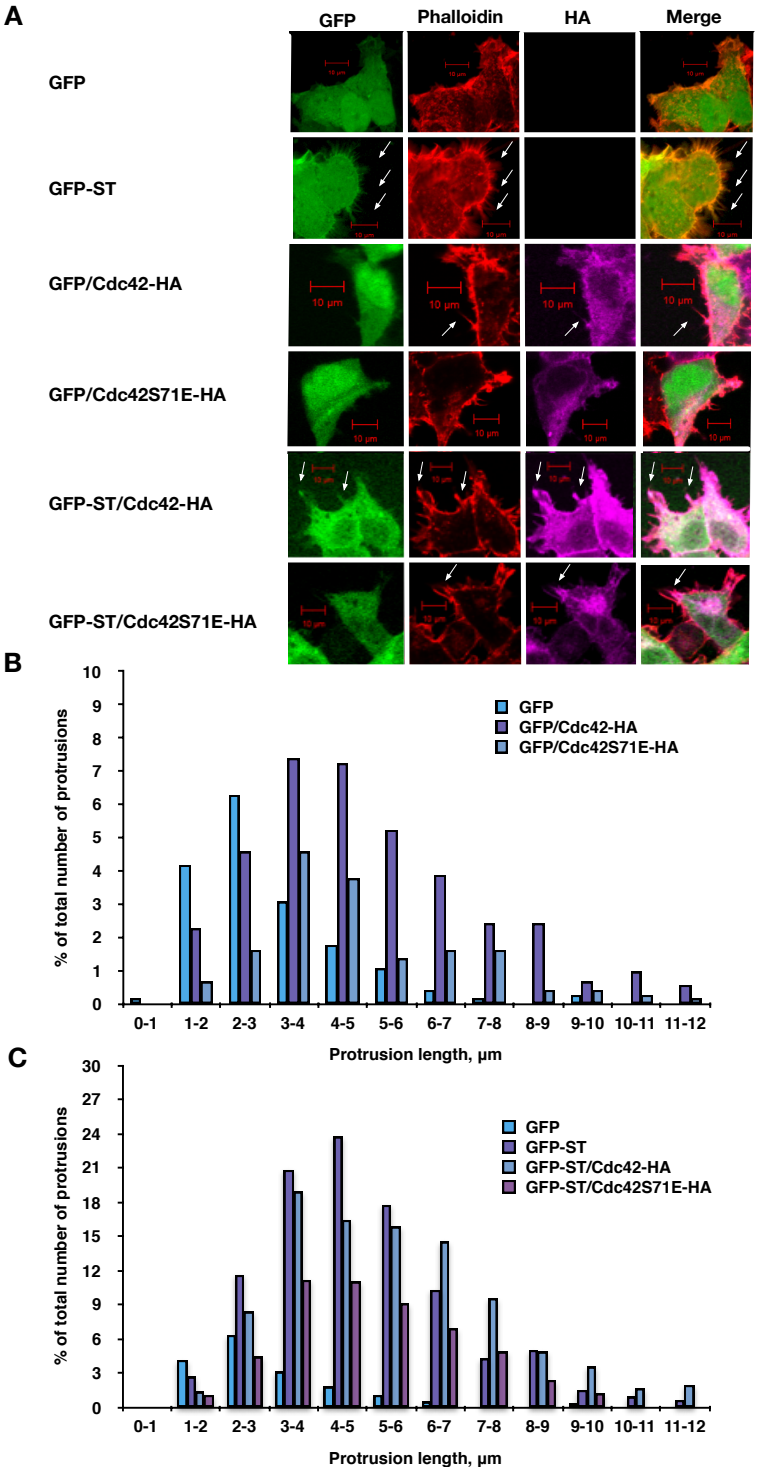


**Figure 4.8: Cell imaging shows that the phosphomimetic Cdc42S71E mutant reduces MCPyV ST-induced filopodia formation.** (A) HEK-293 cells were transfected with 1 µg EGFP, EGFP-ST or co-transfected with 1 µg EGFP-ST and Cdc42-HA or EGFP-ST and Cdc42S71E-HA for 6 h. 24 h later cells were fixed and stained with rhodamine phalloidin. All slides were then analysed using a Zeiss LSM 700 confocal laser scanning microscope. (B) and (C) Actin-based protrusions were counted for 75 cells per condition using ImageJ software. Quantifications are representative examples of 3 biological replicates.

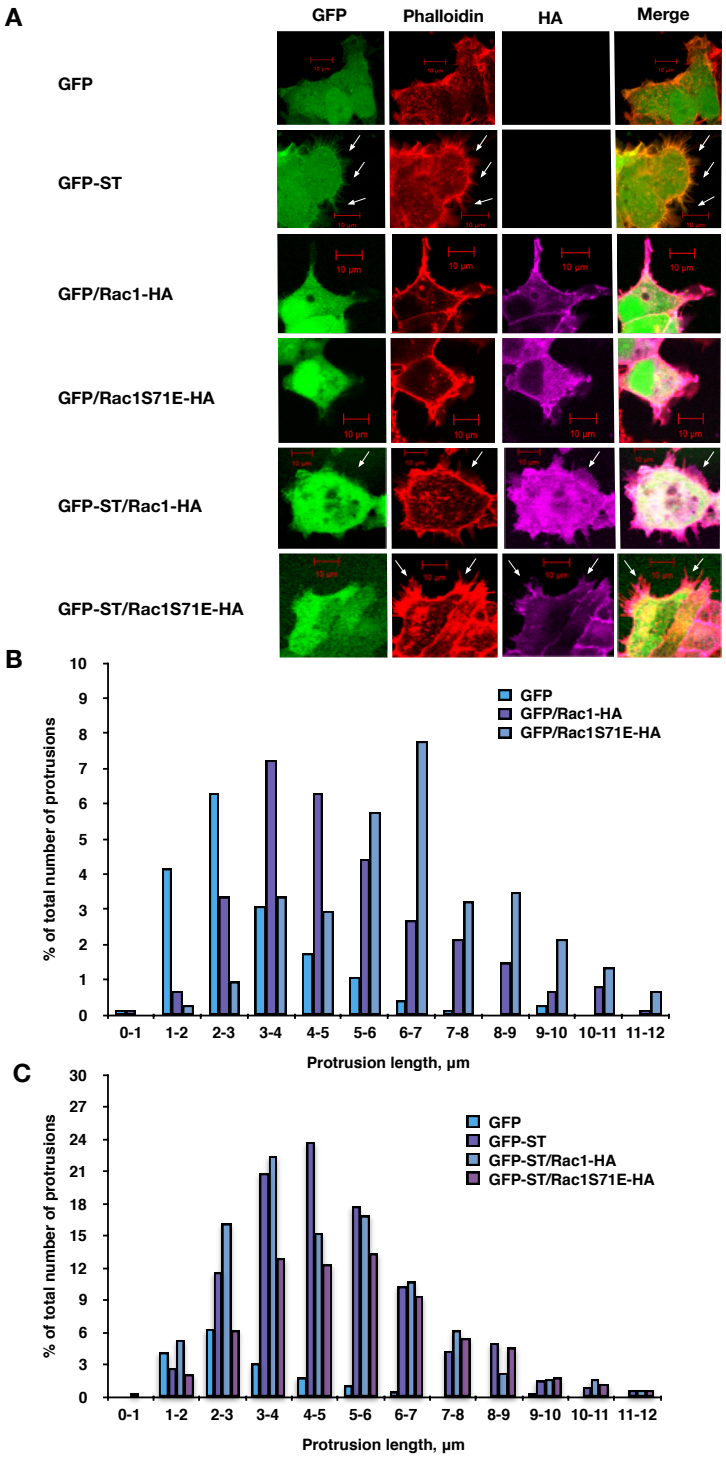


**Figure 4.9: Cell imaging shows that the phosphomimetic Rac1S71E mutant reduces MCPyV ST-induced filopodia formation.** (A) HEK-293 cells were transfected with 1 µg EGFP, EGFP-ST or co-transfected with 1 µg EGFP-ST and Rac1-HA or EGFP-ST and Rac1S71E-HA for 6 h. 24 h later cells were fixed and stained with rhodamine phalloidin. All slides were then analysed using a Zeiss LSM 700 confocal laser scanning microscope. (B) and (C) Actin-based protrusions were counted for 75 cells per condition using ImageJ software. Quantifications are representative examples of 3 biological replicates.

## 4.6 Expression of MCPyV ST does not affect the phosphorylation status of Cdc42 or Rac1

To determine whether the MCPyV ST-PP4C interaction influences the cell motility cascade at the Rho-family GTPase level, phosphorylation of Cdc42 and Rac1 at the Ser71 residue was investigated in the absence and presence of MCPyV ST expression. This particular residue was chosen because it is known to be affected by phosphorylation [430] and because PP4C is a Ser/Thr phosphatase. i293-GFP and i293-GFP-ST cells were transfected with HA-Cdc42 or HA-Rac1, then induced for 48 h. Cell lysates were then probed for phosphorylated Cdc42/Rac1 (residue Ser71) to determine if MCPyV ST expression affects the phosphorylation status of Rho-family GTPases. However, surprisingly, results showed no change in the phosphorylation status of Cdc42/Rac1 (Figure 4.10), indicating that the MCPyV ST-PP4C interaction does not affect the phosphorylation status of Rho-family GTPases directly.

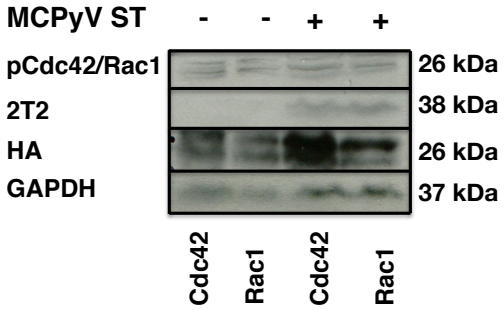


**Figure 4.10: MCPyV ST expression does not affect the phosphorylation status of Cdc42/Rac1.** i293-GFP or i293-GFP-ST were induced with doxycyline hyclate and transfected with 1 µg HA-Cdc42 or HA-Rac1 for 6 h. Cell lysates were probed for phosphorylated Cdc42/Rac1 at the S71 residue. GAPDH was used to measure equal loading. 2T2 was used to probe for MCPyV ST expression.

## 4.7 Integrin activity inhibition affects MCPyV ST-induced cell motility

In the light of the above findings indicating that the phosphorylation status of Cdc42 and Rac1 was unchanged upon MCPyV ST expression, upstream factors

were investigated to uncover a possible target for the MCPyV ST-PP4C interaction. Integrins are known to be important for cell adhesion, polarity, and motility, as they initiate signalling cascades [421]. In addition, integrins have been implicated in cancer progression [422], and their function can be regulated by phosphorylation [426].

In order to assess whether integrins play a role in MCPyV ST-induced cell motility, a range of concentrations of an integrin inhibitor, RGDS, were used. RGDS is a tetrapeptide that has been shown to inhibit the binding of ligands to $\alpha 5\beta 1$ and $\alpha v\beta 3$ integrins [431]. i293-GFP and i293-GFP-ST cells were induced using doxycycline hyclate, while MCC13 cells were transfected with EGFP or EGFP-ST. The cells were then treated with non-toxic concentrations of RGDS (Figure 4.11) for 24 h. Cells were imaged using the IncuCyte kinetic imaging system every 30 min for 24 h (Figure 4.12A and Figure 4.13A). Distances travelled by individual cells were analysed using ImageJ software and showed decreasing cell motility with increasing RGDS concentration in a dose-dependent manner (Figure 4.12B and Figure 4.13B). These results suggested that there is a role for integrin signalling in MCPyV ST-induced cell motility as treatment with RGDS tetrapeptide affected cell motility.

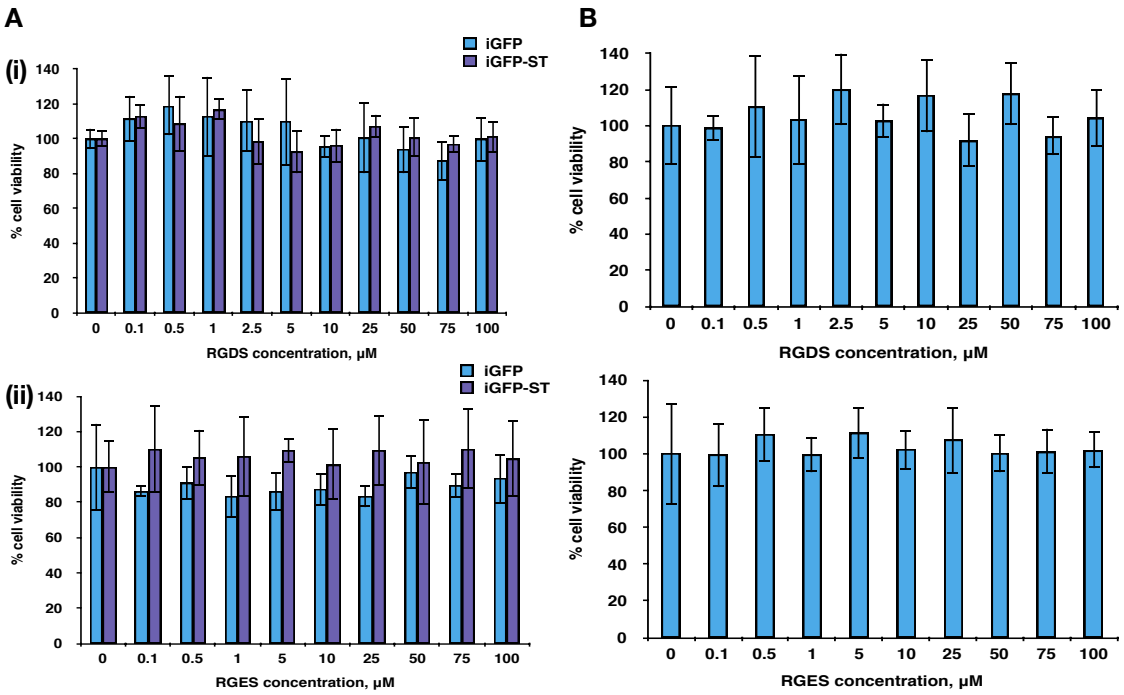


**Figure 4.11: Cell viability assays for RGDS and RGES.** (A) iGFP and iGFP-ST cells were induced for 24 h, then treated with peptides ((i) RGDS, (ii) RGES) at different concentrations for 24 h. (B) MCC13 cells were grown for 24 h, then treated with peptides ((i) RGDS, (ii) RGES) at different concentrations for 24 h. Cell viability was measured using the MTS assay. Highest concentration of inhibitor at >80% viability was used for inhibition studies.

However, in order to confirm that the results obtained are significant, this experiment was repeated using non-toxic concentrations of a control peptide, RGES (Figure 4.11) in i293 and MCC13 cells. Cells were imaged using the IncuCyte kinetic imaging system every 30 min for 24 h (Figure 4.14A and Figure 4.15A). Distances travelled by individual cells were analysed using ImageJ software. Results showed no change in cell motility with increasing RGES concentration (Figure 4.14B and Figure 4.15B). These results confirmed that integrins are important in MCPyV ST-induced cell motility.

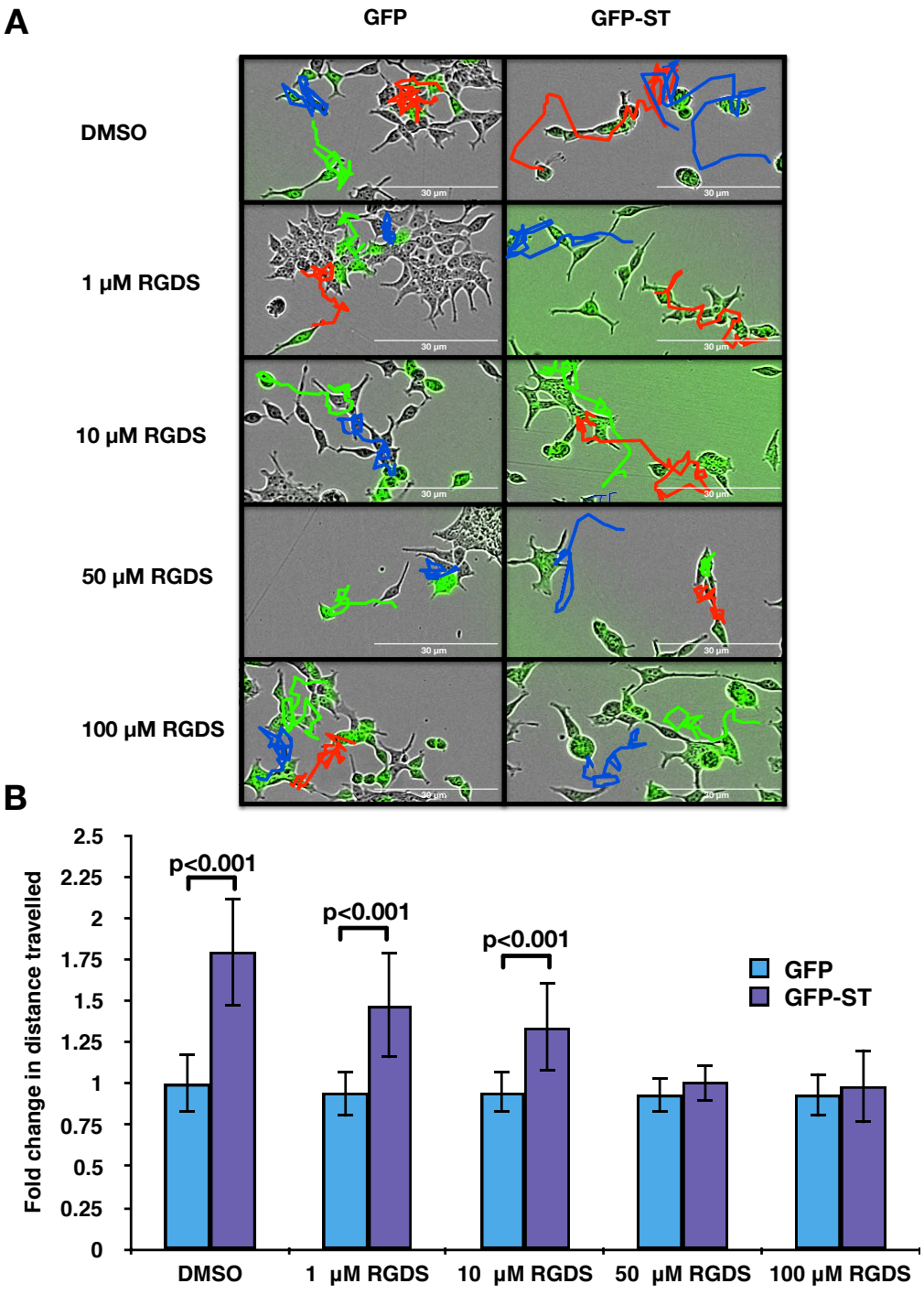


**Figure 4.12: Integrin inhibitor RGDS reduces MCPyV ST-induced cell motility in i293 cells.** (A) i293-GFP and i293-GFP-ST cells were induced using doxycycline hyclate and treated with 1 µg/µl DMSO or 1 µM, 10 µM, 50 µM, or 100 µM RGDS. After 24 h, cell motility was measured using an Incucyte kinetic live cell imaging system. Images were taken for 30 min for a 24 h period. The movement of cells was then tracked using ImageJ software. (B) Average cell movement was calculated (n = 25) and significance was tested using a two-tailed Student's t-test.

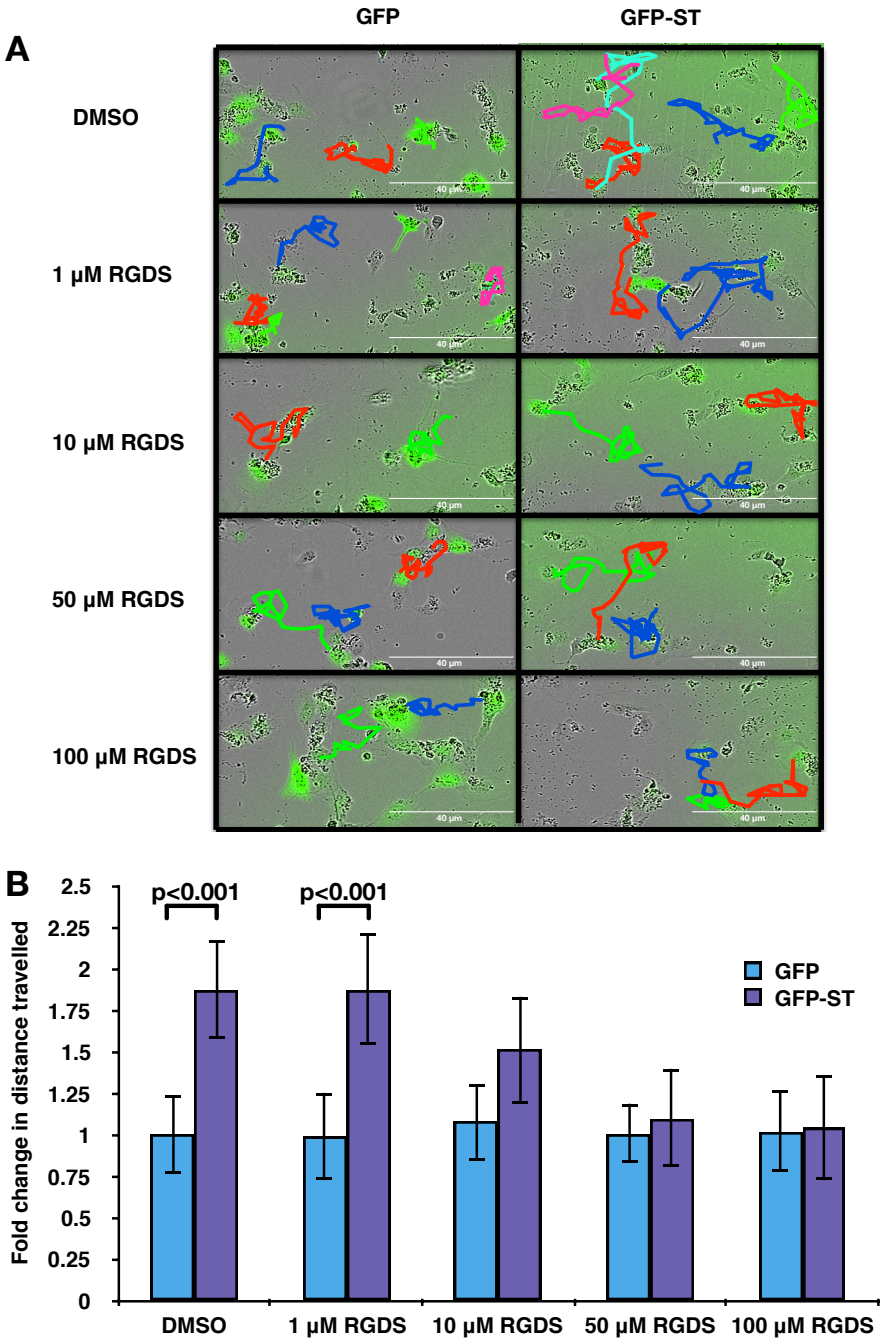


**Figure 4.13: Integrin inhibitor RGDS reduces MCPyV ST-induced cell motility in MCC13 cells.** (A) MCC13 cells were transfected for 24 h with 1µg of EGFP and EGFP-ST, and treated with 1 µg/µl DMSO or 1 µM, 10 µM, 50 µM, or 100 µM RGDS. After 24 h, cell motility was measured using an Incucyte kinetic live cell imaging system. Images were taken for 30 min for a 24 h period. The movement of cells was then tracked using ImageJ software. (B) Average cell movement was calculated (n = 25) and significance was tested using a two-tailed Student's t-test.

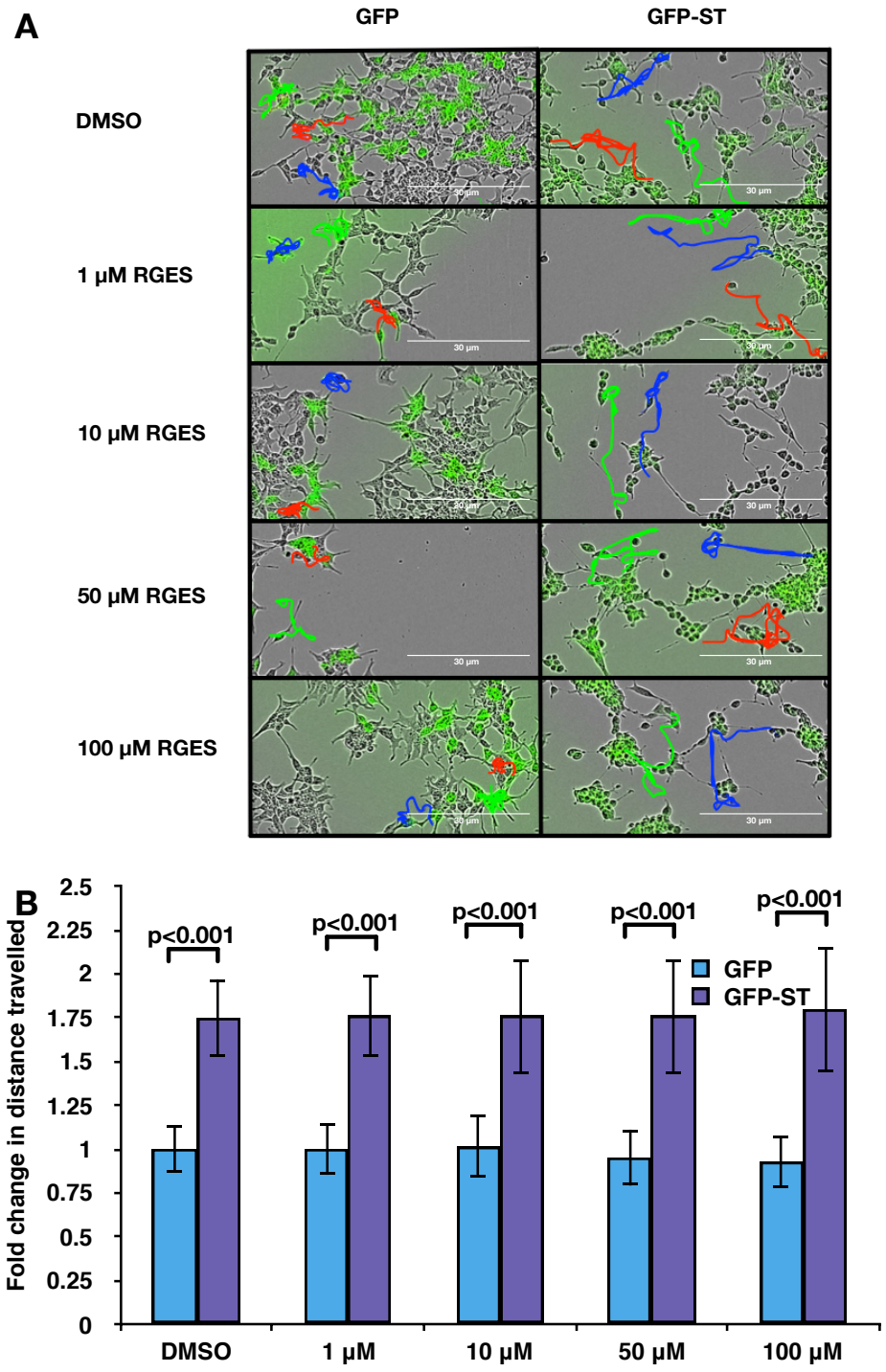


**Figure 4.14: Control peptide RGES does not reduce MCPyV ST-induced cell motility in i293 cells.** (A) i293-GFP and i293-GFP-ST cells were induced using doxycycline hyclate and treated with 1 µg/µl DMSO or 1 µM, 10 µM, 50 µM, or 100 µM RGES. After 24 h, cell motility was measured using an Incucyte kinetic live cell imaging system. Images were taken for 30 min for a 24 h period. The movement of cells was then tracked using ImageJ software. (B) Average cell movement was calculated (n = 25) and significance was tested using a two-tailed Student's t-test.

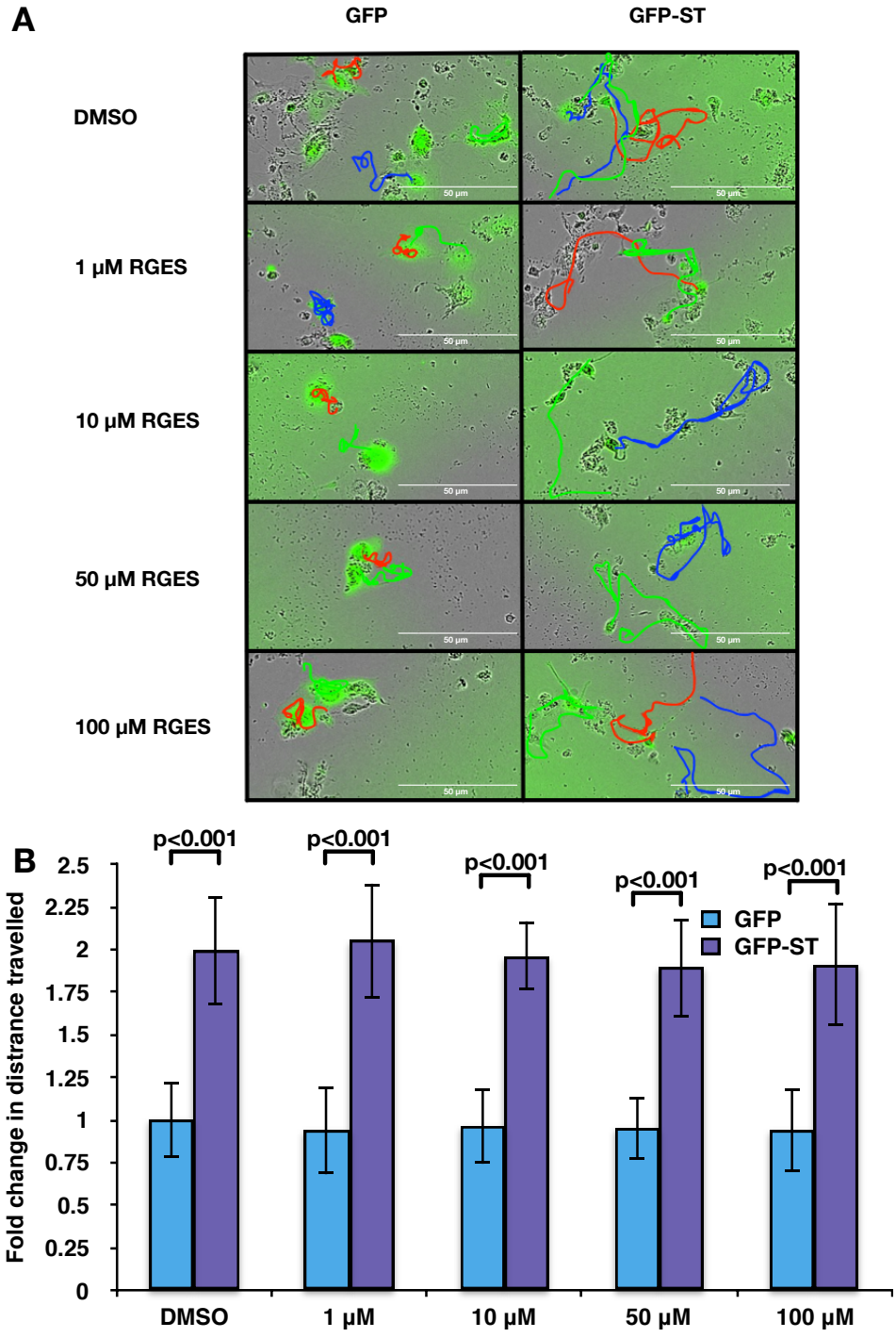


**Figure 4.15: Control peptide RGES does not reduce MCPyV ST-induced cell motility in MCC13 cells.** (A) MCC13 cells were transfected for 24 h with 1 µg of EGFP and EGFP-ST, and treated with 1 µg/µl DMSO or 1 µM, 10 µM, 50 µM, or 100 µM RGES. After 24 h, cell motility was measured using an Incucyte kinetic live cell imaging system. Images were taken for 30 min for a 24 h period. The movement of cells was then tracked using ImageJ software. (B) Average cell movement was calculated (n = 25) and significance was tested using a two-tailed Student's t-test.

## 4.8 Inhibition of integrin activity affects MCPyV ST-induced filopodia formation

As integrin activity was found to be important in MCPyV ST-induced cell motility, it was hypothesised that integrin activity would also affect filopodia formation. To determine whether that is the case, HEK-293 cells were transfected with EGFP or EGFP-ST for 6 h, then treated with 100 μM RGDS or the control peptide RGES for 24 h. Cells then fixed and stained with rhodamine phalloidin to visualise actin-based structures (Figure 4.16A). Quantitative analysis of filopodia showed that treatment of cells expressing MCPyV ST with RGDS show a reduction in filopodia compared to untreated cells expressing MCPyV ST (Figure 4.16B). These results supported previous results that integrins are implicated in MCPyV ST-induced cell motility.

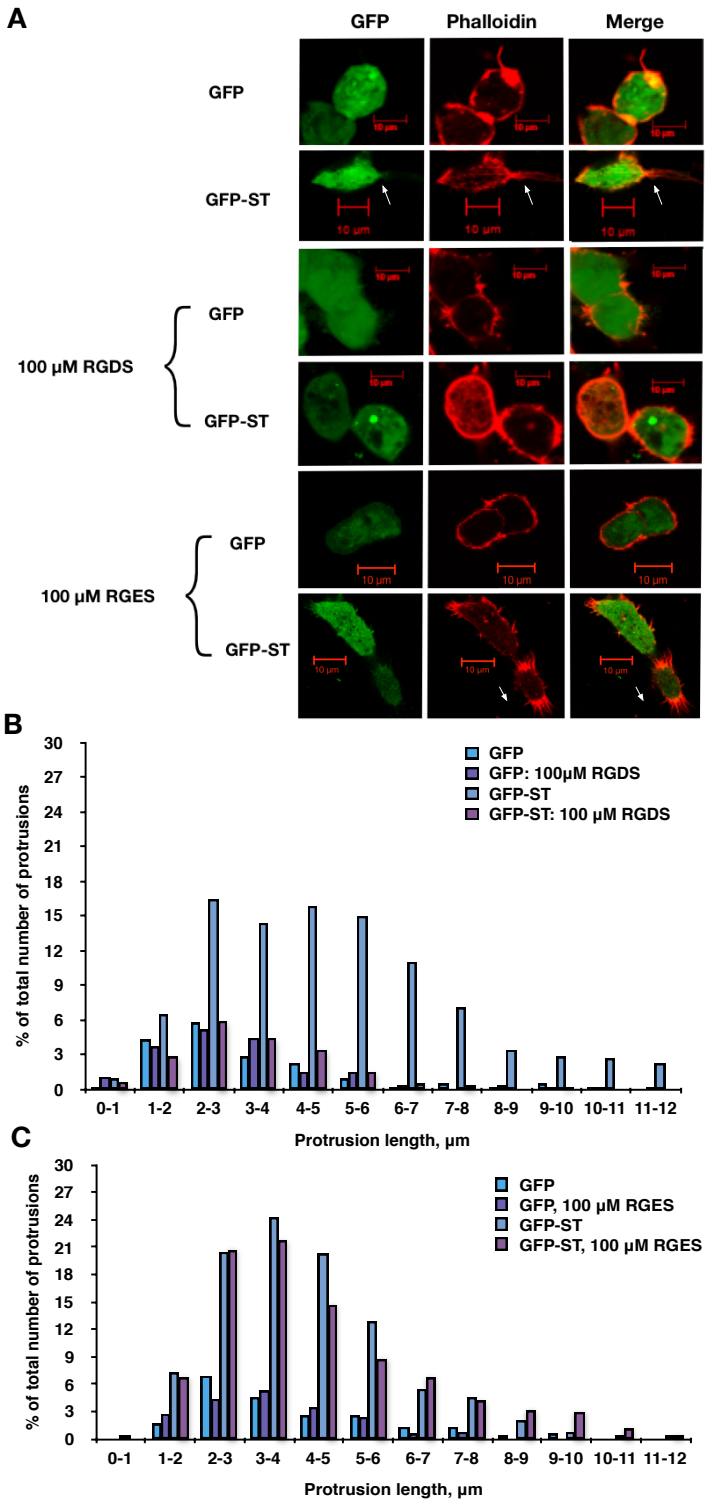


**Figure 4.16: Integrin inhibitor RGDS reduces MCPyV ST-induced filopodia formation.** (A) HEK-293 cells were transfected with 1 µg EGFP or EGFP-ST for 6 h, then treated with 100 µM RGDS or RGES for 24 h. Cells were then fixed and stained with rhodamine phalloidin. All slides were then analysed using a Zeiss LSM 700 confocal laser scanning microscope. (B) and (C) Actin-based protrusions were counted for 75 cells per condition using ImageJ software. Quantifications are representative examples of 3 biological replicates.

## 4.9 Expression of MCPyV ST affects the phosphorylation of β1 integrin at Thr788/789

The importance of integrins in MCPyV ST-induced cell motility and filopodia formation suggested a possibility that integrin phosphorylation could be affected by MCPyV ST-PP4C interaction. Importantly, integrin activity can be regulated by phosphorylation [426]. Specifically, the effect of RGDS on MCPyV ST-induced filopodia formation and cell motility suggested that α5β1 and/or αvβ3 may be involved. As HEK-293 cells do not express αvβ3 [432], α5 and/or β1 were considered for further investigation. Notably, β1 phosphorylation status can be regulated at the Thr788/789 residues [428].

Thus in order to determine whether MCPyV ST expression affected β1 phosphorylation, HEK-293 cells were transfected with EGFP, EGFP-ST, EGFP-ST102A or EGFP-ST103A for 6 h. Cell lysates were probed for phosphorylated β1 integrin at Thr788/789. Results showed a reduction in the phosphorylation levels of β1 integrin at these sites upon MCPyV ST expression. However, phosphorylation levels remained the same upon the expression of the PP4C-non-binding mutants EGFP-ST102A and EGFP-ST103A (Figure 4.16A). Densitometry showed a 3-fold decrease in the phosphorylation levels of β1 at Thr788/789 upon MCPyV ST expression (Figure 4.17B).

These results suggest a potential model for MCPyV ST-induced cell motility (Figure 4.18). Briefly, the MCPyV ST-PP4C interaction leads to the reduction of β1 integrin phosphorylation levels at Thr788/789. This then affects downstream signalling that ultimately enhances filopodia formation and cell motility in MCPyV ST-expressing cells.

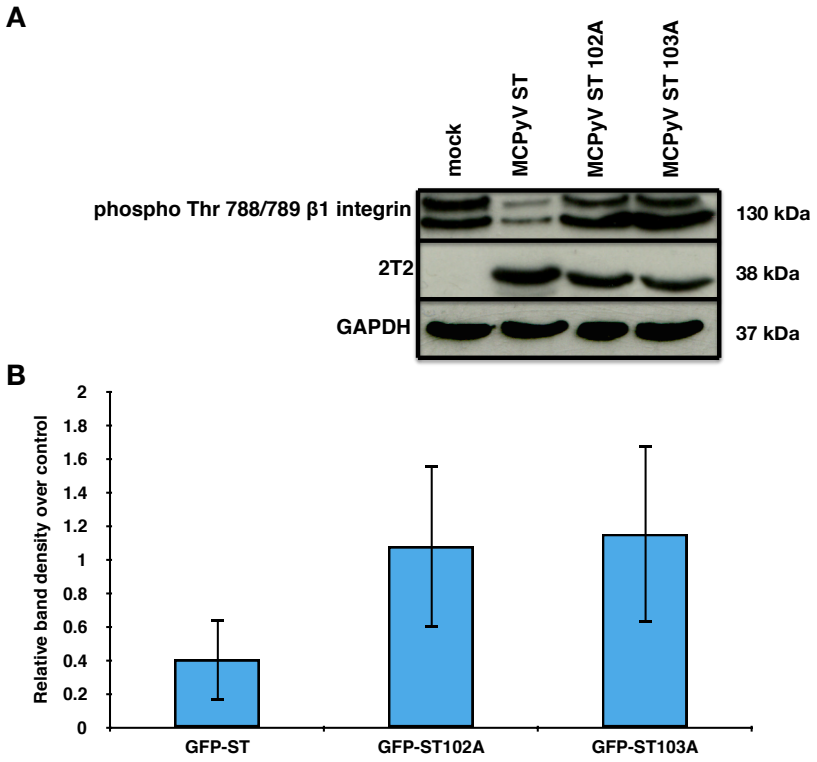


**Figure 4.17: MCPyV ST expression reduces the phosphorylation levels of β1 integrin at Thr 788/789 residues.** (A) HEK-239 cells were transfected with 1 μg EGFP, EGFP-ST, EGFP-ST102A or EGFP-ST103A for 6 h. Cell lysates were probed for phosphorylated Thr 788/789 residues of β1 integrin. GAPDH was used to measure equal loading. 2T2 was used to probe for MCPyV ST expression. (B) Exposed film with immunoblotting results was scanned and uploaded onto ImageJ software, which was used to compare band density (n=3).

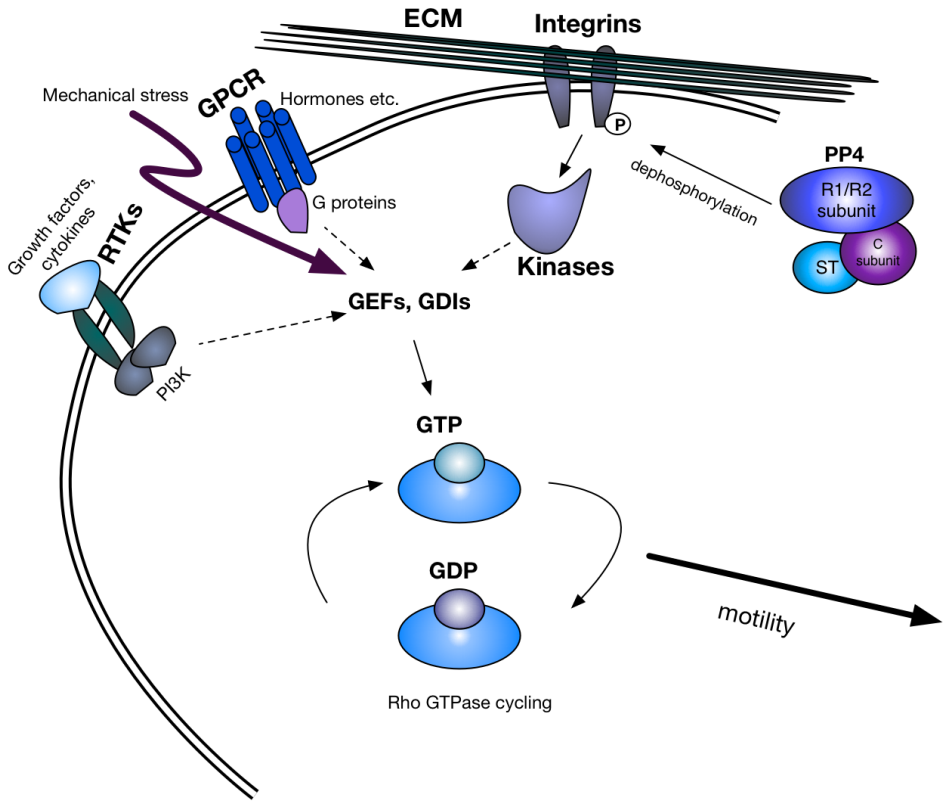


**Figure 4.18: A model for MCPyV ST-induced cell motility.** The MCPyV ST-PP4C leads to the dephosphorylation of β1 integrin. This then leads to the initiation of the cell motility pathway, mediated via the Rho-family GTPases.

## 4.10 Discussion

MCPyV ST can interact with Ser/Thr cellular phosphatases PP2A Aα, PP2A Aβ and PP4C, and these interactions have been well documented [20] [209]. MCPyV ST interaction with PP4C in particular seems to be important in promoting cell motility [210]. While PP4C is not as well characterised as PP2A, it has been implicated in a variety of cellular functions, including apoptosis, DNA mutation, and cell proliferation [433], as well as a number of cell signalling pathways [434]. Moreover, PP4C has been found to be upregulated in some cancers [435]. In addition, it was recently reported that PP4C is involved in destabilising the microtubule network to promote cell motility [210]. Results presented in this chapter implicate PP4C in actin dynamics, as MCPyV ST-induced filopodia formation appears to be dependent upon the MCPyV ST-PP4C interaction.

Having described the role of Rho-family GTPases in MCPyV ST-induced cell motility and filopodia formation in Chapter 3, a potential effect on the phosphorylation status of Cdc42 and Rac1 was explored upon MCPyV ST expression. However, it appears that the MCPyV ST-PP4C interaction does not act at the level of these signal mediators. Therefore, upstream factors were investigated, in particular the cell surface receptors integrins. Data presented in this chapter suggest that integrins, including β1, play a role in MCPyV ST-induced cell motility and filopodia formation.

Integrins are cellular receptors known to be important in the cell motility pathway, particularly in Rho-family GTPase cycling [436]. RGDS, an integrin inhibitor was used to determine whether integrins were important in MCPyV ST-induced cell motility. RGDS is a tetrapeptide found on fibronectin, fibrinogen α, and von Willebrand factor [437] [438], and is known to inhibit α5α1 and ανα3 integrins [431]. Results showed that increasing RGDS concentrations lead to a dose-dependent reduction in MCPyV ST-induced cell motility and filopodia formation.

As β1 integrin is expressed in HEK-293 cells, it was decided to focus on this particular integrin. A further reason was the fact that PP2A has been shown to dephosphorylate β1 integrin at Thr788/789 [428]. It was observed that levels of Thr788/789 phosphorylation were reduced upon MCPyV ST expression, and that the change in phosphorylation is dependent on the interaction of MCPyV ST with PP4C. Thus a mechanism has been put forward, suggesting that the MCPyV ST-PP4C interaction leads to the dephosphorylation of β1 integrin. This in turn activates the cell motility pathway. Moreover, it is possible that other phosphorylation sites, such as Ser785, are involved, although this was not explored in this chapter. Notably, changes in the phosphorylation status Ser785 has been shown to affect cell motility in chicken cell lines [427]. Furthermore, other changes in the phosphorylation status of other integrins may also be important in MCPyV ST-induced cell motility. This area requires further research beyond the scope of this thesis.

The overall findings of Chapters 3 and 4 suggest a possible mechanism (Figure 4.18), wherein the MCPyV ST-PP4C interaction leads to the dephosphorylation of one or more Ser/Thr residues of one or more integrins, including β1. These changes in phosphorylation status then act to initiate the cell motility cascade which, through the Rho-family GTPases, results in increased filopodia formation and cell motility. These findings further contribute to the hypothesis that the

MCPyV ST-PP4C interaction is central in promoting the metastatic phenotype of MCC. Therefore, this interaction is a viable drug target and worth pursuing in future research.

# Chapter 5

# Merkel cell polyomavirus small T antigen-induced cell motility depends on the activity of intracellular chloride channels

## 5.1 Introduction

Cell motility depends on the ability of cells to change their internal volume. This process is driven by changes of the ionic balance in cells [326] [439], which in turn depends on the activity of ion channels. Ion channels allow the passage of ions between the interior of the cell and the interstitial fluid and play a role in a whole range of cellular processes required for the proper functioning of tissues and organs. This makes them frequent drug targets [440].

Some of the major ions involved in cell physiology are sodium, potassium, and chloride. Sodium is the major extracellular ion, and is vital to maintaining the osmolality of interstitial fluid, lymph, and blood [441]. Potassium is the major intracellular cation [441], and a large group of potassium channels are dedicated to tightly controlling potassium influx and efflux. Chloride is the major extracellular anion [441], and a variety of different chloride channels also maintain cellular chloride homeostasis.

In order to control the homeostasis of ions, ion channels are gated. Chloride channel gating, depending on the channel type, may be regulated by transmembrane voltage (voltage-gated channels), cell swelling, binding of signalling molecules (ligand-gated anion channels), various ions (anions, pH, or calcium), phosphorylation of intracellular residues, or binding or hydrolysis of ATP. Voltage-gated chloride channels are involved in setting the resting membrane potential of cells, and as well as chloride, they can conduct other anions, for example bicarbonate, iodide, and nitrite [442]. There are several different families of voltage-gated and ligand-gated chloride channels, including the large CLC family, the cystic fibrosis transmembrane conductance regulator (CFTR) chloride channel, calcium-activated chloride (CaCC) channel family, and the intracellular chloride channel (CLIC) family [443].

The CLIC family consists of seven highly-conserved members: p64 and CLIC1-6, and exist both as soluble proteins and membrane-bound channels. They are unique amongst chloride channels in their capacity to exist as both intracellular soluble proteins and transmembrane channels, being expressed in many different intracellular compartments [444]. As such, members of the CLIC family have been implicated in a variety of cellular functions, including motility [445], angiogenesis [446], brain and skeletal muscle formation [447], apoptosis [448], and

cancer [449]. For example, CLIC1 is upregulated in a number of cancers, including colon cancer [450] and prostate cancer [451].

In this chapter, the link between MCPyV ST-induced cell motility and the activity of chloride channels is explored. This investigation was undertaken due to the involvement of chloride channels in other cancers, and their known role in cell motility. The chapter begins by showing that inhibition of chloride channels reduced MCPyV ST-induced cell motility and filopodia formation. Furthermore, chloride channels of the CLIC family, particularly CLIC1 and CLIC4, are implicated in MCPyV ST-induced cell motility, with increased relocalisation to the cell surface, especially CLIC4, as a potential mechanism of action.

## 5.2 MCPyV ST expression increases the activity of ion channels

Changes in cellular current indicate the activation of ion channels. In order to determine whether MCPyV ST expression induces changes in the activity of ion channels, HEK-293 cells transfected with EGFP or EGFP-ST were patch clamped and the resulting changes in current were measured for single cells. This work was done by Yuahuei Jiang. Results show a dramatic increase in the current of MCPyV ST expressing cells with increasing voltage as compared to controls (Figure 5.1). These results are the first indication that MCPyV ST expression leads to a change in the activity levels of ion channels.

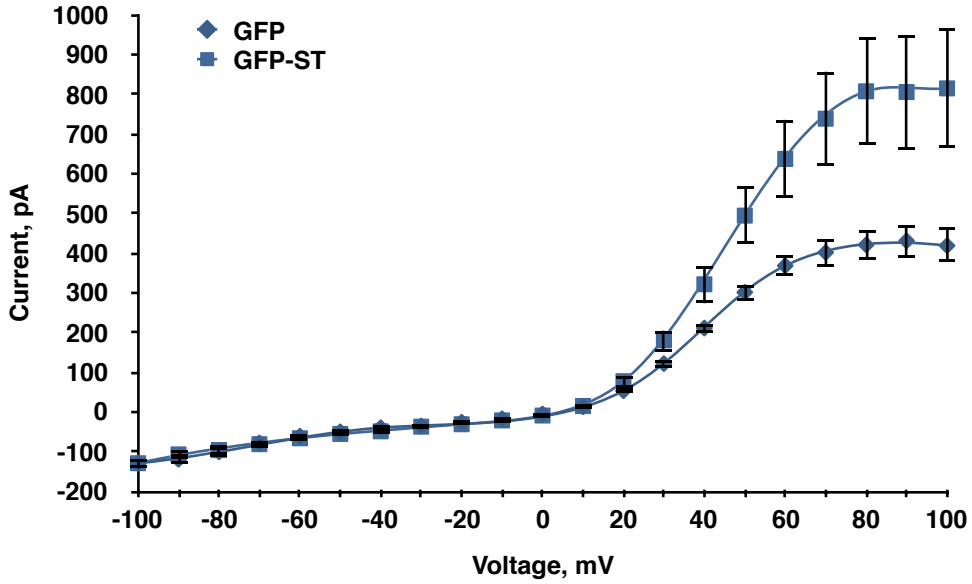


**Figure 5.1: Patch clamping of HEK-293 cells shows an increase in current upon MCPyV ST expression.** HEK-293 cells were transfected with 1 µg EGFP or EGFP-ST for 6 h. 48 h post-transfection cells were patch clamped and membrane currents were recorded from single fluorescing cells. Cells were held at -80 mV and pulses were applied to potentials between ±100 mV. Current-voltage relationships were constructed for each cell by plotting the steady-state current at the end of the pulse against the pipette potential. n = 15 (GFP) or 22 (GFP-ST). This work was performed by Yuahuei Jiang.

Results from the patch clamping studies indicated that there was an overall change in current upon MCPyV ST expression. However, for the scope of this thesis, chloride channels were the focus of further investigation due to their above-mentioned involvement in cell motility and cancer. Furthermore, chloride channels are less well-studied than, for instance, potassium channels, thus any potential involvement of chloride channels in MCPyV ST motility would be completely novel in the context of virus-induced cancer progression.

## 5.3 Broad-spectrum chloride channel inhibitors affect MCPyV ST-induced cell motility

In order to determine whether chloride channels play a role in MCPyV ST-induced cell motility, a selection of inhibitors known to target a broad range of chloride

channels were utilised at non-toxic concentrations as measured by MTS assay (Figure 5.2): DIDS [452], NPPB [453] and RIAA [454].

i293-GFP and i293-GFP-ST cells were induced using doxycycline hyclate, while MCC13 cells were transfected with EGFP or EGFP-ST, and treated with each respective inhibitor for 24 h. Cell motility was then imaged using the IncuCyte kinetic imaging system, every 30 min for 24 h (Figure 5.3A and Figure 5.4A). Distance travelled by individual cells were tracked using ImageJ software. No significant differences were observed among the average distances travelled by control GFP-expressing cells not expressing MCPyV ST, in both untreated and treated cells with the broad-spectrum chloride channel inhibitors (Figure 5.3B and Figure 5.4B). Conversely, MCPyV ST-expressing cells treated with any of the broad-spectrum chloride channel inhibitors showed significant decrease in cell motility compared to untreated cells ($p < 0.001$) (Figure 5.2B and Figure 5.3B). These findings suggested that chloride channels are involved in MCPyV ST-induced cell motility.

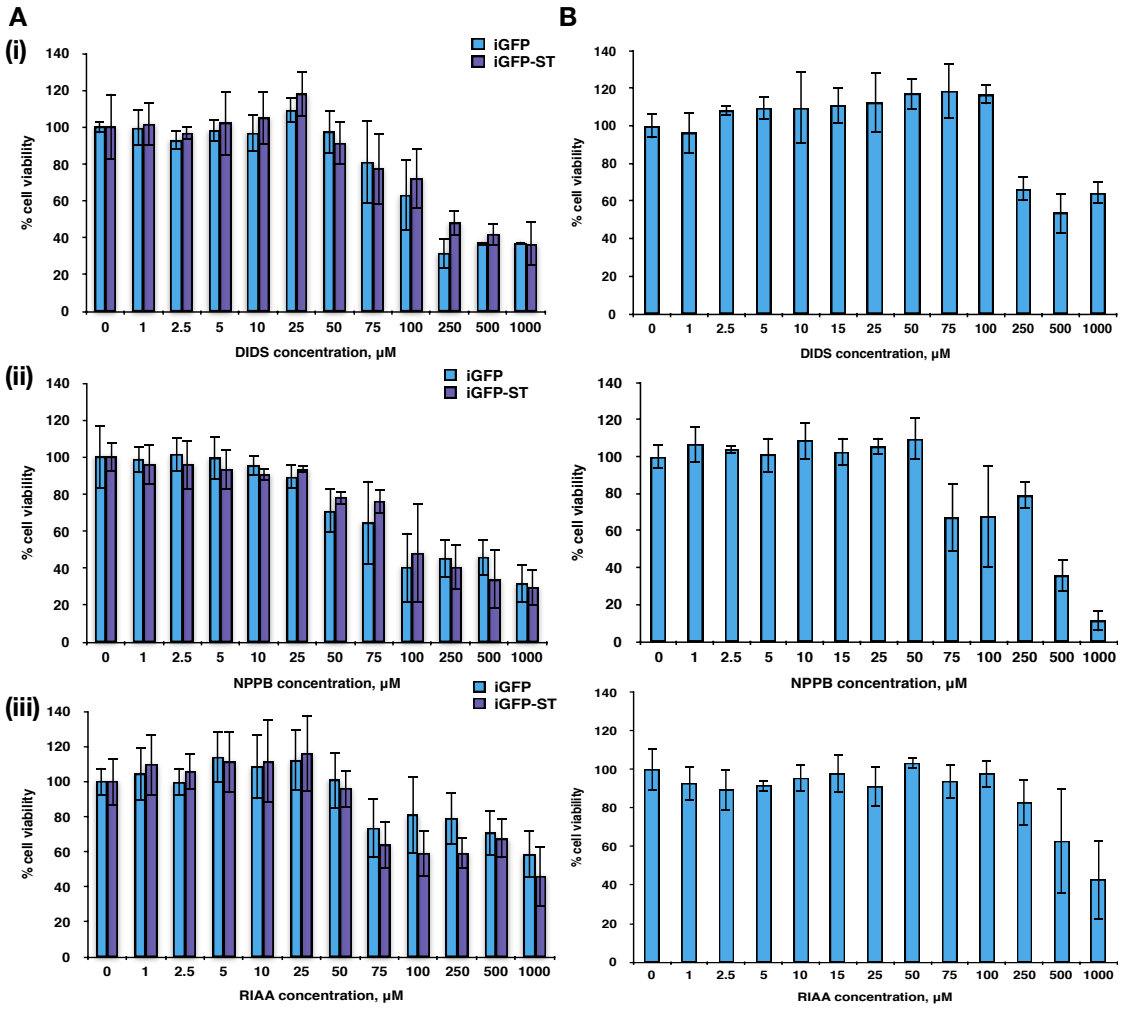


**Figure 5.2: Cell viability assays for broad-spectrum chloride channel inhibitors.** (A) iGFP and iGFP-ST cells were induced for 24 h, then treated with inhibitors ((i) DIDS, (ii) NPPB, (iii) RIAA) at different concentrations for 24 h. (B) MCC13 cells were grown for 24 h, then treated with inhibitors ((i) DIDS, (ii) NPPB, (iii) RIAA) at different concentrations for 24 h. Cell viability was measured using the MTS assay. Highest concentration of each inhibitor at >80% viability was used for further experiments.

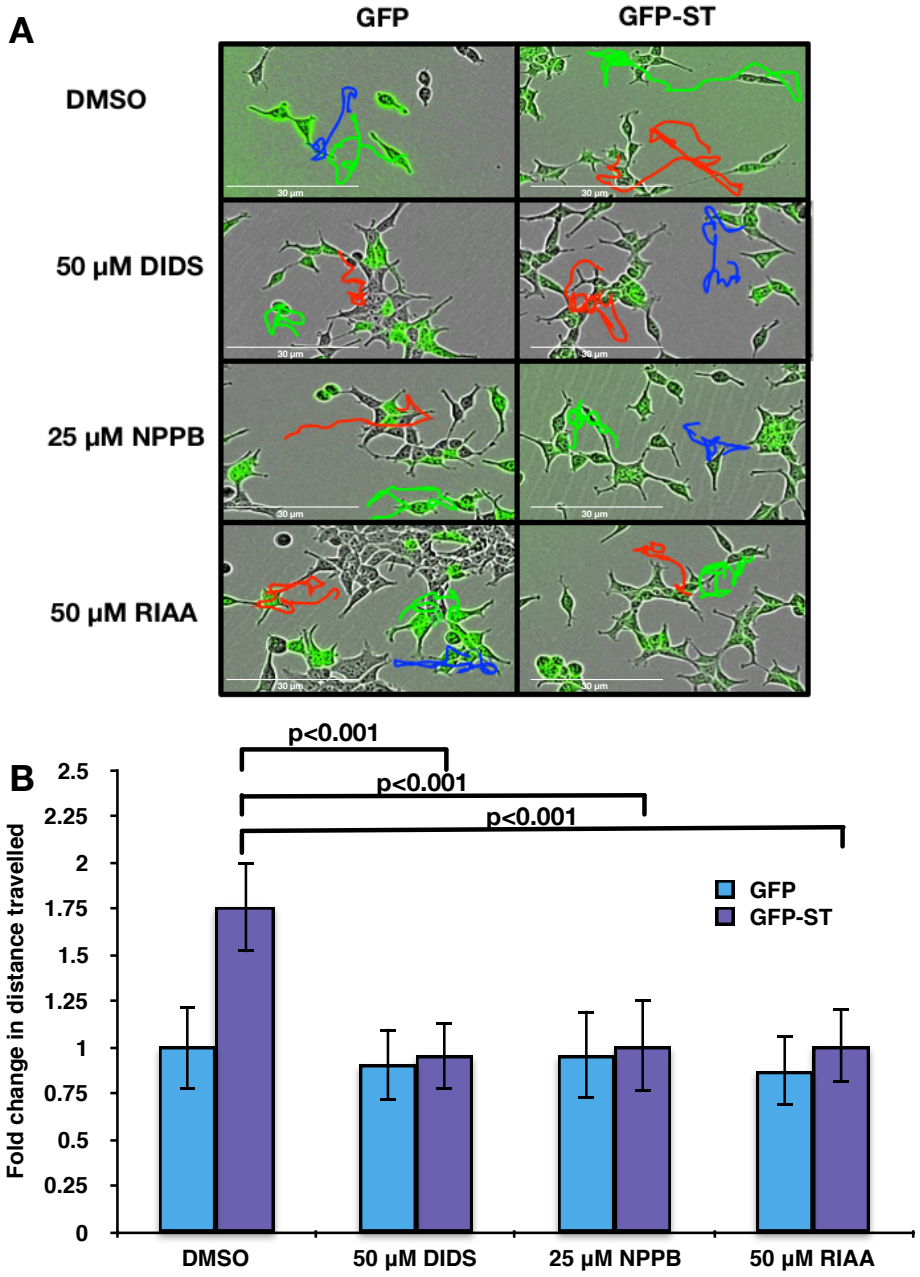


**Figure 5.3: Live cell imaging shows blocking chloride channels with broad-spectrum inhibitors reduces MCPyV ST-induced cell motility in i293 cells.** (A) i293-GFP and i293-GFP-ST cells were induced using doxycycline hyclate and treated with 1 µg/µl DMSO, 50 µM of DIDS or RIAA, or 25 µM of NPPB. After 24 h, cell motility was measured using the IncuCyte kinetic imaging system. Images were taken every 30 min for a 24 h period. (B) The movement of cells was then tracked using ImageJ software (n = 25). Average cell movement was calculated and significance was tested using a a two-tailed Student's t-test.

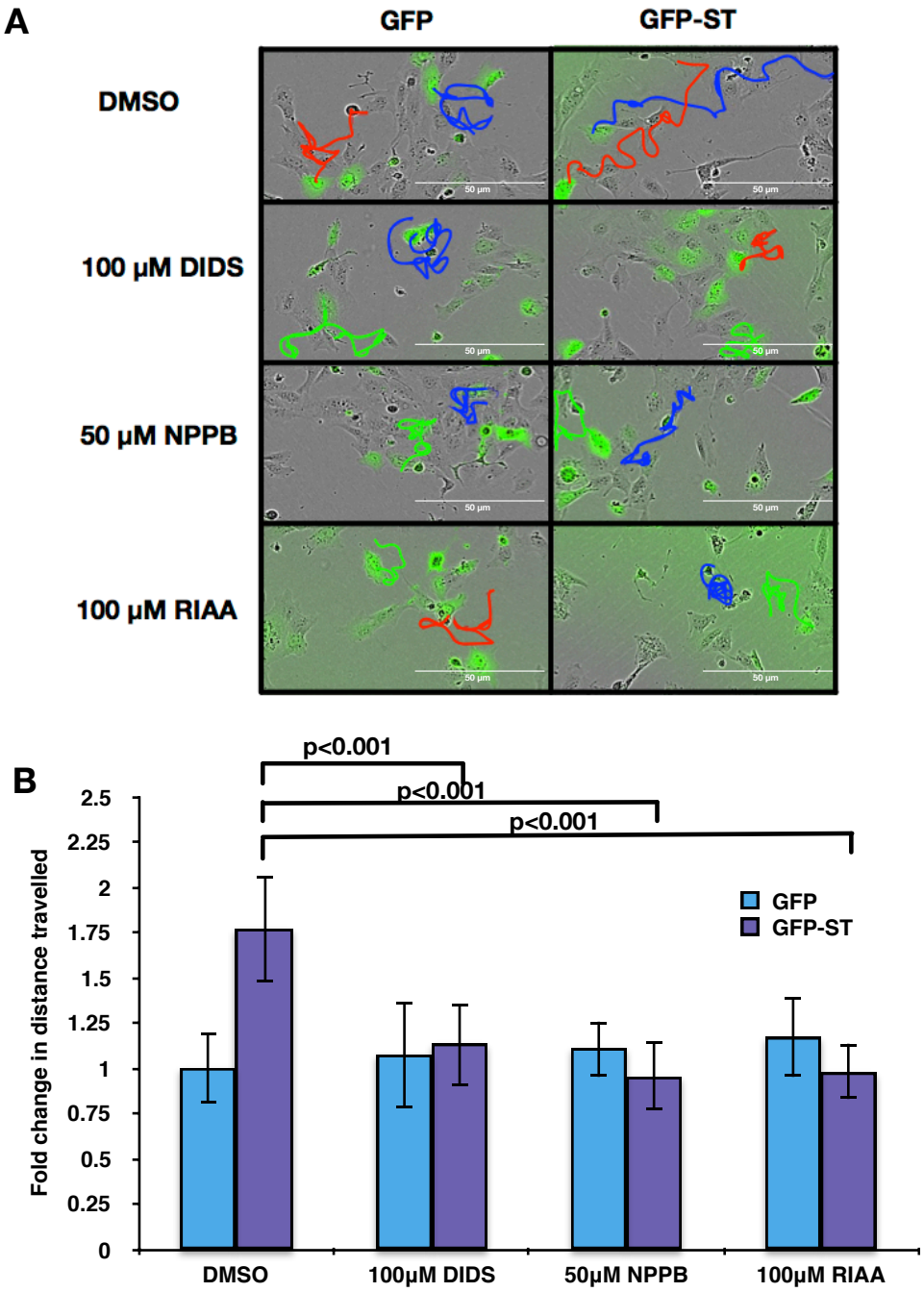


**Figure 5.4: Live cell imaging shows blocking chloride channels with broad-spectrum inhibitors reduces MCPyV ST-induced cell motility in MCC13 cells.** (A) MCC13 cells were transfected for 12 h with 1 µg of EGFP and EGFP-ST, and treated for 24 h with 1 µg/µl DMSO, 100 µM of DIDS or RIAA, or 50 µM of NPPB. After 24 h, cell motility was measured using the IncuCyte kinetic imaging system. Images were taken every 30 min for a 24 h period. (B) The movement of cells was then tracked using ImageJ software (n = 25). Average cell movement was calculated and significance was tested using a a two-tailed Student's t-test.

Finally, to confirm these observations, a haptotaxis migration assay was performed. Haptotaxis migration assays investigate the three-dimensional migration of cells towards a chemoattractant (e.g. FCS) across a permeable chamber. i293-GFP and i293-GFP-ST cells were induced with doxycycline hyclate, transferred to haptotaxis plates, and treated with the three broad-spectrum chloride inhibitors for 24 h. Cells were then allowed to migrate for 24 h according to the assay manufacturer's instructions. Migration was measured by fluorescence after staining cells that migrated into the chambers and resuspending them in the buffer provided (Figure 5.5). Results confirmed that chloride channel inhibitors reduce MCPyV ST-induced cell motility. HEK-293 cells were used as migration controls.

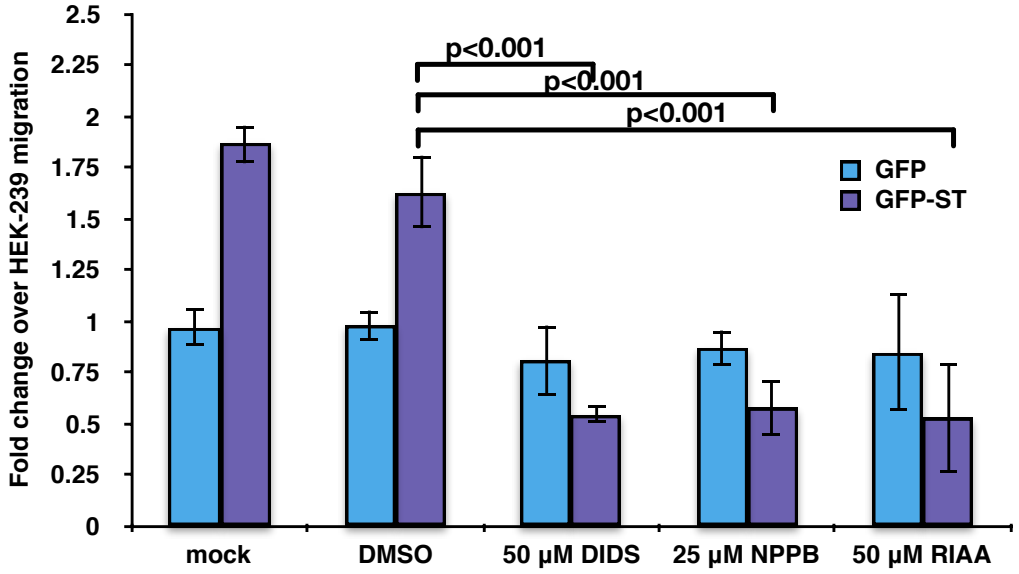


**Figure 5.5: Haptotaxis assay shows blocking chloride channels with broad-spectrum inhibitors reduces MCPyV ST-induced cell migration.** i293-GFP and i293-GFP-ST cells were induced using doxycycline hyclate and treated with 1 µg/µl DMSO, 50 µM of DIDS or RIAA, or 25 µM of NPPB. After 24 h, cells were transferred into migration wells (coated with collagen I), inhibitors were added at appropriate concentrations and allowed to migrate from serum-free to 10% FBS conditions for 24 h. Migratory cells were stained and measured at 560 nm to quantify migration. Average cell migration was calculated and significance was tested using a a two-tailed Student's t-test (n = 3). Untreated HEK-239 cells were used as controls.

## 5.4 Disruption of MCPyV ST-induced cell motility by broad-spectrum chloride channels is not additive

In addition to looking at the effects of individual broad-spectrum chloride channel inhibitors on MCPyV ST-induced cell motility, it was decided to investigate whether this effect was additive by assessing the combined effects of inhibitors. i293-GFP and i293-GFP-ST cells were induced using doxycycline hyclate, while MCC13 cells were transfected with EGFP or EGFP-ST, and treated with pairs of inhibitors for 24 h. Cells were then imaged using the IncuCyte kinetic imaging system, every 30 min for 24 h (Figure 5.6A and Figure 5.7A). Distance travelled by individual cells was tracked using ImageJ software. No additional additive effect was observed either in i293-GFP, i293-GFP-ST, or MCC13 cells upon treatment with pairs of inhibitors, suggesting that the motility reducing effect of individual chloride channel inhibitors was sufficient to block the chloride channels involved in MCPyV ST-induced cell motility (Figure 5.6B and Figure 5.7B). Interestingly, there was no additive effect on control cells expressing GFP either.

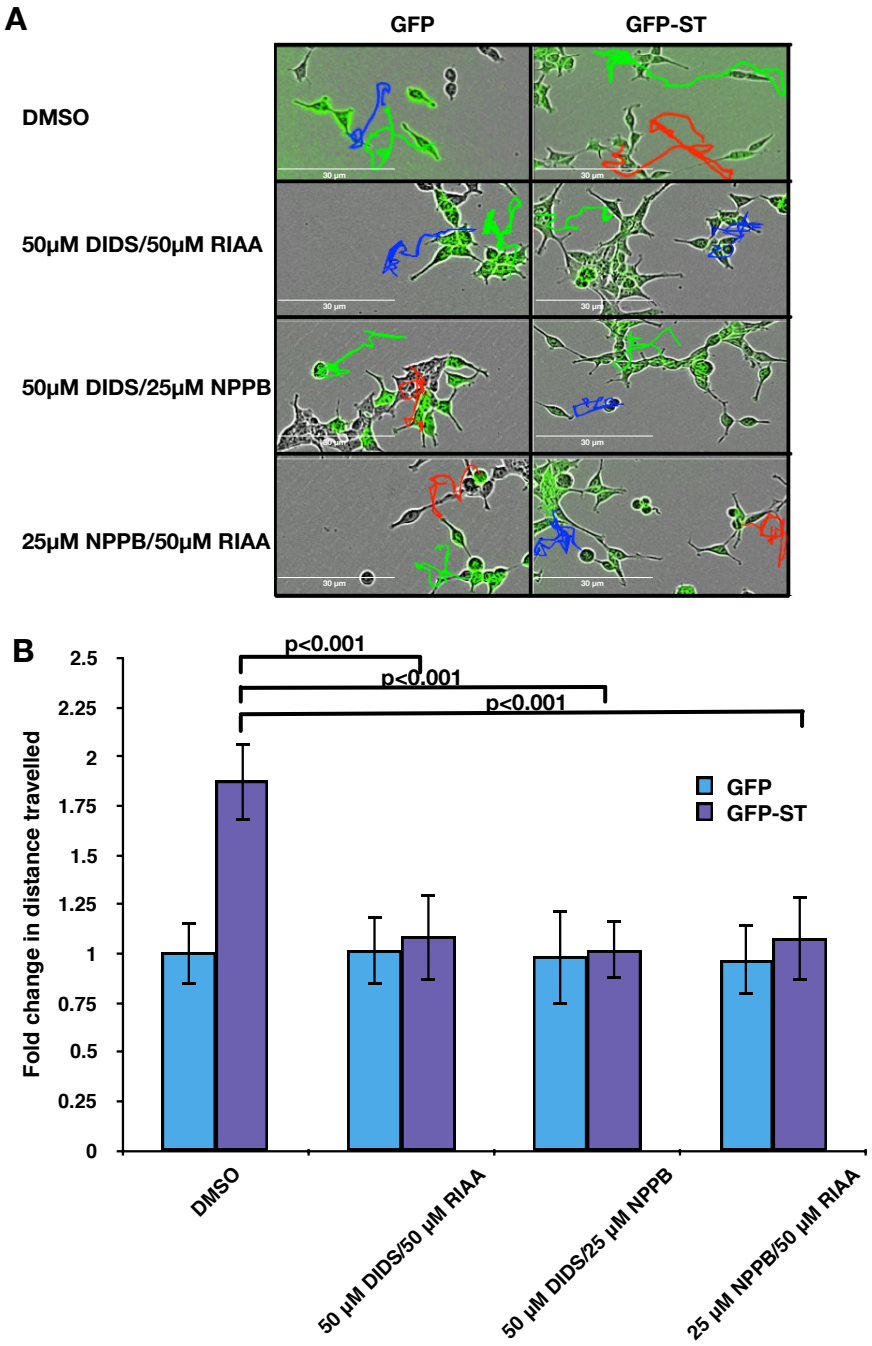


**Figure 5.6: Live cell imaging shows the effect of broad-spectrum chloride channel inhibitors on MCPyV ST-induced cell motility in i293 cells is non-additive.** (A) i293-GFP and i293-GFP-ST cells were induced using doxycycline hyclate for 24 h, and then treated with combinations of two inhibitors (50 μM DIDS/25 μM NPPB, 50 μM DIDS/50 μM RIAA, 25 μM NPPB/50 μM RIAA). After 24 h, cell motility was measured using the IncuCyte kinetic imaging system. Images were taken every 30 min for a 24 h period. (B) Cell movement was then tracked using ImageJ software (n = 25). Average cell movement was calculated and significance was tested using a a two-tailed Student's t-test.

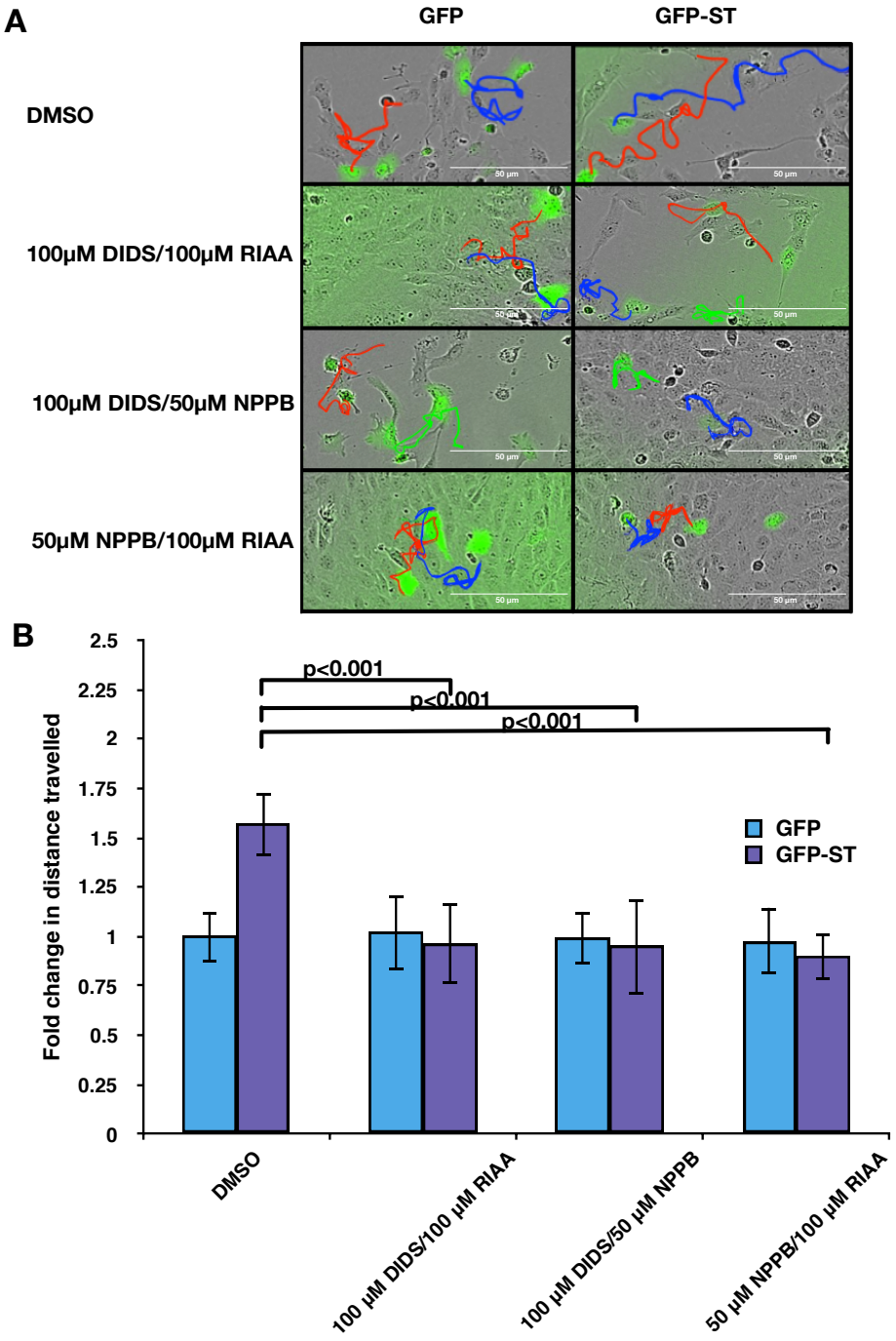


**Figure 5.7: Live cell imaging shows the effect of broad-spectrum chloride channel inhibitors on MCPyV ST-induced cell motility in MCC13 cells is non-additive.** (A) MCC13 cells were transfected for 12 h with 1 µg EGFP or EGFP-ST, then treated with combinations of two inhibitors (100 µM DIDS/50µM NPPB, 100 µM DIDS/100 µM RIAA, 50 µM NPPB/100 µM RIAA). After 24 h, cell motility was measured using the IncuCyte kinetic imaging system. Images were taken every 30 min for a 24 h period. (B) Cell movement was then tracked using ImageJ software (n = 25). Average cell movement was calculated and significance was tested using a a two-tailed Student's t-test.

## 5.5 Disruption of MCPyV ST-induced cell motility by broad-spectrum chloride channels is reversible

Once it was determined that broad-spectrum chloride channels affect MCPyV ST-induced cell motility, it was decided to investigate whether this effect was reversible. i293-GFP and i293-GFP-ST cells were induced using doxycycline hyclate, while MCC13 cells were transfected with EGFP or EGFP-ST, and treated with each respective inhibitor for 24 h. Cells were then imaged using the IncuCyte kinetic imaging system, every 30 min for 24 h, washed, and imaged for further 24 h using the IncuCyte kinetic imaging system. Results showed that in both i293-GFP-ST and MCPyV ST-expressing MCC13 cells motility recovers after washing out the broad-spectrum chloride channel inhibitors, although full recovery is seen only in MCC13 cells (Figure 5.8). These results indicate that the broad-spectrum chloride channel inhibitors act specifically on ion channels, and the effect on MCPyV ST-induced cell motility is not non-specific.

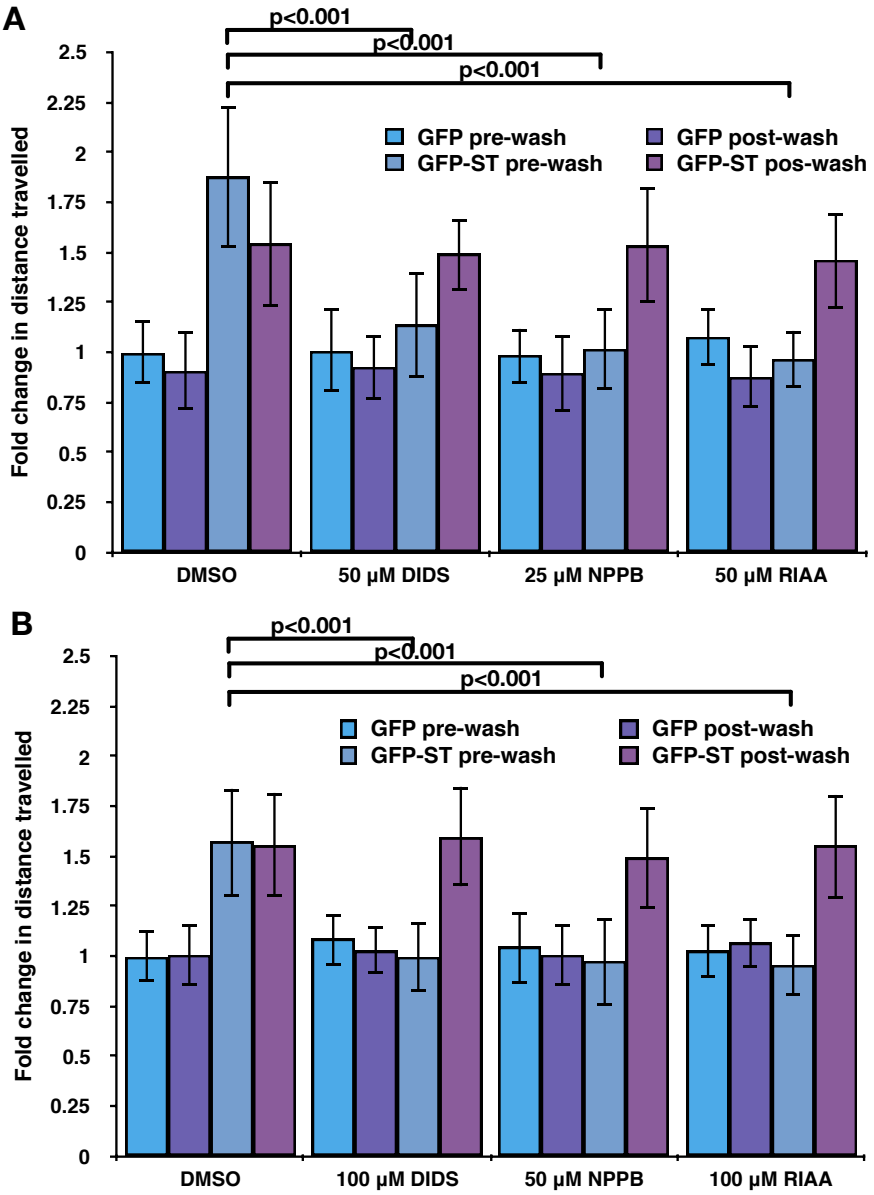


**Figure 5.8: Live cell imaging shows the effect of broad-spectrum chloride channel inhibitors on MCPyV ST-induced cell motility is reversible.** (A) i293-GFP and i293-GFP-ST cells were induced using doxycycline hyclate and treated with 1 µg/µl DMSO, 50 µM DIDS or RIAA, or 25 µM NPPB. After 24 h, cell motility was measured using the IncuCyte kinetic imaging system. Images were taken every 30 min for a 24 h period. Cells were washed with PBS and cell motility was measured every 30 min for a further 24 h using the IncuCyte kinetic imaging system. The movement of cells was then tracked using ImageJ software (n = 25). Average cell movement was calculated and significance was tested using a a two-tailed Student's t-test. (B) MCC13 cells were transfected with 1 µg EGFP or EGFP-ST for 12 h and treated with 1 µg/µl DMSO, 100 µM of DIDS or RIAA, or 50 µM of NPPB. After 24 h, cell motility was measured using the IncuCyte kinetic imaging system. Images were taken every 30 min for a 24 h period. Cells were washed with PBS and cell motility was measured every 30 min for a further 24 h using the IncuCyte kinetic imaging system. The movement of cells was then tracked using ImageJ software (n = 25). Average cell movement was calculated and significance was tested using a a two-tailed Student's t-test.

## 5.6 Broad-spectrum chloride channel inhibitors affect MCPyV ST-induced filopodia formation

Due to the previous results of an observed effect of broad-spectrum chloride channel inhibitors on MCPyV ST-induced cell motility, it was hypothesised that MCPyV ST-induced filopodia formation may also be affected by these inhibitors. In order to explore this possibility, HEK-293 cells were transfected with EGFP or EGFP-ST cells, and treated with the broad-spectrum chloride channel inhibitors (DIDS, NPPB, and RIAA) for 24 h. Cells were then fixed and stained with rhodamine phalloidin to observe actin-based structures (Figure 5.6A). Quantitative analysis of filopodia showed a decrease in filopodia formation when MCPyV ST-expressing cells were treated with any of the broad-spectrum chloride channel inhibitors (Figure 5.6B). Together, these results suggest that inhibiting chloride channels affects MCPyV ST-induced cell motility and filopodia formation.

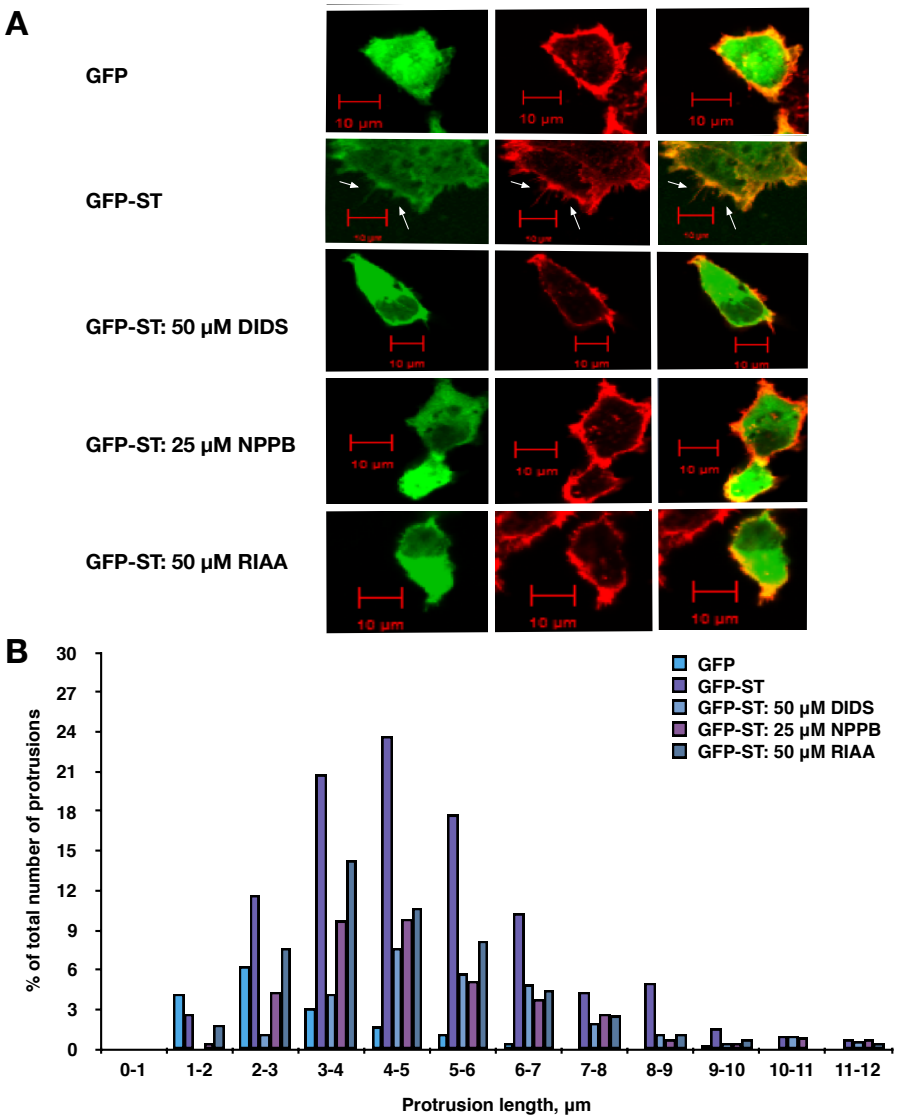


**Figure 5.9: Cell imaging shows that broad-spectrum chloride channe inhibitors reduce MCPyV ST-induced filopodia formation.** (A) HEK-293 cells were transfected with 1 µg EGFP or EGFP-ST for 6 h and treated with 1 µg/µl DMSO, 50 µM of DIDS or RIAA, or 25 µM of NPPB. After 24 h cells were fixed and stained with rhodamine-phalloidin. All slides were then analysed using a Zeiss LSM 700 confocal laser scanning microscope. (B) Actin-based protrusions were counted for 75 cells per condition using ImageJ software.

## 5.7 Quantitative proteomic analysis shows that MCPyV ST expression affects CLIC family protein levels

CLIC family chloride channels have been implicated in cell motility [445] and cancer [450]. Previous work in the Whitehouse laboratory has utilised a SILAC-based quantitative proteomic approach to determine potential alterations in the host cell proteome upon inducible MCPyV ST expression in a HEK-293-derived i293-ST cell line [210]. Further analysis of this data focusing on chloride channels highlighted two CLIC family proteins upregulated upon MCPyV ST expression. These proteins are shown in Table 5.1.

**Table 5.1: Quantitative proteomic analysis shows an increase in CLIC family protein levels upon MCPyV ST expression**

| Protein | Fold change over uninduced | Peptide hits | Function |
|---|---|---|---|
| CLIC1 | 5.7 | 10 | Regulation of fundamental cellular processes via chloride homeostasis [455] |
| CLIC4 | 4.4 | 11 | Regulation of fundamental cellular processes via chloride homeostasis [455] |

To confirm increased levels of CLIC1 and CLIC4 expression upon MCPyV ST induction, i293-ST cells remained uninduced or were induced with doxycycline hyclate for 48 h. In addition, MCC13 cells were transfected with EGFP or EGFP-ST. Cell lysates were then analysed by immunoblotting, and upregulation of CLIC1 and CLIC4 expression was confirmed upon induction of MCPyV ST, in both i293 and in MCC13 cells (Figure 5.10A). CLIC1 increased 2.7-fold in i293-ST and 1.4-fold MCC13 cells, while CLIC4 increased 6-fold in i293-ST cells and 8.8-fold in MCC13 cells (Figure 5.10B).

This increase in chloride channel levels appears to be at the translation stage, as transcription levels, measured by RT-qPCR, are unchanged in i293-ST cells upon MCPyV ST expression (Figure 5.10C). This could be due to previous findings that MPCyV ST deregulates translation rather than transcription [234]. These results indicated that the expression of CLIC family proteins is altered upon MCPyV ST expression, which may have implications in MCPyV ST-induced cell motility.

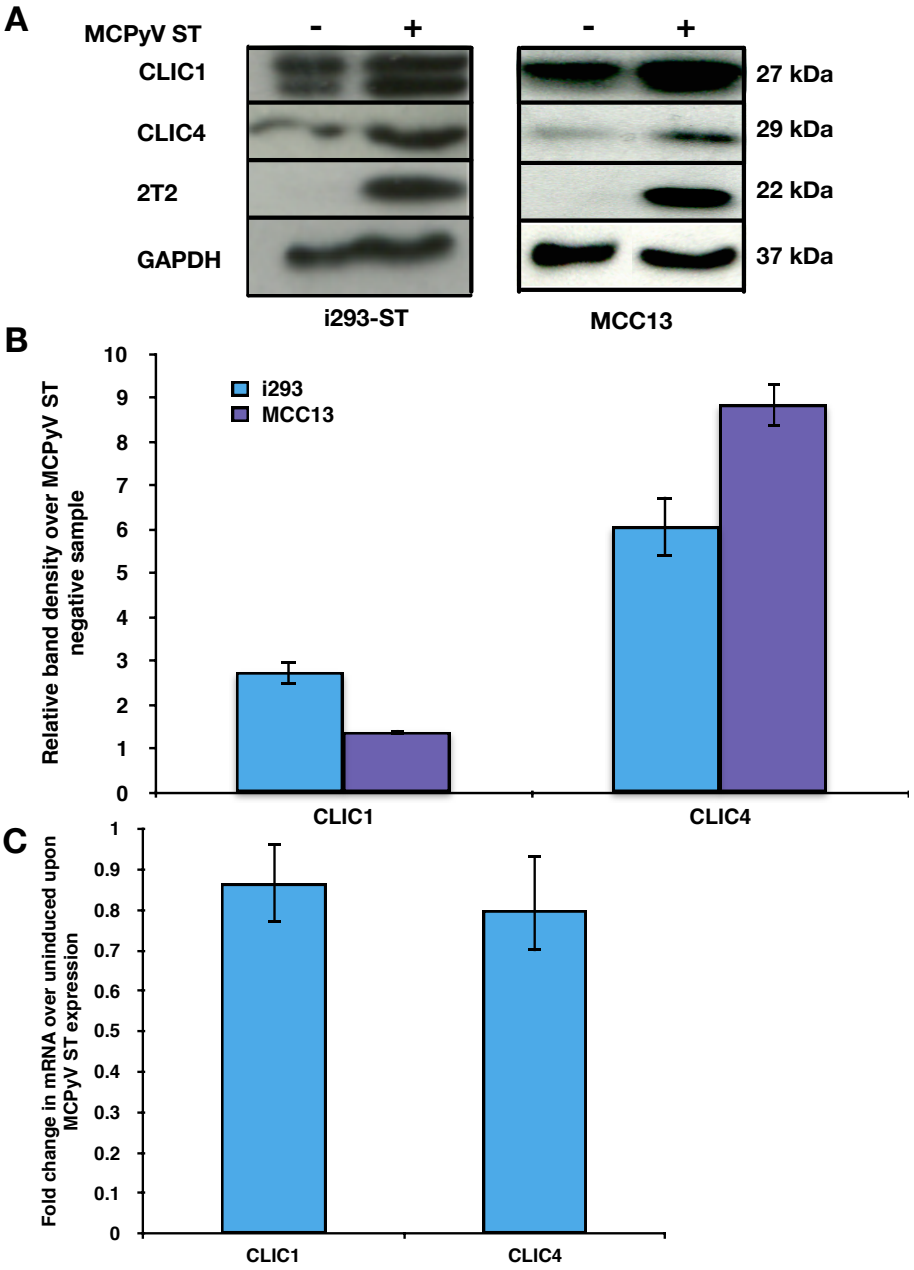


**Figure 5.10: CLIC family proteins are upregulated upon MCPyV ST expression.** (A) i293-ST cells remained uninduced or were incubated for 48 h in the presence of doxycycline hyclate. After induction, cell lysates were probed for CLIC1 and CLIC4 using specific antibodies. MCC13 were transfected with 1 µg EGFP or EGFP-ST for 12 h. Lysates were probed for CLIC1 and CLIC4. GAPDH was used as a measure of equal loading, the 2T2 hybridoma was used to probe for MCPyV ST expression. (B) Exposed film with immunoblotting results was scanned and uploaded onto ImageJ software, which was used to compare band density (n = 3). (C) i293-ST cells remained uninduced or were incubated for 48 h in the presence of doxycycline hyclate. After induction, cellular RNA was extracted using phenol/chloroform, reverse transcribed and RT-qPCR was performed. Transcript levels were analysed using the comparative CT method (n = 3).

## 5.8 MCPyV-positive MCC tumours express CLIC family proteins

In order to investigate whether, like actin-associated proteins, CLIC family proteins are expressed and/or upregulated in MCPyV-positive MCC tumours, two unrelated MCC tumour samples were used (MCC1 and MCC2). Healthy skin was used as a negative control. All samples were homogenised, lysed, and sonicated, and then probed for CLIC1 and CLIC4. CLIC1 appears to be upregulated in MCC1 and MCC2 compared to healthy skin. CLIC4 appears to be expressed to detectable levels in MCC1 and to a lesser degree MCC2, but not in healthy skin (Figure 5.11). Therefore, similar to actin-associated proteins, these differences may be due to varying expression of MCPyV T antigen in samples or due to other unique tumour features. Overall, however, these results confirm the observations made in cell culture experiments, indicating that certain CLIC family proteins are affected upon MCPyV ST expression and may play a role in MCPyV-positive MCC tumourigenesis.

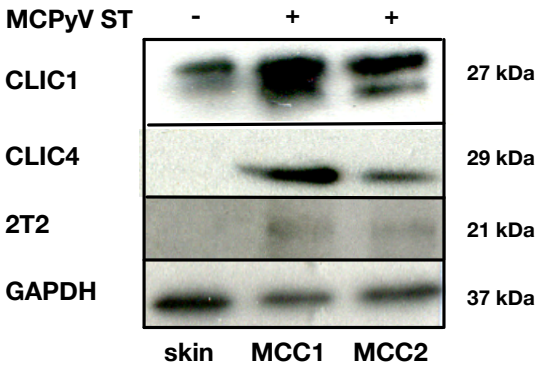


**Figure 5.11: CLIC family proteins are expressed in MCPyV-positive MCC tumours.** Healthy skin, MCC1, and MCC2 were crushed using a mortar and pestle on dry ice, lysed with RIPA buffer for 30 min on ice and then further homogenised by sonication (5 min, 10 s on/10 s off). Tissue lysates were then probed for CLIC1 and CLIC4. GAPDH was used as a measure of equal loading, the 2T2 hybridoma was used to probe for MCPyV ST expression.

## 5.9 Depletion of CLIC1 and CLIC4 disrupts MCPyV ST-induced cell motility

Due to the increased expression of CLIC1 and CLIC4 in MCC tumour samples and MCPyV ST-expressing cell lines, the effect of depleting these chloride channels on MCPyV ST-induced cell motility was investigated. i293-GFP and i293-GFP-ST cells were transfected with scrambled or CLIC1- and/or CLIC4-specific siRNA, then induced with doxycycline hyclate. Similarly, MCC13 cells were transfected with EGFP or EGFP-ST and scrambled or CLIC1 and/or CLIC4 siRNA. Results show good levels of CLIC1 and CLIC4 depletion in both i293 and MCC13 cells, both as single and double knockdowns (Figure 5.12A and Figure 5.13A). Cells were then imaged using the IncuCyte kinetic imaging system, every 30 min for 24 h (Figure 5.12B and Figure 5.13B).

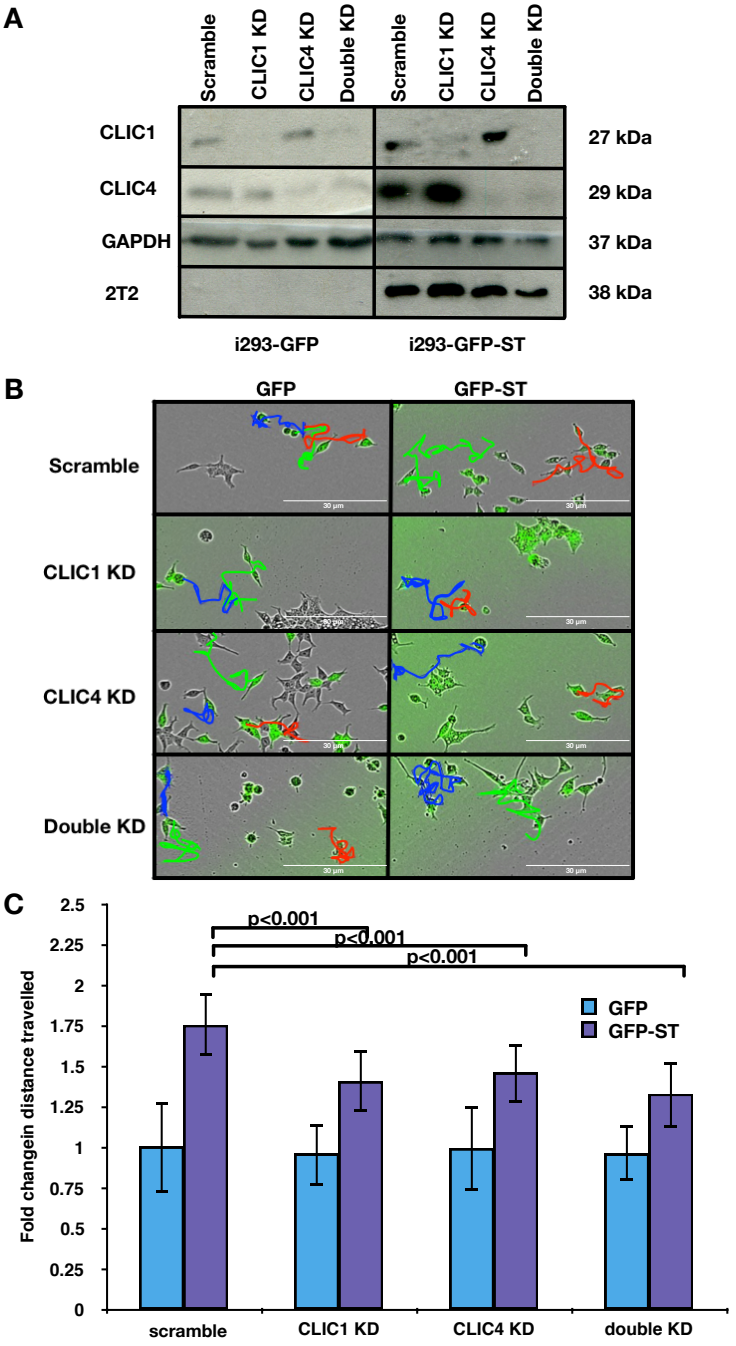


**Figure 5.12: Live cell imaging shows CLIC1 and/or CLIC4 depletion reduces MCPyV ST-induced cell motility in i293 cells.** (A) i293-GFP and i293-GFP-ST cell lysates were probed for successful knockdown with specific CLIC1 and CLIC4 antibodies. GAPDH was used as loading control and 2T2 hybridoma was used to show MCPyV ST expression. (B) i293-GFP and i293-GFP-ST cells were transfected with 10 nmol scrambled or CLIC1 and/or CLIC4 siRNA for 12 h, then induced using doxycycline hyclate for 24 h. 48 h post-knockdown, cell motility was measured using the IncuCyte kinetic imaging system. Images were taken every 30 min for a 24 h period. (C) The movement of cells was then tracked using ImageJ software (n = 25). Average cell movement was calculated and significance was tested using a a two-tailed Student's t-test.

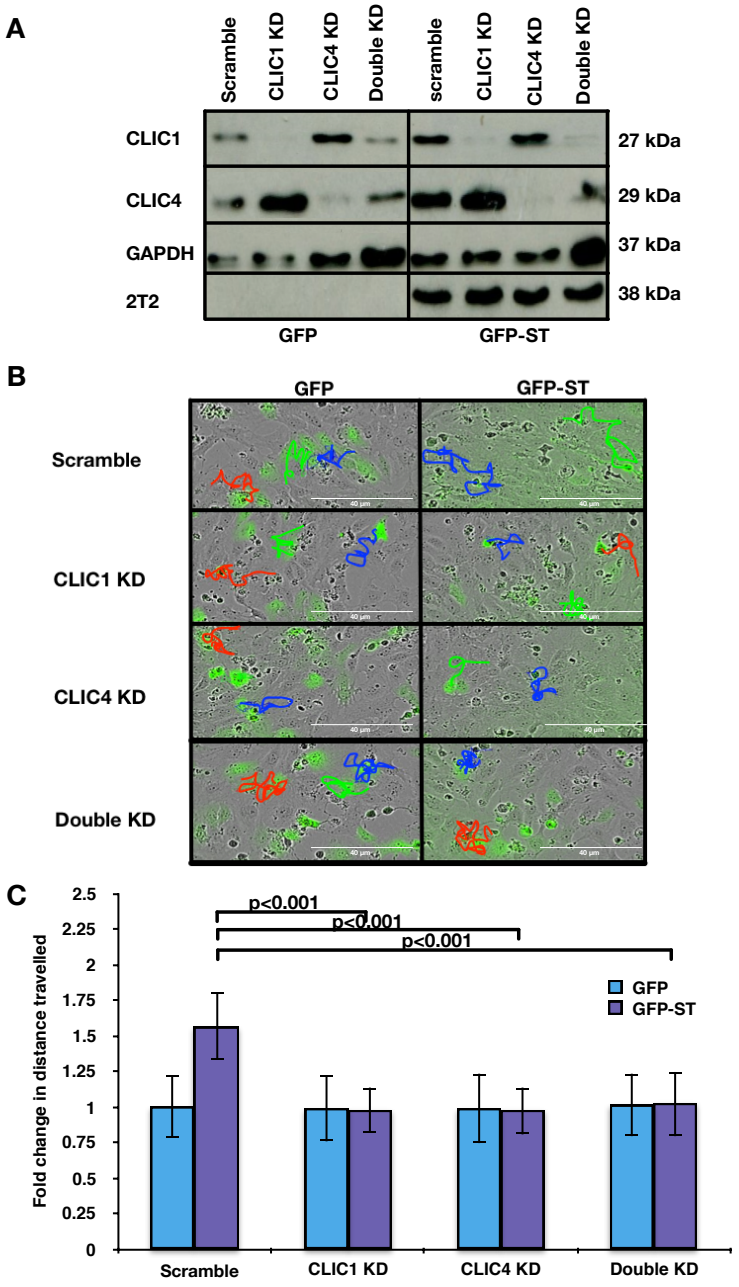


**Figure 5.13: Live cell imaging shows knocking down CLIC1 and/or CLIC4 reduces MCPyV ST-induced cell motility in MCC13 cells.** (A) MCC13 cell lysates were probed for successful knockdown with specific CLIC1 and CLIC4 antibodies. GAPDH was used as loading control and 2T2 hybridoma was used to show MCPyV ST expression. (B) MCC13 cells were transfected with 10 nmol scrambled or CLIC1 and/or CLIC4 siRNA for 12 h, then with 1 µg of EGFP and EGFP-ST for 12 h. 48 h post-knockdown, cell motility was measured using the IncuCyte kinetic imaging system. Images were taken every 30 min for a 24 h period. (C) The movement of cells was then tracked using ImageJ software (n = 25). Average cell movement was calculated and significance was tested using a a two-tailed Student's t-test.

Distance travelled by individual cells were tracked using ImageJ software. No significant differences were observed among the average distances travelled by control cells with knockdown of CLIC1 and/or CLIC4, in both single- and double-knockdown cells (Figure 5.12C and Figure 5.13C). Conversely, cells expressing MCPyV ST which had CLIC1 and/or CLIC4 depleted showed significant decrease in cell motility compared to cells expressing CLIC1 and/or CLIC4 ($p < 0.001$) (Figure 5.9B and Figure 5.10B). Interestingly, in i293 cells the effect was smaller than in MCC13 cells, even though the knockdown levels are comparable (Figure 5.12B and Figure 5.13B). Results do show that depletion of either CLIC1 or CLIC4 leads to a similar level of motility inhibition as the depletion of both at the same time. This could indicate that both channels play an equally important role in MCPyV ST-induced cell motility.

## 5.10 CLIC1 and CLIC4 show increased plasma membrane localisation upon MCPyV ST expression

CLIC family proteins have been shown to relocalise from inside cells to the cell surface in angiogenesis[456] and to invadopodia [457]. Changes to CLIC1 and/or CLIC4 localisation on the surface of cells may lead to changes in the uptake or release of chloride, which may in turn play a role in changes in cell volume which could affect cell motility. Therefore it was determined whether MCPyV ST expression would affect the cell surface localisation of CLIC family proteins using a flow cytometry-based assay.

HEK-293 cells were transfected with EGFP and EGFP-ST, fixed and stained for cell surface CLIC1 and CLIC4. Flow cytometry was performed and results showed changes in the proportion of cells staining for CLIC1 and CLIC4 upon MCPyV ST expression (Figure 5.14A). Gating was set for both CLIC1 and CLIC4 according to their isotype controls (Figure 2.1, Materials and Methods). These changes were quantified and analysis suggested that upon MCPyV ST expression, CLIC1 increases 1.5-fold on the cell surface while CLIC4 increases 2.2-fold on the cell surface (Figure 5.14B). These findings suggest that both CLIC1 and CLIC4 relocalise to the cell surface upon MCPyV ST expression. Interestingly, there seems to be somewhat greater relocalisation by CLIC4. This may indicate a more important role for this CLIC family protein in MCPyV ST-induced cell motility, but more

research needs to be done to explore this possibility, as depletion studies suggest an equal effect by either CLIC1 or CLIC4.

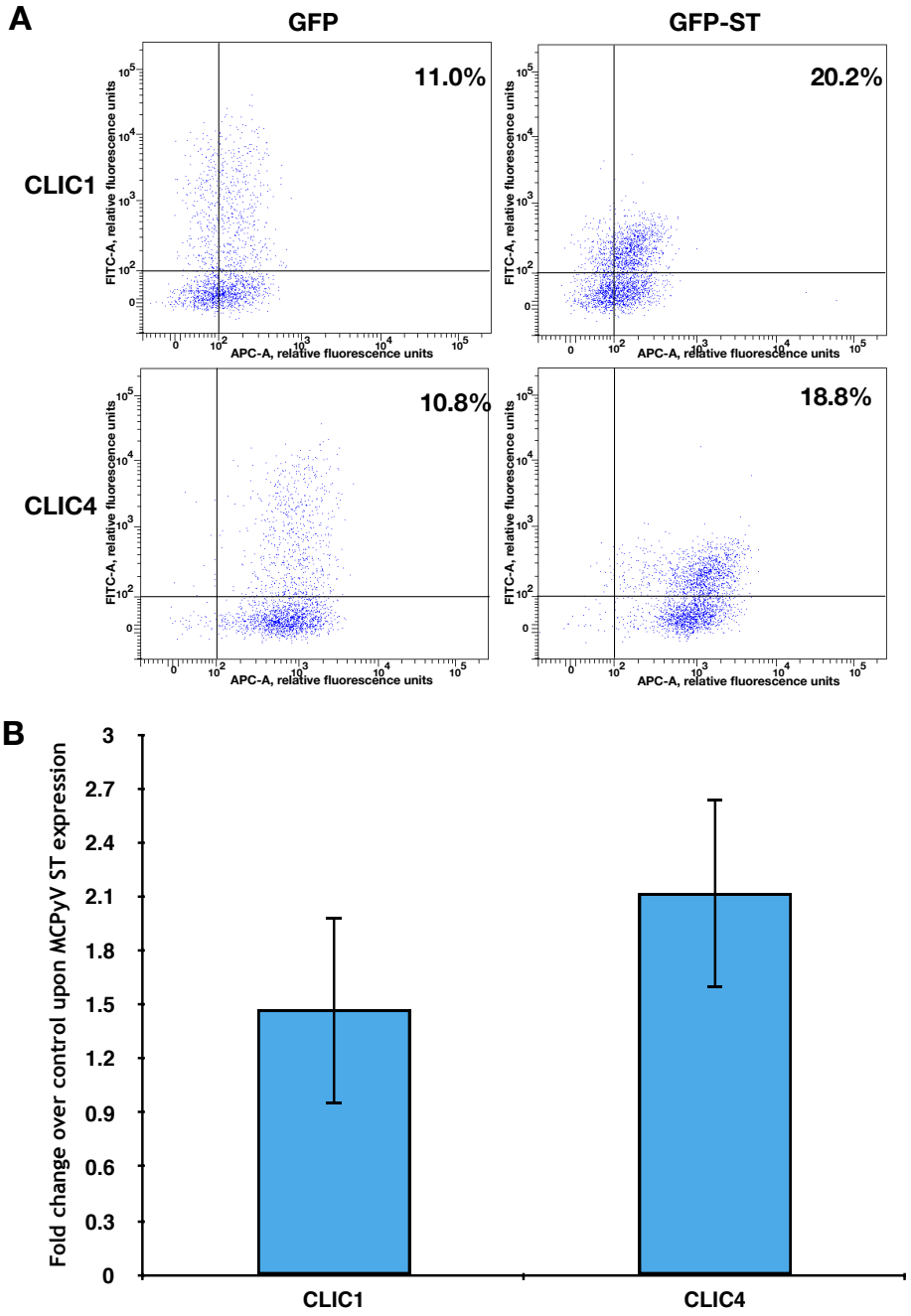


**Figure 5.14: Flow cytometry shows relocalisation of CLIC1 and CLIC4 to the cell surface.** (A) HEK-293 cells were transfected with 1µg EGFP and EGFP-ST for 6 h. Cells were fixed with 2% paraformaldehyde, then stained with specific CLIC1 and CLIC4 antibodies. Flow cytometry was performed and gating was set according to isotype controls (see Figure 2.1). FITC-A corresponds to EGFP fluorescence and APC-A corresponds to secondary antibody staining. (B) Proportions of cells expressing EGFP-ST and stained for CLIC1 or CLIC4 were analysed and compared to proportion of cells expressing EGFP and stained for CLIC1 or CLIC4 (n = 3).

## 5.11 Discussion

MCPyV ST induces cell motility and filopodia formation via the cell motility pathway mediated by Rho-family GTPases (Chapter 3) and initiated via integrin signalling (Chapter 4). In addition, it appears that ion channels are also involved in MCPyV ST-induced cell motility and filopodia formation, potentially via relocalisation to the cell surface initiated by the expression of MCPyV ST. Chloride channels have been implicated in cancer progression [458], although little research has so far been done in this field, particularly in the context of virus-induced cancers.

Data presented in this chapter indicate that expression of MCPyV ST affects cellular ion flow. Chloride channels are implicated in these mechanisms, particularly due to the findings that blockage of these channels by broad-spectrum inhibitors affects MCPyV ST-induced cell motility and filopodia formation. In addition, quantitative proteomic analysis showed that MCPyV ST expression upregulates the protein levels of two CLIC family proteins: CLIC1 and CLIC4. Supporting the role in MCPyV ST-induced motility of these chloride channels, depletion of CLIC1 and CLIC4 leads to the reduction of MCPyV ST-induced cell motility.

The effect of the CLIC family of chloride channels on cell motility has been documented previously for both CLIC1 and CLIC4. Interestingly, CLIC1 has been implicated in regulating the cell surface expression of integrins, including β1 and α3 [445], while CLIC4 is required for transforming growth factor (TGF)-β signalling, leading to increased epithelial to mesenchymal transition [459]. In addition, both CLIC1 and CLIC4 have been implicated in the development and progression of a number of different cancers, including colon cancer [450], prostate cancer [451], pancreatic cancer [460], and ovarian cancer [461].

Results presented in this chapter suggest that chloride channels, specifically CLIC1 and CLIC4, contribute to MCPyV ST-induced cell motility via relocalisation to the cell surface, thus allowing for increased anion flow. Interestingly, CLIC1 relocalisation has previously been implicated in tumourigenesis [462]; however, MCPyV ST expression appears to also affect CLIC4 levels and relocalisation to the cell surface. Therefore, it is possible that CLIC4 plays a significant role in MCPyV ST-induced cell motility and thus MCC metastasis. This would be a novel discovery, as so far CLIC1 has been the most widely-studied of member of the CLIC fam-

ily proteins and implicated more extensively in cell motility. In order to further explore these possibilities, more research on the mechanism by which MCPyV ST acts on CLIC1 and CLIC4 needs to be performed. One avenue of investigation could be the relationship between integrins, which have been implicated in MCPyV ST-induced cell motility in Chapter 4, and the CLIC family proteins.

Furthermore, future investigations into the mechanisms of how MCPyV ST expression promotes relocalisation of CLIC1 and CLIC4, e.g. via changes in phosphorylation, might provide a potential therapeutic target. Another potential mechanism of action could be via the actin cytoskeleton [463], which, as shown in Chapter 3, is also affected by MCPyV ST expression. Finally, blocking CLIC family proteins, CLIC1 and CLIC4, might be another therapeutic pathway. Currently, there are no specific inhibitors available for either channel, and research in this area could prove fruitful in tackling not only MCC, but a host of other metastatic cancers.

# Chapter 6

# Final discussion and future perspectives

## 6.1 Final discussion and future perspectives

MCC is a highly aggressive and metastatic cancer of neuroendocrine origin that presents as nodules on sun-exposed areas of skin. It arises from Merkel cells, which are situated on the basal layer of the epidermis. Merkel cells are mechanoreceptors that are stimulated by light touch, and they form the Merkel cell-neurite complex [170]. MCC tends to spread through the dermal lymphatic system, and is associated with early establishment of distant metastases and a poor 5-year survival rate [177]. MCPyV has been established as the causative agent of MCC in at least 80% of cases [20]. It is found monoclonally integrated in both primary tumours and metastases [20].

MCPyV is a polyomavirus, and expresses two oncogenes from its T antigen locus: LT and ST. MCPyV LT acquires truncating mutations in MCC tumours, rendering it replication-defective [20]. Due to the acquisition of these specific mutations and a monoclonal pattern of integration, MCPyV is thought to be a direct tumourigenic agent rather than a passenger virus. While in most tumourigenic polyomaviruses, such as SV40, LT is thought to be the major oncoprotein, in MCPyV, ST is the major transforming factor [234]. In addition, MCPyV ST has also been shown to promote cell motility [210], so is likely to be involved in MCC metastasis. This is not without precedent, as other tumour viruses, such as SV40, HPV, and EBV can all promote metastasis, via a variety of mechanisms, such as alteration of cell adhesion complexes, production of MMPs, gene expression modulation, and cytoskeletal reorganisation [342] [464] [465].

Previously, identification of MCC tumours was particularly difficult and often mistaken for small-cell carcinoma of the lung, which presents as a visibly similar tumour [179]. Currently, positive CK20 staining along with neuroendocrine biomarkers, e.g. chromatogranin and somatostatin, is used to detect MCC for diagnostic purposes [180]. However, there is still no specific therapeutic regime available for MCC. Therefore, research in this area should ultimately lead to potential drug targets and treatments in order to improve MCC patient survival and care.

The discovery of MCPyV has opened up new avenues of research in MCC treatment, with research into the tumourigenic and metastatic mechanisms induced by MCPyV oncoproteins potentially providing novel drug targets. One such tar-

get is illustrated in the role of MCPyV LT in upregulating a cellular oncogene, survivin, which is essential for the survival of MCPyV-positive MCCs [259]. In fact, YM155, a small molecular inhibitor of surivin, has been shown have a cytostatic effect on MCC tumours in mice xenografts [272]. Furthermore, a small-molecule tyrosine kinase inhibitor, pazopanib, is currently undergoing phase II clinical trials as a potential MCC treatment [273]. Recently, together with determining a host cell line for MCPyV, it was also shown that trametinib is a potent inhibitor of MCPyV infection [220], although the utility of this drug in the later stages of MCC might be low. Therefore the field for new MCPyV-positive MCC drugs, particularly ones that act in later stages of the disease, is wide open.

Previous work in the Whitehouse laboratory performed high-throughput quantitative SILAC-based proteomic analysis [210] using a cell line capable of inducible expression of MCPyV ST to identify differentially-expressed proteins on MCPyV ST expression. SILAC-based analysis coupled with LC-MS/MS and bioinformatics is a way to explore the host cell proteome, and is an informative tool for the study of virus-host interactions [466]. Bioinformatic analysis showed that MCPyV ST expression promotes the differential expression of a number of proteins involved in the regulation of the cytoskeleton and cell motility, both associated with the microtubule network [210] and with the actin cytoskeleton. In addition, MCPyV ST expression was found to promote the expression of proteins associated with cell adhesion, various junctions, and the EMT. This line of research is currently being explored.

Initial findings in multiple cell lines showed that MCPyV ST expression upregulates actin-associated proteins and leads to the increase in the numbers and lengths of actin-based protrusions that were then determined to be filopodia. In addition, enhanced expression of actin-associated proteins was observed in MCC tumours when compared to MCC-negative healthy skin. These changes in actin-associated protein expression and in the presence of early motility markers led to the development of two cell lines, i293-GFP and i293-GFP-ST, in order to explore MCPyV ST-induced cell motility in live cells. Previous observations that MCPyV ST induces cell motility both in inducible and in MCC13 cells were confirmed. In addition, directionality studies showed that MCPyV ST promotes directional motility, and this provides further evidence of MCPyV ST-induced cell motility being metastatic in nature, as directionality is important in metastatic migration [403].

The actin cytoskeleton and cell motility are regulated by Rho-family GTPases. Findings presented in this thesis suggest that Cdc42 and RhoA appear to be involved in MCPyV ST-induced cell motility and filopodia formation, with Rac1 potentially playing a smaller role. Interestingly, other oncogenic viruses also affect the Rho-family GTPases. For instance, SV40 ST activity leads to the rearrangement of filamentous actin networks, including Rac-mediated lamellipodia formation, Cdc42-mediated filopodia formation and the loss of RhoA-dependent stress fibres. SV40 ST expression upregulates Rac1 and Cdc42 and downregulates RhoA [342]. However, no direct changes in Rho-family GTPase levels were observed in MCPyV ST-expressing cells, suggesting that MCPyV ST uses an alternative mechanism to manipulate the actin cytoskeleton. Future research in this area could focus on the many activators and inhibitors of the Rho-family GTPases, in order to determine which ones play a role in MCPyV ST-induced cell motility. There are approximately 60 known activators and 70 known inactivators of Rho-family GTPases [467]. Some of these factors are highly specific for single Rho-family GTPases, e.g. Fgd1 for Cdc42 [468] or p115RhoGEF for Rho [469], while others can act on multiple Rho-family GTPases, e.g. Vav1 on Cdc42, Rac, and Rho [470]. A number of Rho-family GTPase activators, guanine exchange factors (GEFs), are known oncogenes, involved in various cancers, including Dbl in diffuse B cell lymphoma [471], Ect2 in multiple human cancers [472], and Ost in osteosarcoma [473]. Therefore, it may be that a particular GEF or a subset of GEFs are specifically involved in activating Rho-family GTPases in MCPyV-positive MCCs. One potential target for initial investigation could be Vav1, a GEF that has been implicated in neuroblastoma and melanoma, as well as pancreatic, lung, and breast cancers [474]. Regardless, research into the cell motility signalling pathway in the context of MCPyV-positive MCC would further enhance the mechanism proposed in Chapter 4. Furthermore, potential specificity of such activators and/or inhibitors could provide possible drug targets to explore for MCC.

It has been demonstrated that MCPyV ST interacts with multiple cellular Ser/Thr phosphatases, including PP2A A$\alpha$, PP2A A$\beta$, and PP4C [234] [209]. In particular, the MCPyV ST interaction with PP4C seems to be important in promoting cell motility via microtubule stabilisation [210]. In addition, PP4C depletion reduces levels of active Cdc42 and Rac1 in HEK-293 cells, suggesting that it may play a role in actin dynamics [475]. In this thesis, immunoprecipitation studies found

that the exact binding site for PP4C on MCPyV ST is residue 102, allowing the generation of specific MCPyV ST mutants which can specifically distinguish between PP2A Aβ and PP4C binding. This novel mutant was then used to show that the MCPyV ST-PP4C interaction is necessary for cell motility and filopodia formation.

In order to try and determine where in the cell motility pathway the MCPyV ST-PP4C interaction was functioning, changes in Rho-family GTPase phosphorylation status were initially investigated upon MCPyV ST expression. Surprisingly, no changes were observed for Cdc42 or RhoA at the Ser71 residue. Therefore, activators upstream of the Rho-family GTPases were investigated. Upstream of the Rho-family GTPases and their activators in the cell motility pathway are multiple different families of receptors. One such family, the integrins, are important in forming cell-matrix adhesion in cell motility. It was found that inhibiting integrin activity in MCPyV ST-expressing cells reduced motility in a dose-dependent manner, as well as reducing filopodia formation. Finally, findings presented in this thesis show that MCPyV ST expression reduces the phosphorylation levels of β1 integrin at Thr788/789, in contrast to the PP4C non-binding mutants. These findings allow for a mechanism of MCPyV ST-induced cell motility and filopodia formation (illustrated in Figure 4.18), where MCPyV ST interaction with PP4C leads to the dephosphorylation of integrins, which activates the cell motility pathway. PP2A has been shown to dephosphorylate β1 integrin at Thr788/789 [428], and it may be that other phosphorylation sites, such as Ser785 [427] on β1 integrin could be altered upon MCPyV ST expression. Specifically, a dephosphorylated β1 integrin mimic at Ser785 promotes cell spreading and migration in fibroblast and teratocarcinoma cells [427]. Moreover, other integrins as well as other receptors may also play a role in MCPyV ST-induced cell motility and filopodia formation. For example, the sensitivity of MCPyV ST-expressing MCC13 cells to the RGDS peptide suggests a potential role for αvβ3 integrins [431]. Further research in this area would help flesh out the model and add layers of complexity to the signalling that takes place upon MCPyV ST induction of cell motility.

These findings stress the importance of the MCPyV ST-PP4C interaction and highlight it as a novel drug target, particularly in the later stages of MCC, where it has such a poor prognosis. Further research in this area could focus on blocking the specific protein-protein interaction. One example is the potential to use structure-based rational drug design to identify a small molecule inhibitor that

blocks the MCPyV ST-PP4C interaction. The Whitehouse laboratory has generated a predicted MCPyV ST structural model, based upon the known structure of the homologous SV40 ST protein. To identify small molecule inhibitors a virtual high-throughput screening campaign could be conducted using the Leeds proprietary structural screening library. Surface volume analysis (SPROUT, Symbiosis) of the MCPyV ST interface may indicate potential sites for targeting small molecules. Thereafter, docking sites could be virtually modelled and virtual hits prioritised to assess if these inhibitor molecules affect MCPyV ST-induced cell motility. Moreover, in a parallel approach, small molecules could be identified that mimic features of the binding interface of PP4C. Although the issue with this approach is the lack of a crystal structure for PP4C, particularly complexed with MCPyV ST. Another issue would be the therapeutic window, as PP4C is a host factor involved in many different cellular functions. A way to overcome these issues is to use blocking antibodies or peptides to disrupt the MCPyV ST-PP4C interaction. One particularly interesting avenue of research would be developing adhirons to block the PP4C binding site on MCPyV ST. Adhirons are novel, thermostable scaffold proteins with variable regions that can be raised as binders to a protein of interest [476]. Theoretically, an adhiron raised against the 102 residue (and neighbouring residues) of MCPyV ST would prevent the interaction with PP4C without affecting normal cellular functions of the protein phosphatase.

Finally, this thesis also presents novel findings that MCPyV ST-induced cell motility depends on intracellular chloride channels (CLICs), specifically focusing on CLIC1 and CLIC4. Initial patch clamping showed that expression of MCPyV ST affects cellular ion flow, and chloride channels were implicated due to findings that broad-spectrum chloride channel inhibitors reduce MCPyV ST-induced cell motility and filopodia formation. Furthermore, quantitative proteomic and immunoblotting analysis showed that MCPyV ST expression upregulates the protein levels of CLIC1 and CLIC4 in multiple cell lines and in MCPyV-positive MCC tumour samples, while siRNA depletion of these chloride channels leads to the reduction of MCPyV ST-induced cell motility. In addition, CLIC1 and CLIC4 likely contribute to MCPyV ST-induced cell motility by relocalising to the cell surface, allowing for increased ion flow. CLIC1 relocalisation has been previously implicated in cancer, with CLIC1 being visualised on the plasma membrane of glioblastoma cells but not of normal progenitor cells [462], as well as localising to the invadopodia in several cancer cell lines [457]. However, results presented in

this thesis show greater increases of expression and relocalisation of CLIC4 upon MCPyV ST than CLIC1. Therefore, it may be that CLIC4 is more important in MCC tumourigenesis, although more research needs to be done to explore the precise mechanism by which chloride channels act on MCPyV ST-induced cell motility. Interestingly, CLIC1 has been implicated in regulating the cell surface expression of integrins, including β1 and α3 integrins [445]. The MCPyV ST-PP4C interaction has been shown in this thesis to affect β1 integrin, thus linking this dephosphorylation with CLIC activity ought to be explored further. CLIC4 regulates transforming growth factor (TGF)-β signalling, leading to increased epithelial to mesenchymal transition [459], and ongoing work in the Whitehouse laboratory is exploring the role of MCPyV ST in EMT. In addition, both CLIC1 and CLIC4 have been implicated in the development and progression of a number of different cancers, including colon cancer [450], prostate cancer [451], pancreatic cancer [460], and ovarian cancer [461].

Future investigations into the details of how MCPyV ST expression promotes relocalisation of CLIC1 and CLIC4, e.g. via changes in phosphorylation, might provide a potential therapeutic target. Another potential mechanisms of action could be via the actin cytoskeleton [463], which is also affected by MCPyV ST expression, as presented in this thesis. Finally, blocking CLIC family proteins, CLIC1 and CLIC4, might be another therapeutic pathway. There are some chloride channel modulators currently available, with the vast majority working on the cystic fibrosis transmembrane conductance regulator (CFTR) due to its role in cystic fibrosis and on ligand-gated chloride channels (GABA (γ-aminobutyric acid)- and glycine-activated) due to their role in the central nervous system [440]. There are no specific blockers for most CLIC family proteins at the moment, although broad-spectrum chloride channel inhibitors like the ones used in experiments presented in this thesis do have an effect on CLICs. RIAA is thought to block CLIC1 [477], although it has not been used in a therapeutic setting. No specific inhibitors are currently available for CLIC4. Research in this area could prove fruitful in tackling not only MCC, but many other malignancies. Interestingly, the crystal structures of both CLIC1 and CLIC4 have been elucidated, which could provide data to discover additional blockers [478] [479].

Another entire avenue of research to explore regarding MCPyV ST and its role in cancer metastasis is the effect of MCPyV ST on cell-cell and cell-matrix adhesion, EMT, and expression of kinases associated with cell motility. In fact, some

preliminary work being undertaken in the Whitehouse laboratory suggests that kinases like FAK are involved in MCPyV ST-induced cell motility, and that there are changes in the expression of various EMT markers in the presence of MCPyV ST.

In addition, some members of the ADAM (a disintegrin and metalloproteinase) family have been found to be upregulated upon MCPyV ST expression in quantitative proteomic analysis, as well as showing differential cell surface distribution in the presence and absence of MCPyV ST (personal communication, Nnenna Nwogu, Whitehouse laboratory). ADAMs are membrane-anchored glycoproteins and regulatory enzymes associated with cell adhesion and the shedding or cleavage of certain receptors, e.g. integrins [480] [481] [482]. ADAMs are catalytically inactive until autocatalysis, but can cleave the ectodomain of membrane proteins upon activation [483]. Quantitative proteomic analysis suggests that ADAM10 and ADAM17 are upregulated upon MCPyV ST expression. ADAM10 has previously been shown to play a role in cancer. For instance, ADAM10 upregulation in non-small cell lung cancer and nasopharyngeal carcinoma leads to increased cell migration [484] [485]. ADAM17 is overexpressed in some breast cancers [486] and promotes cell invasion in prostate cancer [487]. These two ADAM proteins are currently being investigated in the context of MCPyV ST, and may be potential drug targets. Further research into other enzymes involved in cell adhesion, motility, and invasion, such as MMPs, may yield additional targets.

In summary, this thesis explores the role of MCPyV ST in cell motility. Results presented herein implicate MCPyV ST in reorganising the actin cytoskeleton and promoting cell motility via integrin signalling mediated by the Rho-family GTPases. In addition, interaction between MCPyV ST and the cellular phosphatase PP4C has been shown to be central to MCPyV ST-induced cell motility and filopodia formation. These findings allow a molecular mechanism to be proposed wherein the MCPyV ST-PP4C interaction activates the cell motility pathway via integrin dephosphorylation. Finally, the CLIC family of chloride channels is implicated in facilitating MCPyV ST-induced cell motility via cell surface relocalisation. All these findings increase current understanding of the function of the major MCPyV oncoprotein in MCC and propose new potential therapeutic targets for the treatment of this aggressive and deadly cancer.

# References


[1] C. D. Mathers and D. Loncar, "Projections of global mortality and burden of disease from 2002 to 2030," *PLoS Med*, vol. 3, no. 11, p. e442, 2006. 2

[2] A. B. Mariotto, K. R. Yabroff, Y. Shao, E. J. Feuer, and M. L. Brown, "Projections of the cost of cancer care in the United States: 2010-2020," *J Natl Cancer Inst*, vol. 103, no. 2, pp. 117–128, 2011. 2

[3] J. Maddams, M. Utley, and H. Moller, "Projections of cancer prevalence in the United Kingdom, 2010-2040," *Br J Cancer*, vol. 107, no. 7, pp. 1195–1202, 2012. 2

[4] C. de Martel, J. Ferlay, S. Franceschi, J. Vignat, F. Bray, D. Forman, and M. Plummer, "Global burden of cancers attributable to infections in 2008: a review and synthetic analysis," *The Lancet Oncol*, vol. 13, no. 6, pp. 607–615, 2012. 2

[5] P. Rous, "A sarcoma of the fowl transmissible by an agent separable from the tumor cells," *J Exp Med*, vol. 13, no. 4, pp. 397–411, 1911. 2

[6] P. Rous and J. W. Beard, "The progression to carcinoma of virus-induced rabbit papillomas (shope)," *J Exp Med*, vol. 62, no. 4, pp. 523–548, 1935. 2

[7] P. Rous and J. G. Kidd, "The carcinogenic effect of a papilloma virus on the tarred skin of rabbits: I. Description of the phenomenon," *J Exp Med*, vol. 67, no. 3, pp. 399–428, 1938. 2

[8] L. Gross, "A filterable agent, recovered from Ak leukemic extracts, causing salivary gland carcinomas in C3H mice," *Proc Soc Exp Biol Med*, vol. 83, no. 2, pp. 414–421, 1953. 3, 4

[9] B. E. Eddy, G. S. Borman, G. E. Grubbs, and R. D. Young, "Identification of the oncogenic substance in rhesus monkey kidney cell cultures as simian virus 40," *Virology*, vol. 17, no. 1, pp. 65–75, 1962. 3, 4

[10] D. P. Lane and L. V. Crawford, "T antigen is bound to a host protein in SV40-transformed cells," *Nature*, vol. 278, no. 5701, pp. 261–263, 1979. 3, 19

[11] C. Wychowski, D. Benichou, and M. Girard, "A domain of SV40 capsid polypeptide VP1 that specifies migration into the cell nucleus," *EMBO J*, vol. 5, no. 10, pp. 2569–2576, 1986. 3

[12] W. Eckhart, M. A. Hutchinson, and T. Hunter, "An activity phosphorylating tyrosine in polyoma T antigen immunoprecipitates," *Cell*, vol. 18, no. 4, pp. 925–933, 1979. 3

[13] M. A. Epstein, B. G. Achong, and Y. M. Barr, "Virus particles in cultured lymphoblasts from Burkitt's lymphoma," *Lancet*, vol. 283, no. 7335, pp. 702–703, 1964. 3

[14] B. S. Blumberg and H. J. Alter, "A "new" antigen in leukemia sera," *JAMA*, vol. 191, no. 7, pp. 541–546, 1965. 3

[15] B. J. Poiesz, F. W. Ruscetti, A. F. Gazdar, P. A. Bunn, J. D. Minna, and R. C. Gallo, "Detection and isolation of type C retrovirus particles from fresh and cultured lymphocytes of a patient with cutaneous T-cell lymphoma," *Proc Nat Acad Sci USA*, vol. 77, no. 12, pp. 7415–7419, 1980. 3

[16] M. Durst, L. Gissmann, H. Ikenberg, and H. zur Hausen, "A papillomavirus DNA from a cervical carcinoma and its prevalence in cancer biopsy samples from different geographic regions," *Proc Natl Acad Sci USA*, vol. 80, no. 12, pp. 3812–3815, 1983. 3

[17] M. Boshart, L. Gissmann, H. Ikenberg, A. Kleinheinz, W. Schleuren, and H. zur Hausen, "A new type of papillomavirus DNA, its presence in genital cancer biopsies and in cell lines derived from cervical cancer," *EMBO J*, vol. 3, pp. 1151–1157, 1984. 3

[18] Q. L. Choo, G. Kuo, A. J. Weiner, L. R. Overby, D. W. Bradley, and M. Houghton, "Isolation of a cDNA clone derived from a blood-borne non-A, non-B viral hepatitis genome," *Science*, vol. 244, no. 4902, pp. 359–362, 1989. 3

[19] P. S. Moore and Y. Chang, "Detection of herpesvirus-like DNA sequences in Kaposi's sarcoma in patients with and those without HIV infection," *NEMJ*, vol. 332, no. 18, pp. 1181–1185, 1995. 3

[20] H. Feng, M. Shuda, Y. Chang, and P. S. Moore, "Clonal integration of a polyomavirus in human Merkel cell carcinoma," *Science*, vol. 319, no. 5866, pp. 1096–1100, 2008. 3, 7, 27, 29, 30, 31, 42, 92, 96, 143, 174

[21] R. Johne and H. Muller, "Polyomaviruses of birds: etiologic agents of inflammatory diseases in a tumor virus family," *J Virol*, vol. 81, no. 21, pp. 11554–11559, 2007. 4

[22] M. Y. Halami, G. M. Dorrestein, P. Couteel, G. Heckel, H. Müller, and R. Johne, "Whole-genome characterization of a novel polyomavirus detected in fatally diseased canary birds," *J Gen Virol*, vol. 91, no. 12, pp. 3016–3022, 2010. 4

[23] B. L. Padgett, D. L. Walker, G. M. ZuRhein, R. J. Eckroade, and B. H. Dessel, "Cultivation of papova-like virus from human brain with progressive multifocal leucoencephalopathy," *Lancet*, vol. 1, no. 7712, pp. 1257–1260, 1971. 5, 7

[24] B. L. Padgett and D. L. Walker, "Prevalence of antibodies in human sera against JC virus, an isolate from a case of progressive multifocal leukoencephalopathy," *J Infect Dis*, vol. 127, no. 4, pp. 467–470, 1973. 5

[25] L. A. Shackelton, A. Rambaut, O. G. Pybus, and E. C. Holmes, "JC virus evolution and its association with human populations," *J Virol*, vol. 80, no. 20, pp. 9928–9933, 2006. 5

[26] L. Ricciardiello, L. Laghi, P. Ramamirtham, C. L. Chang, D. K. Chang, A. E. Randolph, and C. R. Boland, "JC virus DNA sequences are frequently present in the human upper and lower gastrointestinal tract," *Gastroenterol*, vol. 119, no. 5, pp. 1228–1235, 2000. 5

[27] M. W. Ferenczy, L. J. Marshall, C. D. S. Nelson, W. J. Atwood, A. Nath, K. Khalili, and E. O. Major, "Molecular biology, epidemiology, and pathogenesis of progressive multifocal leukoencephalopathy, the JC virus-induced demyelinating disease of the human brain," *Clin Microbiol Rev*, vol. 25, no. 3, pp. 471–506, 2012. 6

[28] S. D. Gardner, A. M. Field, D. V. Coleman, and B. Hulme, "New human papovavirus (B.K.) isolated from urine after renal transplantation," *Lancet*, vol. 1, no. 7712, pp. 1253–1257, 1971. 6, 7

[29] A. Egli, L. Infanti, A. Dumoulin, A. Buser, J. Samaridis, C. Stebler, R. Gosert, and H. H. Hirsch, "Prevalence of polyomavirus BK and JC infection and replication in 400 healthy blood donors," *J Infect Dis*, vol. 199, no. 6, pp. 837–846, 2009. 6

[30] G. P. Balba, B. Javaid, and J. G. Timpone Jr., "BK polyomavirus infection in the renal transplant recipient," *Infect Dis Clin N Am*, vol. 27, no. 2, pp. 271–283, 2013. 6

[31] E. van der Meijden, R. W. A. Janssens, C. Lauber, J. N. Bouwes Bavinck, A. E. Gorbalenya, and M. C. W. Feltkamp, "Discovery of a new human polyomavirus associated with <italic>trichodysplasia spinulosa</italic> in an immunocompromized patient," *PLoS Pathog*, vol. 6, no. 7, p. e1001024, 2010. 6, 7

[32] T. Allander, K. Andreasson, S. Gupta, A. Bjerkner, G. Bogdanovic, M. A. A. Persson, T. Dalianis, T. Ramqvist, and B. Andersson, "Identification of a third human polyomavirus," *J Virol*, vol. 81, no. 8, pp. 4130–4136, 2007. 7

[33] A. M. Gaynor, M. D. Nissen, D. M. Whiley, I. M. Mackay, S. B. Lambert, G. Wu, D. C. Brennan, G. A. Storch, T. P. Sloots, and D. Wang, "Identification of a novel polyomavirus from patients with acute respiratory tract infections," *PLoS Pathog*, vol. 3, no. 5, p. e64, 2007. 7

[34] R. M. Schowalter, D. V. Pastrana, K. A. Pumphrey, A. L. Moyer, and C. B. Buck, "Merkel cell polyomavirus and two previously unknown polyomaviruses are chronically shed from human skin," *Cell Host Microbe*, vol. 7, no. 6, pp. 509 – 515, 2010. 7, 33

[35] N. Scuda, J. Hofmann, S. Calvignac-Spencer, K. Ruprecht, P. Liman, J. Kuhn, H. Hengel, and B. Ehlers, "A novel human polyomavirus closely related to the African green monkey-derived lymphotropic polyomavirus," *J Virol*, vol. 85, no. 9, pp. 4586–4590, 2011. 7

[36] E. A. Siebrasse, A. Reyes, E. S. Lim, G. Zhao, R. S. Mkakosya, M. J. Manary, J. I. Gordon, and D. Wang, "Identification of MW polyomavirus, a novel

polyomavirus in human stool," *J Virol*, vol. 86, no. 19, pp. 10321–10326, 2012. 7, 27, 28

[37] C. B. Buck, G. Q. Phan, M. T. Raiji, P. M. Murphy, D. H. McDermott, and A. A. McBride, "Complete genome sequence of a tenth human polyomavirus," *J Virol*, vol. 86, no. 19, p. 10887, 2012. 7

[38] G. Yu, A. L. Greninger, P. Isa, T. G. Phan, M. A. Martinez, M. de la Luz Sanchez, J. F. Contreras, J. I. Santos-Preciado, J. Parsonnet, S. Miller, J. L. DeRisi, E. Delwart, C. F. Arias, and C. Y. Chiu, "Discovery of a novel polyomavirus in acute diarrheal samples from children," *PLoS One*, vol. 7, no. 11, p. e49449, 2012. 7

[39] S. Korup, J. Rietscher, S. Calvignac-Spencer, F. Trusch, J. Hofmann, U. Moens, I. Sauer, S. Voigt, R. Schmuck, and B. Ehlers, "Identification of a novel human polyomavirus in organs of the gastrointestinal tract," *PLoS One*, vol. 8, no. 3, p. e58021, 2013. 7

[40] E. S. Lim, A. Reyes, M. Antonio, D. Saha, U. N. Ikumapayi, M. Adeyemi, O. C. Stine, R. Skelton, D. C. Brennan, R. S. Mkakosya, M. J. Manary, J. I. Gordon, and D. Wang, "Discovery of STL polyomavirus, a polyomavirus of ancestral recombinant origin that encodes a unique T antigen by alternative splicing," *Virology*, vol. 436, no. 2, pp. 295–303, 2013. 7

[41] N. Mishra, M. Pereira, R. H. Rhodes, P. An, J. M. Pipas, K. Jain, A. Kapoor, T. Briese, P. L. Faust, and W. I. Lipkin, "Identification of a novel polyomavirus in a pancreatic transplant recipient with retinal blindness and vasculitic myopathy," *J Infect Dis*, vol. 210, no. 10, pp. 1595–1599, 2014. 7

[42] M. Shuda, H. Feng, H. J. Kwun, S. T. Rosen, O. Gjoerup, P. S. Moore, and Y. Chang, "T antigen mutations are a human tumor-specific signature for Merkel cell polyomavirus," *Proc Nat Acad Sci USA*, vol. 105, no. 42, pp. 16272–16277, 2008. 7, 41, 42, 92

[43] J. J. Carter, M. D. Daugherty, X. Qi, A. Bheda-Malge, G. C. Wipf, K. Robinson, A. Roman, H. S. Malik, and D. A. Galloway, "Identification of an overprinting gene in Merkel cell polyomavirus provides evolutionary insight into the birth of viral genes," *Proc Nat Acad Sci USA*, vol. 110, no. 31, pp. 12744–12749, 2013. 7, 32

[44] J. Cheng, J. A. DeCaprio, M. M. Fluck, and B. S. Schaffhausen, "Cellular transformation by simian virus 40 and murine polyoma virus T antigens," *Semin Cancer Biol*, vol. 19, no. 4, pp. 218–228, 2009. 8, 32

[45] S. Raghava, K. M. Giorda, F. B. Romano, A. P. Heuck, and D. N. Hebert, "The SV40 late protein VP4 is a viroporin that forms pores to disrupt membranes for viral release," *PLoS Pathog*, vol. 7, no. 6, p. e1002116, 2011. 8

[46] N. Gerits and U. Moens, "Agnoprotein of mammalian polyomaviruses," *Virology*, vol. 432, no. 2, pp. 316–326, 2012. 8

[47] M. A. Campanero-Rhodes, A. Smith, W. Chai, S. Sonnino, L. Mauri, R. A. Childs, Y. Zhang, H. Ewers, A. Helenius, A. Imberty, and T. Feizi, "N-glycolyl GM1 ganglioside as a receptor for simian virus 40," *J Virol*, vol. 81, no. 23, pp. 12846–12858, 2007. 9

[48] L. C. Norkin, "Simian virus 40 infection via MHC class I molecules and caveolae," *Immunol Rev*, vol. 168, pp. 13–22, 1999. 10

[49] A. E. Smith, H. Lilie, and A. Helenius, "Ganglioside-dependent cell attachment and endocytosis of murine polyomavirus-like particles," *FEBS Lett*, vol. 555, no. 2, pp. 199–203, 2003. 10

[50] J. A. Low, B. Magnuson, B. Tsai, and M. J. Imperiale, "Identification of gangliosides GD1b and GT1b as receptors for BK virus," *J Virol*, vol. 80, no. 3, pp. 1361–1366, 2006. 10

[51] R. Komagome, H. Sawa, T. Suzuki, Y. Suzuki, S. Tanaka, W. J. Atwood, and K. Nagashima, "Oligosaccharides as receptors for JC virus," *J Virol*, vol. 76, no. 24, pp. 12992–13000, 2002. 10

[52] H. A. Anderson, Y. Chen, and L. C. Norkin, "Bound simian virus 40 translocates to caveolin-enriched membrane domains, and its entry is inhibited by drugs that selectively disrupt caveolae," *Mol Biol Cell*, vol. 7, no. 11, pp. 1825–1834, 1996. 10

[53] W. Querbes, A. Benmerah, D. Tosoni, P. P. Di Fiore, and W. J. Atwood, "A JC virus-induced signal is required for infection of glial cells by a clathrin- and eps15-dependent pathway," *J Virol*, vol. 78, no. 1, pp. 250–256, 2004. 10

[54] N. Ishii, A. Nakanishi, M. Yamada, M. H. Macalalad, and H. Kasamatsu, "Functional complementation of nuclear targeting-defective mutants of simian virus 40 structural proteins," *J Virol*, vol. 68, no. 12, pp. 8209–8216, 1994. 10

[55] Q. Qu, H. Sawa, T. Suzuki, S. Semba, C. Henmi, Y. Okada, M. Tsuda, S. Tanaka, W. J. Atwood, and K. Nagashima, "Nuclear entry mechanism of the human polyomavirus JC virus-like particle: role of importins and the nuclear pore complex," *J Biol Chem*, vol. 279, no. 26, pp. 27735–27742, 2004. 10

[56] I. Bikel and M. R. Loeken, "Involvement of simian virus 40 (SV40) small t antigen in trans activation of SV40 early and late promoters," *J Virol*, vol. 66, no. 3, pp. 1489–1494, 1992. 10, 15

[57] M. Coca-Prados and M. T. Hsu, "Intracellular forms of simian virus 40 nucleoprotein complexes. II. Biochemical and electron microscopic analysis of simian virus 40 virion assembly," *J Virol*, vol. 31, no. 1, pp. 199–208, 1979. 10

[58] X. S. Chen, T. Stehle, and S. C. Harrison, "Interaction of polyomavirus internal protein VP2 with the major capsid protein VP1 and implications for participation of VP2 in viral entry," *EMBO J*, vol. 17, no. 12, pp. 3233–3240, 1998. 10

[59] A. Gordon-Shaag, O. Ben-Nun-Shaul, V. Roitman, Y. Yosef, and A. Oppenheim, "Cellular transcription factor Sp1 recruits simian virus 40 capsid proteins to the viral packaging signal, ses," *J Virol*, vol. 76, no. 12, pp. 5915–5924, 2002. 10

[60] U. Moens, M. Van Ghelue, and M. Johannessen, "Oncogenic potentials of the human polyomavirus regulatory proteins," *Cell Mol Life Sci*, vol. 64, no. 13, pp. 1656–1678, 2007. 10, 11, 19, 31

[61] K. A. Crandall, M. Perez-Losada, R. G. Christensen, D. A. McClellan, and R. P. Viscidi, "Phylogenomics and molecular evolution of polyomaviruses," *Adv Exp Med Biol*, vol. 577, pp. 46–59, 2006. 11

[62] D. Ahuja, M. T. Saenz-Robles, and J. M. Pipas, "SV40 large T antigen targets multiple cellular pathways to elicit cellular transformation," *Oncogene*, vol. 24, no. 52, pp. 7729–7745, 2005. 11, 19

[63] H. Stahl, P. Dröge, and R. Knippers, "DNA helicase activity of SV40 large tumor antigen," *EMBO J*, vol. 5, no. 8, pp. 1939–1944, 1986. 11

[64] F. B. Dean, P. Bullock, Y. Murakami, C. R. Wobbe, L. Weissbach, and J. Hurwitz, "Simian virus 40 (SV40) DNA replication: SV40 large T antigen unwinds DNA containing the SV40 origin of replication," *Proc Natl Acad Sci USA*, vol. 84, no. 1, pp. 16–20, 1987. 11

[65] J. Brady, J. B. Bolen, M. Radonovich, N. Salzman, and G. Khoury, "Stimulation of simian virus 40 late gene expression by simian virus 40 tumor antigen," *Proc Natl Acad Sci USA*, vol. 81, no. 7, pp. 2040–2044, 1984. 11

[66] M. Chowdhury, J. P. Taylor, H. Tada, J. Rappaport, F. Wong-Staal, S. Amini, and K. Khalili, "Regulation of the human neurotropic virus promoter by JCV-T antigen and HIV-1 tat protein," *Oncogene*, vol. 5, no. 12, pp. 1737–1742, 1990. 11

[67] I. Dornreiter, A. Höss, A. K. Arthur, and E. Fanning, "SV40 T antigen binds directly to the large subunit of purified DNA polymerase alpha," *EMBO J*, vol. 9, no. 10, pp. 3329–3336, 1990. 11

[68] T. Melendy and B. Stillman, "An interaction between replication protein A and SV40 T antigen appears essential for primosome assembly during SV40 DNA replication," *J Biol Chem*, vol. 268, no. 5, pp. 3389–3395, 1993. 11

[69] S. Seinsoth, H. Uhlmann-Schiffler, and H. Stahl, "Bidirectional DNA unwinding by a ternary complex of T antigen, nucleolin and topoisomerase I," *EMBO Rep*, vol. 4, no. 3, pp. 263–268, 2003. 12

[70] R. A. Weinberg, "The retinoblastoma protein and cell cycle control," *Cell*, vol. 81, no. 3, pp. 323–330, 1995. 12

[71] B. D. Rowland and R. Bernards, "Re-evaluating cell-cycle regulation by E2Fs," *Cell*, vol. 127, no. 5, pp. 871–874, 2006. 12

[72] J. A. DeCaprio, J. W. Ludlow, J. Figge, J. Y. Shew, C. M. Huang, W. H. Lee, E. Marsilio, E. Paucha, and D. M. Livingston, "SV40 large tumor antigen

forms a specific complex with the product of the retinoblastoma susceptibility gene," *Cell*, vol. 54, no. 2, pp. 275–283, 1988. 12, 19

[73] E. S. Knudsen and J. Y. Wang, "Hyperphosphorylated p107 and p130 bind to T-antigen: identification of a critical regulatory sequence present in RB but not in p107/p130," *Oncogene*, vol. 16, no. 13, pp. 1655–1663, 1998. 12

[74] K. F. Harris, J. B. Christensen, and M. J. Imperiale, "BK virus large T antigen: interactions with the retinoblastoma family of tumor suppressor proteins and effects on cellular growth control," *J Virol*, vol. 70, no. 4, pp. 2378–2386, 1996. 12, 13

[75] A. Srinivasan, K. W. Peden, and J. M. Pipas, "The large tumor antigen of simian virus 40 encodes at least two distinct transforming functions," *J Virol*, vol. 63, no. 12, pp. 5459–5463, 1989. 12

[76] T. Hartmann, X. Xu, M. Kronast, S. Muehlich, K. Meyer, W. Zimmermann, J. Hurwitz, Z.-Q. Pan, S. Engelhardt, and A. Sarikas, "Inhibition of Cullin-RING E3 ubiquitin ligase 7 by simian virus 40 large T antigen," *Proc Natl Acad Sci USA*, vol. 111, no. 9, pp. 3371–3376, 2014. 13

[77] J. Trojanek, S. Croul, T. Ho, J. Y. Wang, A. Darbinyan, M. Nowicki, L. Del Valle, T. Skorski, K. Khalili, and K. Reiss, "T-antigen of the human polyomavirus JC attenuates faithful DNA repair by forcing nuclear interaction between IRS-1 and Rad51," *J Cell Physiol*, vol. 206, no. 1, pp. 35–46, 2006. 13

[78] A. Lassak, L. Del Valle, F. Peruzzi, J. Y. Wang, S. Enam, S. Croul, K. Khalili, and K. Reiss, "Insulin receptor substrate 1 translocation to the nucleus by the human JC virus T-antigen," *J Biol Chem*, vol. 277, no. 19, pp. 17231–17238, 2002. 13, 19

[79] S. Enam, L. Del Valle, C. Lara, D.-D. Gan, C. Ortiz-Hidalgo, J. P. Palazzo, and K. Khalili, "Association of human polyomavirus JCV with colon cancer: evidence for interaction of viral T-antigen and beta-catenin," *Cancer Res*, vol. 62, no. 23, pp. 7093–7101, 2002. 13, 19

[80] D. D. Gan, K. Reiss, T. Carrill, L. Del Valle, S. Croul, A. Giordano, P. Fishman, and K. Khalili, "Involvement of Wnt signaling pathway in murine

medulloblastoma induced by human neurotropic JC virus," *Oncogene*, vol. 20, no. 35, pp. 4864–4870, 2001. 13

[81] L. C. Berger, D. B. Smith, I. Davidson, J. J. Hwang, E. Fanning, and A. G. Wildeman, "Interaction between T antigen and TEA domain of the factor TEF-1 derepresses simian virus 40 late promoter in vitro: identification of T-antigen domains important for transcription control," *J Virol*, vol. 70, no. 2, pp. 1203–1212, 1996. 13, 20

[82] D. R. Borger and J. A. DeCaprio, "Targeting of p300/CREB binding protein coactivators by simian virus 40 is mediated through p53," *J Virol*, vol. 80, no. 9, pp. 4292–4303, 2006. 13

[83] M. Cotsiki, R. L. Lock, Y. Cheng, G. L. Williams, J. Zhao, D. Perera, R. Freire, A. Entwistle, E. A. Golemis, T. M. Roberts, P. S. Jat, and O. V. Gjoerup, "Simian virus 40 large T antigen targets the spindle assembly checkpoint protein Bub1," *Proc Natl Acad Sci USA*, vol. 101, no. 4, pp. 947–952, 2004. 13

[84] X. Wu, D. Avni, T. Chiba, F. Yan, Q. Zhao, Y. Lin, H. Heng, and D. Livingston, "SV40 T antigen interacts with Nbs1 to disrupt DNA replication control," *Genes Dev*, vol. 18, no. 11, pp. 1305–1316, 2004. 13

[85] M. Hollstein, D. Sidransky, B. Vogelstein, and C. C. Harris, "p53 mutations in human cancers," *Science*, vol. 253, no. 5015, pp. 49–53, 1991. 13

[86] T. D. Kierstead and M. J. Tevethia, "Association of p53 binding and immortalization of primary C57BL/6 mouse embryo fibroblasts by using simian virus 40 T-antigen mutants bearing internal overlapping deletion mutations," *J Virol*, vol. 67, no. 4, pp. 1817–1829, 1993. 13

[87] C. Staib, J. Pesch, R. Gerwig, J. K. Gerber, U. Brehm, A. Stangl, and F. Grummt, "p53 inhibits JC virus DNA replication in vivo and interacts with JC virus large T-antigen," *Virology*, vol. 219, no. 1, pp. 237–246, 1996. 13

[88] L. Yamasaki, "Role of the RB tumor suppressor in cancer," *Cancer Treat Res*, vol. 115, pp. 209–239, 2003. 13

[89] K. Segawa, A. Minowa, K. Sugasawa, T. Takano, and F. Hanaoka, "Abrogation of p53-mediated transactivation by SV40 large T antigen," *Oncogene*, vol. 8, no. 3, pp. 543–548, 1993. 13

[90] D. Jiang, A. Srinivasan, G. Lozano, and P. D. Robbins, "SV40 T antigen abrogates p53-mediated transcriptional activity," *Oncogene*, vol. 8, no. 10, pp. 2805–2812, 1993. 13

[91] J. A. Mietz, T. Unger, J. M. Huibregtse, and P. M. Howley, "The transcriptional transactivation function of wild-type p53 is inhibited by SV40 large T-antigen and by HPV-16 E6 oncoprotein," *EMBO J*, vol. 11, no. 13, pp. 5013–5020, 1992. 13

[92] V. Janssens and J. Goris, "Protein phosphatase 2A: a highly regulated family of serine/threonine phosphatases implicated in cell growth and signalling," *Biochem J*, vol. 353, no. 3, pp. 417–439, 2001. 14, 117

[93] H. Usui, M. Imazu, K. Maeta, H. Tsukamoto, K. Azuma, and M. Takeda, "Three distinct forms of type 2A protein phosphatase in human erythrocyte cytosol," *J Biol Chem*, vol. 263, no. 8, pp. 3752–3761, 1988. 14

[94] E. Ogris, D. M. Gibson, and D. C. Pallas, "Protein phosphatase 2A subunit assembly: the catalytic subunit carboxy terminus is important for binding cellular B subunit but not polyomavirus middle tumor antigen," *Oncogene*, vol. 15, no. 8, pp. 911–917, 1997. 14

[95] M. Mumby, "PP2A: unveiling a reluctant tumor suppressor," *Cell*, vol. 130, no. 1, pp. 21–24, 2007. 14

[96] J. Zhou, H. T. Pham, R. Ruediger, and G. Walter, "Characterization of the Aalpha and Abeta subunit isoforms of protein phosphatase 2A: differences in expression, subunit interaction, and evolution," *Biochem J*, vol. 369, no. 2, pp. 387–398, 2003. 15

[97] S. I. Yang, R. L. Lickteig, R. Estes, K. Rundell, G. Walter, and M. C. Mumby, "Control of protein phosphatase 2A by simian virus 40 small-t antigen," *Mol Cell Biol*, vol. 11, no. 4, pp. 1988–1995, 1991. 15

[98] B. Bollag, C. A. Hofstetter, M. M. Reviriego-Mendoza, and R. J. Frisque, "JC virus small t antigen binds phosphatase PP2A and Rb family proteins and Is required for efficient viral DNA replication activity," *PLoS One*, vol. 5, no. 5, p. e10606, 2010. 15

[99] R. Ruediger, M. Hentz, J. Fait, M. Mumby, and G. Walter, "Molecular model of the A subunit of protein phosphatase 2A: interaction with other subunits and tumor antigens," *J Virol*, vol. 68, no. 1, pp. 123–129, 1994. 15

[100] P. Rodriguez-Viciana, C. Collins, and M. Fried, "Polyoma and SV40 proteins differentially regulate PP2A to activate distinct cellular signaling pathways involved in growth control," *Proc Nat Acad Sci USA*, vol. 103, no. 51, pp. 19290–19295, 2006. 15, 21, 44

[101] K. H. Scheidtmann, M. C. Mumby, K. Rundell, and G. Walter, "Dephosphorylation of simian virus 40 large-T antigen and p53 protein by protein phosphatase 2A: inhibition by small-t antigen," *Mol Cell Biol*, vol. 11, no. 4, pp. 1996–2003, 1991. 15

[102] S. Sugano, N. Yamaguchi, and H. Shimojo, "Small t protein of simian virus 40 is required for dense focus formation in a rat cell line," *J Virol*, vol. 41, no. 3, pp. 1073–1075, 1982. 15

[103] I. Bikel, X. Montano, M. E. Agha, M. Brown, M. McCormack, J. Boltax, and D. M. Livingston, "SV40 small t antigen enhances the transformation activity of limiting concentrations of SV40 large T antigen," *Cell*, vol. 48, no. 2, pp. 321–330, 1987. 15

[104] E. Sontag, S. Fedorov, C. Kamibayashi, D. Robbins, M. Cobb, and M. Mumby, "The interaction of SV40 small tumor antigen with protein phosphatase 2A stimulates the map kinase pathway and induces cell proliferation," *Cell*, vol. 75, no. 5, pp. 887–897, 1993. 15

[105] A. Porrás, S. Gaillard, and K. Rundell, "The simian virus 40 small-t and large-T antigens jointly regulate cell cycle reentry in human fibroblasts," *J Virol*, vol. 73, no. 4, pp. 3102–3107, 1999. 15

[106] J. Winston, F. Dong, and W. J. Pledger, "Differential modulation of G1 cyclins and the Cdk inhibitor p27kip1 by platelet-derived growth factor and plasma factors in density-arrested fibroblasts," *J Biol Chem*, vol. 271, no. 19, pp. 11253–11260, 1996. 15

[107] C. S. Moreno, S. Ramachandran, D. G. Ashby, N. Laycock, C. A. Plattner, W. Chen, W. C. Hahn, and D. C. Pallas, "Signaling and transcriptional changes critical for transformation of human cells by simian virus 40 small

tumor antigen or protein phosphatase 2A B56gamma knockdown," *Cancer Res*, vol. 64, no. 19, pp. 6978–6988, 2004. 15, 38

[108] S. M. Dilworth, H. A. Hansson, C. Darnfors, G. Bjursell, C. H. Streuli, and B. E. Griffin, "Subcellular localisation of the middle and large T-antigens of polyoma virus," *EMBO J*, vol. 5, no. 3, pp. 491–499, 1986. 16

[109] A. Schönthal, S. Srinivas, and W. Eckhart, "Induction of c-jun protooncogene expression and transcription factor AP-1 activity by the polyoma virus middle-sized tumor antigen," *Proc Nat Acad Sci USA*, vol. 89, no. 11, pp. 4972–4976, 1992. 16

[110] S. Srinivas, A. Schönthal, and W. Eckhart, "Polyomavirus middle-sized tumor antigen modulates c-Jun phosphorylation and transcriptional activity," *Proc Nat Acad Sci USA*, vol. 91, no. 21, pp. 10064–10068, 1994. 16

[111] C. Wasylyk, P. Flores, A. Gutman, and B. Wasylyk, "PEA3 is a nuclear target for transcription activation by non-nuclear oncogenes," *EMBO J*, vol. 8, no. 11, pp. 3371–3378, 1989. 16

[112] M. Li and R. L. Garcea, "Identification of the threonine phosphorylation sites on the polyomavirus major capsid protein VP1: relationship to the activity of middle T antigen," *J Virol*, vol. 68, no. 1, pp. 320–327, 1994. 16

[113] D. C. Pallas, L. K. Shahrik, B. L. Martin, S. Jaspers, T. B. Miller, D. L. Brautigan, and T. M. Roberts, "Polyoma small and middle T antigens and SV40 small t antigen form stable complexes with protein phosphatase 2A," *Cell*, vol. 60, no. 1, pp. 167–176, 1990. 16

[114] K. P. Mullane, M. Ratnofsky, X. Cullere, and B. Schaffhausen, "Signaling from polyomavirus middle T and small T defines different roles for protein phosphatase 2A," *Mol Cell Biol*, vol. 18, no. 12, pp. 7556–7564, 1998. 16

[115] H. R. Glover, C. E. Brewster, and S. M. Dilworth, "Association between src-kinases and the polyoma virus oncogene middle T-antigen requires PP2A and a specific sequence motif," *Oncogene*, vol. 18, no. 30, pp. 4364–4370, 1999. 16, 17

[116] D. Templeton and W. Eckhart, "N-terminal amino acid sequences of the polyoma middle-size T antigen are important for protein kinase activity

and cell transformation," *Mol Cell Biol*, vol. 4, no. 5, pp. 817–821, 1984. 17, 22

[117] T. Hunter, M. A. Hutchinson, and W. Eckhart, "Polyoma middle-sized T antigen can be phosphorylated on tyrosine at multiple sites in vitro," *EMBO J*, vol. 3, no. 1, pp. 73–79, 1984. 17

[118] K. A. Gottlieb and L. P. Villarreal, "Natural biology of polyomavirus middle T antigen," *Microbiol Mol Biol Rev*, vol. 65, no. 2, pp. 288–318, 2001. 17

[119] J. Zerrahn, U. Knippschild, T. Winkler, and W. Deppert, "Independent expression of the transforming amino-terminal domain of SV40 large I antigen from an alternatively spliced third SV40 early mRNA," *EMBO J*, vol. 12, no. 12, pp. 4739–4746, 1993. 17

[120] S. A. Comerford, N. Schultz, E. A. Hinnant, S. Klapproth, and R. E. Hammer, "Comparative analysis of SV40 17kT and LT function in vivo demonstrates that LT's C-terminus re-programs hepatic gene expression and is necessary for tumorigenesis in the liver," *Oncogenesis*, vol. 1, no. 9, p. e28, 2012. 17, 32

[121] A. Boyapati, M. Wilson, J. Yu, and K. Rundell, "SV40 17KT antigen complements DnaJ mutations in large T antigen to restore transformation of primary human fibroblasts," *Virology*, vol. 315, no. 1, pp. 148–158, 2003. 17

[122] P. W. Trowbridge and R. J. Frisque, "Identification of three new JC virus proteins generated by alternative splicing of the early viral mRNA," *J Neurovirol*, vol. 1, no. 2, pp. 195–206, 1995. 17

[123] C. Prins and R. J. Frisque, "JC virus T' proteins encoded by alternatively spliced early mRNAs enhance T antigen-mediated viral DNA replication in human cells," *J Neurovirol*, vol. 7, no. 3, pp. 250–264, 2001. 17

[124] B. Bollag, L. H. Kilpatrick, S. K. Tyagarajan, M. J. Tevethia, and R. J. Frisque, "JC virus T'135, T'136 and T'165 proteins interact with cellular p107 and p130 in vivo and influence viral transformation potential," *J Neurovirol*, vol. 12, no. 6, pp. 428–442, 2006. 17

[125] J. Abramczuk, S. Pan, G. Maul, and B. B. Knowles, "Tumor induction by simian virus 40 in mice is controlled by long-term persistence of the vi-

ral genome and the immune response of the host," *J Virol*, vol. 49, no. 2, pp. 540–548, 1984. 17

[126] T. Ramqvist and T. Dalianis, "Murine polyomavirus tumour specific transplantation antigens and viral persistence in relation to the immune response, and tumour development," *Semin Cancer Biol*, vol. 19, no. 4, pp. 236–243, 2009. 17

[127] K. Hirai, J. Lehman, and V. Defendi, "Integration of simian virus 40 deoxyribonucleic acid into the deoxyribonucleic acid of primary infected Chinese hamster cells," *J Virol*, vol. 8, no. 5, pp. 708–715, 1971. 18

[128] B. S. Sylla, D. Allard, G. Roy, D. Bourgaux-Ramoisy, and P. Bourgaux, "A mouse DNA sequence that mediates integration and excision of polyoma virus DNA," *Gene*, vol. 29, no. 3, pp. 343–350, 1984. 18

[129] C. W. Mandl and R. J. Frisque, "Characterization of cells transformed by the human polyomavirus JC virus," *J Gen Virol*, vol. 67, pp. 1733–1739, 1986. 18

[130] N. Chenciner, G. Meneguzzi, A. Corallini, M. P. Grossi, P. Grassi, G. Barbanti-Brodano, and G. Milanesi, "Integrated and free viral DNA in hamster tumors induced by BK virus," *Proc Natl Acad Sci USA*, vol. 77, no. 2, pp. 975–979, 1980. 18

[131] D. L. Walker, B. L. Padgett, G. M. ZuRhein, A. E. Albert, and R. F. Marsh, "Human papovavirus (JC): induction of brain tumors in hamsters," *Science*, vol. 181, no. 4100, pp. 674–676, 1973. 18

[132] J. Costa, P. M. Howley, F. Legallais, C. Yee, N. Young, and A. S. Rabson, "Oncogenicity of a nude mouse cell line transformed by a human papovavirus," *J Natl Cancer Inst*, vol. 58, no. 4, pp. 1147–1149, 1977. 18

[133] L. L. Emerson, H. M. Carney, L. J. Layfield, and J. R. Sherbotie, "Collecting duct carcinoma arising in association with BK nephropathy post-transplantation in a pediatric patient. A case report with immunohistochemical and in situ hybridization study," *Pediatr Transplant*, vol. 12, no. 5, pp. 600–605, 2008. 18

[134] M. Narayanan, J. Szymanski, E. Slavcheva, A. Rao, A. Kelly, K. Jones, and G. Jaffers, "BK virus associated renal cell carcinoma: case presentation with

optimized PCR and other diagnostic tests," *Am J Transplant*, vol. 7, no. 6, pp. 1666–1671, 2007. 18

[135] J. Y. Kausman, G. R. Somers, D. M. Francis, and C. L. Jones, "Association of renal adenocarcinoma and BK virus nephropathy post transplantation," *Pediatr Nephrol*, vol. 19, no. 4, pp. 459–462, 2004. 18

[136] S. Loghavi and S. Bose, "Polyomavirus infection and urothelial carcinoma," *Diagn Cytopathol*, vol. 39, no. 7, pp. 531–535, 2011. 18

[137] J. R. Abend, M. Jiang, and M. J. Imperiale, "BK virus and human cancer: innocent until proven guilty," *Semin Cancer Biol*, vol. 19, no. 4, pp. 252–260, 2009. 18

[138] V. Bouvard, R. A. Baan, Y. Grosse, B. Lauby-Secretan, F. El Ghissassi, L. Benbrahim-Tallaa, N. Guha, and K. Straif, "Carcinogenicity of malaria and of some polyomaviruses," *Lancet Oncol*, vol. 13, no. 4, pp. 339–340, 2012. 18

[139] M. Babakir-Mina, M. Ciccozzi, L. Campitelli, S. Aquaro, A. L. Coco, C. F. Perno, and M. Ciotti, "Identification of the novel KI Polyomavirus in paranasal and lung tissues," *J Med Virol*, vol. 81, no. 3, pp. 558–561, 2009. 18

[140] T. Brostoff, F. N. Dela Cruz, M. E. Church, K. D. Woolard, and P. A. Pesavento, "The raccoon polyomavirus genome and tumor antigen transcription are stable and abundant in neuroglial tumors," *J Virol*, vol. 88, no. 21, pp. 12816–12824, 2014. 18

[141] M. T. Saenz-Robles, C. S. Sullivan, and J. M. Pipas, "Transforming functions of simian virus 40," *Oncogene*, vol. 20, no. 54, pp. 7899–7907, 2001. 18

[142] P. Yaciuk, M. C. Carter, J. M. Pipas, and E. Moran, "Simian virus 40 large-T antigen expresses a biological activity complementary to the p300-associated transforming function of the adenovirus E1A gene products," *Mol Cell Biol*, vol. 11, no. 4, pp. 2116–2124, 1991. 19

[143] R. G. Martin, "The transformation of cell growth and transmogrification of DNA synthesis by simian virus 40," *Adv Cancer Res*, vol. 34, pp. 1–68, 1981. 19

[144] K. H. Vousden and D. P. Lane, "p53 in health and disease," *Nat Rev Mol Cell Biol*, vol. 8, no. 4, pp. 275–283, 2007. 19

[145] K. F. Sachsenmeier and J. M. Pipas, "Inhibition of Rb and p53 is insufficient for SV40 T-antigen transformation," *Virology*, vol. 283, no. 1, pp. 40–48, 2001. 19

[146] S. H. Ali, J. S. Kasper, T. Arai, and J. A. DeCaprio, "Cul7/p185/p193 binding to simian virus 40 large T antigen has a role in cellular transformation," *J Virol*, vol. 78, no. 6, pp. 2749–2757, 2004. 19

[147] T. Reya and H. Clevers, "Wnt signalling in stem cells and cancer," *Nature*, vol. 434, no. 7035, pp. 843–850, 2005. 19

[148] P. C. Zuzarte, I. K. Farrance, P. C. Simpson, and A. G. Wildeman, "Tumor cell splice variants of the transcription factor TEF-1 induced by SV40 T-antigen transformation," *Biochim Biophys Acta*, vol. 1517, no. 1, pp. 82–90, 2000. 20

[149] I. Bikel, X. Montano, M. E. Agha, M. Brown, M. McCormack, J. Boltax, and D. M. Livingston, "SV40 small t antigen enhances the transformation activity of limiting concentrations of SV40 large T antigen," *Cell*, vol. 48, no. 2, pp. 321–330, 1987. 20

[150] W. C. Hahn, S. K. Dessain, M. W. Brooks, J. E. King, B. Elenbaas, D. M. Sabatini, J. A. DeCaprio, and R. A. Weinberg, "Enumeration of the simian virus 40 early region elements necessary for human cell transformation," *Mol Cell Biol*, vol. 22, no. 7, pp. 2111–2123, 2002. 20

[151] F. Tiemann, J. Zerrahn, and W. Deppert, "Cooperation of simian virus 40 large and small T antigens in metabolic stabilization of tumor suppressor p53 during cellular transformation," *J Virol*, vol. 69, no. 10, pp. 6115–6121, 1995. 20

[152] F. Martinato, M. Cesaroni, B. Amati, and E. Guccione, "Analysis of Myc-induced histone modifications on target chromatin," *PLoS One*, vol. 3, no. 11, p. e3650, 2008. 20

[153] E. Yeh, M. Cunningham, H. Arnold, D. Chasse, T. Monteith, G. Ivaldi, W. C. Hahn, P. T. Stukenberg, S. Shenolikar, T. Uchida, C. M. Counter, J. R.

Nevins, A. R. Means, and R. Sears, "A signalling pathway controlling c-Myc degradation that impacts oncogenic transformation of human cells," *Nat Cell Biol*, vol. 6, no. 4, pp. 308–318, 2004. 21

[154] B. W. Ozanne, H. J. Spence, L. C. McGarry, and R. F. Hennigan, "Transcription factors control invasion: AP-1 the first among equals," *Oncogene*, vol. 26, no. 1, pp. 1–10, 2007. 21

[155] M. D. Conkright and M. Montminy, "CREB: the unindicted cancer co-conspirator," *Trends Cell Biol*, vol. 15, no. 9, pp. 457–459, 2005. 21

[156] R. Piva, G. Belardo, and M. G. Santoro, "NF-kappaB: a stress-regulated switch for cell survival," *Antioxid Redox Signal*, vol. 8, no. 3-4, pp. 478–486, 2006. 21

[157] T. L. Yuan and L. C. Cantley, "PI3K pathway alterations in cancer: variations on a theme," *Oncogene*, vol. 27, no. 41, pp. 5497–5510, 2008. 21

[158] H. Yuan, T. Veldman, K. Rundell, and R. Schlegel, "Simian virus 40 small tumor antigen activates AKT and telomerase and induces anchorage-independent growth of human epithelial cells," *J Virol*, vol. 76, no. 21, pp. 10685–10691, 2002. 21

[159] J. Kang, M. Yang, B. Li, W. Qi, C. Zhang, K. M. Shokat, D. R. Tomchick, M. Machius, and H. Yu, "Structure and substrate recruitment of the human spindle checkpoint kinase Bub1," *Mol Cell*, vol. 32, no. 3, pp. 394–405, 2008. 21

[160] C. Guo, G. Wu, J. L. Chin, G. Bauman, M. Moussa, F. Wang, N. M. Greenberg, S. S. Taylor, and J. W. Xuan, "Bub1 up-regulation and hyperphosphorylation promote malignant transformation in SV40 tag-induced transgenic mouse models," *Mol Cancer Res*, vol. 4, no. 12, pp. 957–969, 2006. 21

[161] R. Treisman, U. Novak, J. Favaloro, and R. Kamen, "Transformation of rat cells by an altered polyoma virus genome expressing only the middle-T protein," *Nature*, vol. 292, no. 5824, pp. 595–600, 1981. 22

[162] G. G. Carmichael, B. S. Schaffhausen, D. I. Dorsky, D. B. Oliver, and T. L. Benjamin, "Carboxy terminus of polyoma middle-sized tumor antigen is required for attachment to membranes, associated protein kinase activities,

and cell transformation," *Proc Nat Acad Sci USA*, vol. 79, no. 11, pp. 3579–3583, 1982. 22

[163] C. Toker, "Trabecular carcinoma of the skin," *Arch Dermatol*, vol. 105, no. 1, pp. 107–110, 1972. 22

[164] J. Kaae, A. V. Hansen, R. J. Biggar, H. A. Boyd, P. S. Moore, J. Wohlfahrt, and M. Melbye, "Merkel cell carcinoma: incidence, mortality, and risk of other cancers," *J Natl Cancer Inst*, vol. 102, no. 11, pp. 793–801, 2010. 22

[165] S. G. Gupta, L. C. Wang, P. F. Penas, M. Gellenthin, S. J. Lee, and P. Nghiem, "Sentinel lymph node biopsy for evaluation and treatment of patients with Merkel cell carcinoma: The Dana-Farber experience and meta-analysis of the literature," *Arch Dermatol*, vol. 142, no. 6, pp. 685–690, 2006. 22

[166] S. Vernadakis, D. Moris, A. Bankfalvi, N. Makris, and G. C. Sotiropoulos, "Metastatic Merkel cell carcinoma (MCC) of pancreas and breast: a unique case," *World J Surg Oncol*, vol. 11, p. 261, 2013. 22

[167] C. F. Suttie, G. Hruby, L. Horvath, and J. Thompson, "Cardiac metastasis in Merkel cell carcinoma," *J Clin Oncol*, vol. 32, pp. 52–53, 2014. 22

[168] I. Vasileiadis, M. Sofopoulos, N. Arnogiannaki, and S. Georgopoulos, "A Merkel cell carcinoma metastatic to the tonsil: a case report and review of the literature," *J Oral Maxillofac Surg*, vol. 71, no. 10, pp. 1812.e1–6, 2013. 22

[169] F. Merkel, "Tastzellen and Tastkoerperchenbei den Hausthieren und beim Menschen," *Arch MikrAnat*, vol. 11, pp. 636–652, 1875. 22, 23

[170] K. M. Morrison, G. R. Miesegaes, E. A. Lumpkin, and S. M. Maricich, "Mammalian Merkel cells are descended from the epidermal lineage," *Dev Biol*, vol. 336, no. 1, pp. 76–83, 2009. 23, 24, 174

[171] I. Moll, R. Paus, and R. Moll, "Merkel cells in mouse skin: intermediate filament pattern, localization, and hair cycle-dependent density," *J Invest Dermatol*, vol. 106, no. 2, pp. 281–286, 1996. 23

[172] C. A. May and I. Osterland, "Merkel cell distribution in the human eyelid," *Eur J Histochem*, vol. 57, no. 4, p. e33, 2013. 24

[173] N. Ben-Arie, B. A. Hassan, N. A. Bermingham, D. M. Malicki, D. Armstrong, M. Matzuk, H. J. Bellen, and H. Y. Zoghbi, "Functional conservation of atonal and math1 in the cns and pns.," *Development*, vol. 127, pp. 1039–1048, Mar 2000. 24

[174] S. M. Maricich, S. A. Wellnitz, A. M. Nelson, D. R. Lesniak, G. J. Gerling, E. A. Lumpkin, and H. Y. Zoghbi, "Merkel cells are essential for light-touch responses.," *Science*, vol. 324, pp. 1580–1582, Jun 2009. 24

[175] E. Guler-Nizam, U. Leiter, G. Metzler, H. Breuninger, C. Garbe, and T. K. Eigentler, "Clinical course and prognostic factors of Merkel cell carcinoma of the skin," *Br J Dermatol*, vol. 161, no. 1, pp. 90–94, 2009. 24

[176] R. M. C. C. Group, "Merkel cell carcinoma: recent progress and current priorities on etiology, pathogenesis, and clinical management," *J Clin Oncol*, vol. 27, no. 24, pp. 4021–4026, 2009. 24, 25, 26

[177] S. Kuwamoto, "Recent advances in the biology of Merkel cell carcinoma," *Hum Pathol*, vol. 42, no. 8, pp. 1063–1077, 2011. 24, 174

[178] A. S. Leong, G. E. Phillips, A. S. Pieterse, and J. Milios, "Criteria for the diagnosis of primary endocrine carcinoma of the skin (Merkel cell carcinoma). A histological, immunohistochemical and ultrastructural study of 13 cases," *Pathology*, vol. 18, no. 4, pp. 393–399, 1986. 24

[179] M. Bobos, P. Hytiroglou, I. Kostopoulos, G. Karkavelas, and C. S. Papadimitriou, "Immunohistochemical distinction between Merkel cell carcinoma and small cell carcinoma of the lung," *Am J Dermatopathol*, vol. 28, no. 2, pp. 99–104, 2006. 25, 174

[180] K. B. Calder, S. Coplowitz, S. Schlauder, and M. B. Morgan, "A case series and immunophenotypic analysis of CK20-/CK7+ primary neuroendocrine carcinoma of the skin," *J Cutan Pathol*, vol. 34, no. 12, pp. 918–923, 2007. 25, 174

[181] T. Ferringer, H. C. Rogers, and J. S. Metcalf, "Merkel cell carcinoma in situ," *J Cutan Pathol*, vol. 32, no. 2, pp. 162–165, 2005. 25

[182] B. Lemos and P. Nghiem, "Merkel cell carcinoma: more deaths but still no pathway to blame," *J Invest Dermatol*, vol. 127, no. 9, pp. 2100–2103, 2007. 25, 26

[183] N. C. Hodgson, "Merkel cell carcinoma: changing incidence trends," *J Surg Oncol*, vol. 89, no. 1, pp. 1–4, 2005. 25

[184] M. Agelli, L. X. Clegg, J. C. Becker, and D. E. Rollison, "The etiology and epidemiology of Merkel cell carcinoma," *Curr Probl Cancer*, vol. 34, no. 1, pp. 14–37, 2010. 25

[185] B. A. Reichgelt and O. Visser, "Epidemiology and survival of Merkel cell carcinoma in the Netherlands. A population-based study of 808 cases in 1993-2007," *Eur J Cancer*, vol. 47, no. 4, pp. 579–585, 2011. 25

[186] J. Albores-Saavedra, K. Batich, F. Chable-Montero, N. Sagy, A. M. Schwartz, and D. E. Henson, "Merkel cell carcinoma demographics, morphology, and survival based on 3870 cases: a population based study," *J Cutan Pathol*, vol. 37, no. 1, pp. 20–27, 2010. 25

[187] J. C. Becker, "Merkel cell carcinoma," *Ann Oncol*, vol. 21, pp. 81–85, 2010. 25

[188] K. G. Paulson, J. G. Iyer, D. R. Byrd, and P. Nghiem, "Pathologic nodal evaluation is increasingly commonly performed for patients with Merkel cell carcinoma," *J Am Acad Dermatol*, vol. 69, no. 4, pp. 653–654, 2013. 25

[189] J. Burack and E. L. Altschuler, "Sustained remission of metastatic Merkel cell carcinoma with treatment of HIV infection," *J R Soc Med*, vol. 96, no. 5, pp. 238–239, 2003. 26

[190] J. C. Wooff, J. R. Trites, N. M. G. Walsh, and M. J. Bullock, "Complete spontaneous regression of metastatic merkel cell carcinoma: a case report and review of the literature," *Am J Dermatopathol*, vol. 32, no. 6, pp. 614–617, 2010. 26

[191] H. H. Wong and J. Wang, "Merkel cell carcinoma," *Arch Pathol Lab Med*, vol. 134, no. 11, pp. 1711–1716, 2010. 26

[192] B. D. Lemos, B. E. Storer, J. G. Iyer, J. L. Phillips, C. K. Bichakjian, L. C. Fang, T. M. Johnson, N. J. Liegeois-Kwon, C. C. Otley, K. G. Paulson, M. I. Ross, S. S. Yu, N. C. Zeitouni, D. R. Byrd, V. K. Sondak, J. E. Gershenwald, A. J. Sober, and P. Nghiem, "Pathologic nodal evaluation improves prognostic accuracy in Merkel cell carcinoma: analysis of 5823 cases as the basis of the

first consensus staging system," *J Am Acad Dermatol*, vol. 63, no. 5, pp. 751–761, 2010. 26

[193] M. Agelli and L. X. Clegg, "Epidemiology of primary Merkel cell carcinoma in the United States," *J Am Acad Dermatol*, vol. 49, no. 5, pp. 832–841, 2003. 26, 92

[194] A. A. Sarnaik, M. H. Lien, P. Nghiem, and C. K. Bichakjian, "Clinical recognition, diagnosis, and staging of Merkel cell carcinoma, and the role of the multidisciplinary management team," *Curr Probl Cancer*, vol. 34, no. 1, pp. 38–46, 2010. 26

[195] R. H. Decker and L. D. Wilson, "Role of radiotherapy in the management of Merkel cell carcinoma of the skin," *J Natl Compr Canc Netw*, vol. 4, no. 7, pp. 713–718, 2006. 26

[196] P. T. Tai, E. Yu, E. Winquist, A. Hammond, L. Stitt, J. Tonita, and J. Gilchrist, "Chemotherapy in neuroendocrine/Merkel cell carcinoma of the skin: case series and review of 204 cases," *J Clin Oncol*, vol. 18, no. 12, pp. 2493–2499, 2000. 26, 46

[197] S. J. Rodig, J. Cheng, J. Wardzala, A. DoRosario, J. J. Scanlon, A. C. Laga, A. Martinez-Fernandez, J. A. Barletta, A. M. Bellizzi, S. Sadasivam, D. T. Holloway, D. J. Cooper, T. S. Kupper, L. C. Wang, and J. A. DeCaprio, "Improved detection suggests all Merkel cell carcinomas harbor Merkel polyomavirus," *J Clin Invest*, vol. 122, no. 12, pp. 4645–4653, 2012. 27

[198] J. M. Kean, S. Rao, M. Wang, and R. L. Garcea, "Seroepidemiology of human polyomaviruses," *PLoS Pathog*, vol. 5, no. 3, p. e1000363, 2009. 27

[199] T. Dalianis, T. Ramqvist, K. Andreasson, J. M. Kean, and R. L. Garcea, "KI, WU and Merkel cell polyomaviruses: a new era for human polyomavirus research," *Semin Cancer Biol*, vol. 19, no. 4, pp. 270–275, 2009. 27

[200] R. Johne, C. B. Buck, T. Allander, W. J. Atwood, R. L. Garcea, M. J. Imperiale, E. O. Major, T. Ramqvist, and L. C. Norkin, "Taxonomical developments in the family Polyomaviridae," *Arch Virol*, vol. 156, no. 9, pp. 1627–1634, 2011. 28

[201] C. F. De Gascun and M. J. Carr, "Human polyomavirus reactivation: disease pathogenesis and treatment approaches," *Clin Dev Immunol*, vol. 2013, p. e373579, 2013. 28

[202] M. Matsushita, T. Iwasaki, S. Kuwamoto, M. Kato, K. Nagata, I. Murakami, Y. Kitamura, and K. Hayashi, "Merkel cell polyomavirus (MCPyV) strains in Japanese merkel cell carcinomas (MCC) are distinct from Caucasian type MCPyVs: genetic variability and phylogeny of MCPyV genomes obtained from Japanese MCPyV-infected MCCs," *Virus Genes*, vol. 48, no. 2, pp. 233–242, 2014. 28

[203] H. J. Kwun, A. Guastafierro, M. Shuda, G. Meinke, A. Bohm, P. S. Moore, and Y. Chang, "The minimum replication origin of Merkel cell polyomavirus has a unique large T-antigen loading architecture and requires small T-antigen expression for optimal replication," *J Virol*, vol. 83, no. 23, pp. 12118–12128, 2009. 30, 36, 37

[204] D. Topalis, G. Andrei, and R. Snoeck, "The large tumor antigen: a "Swiss Army knife" protein possessing the functions required for the polyomavirus life cycle," *Antiviral Res*, vol. 97, no. 2, pp. 122–136, 2013. 30

[205] T. Nakamura, Y. Sato, D. Watanabe, H. Ito, N. Shimonohara, T. Tsuji, N. Nakajima, Y. Suzuki, K. Matsuo, H. Nakagawa, T. Sata, and H. Katano, "Nuclear localization of Merkel cell polyomavirus large T antigen in Merkel cell carcinoma," *Virology*, vol. 398, no. 2, pp. 273–279, 2010. 30

[206] J. Li, X. Wang, J. Diaz, S. H. Tsang, C. B. Buck, and J. You, "Merkel cell polyomavirus large T antigen disrupts host genomic integrity and inhibits cellular proliferation," *J Virol*, vol. 87, no. 16, pp. 9173–9188, 2013. 30, 43

[207] X. Liu, J. Hein, S. C. W. Richardson, P. H. Basse, T. Toptan, P. S. Moore, O. V. Gjoerup, and Y. Chang, "Merkel cell polyomavirus large T antigen disrupts lysosome clustering by translocating human Vam6p from the cytoplasm to the nucleus," *J Bio Chem*, vol. 286, no. 19, pp. 17079–17090, 2011. 30, 36, 41

[208] G. J. Seo, C. J. Chen, and C. S. Sullivan, "Merkel cell polyomavirus encodes a microRNA with the ability to autoregulate viral gene expression," *Virology*, vol. 383, no. 2, pp. 183–187, 2009. 31, 33, 35

[209] D. A. Griffiths, H. Abdul-Sada, L. M. Knight, B. R. Jackson, K. Richards, E. L. Prescott, A. H. S. Peach, G. E. Blair, A. Macdonald, and A. Whitehouse, "Merkel cell polyomavirus small T antigen targets the NEMO adaptor protein to disrupt inflammatory signaling," *J Virol*, vol. 87, no. 24, pp. 13853–13867, 2013. 31, 38, 65, 100, 117, 118, 143, 176

[210] L. M. Knight, G. Stakaityte, J. J. Wood, H. Abdul-Sada, D. A. Griffiths, G. J. Howell, R. Wheat, G. E. Blair, N. M. Steven, A. Macdonald, D. J. Blackbourn, and A. Whitehouse, "Merkel cell polyomavirus small T antigen mediates microtubule destabilization to promote cell motility and migration," *J Virol*, vol. 89, no. 1, pp. 35–47, 2015. 31, 61, 65, 93, 103, 114, 117, 143, 162, 174, 175, 176

[211] H. J. Kwun, M. Shuda, H. Feng, C. J. Camacho, P. S. Moore, and Y. Chang, "Merkel cell polyomavirus small T antigen controls viral replication and oncoprotein expression by targeting the cellular ubiquitin ligase SCFFbw7," *Cell Host Microbe*, vol. 14, no. 2, pp. 125–135, 2013. 31, 37, 44

[212] S. H. Tsang, R. Wang, E. Nakamaru-Ogiso, S. A. B. Knight, C. B. Buck, and J. You, "The oncogenic small tumor antigen of Merkel cell polyomavirus Is an iron-sulfur cluster protein that enhances viral DNA replication," *J Virol*, vol. 90, no. 3, pp. 1544–1556, 2015. 31

[213] Y. L. Tolstov, D. V. Pastrana, H. Feng, J. C. Becker, F. J. Jenkins, S. Moschos, Y. Chang, C. B. Buck, and P. S. Moore, "Human Merkel cell polyomavirus infection II. MCV is a common human infection that can be detected by conformational capsid epitope immunoassays," *Int J Cancer*, vol. 125, no. 6, pp. 1250–1256, 2009. 32

[214] A. Touzé, J. Gaitan, F. Arnold, R. Cazal, M. J. Fleury, N. Combelas, P.-Y. Sizaret, S. Guyetant, A. Maruani, M. Baay, M. Tognon, and P. Coursaget, "Generation of Merkel cell polyomavirus (MCV)-like particles and their application to detection of MCV antibodies," *J Clin Microbiol*, vol. 48, no. 5, pp. 1767–1770, 2010. 32

[215] R. M. Schowalter and C. B. Buck, "The Merkel cell polyomavirus minor capsid protein," *PLoS Pathog*, vol. 9, no. 8, p. e1003558, 2013. 32, 33

[216] U. Neu, H. Hengel, B. S. Blaum, R. M. Schowalter, D. Macejak, M. Gilbert, W. W. Wakarchuk, A. Imamura, H. Ando, M. Kiso, N. Arnberg, R. L.

Garcea, T. Peters, C. B. Buck, and T. Stehle, "Structures of Merkel cell polyomavirus VP1 complexes define a sialic acid binding site required for infection," *PLoS Pathog*, vol. 8, no. 7, p. e1002738, 2012. 32, 33, 34

[217] C. S. Sullivan, A. T. Grundhoff, S. Tevethia, J. M. Pipas, and D. Ganem, "SV40-encoded microRNAs regulate viral gene expression and reduce susceptibility to cytotoxic T cells," *Nature*, vol. 435, no. 7042, pp. 682–686, 2005. 33

[218] G. J. Seo, L. H. L. Fink, B. O'Hara, W. J. Atwood, and C. S. Sullivan, "Evolutionarily conserved function of a viral microRNA," *J Virol*, vol. 82, no. 20, pp. 9823–9828, 2008. 33

[219] S. Lee, K. G. Paulson, E. P. Murchison, O. K. Afanasiev, C. Alkan, J. H. Leonard, D. R. Byrd, G. J. Hannon, and P. Nghiem, "Identification and validation of a novel mature microRNA encoded by the Merkel cell polyomavirus in human Merkel cell carcinomas," *J Clin Virol*, vol. 52, no. 3, pp. 272–275, 2011. 33

[220] W. Liu, R. Yang, A. S. Payne, R. M. Schowalter, M. E. Spurgeon, P. F. Lambert, X. Xu, C. B. Buck, and J. You, "Identifying the target cells and mechanisms of Merkel cell polyomavirus infection," *Cell Host Microbe*, vol. 19, pp. 775–787, 2016. 33, 34, 41, 46, 64, 175

[221] R. M. Schowalter, W. C. Reinhold, and C. B. Buck, "Entry tropism of BK and Merkel cell polyomaviruses in cell culture," *PLoS One*, vol. 7, no. 7, p. e42181, 2012. 33

[222] F. Neumann, S. Borchert, C. Schmidt, R. Reimer, H. Hohenberg, N. Fischer, and A. Grundhoff, "Replication, gene expression and particle production by a consensus Merkel Cell Polyomavirus (MCPyV) genome," *PLoS One*, vol. 6, no. 12, p. e29112, 2011. 33, 41

[223] R. M. Schowalter, D. V. Pastrana, and C. B. Buck, "Glycosaminoglycans and sialylated glycans sequentially facilitate Merkel cell polyomavirus infectious entry," *PLoS Pathog*, vol. 7, no. 7, p. e1002161, 2011. 34

[224] P. H. Bauer, C. Cui, T. Stehle, S. C. Harrison, J. A. DeCaprio, and T. L. Benjamin, "Discrimination between sialic acid-containing receptors and pseu-

doreceptors regulates polyomavirus spread in the mouse," *J Virol*, vol. 73, no. 7, pp. 5826–5832, 1999. 34

[225] M. Sapp and P. M. Day, "Structure, attachment and entry of polyoma- and papillomaviruses," *Virology*, vol. 384, no. 2, pp. 400–409, 2009. 34

[226] C. A. J. Horvath, G. A. V. Boulet, V. M. Renoux, P. O. Delvenne, and J.-P. J. Bogers, "Mechanisms of cell entry by human papillomaviruses: an overview," *Virol J*, vol. 7, p. 11, 2010. 34

[227] H. Feng, H. J. Kwun, X. Liu, O. Gjoerup, D. B. Stolz, Y. Chang, and P. S. Moore, "Cellular and viral factors regulating Merkel cell polyomavirus replication," *PLoS One*, vol. 6, no. 7, p. e22468, 2011. 35, 36

[228] R. Wessel, J. Schweizer, and H. Stahl, "Simian virus 40 T-antigen DNA helicase is a hexamer which forms a binary complex during bidirectional unwinding from the viral origin of DNA replication," *J Virol*, vol. 66, no. 2, pp. 804–815, 1992. 36

[229] C. J. Harrison, G. Meinke, H. J. Kwun, H. Rogalin, P. J. Phelan, P. A. Bullock, Y. Chang, P. S. Moore, and A. Bohm, "Asymmetric assembly of Merkel cell polyomavirus large T-antigen origin binding domains at the viral origin," *J Mol Biol*, vol. 409, no. 4, pp. 529–542, 2011. 36

[230] X. Wang, J. Li, R. M. Schowalter, J. Jiao, C. B. Buck, and J. You, "Bromodomain protein Brd4 plays a key role in Merkel cell polyomavirus DNA replication," *PLOS Path*, vol. 8, no. 11, p. e1003021, 2012. 36

[231] S. H. Tsang, X. Wang, J. Li, C. B. Buck, and J. You, "Host DNA damage response factors localize to Merkel cell polyomavirus DNA replication sites to support efficient viral DNA replication," *J Virol*, vol. 88, pp. 3285–3297, 2014. 36, 37

[232] K. A. Gillespie, K. P. Mehta, L. A. Laimins, and C. A. Moody, "Human papillomaviruses recruit cellular DNA repair and homologous recombination factors to viral replication centers," *J Virol*, vol. 86, pp. 9520–9526, 2012. 37

[233] X. Wang, C. M. Helfer, N. Pancholi, J. E. Bradner, and J. You, "Recruitment of Brd4 to the human papillomavirus type 16 DNA replication complex is essential for replication of viral DNA," *J Virol*, vol. 87, no. 7, pp. 3871–3884, 2013. 37

[234] M. Shuda, H. J. Kwun, H. Feng, Y. Chang, and P. S. Moore, "Human Merkel cell polyomavirus small T antigen is an oncoprotein targeting the 4E-BP1 translation regulator," *J Clin Invest*, vol. 121, no. 9, pp. 3623–3634, 2011. 37, 43, 44, 45, 65, 94, 96, 117, 162, 174, 176

[235] M. Welcker and B. E. Clurman, "FBW7 ubiquitin ligase: a tumour suppressor at the crossroads of cell division, growth and differentiation," *Nat Rev Cancer*, vol. 8, no. 2, pp. 83–93, 2008. 37

[236] K. Takeda and S. Akira, "Toll-like receptors in innate immunity," *Int Immunol*, vol. 17, no. 1, pp. 1–14, 2005. 38, 39

[237] M. Karin and M. Delhase, "The I kappa B kinase (IKK) and NF-kappa B: key elements of proinflammatory signalling," *Semin Immunol*, vol. 12, no. 1, pp. 85–98, 2000. 38

[238] G. Le Negrate, "Viral interference with innate immunity by preventing NF-kappaB activity," *Cell Microbiol*, vol. 14, no. 2, pp. 168–181, 2012. 38

[239] M. Joo, Y. S. Hahn, M. Kwon, R. T. Sadikot, T. S. Blackwell, and J. W. Christman, "Hepatitis C virus core protein suppresses NF-kappaB activation and cyclooxygenase-2 expression by direct interaction with IkappaB kinase beta," *J Virol*, vol. 79, no. 12, pp. 7648–7657, 2005. 38

[240] D. Spitkovsky, S. P. Hehner, T. G. Hofmann, A. Moller, and M. L. Schmitz, "The human papillomavirus oncoprotein E7 attenuates NF-kappa B activation by targeting the Ikappa B kinase complex," *J Biol Chem*, vol. 277, no. 28, pp. 25576–25582, 2002. 38

[241] P. M. Fliss, T. P. Jowers, M. M. Brinkmann, B. Holstermann, C. Mack, P. Dickinson, H. Hohenberg, P. Ghazal, and W. Brune, "Viral mediated redirection of NEMO/IKKgammato autophagosomes curtails the inflammatory cascade," *PLoS Pathog*, vol. 8, no. 2, p. e1002517, 2012. 38

[242] C. M. H. Randall, J. A. Jokela, and J. L. Shisler, "The MC159 protein from the molluscum contagiosum poxvirus inhibits NF-kappaB activation by interacting with the IkappaB kinase complex," *J Immunol*, vol. 188, no. 5, pp. 2371–2379, 2012. 38

[243] I. Fathallah, P. Parroche, H. Gruffat, C. Zannetti, H. Johansson, J. Yue, E. Manet, M. Tommasino, B. S. Sylla, and U. A. Hasan, "EBV latent membrane protein 1 Is a negative regulator of TLR9," *J Immunol*, vol. 185, no. 11, pp. 6439–6447, 2010. 38

[244] U. A. Hasan, E. Bates, F. Takeshita, A. Biliato, R. Accardi, V. Bouvard, M. Mansour, I. Vincent, L. Gissmann, T. Iftner, M. Sideri, F. Stubenrauch, and M. Tommasino, "TLR9 expression and function is abolished by the cervical cancer-associated human papillomavirus type 16," *J Immunol*, vol. 178, no. 5, pp. 3186–3197, 2007. 38

[245] I. E. Vincent, C. Zannetti, J. Lucifora, H. Norder, U. Protzer, P. Hainaut, F. Zoulim, M. Tommasino, C. Trépo, U. Hasan, and I. Chemin, "Hepatitis B virus impairs TLR9 expression and function in plasmacytoid dendritic cells," *PLoS One*, vol. 6, no. 10, p. e26315, 2011. 38

[246] H. Tsujimura, T. Tamura, H. J. Kong, A. Nishiyama, K. J. Ishii, D. M. Klinman, and K. Ozato, "Toll-like receptor 9 signaling activates NF-kappaB through IFN regulatory factor-8/IFN consensus sequence binding protein in dendritic cells," *J Immunol*, vol. 172, no. 11, pp. 6820–6827, 2004. 39

[247] N. Shahzad, M. Shuda, T. Gheit, H. J. Kwun, I. Cornet, D. Saidj, C. Zannetti, U. Hasan, Y. Chang, P. S. Moore, R. Accardi, and M. Tommasino, "The T antigen locus of Merkel cell polyomavirus downregulates human Toll-like receptor 9 expression," *J Virol*, vol. 87, no. 23, pp. 13009–13019, 2013. 39

[248] K. Khalili, M. K. White, H. Sawa, K. Nagashima, and M. Safak, "The agnoprotein of polyomaviruses: A multifunctional auxiliary protein," *J Cell Physiol*, vol. 204, no. 1, pp. 1–7, 2005. 41

[249] R. Daniels, D. Sadowicz, and D. N. Hebert, "A very late viral protein triggers the lytic release of SV40," *PLoS Pathog*, vol. 3, no. 7, p. e98, 2007. 41

[250] E. T. Clayson, L. V. Brando, and R. W. Compans, "Release of simian virus 40 virions from epithelial cells is polarized and occurs without cell lysis," *J Virol*, vol. 63, no. 5, pp. 2278–2288, 1989. 41

[251] R. Houben, M. Shuda, R. Weinkam, D. Schrama, H. Feng, Y. Chang, P. S. Moore, and J. C. Becker, "Merkel cell polyomavirus-infected Merkel cell

carcinoma cells require expression of viral T antigens," *J Virol*, vol. 84, no. 14, pp. 7064–7072, 2010. 41

[252] H. C. Laude, B. Jonchère, E. Maubec, A. Carlotti, E. Marinho, B. Couturaud, M. Peter, X. Sastre-Garau, M.-F. Avril, N. Dupin, and F. Rozenberg, "Distinct Merkel cell polyomavirus molecular features in tumour and non tumour specimens from patients with Merkel cell carcinoma," *PLoS Pathog*, vol. 6, no. 8, p. e1001076, 2010. 41

[253] A. Kassem, A. Schopflin, C. Diaz, W. Weyers, E. Stickeler, M. Werner, and A. Zur Hausen, "Frequent detection of Merkel cell polyomavirus in human Merkel cell carcinomas and identification of a unique deletion in the VP1 gene," *Cancer Res*, vol. 68, no. 13, pp. 5009–5013, 2008. 41, 42

[254] X. Sastre-Garau, M. Peter, M.-F. Avril, H. Laude, J. Couturier, F. Rozenberg, A. Almeida, F. Boitier, A. Carlotti, B. Couturaud, and N. Dupin, "Merkel cell carcinoma of the skin: pathological and molecular evidence for a causative role of MCV in oncogenesis," *J Pathol*, vol. 218, no. 1, pp. 48–56, 2009. 42

[255] J. A. DeCaprio and R. L. Garcea, "A cornucopia of human polyomaviruses," *Nat Rev Micro*, vol. 11, no. 4, pp. 264–276, 2013. 42

[256] S. K. Demetriou, K. Ona-Vu, E. M. Sullivan, T. K. Dong, S.-W. Hsu, and D. H. Oh, "Defective DNA repair and cell cycle arrest in cells expressing Merkel cell polyomavirus T antigen," *Int J Cancer*, vol. 131, no. 8, pp. 1818–1827, 2012. 42

[257] M. Shuda, R. Arora, H. J. Kwun, H. Feng, R. Sarid, M.-T. Fernandez-Figueras, Y. Tolstov, O. Gjoerup, M. M. Mansukhani, S. H. Swerdlow, P. M. Chaudhary, J. M. Kirkwood, M. A. Nalesnik, J. A. Kant, L. M. Weiss, P. S. Moore, and Y. Chang, "Human Merkel cell polyomavirus infection I. MCV T antigen expression in Merkel cell carcinoma, lymphoid tissues and lymphoid tumors," *Int J Cancer*, vol. 125, no. 6, pp. 1243–1249, 2009. 43

[258] J. Cheng, O. Rozenblatt-Rosen, K. G. Paulson, P. Nghiem, and J. A. DeCaprio, "Merkel cell polyomavirus large T antigen has growth-promoting and inhibitory activities," *J Virol*, vol. 87, no. 11, pp. 6118–6126, 2013. 43

[259] R. Arora, M. Shuda, A. Guastafierro, H. Feng, T. Toptan, Y. Tolstov, D. Normolle, L. L. Vollmer, A. Vogt, A. Domling, J. L. Brodsky, Y. Chang, and P. S. Moore, "Survivin is a therapeutic target in Merkel cell carcinoma," *Sci Transl Med*, vol. 4, no. 133, p. 133ra56, 2012. 43, 46, 175

[260] M. S. Coumar, F.-Y. Tsai, J. R. Kanwar, S. Sarvagalla, and C. H. A. Cheung, "Treat cancers by targeting survivin: just a dream or future reality?," *Cancer Treat Rev*, vol. 39, no. 7, pp. 802–811, 2013. 43

[261] N. J. Buchkovich, Y. Yu, C. A. Zampieri, and J. C. Alwine, "The TORrid affairs of viruses: effects of mammalian DNA viruses on the PI3K-Akt-mTOR signalling pathway," *Nat Rev Microbiol*, vol. 6, no. 4, pp. 266–275, 2008. 44

[262] R. J. O. Dowling, I. Topisirovic, T. Alain, M. Bidinosti, B. D. Fonseca, E. Petroulakis, X. Wang, O. Larsson, A. Selvaraj, Y. Liu, S. C. Kozma, G. Thomas, and N. Sonenberg, "mTORC1-mediated cell proliferation, but not cell growth, controlled by the 4E-BPs," *Science*, vol. 328, no. 5982, pp. 1172–1176, 2010. 44

[263] Q.-B. She, E. Halilovic, Q. Ye, W. Zhen, S. Shirasawa, T. Sasazuki, D. B. Solit, and N. Rosen, "4E-BP1 is a key effector of the oncogenic activation of the AKT and ERK signaling pathways that integrates their function in tumors," *Cancer Cell*, vol. 18, no. 1, pp. 39–51, 2010. 44

[264] J. D. Richter and N. Sonenberg, "Regulation of cap-dependent translation by eIF4E inhibitory proteins," *Nature*, vol. 433, no. 7025, pp. 477–480, 2005. 44

[265] A. Pause, G. J. Belsham, A. C. Gingras, O. Donze, T. A. Lin, J. C. J. Lawrence, and N. Sonenberg, "Insulin-dependent stimulation of protein synthesis by phosphorylation of a regulator of 5'-cap function," *Nature*, vol. 371, no. 6500, pp. 762–767, 1994. 44

[266] A.-C. Gingras, S. P. Gygi, B. Raught, R. D. Polakiewicz, R. T. Abraham, M. F. Hoekstra, R. Aebersold, and N. Sonenberg, "Regulation of 4E-BP1 phosphorylation: a novel two-step mechanism," *Genes Dev*, vol. 13, no. 11, pp. 1422–1437, 1999. 44

[267] S. Angermeyer, S. Hesbacher, J. C. Becker, D. Schrama, and R. Houben, "Merkel cell polyomavirus-positive Merkel cell carcinoma cells do not re-

quire expression of the viral small T antigen," *J Invest Dermatol*, vol. 133, no. 8, pp. 2059–2064, 2013. 45

[268] T. Jouary, C. Leyral, B. Dreno, A. Doussau, B. Sassolas, M. Beylot-Barry, C. Renaud-Vilmer, B. Guillot, P. Bernard, C. Lok, C. Bedane, F. Cambazard, L. Misery, E. Esteve, S. Dalac, L. Machet, F. Grange, P. Young, F. Granel-Brocard, F. Truchetet, B. Vergier, M. M. Delaunay, and J. J. Grob, "Adjuvant prophylactic regional radiotherapy versus observation in stage I Merkel cell carcinoma: a multicentric prospective randomized study," *Ann Oncol*, vol. 23, no. 4, pp. 1074–1080, 2012. 46

[269] E. Pape, N. Rezvoy, N. Penel, J. Salleron, V. Martinot, P. Guerreschi, V. Dziwniel, S. Darras, X. Mirabel, and L. Mortier, "Radiotherapy alone for Merkel cell carcinoma: a comparative and retrospective study of 25 patients," *J Am Acad Dermatol*, vol. 65, no. 5, pp. 983–990, 2011. 46

[270] C. Willmes, C. Adam, M. Alb, L. Volkert, R. Houben, J. C. Becker, and D. Schrama, "Type I and II IFNs inhibit Merkel cell carcinoma via modulation of the Merkel cell polyomavirus T antigens," *Cancer Res*, vol. 72, no. 8, pp. 2120–2128, 2012. 46

[271] C. Biver-Dalle, T. Nguyen, A. Touze, C. Saccomani, S. Penz, S. Cunat-Peultier, M.-O. Riou-Gotta, P. Humbert, P. Coursaget, and F. Aubin, "Use of interferon-alpha in two patients with Merkel cell carcinoma positive for Merkel cell polyomavirus," *Acta Oncol*, vol. 50, no. 3, pp. 479–480, 2011. 46

[272] L. R. Dresang, A. Guastafierro, R. Arora, D. Normolle, Y. Chang, and P. S. Moore, "Response of Merkel cell polyomavirus-positive Merkel cell carcinoma xenografts to a survivin inhibitor," *PLoS One*, vol. 8, no. 11, p. e80543, 2013. 46, 175

[273] M. S. Davids, A. Charlton, S.-S. Ng, M.-L. Chong, K. Laubscher, M. Dar, J. Hodge, R. Soong, and B. C. Goh, "Response to a novel multitargeted tyrosine kinase inhibitor pazopanib in metastatic Merkel cell carcinoma," *J Clin Oncol*, vol. 27, no. 26, pp. e97–100, 2009. 46, 175

[274] A. Sugamata, K. Goya, and N. Yoshizawa, "A case of complete spontaneous regression of extremely advanced Merkel cell carcinoma," *J Surg Case Rep*, vol. 2011, no. 10, p. 7, 2011. 47

[275] J. G. Iyer, O. K. Afanasiev, C. McClurkan, K. Paulson, K. Nagase, L. Jing, J. O. Marshak, L. Dong, J. Carter, I. Lai, E. Farrar, D. Byrd, D. Galloway, C. Yee, D. M. Koelle, and P. Nghiem, "Merkel cell polyomavirus-specific CD8(+) and CD4(+) T-cell responses identified in Merkel cell carcinomas and blood," *Clin Cancer Res*, vol. 17, no. 21, pp. 6671–6680, 2011. 47

[276] R. Lyngaa, N. W. Pedersen, D. Schrama, C. A. Thrue, D. Ibrani, O. Met, P. Thor Straten, P. Nghiem, J. C. Becker, and S. R. Hadrup, "T-cell responses to oncogenic merkel cell polyomavirus proteins distinguish patients with merkel cell carcinoma from healthy donors," *Clin Cancer Res*, vol. 20, no. 7, pp. 1768–1778, 2014. 47

[277] Q. Zeng, B. P. Gomez, R. P. Viscidi, S. Peng, L. He, B. Ma, T.-C. Wu, and C.-F. Hung, "Development of a DNA vaccine targeting Merkel cell polyomavirus," *Vaccine*, vol. 30, no. 7, pp. 1322–1329, 2012. 47

[278] B. Gomez, L. He, Y. C. Tsai, T.-C. Wu, R. P. Viscidi, and C.-F. Hung, "Creation of a Merkel cell polyomavirus small T antigen-expressing murine tumor model and a DNA vaccine targeting small T antigen," *Cell Biosci*, vol. 3, no. 1, p. 29, 2013. 47

[279] O. K. Afanasiev, L. Yelistratova, N. Miller, K. Nagase, K. Paulson, J. G. Iyer, D. Ibrani, D. M. Koelle, and P. Nghiem, "Merkel polyomavirus-specific T cells fluctuate with Merkel cell carcinoma burden and express therapeutically targetable PD-1 and Tim-3 exhaustion markers," *Clin Cancer Res*, vol. 19, no. 19, pp. 5351–5360, 2013. 47

[280] T. D. Pollard and J. A. Cooper, "Actin, a central player in cell shape and movement," *Science*, vol. 326, no. 5957, pp. 1208–1212, 2009. 48

[281] D. Pruyne, M. Evangelista, C. Yang, E. Bi, S. Zigmond, A. Bretscher, and C. Boone, "Role of formins in actin assembly: nucleation and barbed-end association," *Science*, vol. 297, no. 5581, pp. 612–615, 2002. 48

[282] F. Li and H. N. Higgs, "Dissecting requirements for auto-inhibition of actin nucleation by the formin, mDia1," *J Biol Chem*, vol. 280, no. 8, pp. 6986–6992, 2005. 48

[283] K. G. Campellone and M. D. Welch, "A nucleator arms race: cellular control of actin assembly," *Nat Rev Mol Cell Biol*, vol. 11, no. 4, pp. 237–251, 2010. 48

[284] N. Tomasevic, Z. Jia, A. Russell, T. Fujii, J. J. Hartman, S. Clancy, M. Wang, C. Beraud, K. W. Wood, and R. Sakowicz, "Differential regulation of WASP and N-WASP by Cdc42, Rac1, Nck, and PI(4,5)P2," *Biochemistry*, vol. 46, no. 11, pp. 3494–3502, 2007. 49

[285] A. Nurnberg, T. Kitzing, and R. Grosse, "Nucleating actin for invasion," *Nat Rev Cancer*, vol. 11, no. 3, pp. 177–187, 2011. 49, 50

[286] A. G. Ammer and S. A. Weed, "Cortactin branches out: roles in regulating protrusive actin dynamics," *Cell Motil Cytoskeleton*, vol. 65, no. 9, pp. 687–707, 2008. 49

[287] A. M. Weaver, A. V. Karginov, A. W. Kinley, S. A. Weed, Y. Li, J. T. Parsons, and J. A. Cooper, "Cortactin promotes and stabilizes Arp2/3-induced actin filament network formation," *Curr Biol*, vol. 11, no. 5, pp. 370–374, 2001. 49, 94

[288] W. Brieher, "Mechanisms of actin disassembly," *Mol Biol Cell*, vol. 24, no. 15, pp. 2299–2302, 2013. 50

[289] A. Bretscher, "Fimbrin is a cytoskeletal protein that crosslinks F-actin in vitro," *Proc Natl Acad Sci USA*, vol. 78, no. 11, pp. 6849–6853, 1981. 50

[290] S. Yamashiro, Y. Yamakita, S. Ono, and F. Matsumura, "Fascin, an actin-bundling protein, induces membrane protrusions and increases cell motility of epithelial cells," *Mol Biol Cell*, vol. 9, no. 5, pp. 993–1006, 1998. 50

[291] A. Arjonen, R. Kaukonen, and J. Ivaska, "Filopodia and adhesion in cancer cell motility," *Cell Adh Migr*, vol. 5, no. 5, pp. 421–430, 2011. 50

[292] P. Hahne, A. Sechi, S. Benesch, and J. V. Small, "Scar/WAVE is localised at the tips of protruding lamellipodia in living cells," *FEBS Lett*, vol. 492, no. 3, pp. 215–220, 2001. 50

[293] H. Yamaguchi, M. Lorenz, S. Kempiak, C. Sarmiento, S. Coniglio, M. Symons, J. Segall, R. Eddy, H. Miki, T. Takenawa, and J. Condeelis,

"Molecular mechanisms of invadopodium formation: the role of the N-WASP-Arp2/3 complex pathway and cofilin," *J Cell Biol*, vol. 168, no. 3, pp. 441–452, 2005. 50

[294] K. Manakova, H. Yan, J. Lowengrub, and J. Allard, "Cell surface mechanochemistry and the determinants of bleb formation, healing, and travel velocity," *Biophys J*, vol. 110, no. 7, pp. 1636–1647, 2016. 50

[295] S. Suetsugu, D. Yamazaki, S. Kurisu, and T. Takenawa, "Differential roles of WAVE1 and WAVE2 in dorsal and peripheral ruffle formation for fibroblast cell migration," *Dev Cell*, vol. 5, no. 4, pp. 595–609, 2003. 52

[296] R. A. Worthylake, S. Lemoine, J. M. Watson, and K. Burridge, "RhoA is required for monocyte tail retraction during transendothelial migration," *J Cell Biol*, vol. 154, no. 1, pp. 147–160, 2001. 52

[297] M. Chrzanowska-Wodnicka and K. Burridge, "Rho-stimulated contractility drives the formation of stress fibers and focal adhesions," *J Cell Biol*, vol. 133, no. 6, pp. 1403–1415, 1996. 52, 92

[298] S. Ahmed, W. I. Goh, and W. Bu, "I-BAR domains, IRSp53 and filopodium formation," *Semin Cell Dev Biol*, vol. 21, no. 4, pp. 350–356, 2010. 52, 100

[299] K. Rottner and T. E. B. Stradal, "Actin dynamics and turnover in cell motility," *Curr Opin Cell Biol*, vol. 23, no. 5, pp. 569–578, 2011. 52

[300] J. L. Ross, M. Y. Ali, and D. M. Warshaw, "Cargo transport: molecular motors navigate a complex cytoskeleton," *Curr Opin Cell Biol*, vol. 20, no. 1, pp. 41–47, 2008. 52

[301] H. de Forges, A. Bouissou, and F. Perez, "Interplay between microtubule dynamics and intracellular organization," *Int J Biochem Cell Biol*, vol. 44, no. 2, pp. 266–274, 2012. 52

[302] J. C. Gatlin and K. Bloom, "Microtubule motors in eukaryotic spindle assembly and maintenance," *Semin Cell Dev Biol*, vol. 21, no. 3, pp. 248–254, 2010. 52

[303] I. Kaverina and A. Straube, "Regulation of cell migration by dynamic microtubules," *Semin Cell Dev Biol*, vol. 22, no. 9, pp. 968–974, 2011. 52

[304] B. R. Brinkley, "Microtubule organizing centers," *Annu Rev Cell Biol*, vol. 1, no. 1, pp. 145–172, 1985. 52

[305] D. Sept, "Microtubule polymerization: one step at a time," *Curr Biol*, vol. 17, no. 17, pp. 764–766, 2007. 52

[306] Y. Komarova, C. O. De Groot, I. Grigoriev, S. M. Gouveia, E. L. Munteanu, J. M. Schober, S. Honnappa, R. M. Buey, C. C. Hoogenraad, M. Dogterom, G. G. Borisy, M. O. Steinmetz, and A. Akhmanova, "Mammalian end binding proteins control persistent microtubule growth," *J Cell Biol*, vol. 184, no. 5, pp. 691–706, 2009. 53

[307] H. Herrmann, H. Bar, L. Kreplak, S. V. Strelkov, and U. Aebi, "Intermediate filaments: from cell architecture to nanomechanics," *Nat Rev Mol Cell Biol*, vol. 8, no. 7, pp. 562–573, 2007. 53

[308] A.-M. Chioni, W. J. Brackenbury, J. D. Calhoun, L. L. Isom, and M. B. A. Djamgoz, "A novel adhesion molecule in human breast cancer cells: voltage-gated Na+ channel beta1 subunit," *Int J Biochem Cell Biol*, vol. 41, no. 5, pp. 1216–1227, 2009. 53

[309] A. El Chemaly, Y. Okochi, M. Sasaki, S. Arnaudeau, Y. Okamura, and N. Demaurex, "VSOP/Hv1 proton channels sustain calcium entry, neutrophil migration, and superoxide production by limiting cell depolarization and acidification," *J Exp Med*, vol. 207, no. 1, pp. 129–139, 2010. 54

[310] S. Chifflet, J. A. Hernández, and S. Grasso, "A possible role for membrane depolarization in epithelial wound healing," *Am J Physiol*, vol. 288, no. 6, pp. 1420–1430, 2005. 54

[311] K. Szászi, G. Sirokmány, C. D. Ciano-Oliveira, O. D. Rotstein, and A. Kapus, "Depolarization induces Rho-Rho kinase-mediated myosin light chain phosphorylation in kidney tubular cells," *Am J Physiol*, vol. 289, no. 3, pp. 673–685, 2005. 54

[312] C. Callies, J. Fels, I. Liashkovich, K. Kliche, P. Jeggle, K. Kusche-Vihrog, and H. Oberleithner, "Membrane potential depolarization decreases the stiffness of vascular endothelial cells," *J Cell Sci*, vol. 124, no. 11, pp. 1936–1942, 2011. 54

[313] S. Pillozzi and A. Arcangeli, *Physical and functional interaction between integrins and hERG1 channels in cancer cells*, pp. 55–67. New York, NY: Springer New York, 2010. 54

[314] K. M. Tyner, R. Kopelman, and M. A. Philbert, ""Nanosized voltmeter" enables cellular-wide electric field mapping," *Biophys J*, vol. 93, no. 4, pp. 1163–1174, 2007. 54

[315] W. S. Schneider, P. Pagel, C. Rotsch, T. Danker, H. Oberleithner, M. Radmacher, and A. Schwab, "Volume dynamics in migrating epithelial cells measured with atomic force microscopy," *Pflügers Archiv*, vol. 439, no. 3, pp. 297–303, 2000. 54

[316] S. Watkins and H. Sontheimer, "Hydrodynamic cellular volume changes enable glioma cell invasion," *J Neurosci*, vol. 31, no. 47, pp. 17250–17259, 2011. 54

[317] G. S. Worthen, P. M. Henson, S. Rosengren, G. P. Downey, and D. M. Hyde, "Neutrophils increase volume during migration in vivo and in vitro," *Am J Respir Cell Mol Biol*, vol. 10, no. 1, pp. 1–7, 1994. 54

[318] T. Ito, A. Suzuki, and T. P. Stossel, "Regulation of water flow by actin-binding protein-induced actin gelatin," *Biophys J*, vol. 61, no. 5, pp. 1301–1305, 1992. 54

[319] T. Ito and M. Yamazaki, "The "Le Chatelier's principle"-governed response of actin filaments to osmotic stress," *J Phys Chem B*, vol. 110, no. 27, pp. 13572–13581, 2006. 54

[320] T. J. Mitchison, G. T. Charras, and L. Mahadevan, "Implications of a poroelastic cytoplasm for the dynamics of animal cell shape," *Semin Cell Dev Biol*, vol. 19, no. 3, pp. 215–223, 2008. 54

[321] V. M. Laurent, S. Kasas, A. Yersin, T. E. Schaffer, S. Catsicas, G. Dietler, A. B. Verkhovsky, and J.-J. Meister, "Gradient of rigidity in the lamellipodia of migrating cells revealed by atomic force microscopy," *Biophys J*, vol. 89, no. 1, pp. 667–675, 2005. 54

[322] B. R. Haas and H. Sontheimer, "Inhibition of the sodium-potassium-chloride cotransporter isoform-1 reduces glioma invasion," *Cancer Res*, vol. 70, no. 13, pp. 5597–5606, 2010. 54

[323] C. B. Ransom, J. T. O'Neal, and H. Sontheimer, "Volume-activated chloride currents contribute to the resting conductance and invasive migration of human glioma cells," *J Neurosci*, vol. 21, no. 19, pp. 7674–7683, 2001. 54

[324] R. C. Huebert, M. M. Vasdev, U. Shergill, A. Das, B. Q. Huang, M. R. Charlton, N. F. LaRusso, and V. H. Shah, "Aquaporin-1 facilitates angiogenic invasion in the pathological neovasculature that accompanies cirrhosis," *Hepatology*, vol. 52, no. 1, pp. 238–248, 2010. 55

[325] K. Yoshida and T. Soldati, "Dissection of amoeboid movement into two mechanically distinct modes," *J Cell Sci*, vol. 119, no. 18, pp. 3833–3844, 2006. 55

[326] E. K. Hoffmann, I. H. Lambert, and S. F. Pedersen, "Physiology of cell volume regulation in vertebrates," *Physiol Rev*, vol. 89, no. 1, pp. 193–277, 2009. 55, 147

[327] G. Cruse, S. M. Duffy, C. E. Brightling, and P. Bradding, "Functional KCa3.1 K+ channels are required for human lung mast cell migration," *Thorax*, vol. 61, no. 10, pp. 880–885, 2006. 55

[328] M. P. Matheu, C. Beeton, A. Garcia, V. Chi, S. Rangaraju, O. Safrina, K. Monaghan, M. I. Uemura, D. Li, S. Pal, L. M. de la Maza, E. Monuki, A. Flugel, M. W. Pennington, I. Parker, K. G. Chandy, and M. D. Cahalan, "Imaging of effector memory T cells during a delayed-type hypersensitivity reaction and suppression by Kv1.3 channel block," *Immunity*, vol. 29, no. 4, pp. 602–614, 2008. 55

[329] N. K. Jorgensen, S. F. Pedersen, H. B. Rasmussen, M. Grunnet, D. A. Klaerke, and S.-P. Olesen, "Cell swelling activates cloned Ca(2+)-activated K(+) channels: a role for the F-actin cytoskeleton," *Biochim Biophys Acta*, vol. 1615, no. 1-2, pp. 115–125, 2003. 55

[330] S. B. Rizoli, O. D. Rotstein, J. Parodo, M. J. Phillips, and A. Kapus, "Hypertonic inhibition of exocytosis in neutrophils: central role for osmotic actin skeleton remodeling," *Am J Physiol*, vol. 279, no. 3, pp. 619–633, 2000. 55

[331] A. Schwab, B. Schuricht, P. Seeger, J. Reinhardt, and P. C. Dartsch, "Migration of transformed renal epithelial cells is regulated by K+ channel modu-

lation of actin cytoskeleton and cell volume," *Pflügers Archiv*, vol. 438, no. 3, pp. 330–337, 1999. 55

[332] C. Di Ciano, Z. Nie, K. Szászi, A. Lewis, T. Uruno, X. Zhan, O. D. Rotstein, A. Mak, and A. Kapus, "Osmotic stress-induced remodeling of the cortical cytoskeleton," *Am J Physiol*, vol. 283, no. 3, pp. 850–865, 2002. 56

[333] M. Rasmussen, R. T. Alexander, B. V. Darborg, N. Møbjerg, E. K. Hoffmann, A. Kapus, and S. F. Pedersen, "Osmotic cell shrinkage activates ezrin/radixin/moesin (ERM) proteins: activation mechanisms and physiological implications," *Am J Physiol*, vol. 294, no. 1, pp. 197–212, 2008. 56

[334] T. K. Klausen, C. Hougaard, E. K. Hoffmann, and S. F. Pedersen, "Cholesterol modulates the volume-regulated anion current in Ehrlich-Lettre ascites cells via effects on Rho and F-actin," *Am J Physiol*, vol. 291, no. 4, pp. 757–771, 2006. 56

[335] C. Di Ciano-Oliveira, G. Sirokmány, K. Szászi, W. T. Arthur, A. Masszi, M. Peterson, O. D. Rotstein, and A. Kapus, "Hyperosmotic stress activates Rho: differential involvement in Rho kinase-dependent MLC phosphorylation and NKCC activation," *Am J Physiol*, vol. 285, no. 3, pp. 555–566, 2003. 56

[336] G. R. Felice, P. Eason, M. V. Nermut, and S. Kellie, "pp60v-src association with the cytoskeleton induces actin reorganization without affecting polymerization status," *Eur J Cell Biol*, vol. 52, no. 1, pp. 47–59, 1990. 56

[337] K. Shriver and L. Rohrschneider, "Organization of pp60src and selected cytoskeletal proteins within adhesion plaques and junctions of Rous sarcoma virus-transformed rat cells," *J Cell Biol*, vol. 89, no. 3, pp. 525–535, 1981. 56

[338] B. M. Sefton, T. Hunter, E. H. Ball, and S. J. Singer, "Vinculin: a cytoskeletal target of the transforming protein of Rous sarcoma virus," *Cell*, vol. 24, no. 1, pp. 165–174, 1981. 56

[339] Y. Yoo, H. J. Ho, C. Wang, and J.-L. Guan, "Tyrosine phosphorylation of cofilin at Y68 by v-Src leads to its degradation through ubiquitin-proteasome pathway," *Oncogene*, vol. 29, no. 2, pp. 263–272, 2010. 56

[340] T. David-Pfeuty and S. J. Singer, "Altered distributions of the cytoskeletal proteins vinculin and alpha-actinin in cultured fibroblasts transformed by Rous sarcoma virus," *Proc Natl Acad Sci USA*, vol. 77, no. 11, pp. 6687–6691, 1980. 56

[341] A. Graessmann, M. Graessmann, R. Tjian, and W. C. Topp, "Simian virus 40 small-t protein is required for loss of actin cable networks in rat cells," *J Virol*, vol. 33, no. 3, pp. 1182–1191, 1980. 56

[342] V. Nunbhakdi-Craig, L. Craig, T. Machleidt, and E. Sontag, "Simian virus 40 small tumor antigen induces deregulation of the actin cytoskeleton and tight junctions in kidney epithelial cells," *J Virol*, vol. 77, no. 5, pp. 2807–2818, 2003. 56, 63, 114, 174, 176

[343] G. Mosialos, S. Yamashiro, R. W. Baughman, P. Matsudaira, L. Vara, F. Matsumura, E. Kieff, and M. Birkenbach, "Epstein-Barr virus infection induces expression in B lymphocytes of a novel gene encoding an evolutionarily conserved 55-kilodalton actin-bundling protein," *J Virol*, vol. 68, no. 11, pp. 7320–7328, 1994. 56

[344] L. C. Spender, W. Lucchesi, G. Bodelon, A. Bilancio, C. E. Karstegl, T. Asano, O. Dittrich-Breiholz, M. Kracht, B. Vanhaesebroeck, and P. J. Farrell, "Cell target genes of Epstein-Barr virus transcription factor EBNA-2: induction of the p55alpha regulatory subunit of PI3-kinase and its role in survival of EREB2.5 cells," *J Gen Virol*, vol. 87, no. 10, pp. 2859–2867, 2006. 56

[345] E. Lara-Pezzi, J. M. Serrador, M. C. Montoya, D. Zamora, M. Yanez-Mo, M. Carretero, H. Furthmayr, F. Sanchez-Madrid, and M. Lopez-Cabrera, "The hepatitis B virus X protein (HBx) induces a migratory phenotype in a CD44-dependent manner: possible role of HBx in invasion and metastasis," *Hepatology*, vol. 33, no. 5, pp. 1270–1281, 2001. 56, 64

[346] S. T. Charette and D. J. McCance, "The E7 protein from human papillomavirus type 16 enhances keratinocyte migration in an Akt-dependent manner," *Oncogene*, vol. 26, no. 52, pp. 7386–7390, 2007. 57

[347] C. Grossmann, S. Podgrabinska, M. Skobe, and D. Ganem, "Activation of NF-kappaB by the latent vFLIP gene of Kaposi's sarcoma-associated herpesvirus is required for the spindle shape of virus-infected endothelial

cells and contributes to their proinflammatory phenotype," *J Virol*, vol. 80, no. 14, pp. 7179–7185, 2006. 57

[348] M. P. Taylor, O. O. Koyuncu, and L. W. Enquist, "Subversion of the actin cytoskeleton during viral infection," *Nat Rev Microbiol*, vol. 9, no. 6, pp. 427–439, 2011. 58

[349] T. Lämmermann and M. Sixt, "Mechanical modes of "amoeboid" cell migration," *Curr Opin Cell Biol*, vol. 21, no. 5, pp. 636–644, 2009. 59

[350] P. Friedl and K. Wolf, "Plasticity of cell migration: a multiscale tuning model," *J Cell Biol*, vol. 188, no. 1, pp. 11–19, 2010. 59

[351] O. Ilina and P. Friedl, "Mechanisms of collective cell migration at a glance," *J Cell Sci*, vol. 122, no. 18, pp. 3203–3208, 2009. 59

[352] K. Nabeshima, T. Inoue, Y. Shimao, and T. Sameshima, "Matrix metalloproteinases in tumor invasion: role for cell migration," *Pathol Int*, vol. 52, no. 4, pp. 255–264, 2002. 59

[353] S. Etienne-Manneville, "Polarity proteins in migration and invasion," *Oncogene*, vol. 27, no. 55, pp. 6970–6980, 2008. 59

[354] D. I. Johnson, "Cdc42: an essential Rho-type GTPase controlling eukaryotic cell polarity," *Microbiol Mol Biol Rev*, vol. 63, no. 1, pp. 54–105, 1999. 59

[355] P. T. Caswell and J. C. Norman, "Integrin trafficking and the control of cell migration," *Traffic*, vol. 7, no. 1, pp. 14–21, 2006. 61

[356] D. J. Webb, J. T. Parsons, and A. F. Horwitz, "Adhesion assembly, disassembly and turnover in migrating cells – over and over and over again," *Nat Cell Biol*, vol. 4, no. 4, pp. 97–100, 2002. 61

[357] Y.-L. Hu, S. Lu, K. W. Szeto, J. Sun, Y. Wang, J. C. Lasheras, and S. Chien, "FAK and paxillin dynamics at focal adhesions in the protrusions of migrating cells," *Sci Rep*, vol. 4, p. 6024, 2014. 61

[358] D. A. Calderwood and M. H. Ginsberg, "Talin forges the links between integrins and actin," *Nat Cell Biol*, vol. 5, no. 8, pp. 694–697, 2003. 61

[359] J. D. Humphries, P. Wang, C. Streuli, B. Geiger, M. J. Humphries, and C. Ballestrem, "Vinculin controls focal adhesion formation by direct interactions with talin and actin," *J Cell Biol*, vol. 179, no. 5, pp. 1043–1057, 2007. 61

[360] D. F. Kelly and K. A. Taylor, "Identification of the beta1-integrin binding site on alpha-actinin by cryoelectron microscopy," *J Struct Biol*, vol. 149, no. 3, pp. 290–302, 2005. 61

[361] M. Pfaff, X. Du, and M. H. Ginsberg, "Calpain cleavage of integrin beta cytoplasmic domains 1," *FEBS Letters*, vol. 460, no. 1, pp. 17–22, 1999. 61

[362] P. Mehlen and A. Puisieux, "Metastasis: a question of life or death," *Nat Rev Cancer*, vol. 6, no. 6, pp. 449–458, 2006. 61

[363] U. Cavallaro and G. Christofori, "Cell adhesion and signalling by cadherins and Ig-CAMs in cancer," *Nat Rev Cancer*, vol. 4, no. 2, pp. 118–132, 2004. 62

[364] I. R. Beavon, "The E-cadherin-catenin complex in tumour metastasis: structure, function and regulation," *Eur J Cancer*, vol. 36, no. 13, pp. 1607–1620, 2000. 62, 63

[365] A. Le Bivic, Y. Sambuy, K. Mostov, and E. Rodriguez-Boulan, "Vectorial targeting of an endogenous apical membrane sialoglycoprotein and uvomorulin in MDCK cells," *J Cell Biol*, vol. 110, no. 5, pp. 1533–1539, 1990. 62

[366] J. E. Lewis, P. J. Jensen, K. R. Johnson, and M. J. Wheelock, "E-cadherin mediates adherens junction organization through protein kinase C," *J Cell Sci*, vol. 107, pp. 3615–3621, 1994. 62

[367] R. Kalluri and R. A. Weinberg, "The basics of epithelial-mesenchymal transition," *J Clin Invest*, vol. 119, no. 6, pp. 1420–1428, 2009. 63

[368] M. Yilmaz and G. Christofori, "Mechanisms of motility in metastasizing cells," *Mol Cancer Res*, vol. 8, no. 5, pp. 629–642, 2010. 63

[369] A. L. Talis, J. M. Huibregtse, and P. M. Howley, "The role of E6AP in the regulation of p53 protein levels in human papillomavirus (HPV)-positive and HPV-negative cells," *J Biol Chem*, vol. 273, no. 11, pp. 6439–6445, 1998. 63

[370] R. A. Watson, M. Thomas, L. Banks, and S. Roberts, "Activity of the human papillomavirus E6 PDZ-binding motif correlates with an enhanced morphological transformation of immortalized human keratinocytes," *J Cell Sci*, vol. 116, no. 24, pp. 4925–4934, 2003. 63

[371] J.-O. Lee, H. J. Kwun, J. K. Jung, K. H. Choi, D. S. Min, and K. L. Jang, "Hepatitis B virus X protein represses E-cadherin expression via activation of DNA methyltransferase 1," *Oncogene*, vol. 24, no. 44, pp. 6617–6625, 2005. 63

[372] A. C. Han, A. P. Soler, C. K. Tang, K. A. Knudsen, and H. Salazar, "Nuclear localization of E-cadherin expression in Merkel cell carcinoma," *Arch Pathol Lab Med*, vol. 124, no. 8, pp. 1147–1151, 2000. 63

[373] J. P. Thiery, "Epithelial-mesenchymal transitions in tumour progression," *Nat Rev Cancer*, vol. 2, no. 6, pp. 442–454, 2002. 63

[374] E. Sahai, "Mechanisms of cancer cell invasion," *Curr Opin Genes Dev*, vol. 15, no. 1, pp. 87–96, 2005. 63, 64, 65

[375] G. P. Gupta and J. Massague, "Cancer metastasis: building a framework," *Cell*, vol. 127, no. 4, pp. 679–695, 2006. 64

[376] R. P. Verma and C. Hansch, "Matrix metalloproteinases (MMPs): chemical–biological functions and (Q)SARs," *Bioorg Med Chem*, vol. 15, no. 6, pp. 2223–2268, 2007. 64

[377] D. Zhu, M. Ye, and W. Zhang, "E6/E7 oncoproteins of high risk HPV-16 upregulate MT1-MMP, MMP-2 and MMP-9 and promote the migration of cervical cancer cells," *Int J Clin Exp Pathol*, vol. 8, no. 5, pp. 4981–4989, 2015. 64

[378] N. E. Sounni, L. Devy, A. Hajitou, F. Frankenne, M. C., C. Gilles, C. Deroanne, E. W. Thompson, J. M. Foidart, and A. Noel, "MT1-MMP expression promotes tumor growth and angiogenesis through an up-regulation of vascular endothelial growth factor expression," *FASEB J*, vol. 16, no. 6, pp. 555–564, 2002. 64

[379] S. Kondo, S. Y. Seo, T. Yoshizaki, N. Wakisaka, M. Furukawa, I. Joab, K. L. Jang, and J. S. Pagano, "EBV latent membrane protein 1 up-regulates

hypoxia-inducible factor 1alpha through Siah1-mediated down-regulation of prolyl hydroxylases 1 and 3 in nasopharyngeal epithelial cells," *Cancer Res*, vol. 66, no. 20, pp. 9870–9877, 2006. 64

[380] G. R. Mundy, "Metastasis to bone: causes, consequences and therapeutic opportunities," *Nat Rev Cancer*, vol. 2, no. 8, pp. 584–593, 2002. 65

[381] J. R. Boyne and A. Whitehouse, "Nucleolar trafficking is essential for nuclear export of intronless herpesvirus mRNA," *Proc Natl Acad Sci USA*, vol. 103, no. 41, pp. 15190–15195, 2006. 90

[382] M. Heath, N. Jaimes, B. Lemos, A. Mostaghimi, L. Wang, P. Penas, and P. Nghiem, "Clinical characteristics of Merkel cell carcinoma at diagnosis in 195 patients: the AEIOU features," *J Am Acad Dermatol*, vol. 58, no. 3, pp. 375–381, 2008. 92

[383] A. F. Chambers, A. C. Groom, and I. C. MacDonald, "Metastasis: dissemination and growth of cancer cells in metastatic sites," *Nat Rev Cancer*, vol. 2, no. 8, pp. 563–572, 2002. 92

[384] W. Wang, J. B. Wyckoff, V. C. Frohlich, Y. Oleynikov, S. Huttelmaier, J. Zavadil, L. Cermak, E. P. Bottinger, R. H. Singer, J. G. White, J. E. Segall, and J. S. Condeelis, "Single cell behavior in metastatic primary mammary tumors correlated with gene expression patterns revealed by molecular profiling," *Cancer Res*, vol. 62, no. 21, pp. 6278–6288, 2002. 92

[385] B. L. Rothschild, A. H. Shim, A. G. Ammer, L. C. Kelley, K. B. Irby, J. A. Head, L. Chen, M. Varella-Garcia, P. G. Sacks, B. Frederick, D. Raben, and S. A. Weed, "Cortactin overexpression regulates actin-related protein 2/3 complex activity, motility, and invasion in carcinomas with chromosome 11q13 amplification," *Cancer Res*, vol. 66, no. 16, pp. 8017–8025, 2006. 92

[386] H. S. Fernando, A. J. Sanders, H. G. Kynaston, and W. G. Jiang, "WAVE1 is associated with invasiveness and growth of prostate cancer cells," *J Urol*, vol. 180, no. 4, pp. 1515–1521, 2008. 92

[387] F. Xue, D. M. Janzen, and D. A. Knecht, "Contribution of filopodia to cell migration: a mechanical link between protrusion and contraction," *Int J Cell Biol*, vol. 2010, p. 507821, 2010. 92

[388] A. Hall, "Rho GTPases and the actin cytoskeleton," *Science*, vol. 279, no. 5350, pp. 509–514, 1998. 92, 107

[389] S. Krugmann, I. Jordens, K. Gevaert, M. Driessens, J. Vandekerckhove, and A. Hall, "Cdc42 induces filopodia by promoting the formation of an IRSp53:Mena complex," *Curr Biol*, vol. 11, no. 21, pp. 1645–1655, 2001. 92

[390] A. J. Ridley, H. F. Paterson, C. L. Johnston, D. Diekmann, and A. Hall, "The small GTP-binding protein rac regulates growth factor-induced membrane ruffling," *Cell*, vol. 70, no. 3, pp. 401–410, 1992. 92

[391] H. Zamudio-Meza, A. Castillo-Alvarez, C. Gonzalez-Bonilla, and I. Meza, "Cross-talk between Rac1 and Cdc42 GTPases regulates formation of filopodia required for dengue virus type-2 entry into HMEC-1 cells," *J Gen Virol*, vol. 90, no. 12, pp. 2902–2911, 2009. 92

[392] L. E. Arias-Romero and J. Chernoff, "Targeting Cdc42 in cancer," *Expert Opin Ther Targets*, vol. 17, no. 11, pp. 1263–1273, 2013. 93

[393] M. J. Davis, B. H. Ha, E. C. Holman, R. Halaban, J. Schlessinger, and T. J. Boggon, "RAC1P29S is a spontaneously activating cancer-associated GTPase," *Proc Natl Acad Sci USA*, vol. 110, no. 3, pp. 912–917, 2013. 93

[394] A. J. Ridley, "RhoA, RhoB and RhoC have different roles in cancer cell migration," *J Microsc*, vol. 251, no. 3, pp. 242–249, 2013. 93

[395] G. Fritz, I. Just, and B. Kaina, "Rho GTPases are over-expressed in human tumors," *Int J Cancer*, vol. 81, no. 5, pp. 682–687, 1999. 93

[396] G. Fritz, C. Brachetti, F. Bahlmann, M. Schmidt, and B. Kaina, "Rho GTPases in human breast tumours: expression and mutation analyses and correlation with clinical parameters," *Br J Cancer*, vol. 87, no. 6, pp. 635–644, 2002. 93

[397] Y. Pan, F. Bi, N. Liu, Y. Xue, X. Yao, Y. Zheng, and D. Fan, "Expression of seven main Rho family members in gastric carcinoma," *Biochem Biophys Res Commun*, vol. 315, no. 3, pp. 686–691, 2004. 93

[398] B. Belletti and G. Baldassarre, "Stathmin: a protein with many tasks. New biomarker and potential target in cancer," *Expert Opin Ther Targets*, vol. 15, no. 11, pp. 1249–1266, 2011. 93

[399] P. Lappalainen and D. G. Drubin, "Cofilin promotes rapid actin filament turnover in vivo," *Nature*, vol. 388, no. 6637, pp. 78–82, 1997. 94

[400] I. Rouiller, X.-P. Xu, K. J. Amann, C. Egile, S. Nickell, D. Nicastro, R. Li, T. D. Pollard, N. Volkmann, and D. Hanein, "The structural basis of actin filament branching by the Arp2/3 complex," *J Cell Biol*, vol. 180, no. 5, pp. 887–895, 2008. 94

[401] C. Yang, L. Czech, S. Gerboth, S.-i. Kojima, G. Scita, and T. Svitkina, "Novel roles of formin mDia2 in lamellipodia and filopodia formation in motile cells," *PLoS Biol*, vol. 5, no. 11, p. e317, 2007. 100

[402] A. B. Bohil, B. W. Robertson, and R. E. Cheney, "Myosin-X is a molecular motor that functions in filopodia formation," *Proc Natl Acad Sci USA*, vol. 103, no. 33, pp. 12411–12416, 2006. 100

[403] J. Varani, S. E. G. Fligeil, and P. Perone, "Directional motility in strongly malignant murine tumor cells," *Int J Cancer*, vol. 35, no. 4, pp. 559–564, 1985. 104, 114, 175

[404] I. Nemere, A. Kupfer, and S. J. Singer, "Reorientation of the Golgi apparatus and the microtubule-organizing center inside macrophages subjected to a chemotactic gradient," *Cell Motility*, vol. 5, no. 1, pp. 17–29, 1985. 105

[405] N. Reymond, J. H. Im, R. Garg, F. M. Vega, B. Borda d'Agua, P. Riou, S. Cox, F. Valderrama, R. J. Muschel, and A. J. Ridley, "Cdc42 promotes transendothelial migration of cancer cells through beta1 integrin," *J Cell Biol*, vol. 199, pp. 653–668, Nov 2012. 107

[406] H. K. Bid, R. D. Roberts, P. K. Manchanda, and P. J. Houghton, "RAC1: an emerging therapeutic option for targeting cancer angiogenesis and metastasis," *Mol Cancer Ther*, vol. 12, no. 10, pp. 1925–1934, 2013. 107

[407] M. Kakiuchi, T. Nishizawa, H. Ueda, K. Gotoh, A. Tanaka, A. Hayashi, S. Yamamoto, K. Tatsuno, H. Katoh, Y. Watanabe, T. Ichimura, T. Ushiku, S. Funahashi, K. Tateishi, I. Wada, N. Shimizu, S. Nomura, K. Koike, Y. Seto, M. Fukayama, H. Aburatani, and S. Ishikawa, "Recurrent gain-of-function mutations of RHOA in diffuse-type gastric carcinoma," *Nat Genet*, vol. 46, no. 6, pp. 583–587, 2014. 107

[408] Z. Surviladze, A. Waller, J. J. Strouse, C. Bologa, O. Ursu, V. Salas, J. F. Parkinson, G. K. Phillips, E. Romero, A. Wandinger-Ness, L. A. Sklar, C. Schroeder, D. Simpson, J. Noth, J. Wang, J. Golden, and J. Aube, "A potent and selective inhibitor of Cdc42 GTPase," *Probe Reports from the NIH Molecular Libraries Program*, 2010. 107

[409] A. Friesland, Y. Zhao, Y.-H. Chen, L. Wang, H. Zhou, and Q. Lu, "Small molecule targeting Cdc42-intersectin interaction disrupts Golgi organization and suppresses cell motility," *Proc Natl Acad Sci USA*, vol. 110, no. 4, pp. 1261–1266, 2013. 107

[410] Y. Gao, J. B. Dickerson, F. Guo, J. Zheng, and Y. Zheng, "Rational design and characterization of a Rac GTPase-specific small molecule inhibitor," *Proc Nat Acad Sci USA*, vol. 101, no. 20, pp. 7618–7623, 2004. 107

[411] X. Shang, F. Marchioni, N. Sipes, C. R. Evelyn, M. Jerabek-Willemsen, S. Duhr, W. Seibel, M. Wortman, and Y. Zheng, "Rational design of small molecule inhibitors targeting RhoA subfamily Rho GTPases," *Chem Biol*, vol. 19, no. 6, pp. 699–710, 2012. 107

[412] A. Schmidt and A. Hall, "Guanine nucleotide exchange factors for Rho GTPases: turning on the switch," *Genes Dev*, vol. 16, no. 13, pp. 1587–1609, 2002. 115

[413] J. Cherfils and M. Zeghouf, "Regulation of small GTPases by GEFs, GAPs, and GDIs," *Physiol Rev*, vol. 93, no. 1, pp. 269–309, 2013. 115

[414] S. K. Mitra, D. A. Hanson, and D. D. Schlaepfer, "Focal adhesion kinase: in command and control of cell motility," *Nat Rev Mol Cell Biol*, vol. 6, no. 1, pp. 56–68, 2005. 117

[415] S. Basu, "PP2A in the regulation of cell motility and invasion," *Curr Protein Pept Sci*, vol. 12, no. 1, pp. 3–11, 2011. 117

[416] H. J. Kwun, M. Shuda, C. J. Camacho, A. M. Gamper, M. Thant, Y. Chang, and P. S. Moore, "Restricted protein phosphatase 2A targeting by Merkel cell polyomavirus small T antigen," *J Virol*, vol. 89, no. 8, pp. 4191–4200, 2015. 117

[417] U. S. Cho, S. Morrone, A. A. Sablina, J. D. Arroyo, W. C. Hahn, and W. Xu, "Structural basis of PP2A inhibition by small t antigen," *PLoS Biol*, vol. 5, no. 8, p. e202, 2007. 117

[418] J. S. Bennett, B. W. Berger, and P. C. Billings, "The structure and function of platelet integrins," *J Thromb Haemost*, vol. 7, pp. 200–205, 2009. 117

[419] R. O. Hynes, "Integrins: versatility, modulation, and signaling in cell adhesion," *Cell*, vol. 69, no. 1, pp. 11–25, 1992. 117

[420] R. O. Hynes, "Integrins: bidirectional, allosteric signaling machines," *Cell*, vol. 110, no. 6, pp. 673–687, 2002. 117

[421] S. P. Holly, M. K. Larson, and L. V. Parise, "Multiple roles of integrins in cell motility," *Exp Cell Res*, vol. 261, pp. 69–74, Nov 2000. 117, 133

[422] J. S. Desgrosellier and D. A. Cheresh, "Integrins in cancer: biological implications and therapeutic opportunities," *Nat Rev Cancer*, vol. 10, no. 1, pp. 9–22, 2010. 117, 133

[423] M. H. Ginsberg, A. Partridge, and S. J. Shattil, "Integrin regulation," *Curr Opin Cell Biol*, vol. 17, no. 5, pp. 509–516, 2005. 117

[424] E. G. Arias-Salgado, S. Lizano, S. Sarkar, J. S. Brugge, M. H. Ginsberg, and S. J. Shattil, "Src kinase activation by direct interaction with the integrin beta cytoplasmic domain," *Proc Nat Acad Sci USA*, vol. 100, no. 23, pp. 13298–13302, 2003. 118

[425] K. V. Vijayan, Y. Liu, T.-T. Li, and P. F. Bray, "Protein phosphatase 1 associates with the integrin alphaIIb subunit and regulates signaling," *J Biol Chem*, vol. 279, no. 32, pp. 33039–33042, 2004. 118

[426] S. C. Fagerholm, T. J. Hilden, and C. G. Gahmberg, "P marks the spot: site-specific integrin phosphorylation regulates molecular interactions," *Trends Biochem Sci*, vol. 29, no. 9, pp. 504–512, 2004. 118, 133, 141

[427] J. P. Mulrooney, T. Hong, and L. B. Grabel, "Serine 785 phosphorylation of the beta1 cytoplasmic domain modulates beta1A-integrin-dependent functions," *J Cell Sci*, vol. 114, no. Pt 13, pp. 2525–2533, 2001. 118, 144, 177

[428] S.-M. Kim, M. S. Kwon, C. S. Park, K.-R. Choi, J.-S. Chun, J. Ahn, and W. K. Song, "Modulation of Thr phosphorylation of integrin beta1 during muscle differentiation," *J Biol Chem*, vol. 279, no. 8, pp. 7082–7090, 2004. 118, 141, 144, 177

[429] M.-A. Forget, R. R. Desroisiers, D. Gingras, and R. Beliveau, "Phosphorylation states of Cdc42 and RhoA regulate their interactions with Rho GDP dissociation inhibitor and their extraction from biological membranes," *Biochem J*, vol. 361, no. 2, pp. 243–254, 2002. 129

[430] J. Schwarz, J. Proff, A. HâĂřvemeier, M. Ladwein, K. Rottner, B. Barlag, A. Pich, H. Tatge, I. Just, and R. Gerhard, "Serine-71 phosphorylation of Rac1 modulates downstream signaling," *PLoS One*, vol. 7, no. 9, p. e44358, 2012. 129, 132

[431] R. B. Basani, G. D'Andrea, N. Mitra, G. Vilaire, M. Richberg, M. A. Kowalska, J. S. Bennett, and M. Poncz, "RGD-containing peptides inhibit fibrinogen binding to platelet alphaIIbbeta3 by inducing an allosteric change in the amino-terminal portion of alphaIIb," *J Biol Chem*, vol. 276, no. 17, pp. 13975–13981, 2001. 133, 144, 177

[432] K. O. Simon, E. M. Nutt, D. G. Abraham, G. A. Rodan, and L. T. Duong, "The alphavbeta3 integrin regulates alpha5beta1-mediated cell migration toward fibronectin," *J Biol Chem*, vol. 272, no. 46, pp. 29380–29389, 1997. 141

[433] M. Mourtada-Maarabouni and G. T. Williams, "Protein phosphatase 4 regulates apoptosis, proliferation and mutation rate of human cells," *Biochim Biophys Acta*, vol. 1783, no. 8, pp. 1490–1502, 2008. 143

[434] P. T. W. Cohen, A. Philp, and C. Vazquez-Martin, "Protein phosphatase 4–from obscurity to vital functions," *FEBS Lett*, vol. 579, no. 15, pp. 3278–3286, 2005. 143

[435] B. Wang, A. Zhao, L. Sun, X. Zhong, J. Zhong, H. Wang, M. Cai, J. Li, Y. Xu, J. Liao, J. Sang, D. Chowdhury, G. P. Pfeifer, Y. Yen, and X. Xu, "Protein phosphatase PP4 is overexpressed in human breast and lung tumors," *Cell Res*, vol. 18, no. 9, pp. 974–977, 2008. 143

[436] S. Huveneers and E. H. J. Danen, "Adhesion signaling - crosstalk between integrins, Src and Rho," *J Cell Sci*, vol. 122, no. 8, pp. 1059–1069, 2009. 144

[437] D. M. Haverstick, J. F. Cowan, K. M. Yamada, and S. A. Santoro, "Inhibition of platelet adhesion to fibronectin, fibrinogen, and von Willebrand factor substrates by a synthetic tetrapeptide derived from the cell-binding domain of fibronectin," *Blood*, vol. 66, no. 4, pp. 946–952, 1985. 144

[438] M. D. Pierschbacher and E. Ruoslahti, "Cell attachment activity of fibronectin can be duplicated by small synthetic fragments of the molecule," *Nature*, vol. 309, no. 5963, pp. 30–33, 1984. 144

[439] H. Jiang and S. X. Sun, "Cellular pressure and volume regulation and implications for cell mechanics," *Biophys J*, vol. 105, no. 3, pp. 609–619, 2013. 147

[440] A. S. Verkman and L. J. V. Galietta, "Chloride channels as drug targets," *Nat Rev Drug Discov*, vol. 8, no. 2, pp. 153–171, 2009. 147, 179

[441] J. Terry, "The major electrolytes: sodium, potassium, and chloride," *J Intraven Nurs*, vol. 17, no. 5, pp. 240–247, 1994. 147

[442] T. J. Jentsch, V. Stein, F. Weinreich, and A. A. Zdebik, "Molecular structure and physiological function of chloride channels," *Physiol Rev*, vol. 82, no. 2, pp. 503–568, 2002. 147

[443] M. Suzuki, T. Morita, and T. Iwamoto, "Diversity of Cl- channels," *Cell Mol Life Sci*, vol. 63, no. 1, pp. 12–24, 2005. 147

[444] H. Singh, "Two decades with dimorphic Chloride Intracellular Channels (CLICs)," *FEBS Letters*, vol. 584, no. 10, pp. 2112–2121, 2010. 147

[445] J. J. Tung and J. Kitajewski, "Chloride intracellular channel 1 functions in endothelial cell growth and migration," *J Angiogen Res*, vol. 2, pp. 23–23, 2010. 147, 162, 171, 179

[446] J. J. Tung, O. Hobert, M. Berryman, and J. Kitajewski, "Chloride intracellular channel 4 is involved in endothelial proliferation and morphogenesis in vitro," *Angiogenesis*, vol. 12, no. 3, pp. 209–220, 2009. 147

[447] D. Chalothorn, H. Zhang, J. E. Smith, J. C. Edwards, and J. E. Faber, "Chloride intracellular channel-4 Is a determinant of native collateral formation in skeletal muscle and brain," *Circ Res*, vol. 105, no. 1, pp. 89–98, 2009. 147

[448] E. Fernández-Salas, K. S. Suh, V. V. Speransky, W. L. Bowers, J. M. Levy, T. Adams, K. R. Pathak, L. E. Edwards, D. D. Hayes, C. Cheng, A. C. Steven, W. C. Weinberg, and S. H. Yuspa, "mtCLIC/CLIC4, an organellular chloride channel protein, is increased by DNA damage and participates in the apoptotic response to p53," *Mol Cell Biol*, vol. 22, no. 11, pp. 3610–3620, 2002. 147

[449] K. S. Suh and S. H. Yuspa, "Intracellular chloride channels: critical mediators of cell viability and potential targets for cancer therapy," *Curr Pharm Des*, vol. 11, no. 21, pp. 2753–2764, 2005. 148

[450] P. Wang, C. Zhang, P. Yu, B. Tang, T. Liu, H. Cui, and J. Xu, "Regulation of colon cancer cell migration and invasion by CLIC1-mediated RVD," *Mol Cell Biochem*, vol. 365, no. 1-2, pp. 313–321, 2012. 148, 162, 171, 179

[451] Y. Tian, Y. Guan, Y. Jia, Q. Meng, and J. Yang, "Chloride intracellular channel 1 regulates prostate cancer cell proliferation and migration through the MAPK/ERK pathway," *Cancer Biother Radiopharm*, vol. 29, no. 8, pp. 339–344, 2014. 148, 171, 179

[452] F. Jessen, C. Sjøholm, and E. K. Hoffmann, "Identification of the anion exchange protein of Ehrlich cells: A kinetic analysis of the inhibitory effects of 4,4âĂš-diisothiocyano-2,2âĂš-stilbene-disulfonic acid (DIDS) and labeling of membrane proteins with 3H-DIDS," *J Membr Biol*, vol. 92, no. 3, pp. 195–205, 1986. 150

[453] D. J. Keeling, A. G. Taylor, and P. L. Smith, "Effects of NPPB (5-nitro-2-(3-phenylpropylamino)benzoic acid) on chloride transport in intestinal tissues and the T84 cell line," *Biochim Biophys Acta*, vol. 1115, no. 1, pp. 42–48, 1991. 150

[454] D. W. Landry, M. Reitman, E. J. J. Cragoe, and Q. Al-Awqati, "Epithelial chloride channel. Development of inhibitory ligands," *J Gen Physiol*, vol. 90, no. 6, pp. 779–798, 1987. 150

[455] T. J. Jentsch, V. Stein, F. Weinreich, and A. A. Zdebik, "Molecular structure and physiological function of chloride channels," *Physiol Rev*, vol. 82, no. 2, pp. 503–568, 2002. 162

[456] L. M. Knowles, G. Malik, B. L. Hood, T. P. Conrads, and J. Pilch, "CLT1 targets angiogenic endothelium through CLIC1 and fibronectin," *Angiogenesis*, vol. 15, no. 1, pp. 115–129, 2012. 168

[457] L. A. Gurski, L. M. Knowles, P. H. Basse, J. K. Maranchie, S. C. Watkins, and J. Pilch, "Relocation of CLIC1 promotes tumor cell invasion and colonization of fibrin," *Mol Cancer Res*, vol. 13, no. 2, pp. 273–280, 2015. 168, 178

[458] M. Peretti, M. Angelini, N. Savalli, T. Florio, S. H. Yuspa, and M. Mazzanti, "Chloride channels in cancer: Focus on chloride intracellular channel 1 and 4 (CLIC1 AND CLIC4) proteins in tumor development and as novel therapeutic targets," *Biochim Biophys Acta*, vol. 1848, no. 10, pp. 2523–2531, 2015. 171

[459] A. Shukla, R. Edwards, Y. Yang, A. Hahn, K. Folkers, J. Ding, V. C. Padmakumar, C. Cataisson, K. S. Suh, and S. H. Yuspa, "CLIC4 regulates TGF-beta-dependent myofibroblast differentiation to produce a cancer stroma," *Oncogene*, vol. 33, no. 7, pp. 842–850, 2014. 171, 179

[460] J. Lu, Q. Dong, B. Zhang, X. Wang, B. Ye, F. Zhang, X. Song, G. Gao, J. Mu, Z. Wang, F. Ma, and J. Gu, "Chloride intracellular channel 1 (CLIC1) is activated and functions as an oncogene in pancreatic cancer," *Med Oncol*, vol. 32, no. 6, p. 616, 2015. 171, 179

[461] Q. Yao, X. Qu, Q. Yang, M. Wei, and B. Kong, "CLIC4 mediates TGF-beta1-induced fibroblast-to-myofibroblast transdifferentiation in ovarian cancer," *Oncol Rep*, vol. 22, no. 3, pp. 541–548, 2009. 171, 179

[462] M. Setti, N. Savalli, D. Osti, C. Richichi, M. Angelini, P. Brescia, L. Fornasari, M. S. Carro, M. Mazzanti, and G. Pelicci, "Functional role of CLIC1 ion channel in glioblastoma-derived stem/progenitor cells," *J Natl Cancer Inst*, vol. 105, no. 21, pp. 1644–1655, 2013. 171, 178

[463] H. Singh, M. A. Cousin, and R. H. Ashley, "Functional reconstitution of mammalian "chloride intracellular channels" CLIC1, CLIC4 and CLIC5 re-

veals differential regulation by cytoskeletal actin," *FEBS Journal*, vol. 274, no. 24, pp. 6306–6316, 2007. 172, 179

[464] A. Yasmeen, T. A. Bismar, M. Kandouz, W. D. Foulkes, P.-Y. Desprez, and A.-E. Al Moustafa, "E6/E7 of HPV type 16 promotes cell invasion and metastasis of human breast cancer cells," *Cell Cycle*, vol. 6, no. 16, pp. 2038–2042, 2007. 174

[465] R. Kaul, M. Murakami, T. Choudhuri, and E. S. Robertson, "Epstein-Barr virus latent nuclear antigens can induce metastasis in a nude mouse model," *J Virol*, vol. 81, no. 19, pp. 10352–10361, 2007. 174

[466] D. C. Munday, R. Surtees, E. Emmott, B. K. Dove, P. Digard, J. N. Barr, A. Whitehouse, D. Matthews, and J. A. Hiscox, "Using SILAC and quantitative proteomics to investigate the interactions between viral and host proteomes," *Proteomics*, vol. 12, no. 4-5, pp. 666–672, 2012. 175

[467] S. Etienne-Manneville and A. Hall, "Rho GTPases in cell biology," *Nature*, vol. 420, pp. 629–635, 12 2002. 176

[468] Y. Zheng, D. J. Fischer, M. F. Santos, G. Tigyi, N. G. Pasteris, J. L. Gorski, and Y. Xu, "The faciogenital dysplasia gene product FGD1 functions as a Cdc42Hs-specific guanine-nucleotide exchange factor," *J Biol Chem*, vol. 271, no. 52, pp. 33169–33172, 1996. 176

[469] M. J. Hart, S. Sharma, N. elMasry, R.-G. Qiu, P. McCabe, P. Polakis, and G. Bollag, "Identification of a novel guanine nucleotide exchange factor for the Rho GTPase," *J Biol Chem*, vol. 271, no. 41, pp. 25452–25458, 1996. 176

[470] M. F. Olson, N. G. Pasteris, J. L. Gorski, and A. Hall, "Faciogenital dysplasia protein (FGD1) and Vav, two related proteins required for normal embryonic development, are upstream regulators of Rho GTPases," *Curr Biol*, vol. 6, no. 12, pp. 1628–1633, 1996. 176

[471] A. Eva and S. A. Aaronson, "Isolation of a new human oncogene from a diffuse B-cell lymphoma," *Nature*, vol. 316, no. 6025, pp. 273–275, 1985. 176

[472] A. P. Fields and V. Justilien, "The guanine nucleotide exchange factor (GEF) Ect2 is an oncogene in human cancer," *Adv Enzyme Regul*, vol. 50, no. 1, pp. 190–200, 2010. 176

[473] Y. Horii, J. F. Beeler, K. Sakaguchi, M. Tachibana, and T. Miki, "A novel oncogene, ost, encodes a guanine nucleotide exchange factor that potentially links Rho and Rac signaling pathways," *EMBO J*, vol. 13, no. 20, pp. 4776–4786, 1994. 176

[474] S. Katzav, "Vav1: A Dr. Jekyll and Mr. Hyde protein – good for the hematopoietic system, bad for cancer," *Oncotarget*, vol. 6, no. 30, pp. 28731–28742, 2015. 176

[475] C. Martin-Granados, A. Philp, S. K. Oxenham, A. R. Prescott, and P. T. W. Cohen, "Depletion of protein phosphatase 4 in human cells reveals essential roles in centrosome maturation, cell migration and the regulation of Rho GTPases," *Int J Biochem Cell Biol*, vol. 40, no. 10, pp. 2315–2332, 2008. 176

[476] C. Tiede, A. A. S. Tang, S. E. Deacon, U. Mandal, J. E. Nettleship, R. L. Owen, S. E. George, D. J. Harrison, R. J. Owens, D. C. Tomlinson, and M. J. McPherson, "Adhiron: a stable and versatile peptide display scaffold for molecular recognition applications," *Protein Eng Des Sel*, vol. 27, no. 5, pp. 145–155, 2014. 178

[477] S. M. Valenzuela, M. Mazzanti, R. Tonini, M. R. Qiu, K. Warton, E. A. Musgrove, T. J. Campbell, and S. N. Breit, "The nuclear chloride ion channel NCC27 is involved in regulation of the cell cycle," *J Physiol*, vol. 529, pp. 541–552, 2000. 179

[478] S. J. Harrop, M. Z. DeMaere, W. D. Fairlie, T. Reztsova, S. M. Valenzuela, M. Mazzanti, R. Tonini, M. R. Qiu, L. Jankova, K. Warton, A. R. Bauskin, W. M. Wu, S. Pankhurst, T. J. Campbell, S. N. Breit, and P. M. Curmi, "Crystal structure of a soluble form of the intracellular chloride ion channel CLIC1 (NCC27) at 1.4-A resolution," *J Biol Chem*, vol. 276, no. 48, pp. 44993–45000, 2001. 179

[479] D. R. Littler, N. N. Assaad, S. J. Harrop, L. J. Brown, G. J. Pankhurst, P. Luciani, M.-I. Aguilar, M. Mazzanti, M. A. Berryman, S. N. Breit, and P. M. G. Curmi, "Crystal structure of the soluble form of the redox-regulated chloride ion channel protein CLIC4," *FEBS J*, vol. 272, no. 19, pp. 4996–5007, 2005. 179

[480] T. G. Wolfsberg, P. Primakoff, D. G. Myles, and J. M. White, "ADAM, a novel family of membrane proteins containing A Disintegrin And Metalloprotease domain: multipotential functions in cell-cell and cell-matrix interactions," *J Cell Biol*, vol. 131, no. 2, pp. 275–278, 1995. 180

[481] C. P. Blobel, "ADAMs: key components in EGFR signalling and development," *Nat Rev Mol Cell Biol*, vol. 6, no. 1, pp. 32–43, 2005. 180

[482] M. L. Moss and M. H. Lambert, "Shedding of membrane proteins by ADAM family proteases," *Essays Biochem*, vol. 38, pp. 141–153, 2002. 180

[483] D. R. Edwards, M. M. Handsley, and C. J. Pennington, "The ADAM metalloproteinases," *Mol Aspects Med*, vol. 29, no. 5, pp. 258–289, 2008. 180

[484] J. Guo, L. He, P. Yuan, P. Wang, Y. Lu, F. Tong, Y. Wang, Y. Yin, J. Tian, and J. Sun, "ADAM10 overexpression in human non-small cell lung cancer correlates with cell migration and invasion through the activation of the Notch1 signaling pathway," *Oncol Rep*, vol. 28, no. 5, pp. 1709–1718, 2012. 180

[485] B. You, Y. Shan, S. Shi, X. Li, and Y. You, "Effects of ADAM10 upregulation on progression, migration, and prognosis of nasopharyngeal carcinoma," *Cancer Sci*, vol. 106, no. 11, pp. 1506–1514, 2015. 180

[486] A. Trad, H. P. Hansen, M. Shomali, M. Peipp, K. Klausz, N. Hedemann, K. Yamamoto, A. Mauermann, C. Desel, I. Lorenzen, H. Lemke, S. Rose-John, and J. Grotzinger, "ADAM17-overexpressing breast cancer cells selectively targeted by antibody-toxin conjugates," *Cancer Immunol Immunother*, vol. 62, no. 3, pp. 411–421, 2013. 180

[487] L.-J. Xiao, P. Lin, F. Lin, X. Liu, W. Qin, H.-F. Zou, L. Guo, W. Liu, S.-J. Wang, and X.-G. Yu, "ADAM17 targets MMP-2 and MMP-9 via EGFR-MEK-ERK pathway activation to promote prostate cancer cell invasion," *Int J Oncol*, vol. 40, no. 5, pp. 1714–1724, 2012. 180